Motion Cueing in Driving Simulators for Research Applications

by

Andrew Hamish John Jamson

Submitted in accordance with the requirements for the degree of
Doctor of Philosophy

The University of Leeds
Institute for Transport Studies

November 2010

The candidate confirms that the work submitted is his own and that appropriate credit has been given where reference has been made to the work of others.

UNIVERSITY OF LEEDS

ACKNOWLEDGEMENTS

Firstly, I would like to acknowledge my long-standing colleague, Tony Horrobin. Without his dedication and unstinting hard work, neither the development of the University of Leeds Driving Simulator nor the technical implementation of the work presented here would have been possible. Throughout both, his devotion and commitment has been truly admirable. I have even learnt to decipher his occasional monosyllabic sentences, normally limited to the occasions when I significantly increased his already ample workload.

Naturally, I would also like to thank my supervisor, Professor Oliver Carsten. When I entered supervision meetings full of doubt and self-criticism, his insight and encouragement ensured that I left feeling revived and enthused. I doubt I would have been able to complete this work without his support.

I also need to state my gratitude to my unofficial supervisor, Dr Sunjoo Advani. His comprehension of the area of motion cueing in simulation was genuinely inspirational. His willingness to share his expertise and acumen was way beyond any reasonable call of duty.

The support of Eddie van Duivenbode at Bosch Rexroth B.V. is also acknowledged with appreciation. Back in 2006 when his company commissioned the motion system at the University's simulator, his assistance was expected. His continuing support some four years later, particularly in the area of MATLAB/Simulink modelling was less so. Thanks, Eddie.

Finally, I need to acknowledge my life supervisor, my wife Samantha. She has been equally responsible for my two most cherished long-term projects, my children Ruby and Charlie. I am truly grateful for the boundless energy and encouragement that all three of them continually provide. Their backing during the period that I undertook this work ensured its successful completion.

ABSTRACT

This research investigated the perception of self-motion in driving simulation, focussing on the dynamic cues produced by a motion platform. The study was undertaken in three stages, evaluating various motion cueing techniques based on both subjective ratings of realism and objective measures of driver performance.

Using a Just Noticeable Difference methodology, Stage 1 determined the maximum perceptible motion scaling for platform movement in both translation and tilt. Motion cues scaled by 90% or more could not be perceptibly differentiated from unscaled motion.

This result was used in Stage 2's examination of the most appropriate point in space at which the platform translations and rotations should be centred (Motion Reference Point, MRP). Participants undertook two tracking tasks requiring both longitudinal (braking) and lateral (steering) vehicle control. Whilst drivers appeared unable to perceive a change in MRP from head level to a point 1.1m lower, the higher position (closer to the vestibular organs) did result in marginally smoother braking, corresponding to the given requirements of the longitudinal driving task.

Stage 3 explored the perceptual trade-off between the specific force error and tilt rate error generated by the platform. Three independent experimental factors were manipulated: motion scale-factor, platform tilt rate and additional platform displacement afforded by a XY-table. For the longitudinal task, slow tilt that remained sub-threshold was perceived as the most realistic, especially when supplemented by the extra surge of the XY-table. However, braking task performance was superior when a more rapid tilt was experienced. For the lateral task, perceived realism was enhanced when motion cues were scaled by

50%, particularly with added XY-sway. This preference was also supported by improvements in task accuracy. Participants ratings were unmoved by changing tilt rate, although rapid tilt did result in more precise lane control.

Several interactions were also observed, most notably between platform tilt rate and XY-table availability. When the XY-table was operational, driving task performance varied little between sub-threshold and more rapid tilt. However, while the XY-table was inactive, both driving tasks were better achieved in conditions of high tilt rate.

An interpretation of these results suggests that without the benefit of significant extra translational capability, priority should be given to the minimisation of specific force error through motion cues presented at a perceptibly high tilt rate. However, XY-table availability affords the simulator engineer the luxury of attaining a slower tilt that provides both accurate driving task performance and accomplishes maximum perceived realism.

CONTENTS

FIGURES

TABLES

GLOSSARY OF TERMS

Analysis of Variance	collection of statistical models in which the observed variance in a particular variable is partitioned into components attributable to different sources of variation
Bode plot	graphical depiction of system transfer function in frequency domain of input/output amplitude (Bode magnitude) and timing (Bode phase)
Cartesian	coordinate system specifying point in space relative to three fixed perpendicular planes
Classical filter	well-established motion drive algorithm filtering vehicle dynamic input and commanding motion platform output in translation and rotation
Cut-off frequency	break frequency at which system throughput is attenuated
Degree-of-freedom	motion system displacement along a single orthogonal axis
Disparity	relative lateral displacement of the retinal images in the left and right eyes of the same object in space
Dome	typically spherical construction housing a simulator's vehicle cab and display system

Frequency domain	Description of system input and output as function of angular frequency rather than time
Heave	motion platform vertical movement in translation along its z-axis (analogous to SAE J670 vehicle axis system)
Hexapod	[Gough-]Stewart platform, actuated mechanism allowing movement along the three linear and three angular axes of Cartesian frame (six degrees-of-freedom)
High-pass filter	Attenuation of signals below filter's cut-off frequency, higher frequencies unmodified
Lateral	horizontal left / right motion, along the y-axis of the SAE J670 vehicle axis system
Longitudinal	horizontal fore / aft motion, along the x-axis of the SAE J670 vehicle axis system
Low-pass filter	Attenuation of signals above filter's cut-off frequency, lower frequencies unmodified
Motion cueing	the technique or algorithm which commands the movement of a motion platform to simulate the vestibular system of the occupant of the simulator
Motion Drive Algorithm	mathematical filtering of vehicle dynamic input, output commanding motion platform movement

Motion platform	interchangeable with motion system or motion base
Motion Reference Point	the point in space at which the platform translations and rotations are centred
Optic flow	dynamic pattern of retinal motion used to decipher an apparent visual motion
Paired Comparison	statistical technique to compare entities in pairs to judge which of each entity is preferred or has a greater amount of some quantitative property
Pitch	motion platform movement in rotation around the y-axis (analogous to SAE J670 vehicle axis system)
Proprioceptor	receptor on nerve endings in muscles, tendons and joints disambiguating sensory information into position of limb and corresponding body movement in space
Roll	motion platform movement in rotation around the x-axis (analogous to SAE J670 vehicle axis system)
Scale-factor	the factor by which motion platform's output (vestibular cues stimulated by the platform) are deliberately attenuated from its inputs (demanded cue)
Specific force	perceived acceleration with respect to gravity

Sway	motion platform horizontal movement left and right in translation along its y-axis (analogous to SAE J670 vehicle axis system)
Surge	motion platform horizontal movement forward and backward in translation along its x-axis (analogous to SAE J670 vehicle axis system)
Tilt	angular displacement of the motion platform in pitch or roll
Tilt-coordination	angular displacement of the motion platform in order to trade the gravity vector for a perception of acceleration
Tilt rate	angular velocity of the motion platform in pitch or roll
Tracking task	task associated with the following of some target or goal
Transfer function	mathematical system description of input/output relationship
Translation	linear movement of a motion platform in surge (longitudinal), sway (lateral) or heave (vertical)
Vection	perception of self-motion
Vehicle dynamics	mathematical description of a vehicle's function influencing its equations of motion

Vestibular	sensory balance and perception of acceleration, imparted by otoliths and semi-circular canals located in the inner ear
Washout	slow return of motion platform to its neutral position handled by second order high-pass filter
XY-table	moving sled allowing significant relocation of motion platform in either surge or sway
Yaw	motion platform movement in rotation around the z-axis (analogous to SAE J670 vehicle axis system)

CHAPTER 1

RESEARCH DRIVING SIMULATORS

Research driving simulators, as opposed those employed in the development of driver training, are primarily used to facilitate scientific evaluations of driver behaviour. They enjoy many benefits over naturalistic studies using instrumented vehicles with their main advantage being a considerable versatility to configure virtual scenarios that exactly match the requirement of a particular investigation. Environmental conditions can be manipulated such as day/night operation, weather conditions and state of the road surface. The parameters of the driven vehicle can be altered: for example suspension design, tyre construction and steering characteristics can be matched to an existing or prototype vehicle. New and novel road schemes, methods of signage and highway infrastructure can be modelled virtually and evaluated prior to the logistical challenge of modifying large areas of roadway. Furthermore, there is the ethical advantage of an inherently safe environment for the participants of a particular study. This makes research driving simulators particularly useful for investigations into fatigue, impairment and medical issues.

Simulator designers strive to reproduce high quality visual, auditory and kinaesthetic cues within their facilities in order to artificially recreate a realistic driving environment. However, financial or logistical constraints may limit a simulator's capabilities, potentially moderating its ability to fully stimulate the entire range of drivers' sensory modalities. Clearly, these limitations have the potential to influence the efficacy of a particular research study in terms of the reliability of driving data extracted from the simulator. A badly designed simulator could invoke unrealistic driver behaviour that, in turn, may lead to poor quality driver behavioural research.

A simulator's capabilities have some bearing on its validity in a number of ways. First, there is the issue of motivation. Participants are clearly aware that they are not exposed to any physical danger whilst driving, but to what extent

does the simulated drive absorb them? How real does the simulated driving experience feel to them? Essentially, is the simulator “emotionally” valid? Next, there is the issue of “physical” validity: how does the simulator’s dynamic behaviour match that of the vehicle it is imitating? Do similar applications of the driver controls induce the same vehicle performance in natural and virtual conditions? Thirdly, there is “face” validity: how is the simulator perceived in terms of its look and feel? Do the vehicle interior and controls resemble those in the real vehicle? After this, “perceptual” validity must be considered. Do drivers acquire the appropriate visual, auditory, proprioceptive and vestibular cues in order to make accurate estimations of distance, speed and acceleration? Finally, a simulator’s “behavioural” validity is probably the most important: to what extent, is a driver’s control of the vehicle comparable under both simulated and natural conditions?

At present, more than 100 large-scale research driving simulators exist worldwide, owned, operated and often constructed by universities, government research institutions and vehicle manufacturers. Several more are currently under construction, but as yet, neither a standardised technique nor an international legislator exist to assess validity in terms of the specific characteristics of the many and varied subsystems that make up an individual driving simulator.

The technologies developed leading to the advent of Full Flight Simulators (FSS) also play a significant role in the make-up of research driving simulators. Before a FSS can be utilised in the training of flight crew, it must first be certified by the local National Aviation Authority. This evaluation is made against a list of tests dictated by the procedural and methodical nature of commercial pilot training. By initially defining the tasks required of the simulator operator (in this case the pilot), the demands required of the simulator itself can be subsequently identified. With this classification, it becomes possible to define the acceptable simulator characteristics by assessing the ability of the FSS to facilitate the training of flight crew within the operational range of the simulator defined by those characteristics.

Driving, on the other hand, is much less regulated and arguably more wide-ranging activity than commercial flying. Varying tasks are constantly demanded of the driver to maintain safe and controlled operation of the vehicle based on a perception of the entire driving environment; for example, potential hazards unfolding in the visual scene, the performance of the driven vehicle, navigation, control and handling. Defining this plethora of tasks in order to, in turn, define an acceptable driving simulator operational range therefore becomes an exceptionally difficult challenge. Hence, research driving simulator validation is, in general, a sporadic, under-funded and under-researched area, severely lacking common consistent and robust validation procedures.

1.1. Aims and objectives

The remainder of this chapter introduces the key sub-systems within a typical driving simulator and their evolution throughout the historical development of such facilities. The aim is to highlight the key characteristics of these sub-systems and the potential influence that each may have on the perception of self-motion or "*vection"* (Howard & Templeton, 1966) within a virtual driving environment and hence its validity. The optimal configuration of each sub-system remains a significant cause for debate and still poses a major challenge when considering the ability of simulators to extract realistic driver behaviour. If a difference is observed between real and virtual conditions, how easy is it to explain what factors specifically cause these differences? It will be argued that accurate perception of vection is predominantly influenced by three main human sensory modalities: stimulation of the visual system, the vestibular system and the auditory system (Kemeny & Panerai, 2003). However, a plethora of simulation parameters may affect this sensation, shaping a driver's judgment of the overall virtual environment.

If perception is influenced by the vagaries of the simulator's different subsystems and their ability to fully stimulate the breadth of a drivers' sensory modalities, these limitations have the potential to influence the efficacy of a particular investigation in terms of the reliability of driving data extracted from

the simulator (Kaptein, Theeuwes & van der Horst, 1996). However, if the driving tasks are tightly defined, it can be possible to develop a validation technique that meets the requirements of those particular tasks. The important questions during such a task analysis then become:

- What is the role of human perception in performing these tasks in reality?
- How can the available resources and the simulator's characteristics (hardware and software) be best optimized to re-create these perceptions?

Due to the extensive subsystems within a driving simulator, the scope of the research presented here focuses on just one modality: the perception of motion through the vestibular channel, excited by the simulator's motion system. This subsystem was selected for two reasons. First, the perception of motion cues and their impact on vection is highly significant in driving simulation (Kemeny & Panerai, 2003). Secondly, whilst more fully explored in the realm of flight simulation, the addition of dynamic cues and the exploitation of motion systems has received limited attention from the driving simulator community at large.

Equally as important as defining a scope for the research is identifying its success criteria. This research aims to assess the impact of perceived motion on driving simulator validity at both perceptual and behavioural levels. First, simple yet typical driving scenarios are defined that permit an objective assessment of driver performance against the accurate achievement of specific driving tasks. Next, whilst holding the remaining simulator characteristics constant, the behaviour of the motion system is characterised according to its key attributes. By comparing subjective assessments of realism and objective measures of task performance, the effect of the manipulation of these attributes is assessed. It is therefore possible to draw conclusions on which motion cueing conditions achieve a strong perceived correlation between real and virtual conditions and those that obtain solid behavioural correspondence. Of great interest is whether these conditions do actually match.

This experimental approach is innovative and attempts to build on existing simulation literature in the undertaking of an in-depth and comprehensive study into the perception of motion within research driving simulators. In the process, it aims to fill a significant gap in the existing literature, whilst at the same time providing results that are relevant to those driving simulator developers privileged enough to benefit from a motion system.

1.2. Key sub-systems of a research driving simulator

Figure 1-1 below shows the key sub-systems of a research driving simulator and how they interact with one another. Originating from the driver making control inputs from the vehicle cab, each successive sub-system plays a vital role in the provision of the various modalities required to form a sound perception of the virtual driving environment.

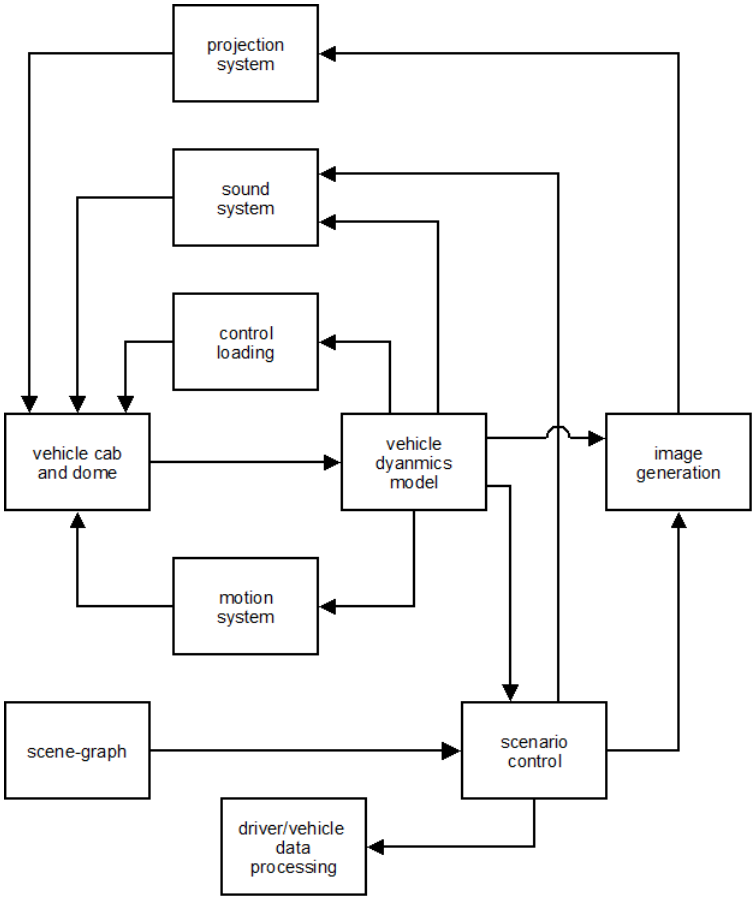

Figure 1-1: key sub-systems of a research driving simulator

Vehicle cab and dome. At the centre of any simulation is the driver and the vehicle cab in which he or she sits. For low-cost simulators, this typically consists of either a full or cut-down real vehicle cockpit. Very cheap desktop simulators may only include a representation of the physical driver controls, i.e. steering wheel and foot pedals. Dashboard instrumentation is commonly fully operational to give the driver indications of driving speed, engine speed, fuel level and other information concerning the vehicle's operation. In simulators benefiting from a motion system, the whole cab may reside within a simulation dome. This is normally a stiff but lightweight construction such that it does not resonate at the usual frequencies of operation of the motion system. The dome prevents unwanted extraneous sounds and light from polluting the simulation environment, and its inner surface is used as a screen onto which to display the visual images from the projection system.

Vehicle dynamics model. Vehicle dynamics are critical to a robust simulator (see Gillespie, 1992, for a review). The model analyses the driver's use of the vehicle controls, such as the steering wheel, accelerator, brake etc. and simulates the dynamic behaviour of a real-life vehicle.

Scene-graph. The scene-graph holds the data that define the virtual world in a hierarchical database structure. Initially, the 3-D model of the roadway describes only static roadside furniture, e.g. roadways, buildings, trees, signposts. It includes both low-level descriptions of object geometry and their appearance, as well as higher-level, spatial information of their location within the virtual environment. Additional data defining attributes of particular objects, e.g. road friction, can be included in the scene-graph. Its function is to provide an efficient structure of the graphical data that supports optimal performance in terms of speed of rendering of the image generation process falling later in the simulation loop (see Foley, van Dam, Feiner & Hughes, 1990, for a review).

Scenario control. Scenario control refers to the process of choreographing particular traffic scenarios or events within the virtual driving environment. It achieves this through a modification of the scene-graph to add all the real-time

agents based on a model of their behaviour, such as other vehicles, pedestrians or traffic lights. Fundamental to scenario control is the underlying description of the roadway, the Logical Road Network - LRN (van Wolffelaar, 1996; Bailey, Jamson, Wright & Parkes, 1999). Scenario control uses the LRN to provide information in order to support the behaviour and interaction of the real-time agents. For example, intelligent virtual traffic effectively uses the LRN to "perceive" the road as a human driver in order to make intelligent decisions such as intersection priorities and overtaking (e.g. Cremer, Kearney & Papelis, 1995).

Driver/vehicle data processing. One of the fundamental reasons for using a research driving simulator is the abundance of driver behavioural and performance measures that can be easily recorded. These data may refer to the driver's use of the vehicle controls, the corresponding behaviour of the vehicle or specific behavioural metrics that are commonly used to quantify driver behaviour, such as coherence in a car following task (Brookhuis, de Vries, & de Waard, 1991), steering reversal rate (McLean & Hoffmann, 1975) or time-to-line crossing (Godthelp & Konnings, 1981).

Image generation. Image generation describes the computational process of visually rendering the virtual environment from the point of view of the driver. The process acts on the complete hierarchical visual scene-graph, both the initial static objects in the 3-D model of the roadway and those moving agents appended to the scene-graph by the scenario control module. The image generation module, taking account of the viewer's position from the vehicle dynamics module, then uses standard libraries to render a perspective view of the complete scene-graph. These libraries efficiently manage the computational drawing process in order to maximise the frame rate and complexity of the visual scene. Visual effects such as weather conditions and lighting conditions can be added along with features such as multiple visual display channels to create wide field of views.

Control loading. The “feel” of a simulated drive helps to create a sense of realism in a driving simulator; hence, it is convenient that the vehicle controls have the same characteristics as the actual vehicle that the simulator is mimicking. The main feedback to a simulator driver is through the steering emanating from those generated at the tyre-road interface as modeled by the vehicle dynamics. Control feedback through the foot pedals, and in particular the feel of the brake, is also significant.

Sound system. High quality reproduction of auditory cues and their acoustic spatialisation within the simulated environment enriches the driver’s perception of the virtual driving scene. Sounds of both internal (engine noise, aerodynamic noise, road rumble, tyre screech) and external objects (other traffic, environmental noise) are recorded and synthesised. These sounds are then modified according to the current driving state (e.g. vehicle speed, engine speed, Doppler effects) taking into account the complex acoustic field inside the vehicle cab. Finally, the modified sounds are played back to the driver, often through a multi-channel surround sound system.

Projection system. The projection system physically displays the virtual driving scene rendered by the image generation module. This can take place over a single visual channel or over a number of projected images, whose images are blended and colour-balanced, to create a wide field of view. Projection screens for narrow field of views (less than 50-60°) tend to be flat surfaces, having the advantage they are cheap and easy to modify. Multi-channel systems, affording a much wider view, normally require either cylindrical or spherical projection screens in order to keep a relaxed eye-point: a constant distance from the eye to the screen surface, whatever the viewing angle.

Motion system. A motion system is designed to artificially recreate the dynamic cues of both longitudinal (braking and ride) and lateral (cornering and stability) vehicle accelerations. Dynamic cueing in a driving simulator is possible using motion platforms which were initially developed for flight simulation

applications, progressively used more frequently in the automotive field. Developments in vehicle simulation applications started relatively recently (Nordmark, Lidström & Palmkvist, 1984; Drosdol & Panik, 1985) compared to the initial hexapod design used in early flight simulators (Stewart, 1965).

A full description and wide-ranging literature review focussing solely on the motion system can be found later in Chapter 2. A thorough understanding of its design, functionality and operation is important when it comes to comprehending the rationale for the experimental work undertaken, outlined in Chapter 4. Until that point, the next section briefly outlines a potted history of research driving simulator development. In order to preserve relevance to this work, the review focuses almost entirely on the development of facilities with significant motion capabilities.

1.3. Significant milestones throughout the history of driving simulator development

Fully interactive research driving simulators, in which drivers could actually control their vehicle in a virtual environment, were in existence long before the development of modern computer-generated visual displays. In 1965, the American Society of Mechanical Engineers published a report outlining the development of a driving simulator in which drivers were seated in a stationary vehicle cab in front of a projection system replaying colour film recorded from a real world scene (Wojcik & Hulbert, 1965). Auditory and vibratory inputs were provided to increase the simulator's limited realism. However, since the simulator was non-interactive and participants had no real control over the speed or position of their vehicle, it was recognised that the facility was more suited to the physiological and perceptual aspects of the driving task rather than those requiring motor skills. One year later, researchers at the Human Resources Research Organization developed a similar system (McKnight & Hunter, 1966), and the era of research driving simulators had begun.

By 1975, at least sixteen driving simulators were operating in the U.S. (Allen, Klein & Ziedman, 1979), however, it was not until 1980 that the Department of Transportation and the Federal Highways Administration decided to fund a feasibility study into construction of a fully interactive national facility based on a network of computers. Three years later, the system was installed at the Turner-Fairbank Highways Research Center and was dubbed HYSIM, Highway Driving Simulator.

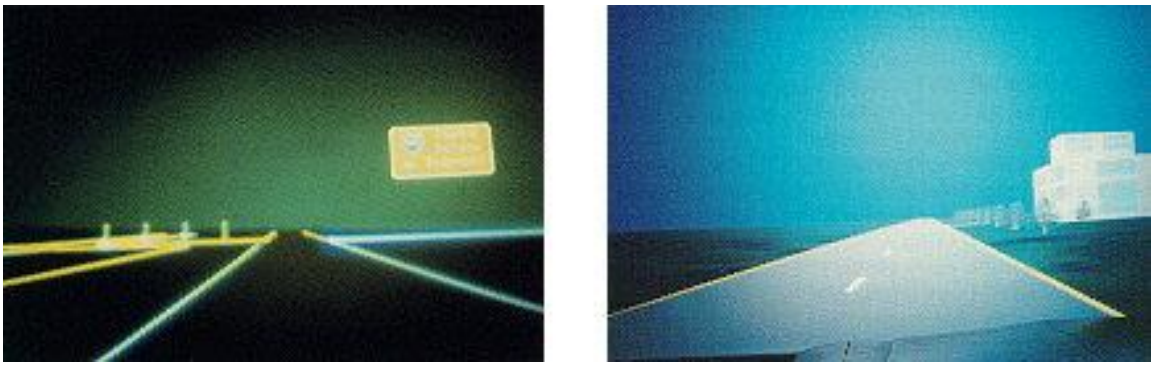

Figure 1-2: Visual scene of the original and subsequently upgrade HYSIM

In Europe, the first significant computer-based research driving simulator was developed by German vehicle manufacturer Volkswagen during the early 1970s. A single, flat screen was mounted in front of the driver seated, without a vehicle cab, on a motion system allowing limited movement in pitch, roll and yaw.

In 1984, this concept was further developed at the Institut für Kraftfahrvehsen und Kolbenmaschinen (IKK) in Hamburg. A VW Golf cab was mounted on a sled allowing only lateral motion with a narrow field of view image projected in front of the driver. After well over a decade of operation, the simulator was subsequently modified to become the Modular Automobile Road Simulator, MARS (Tomaske, 1999). The sled was retained, but it now carried a hexapod motion system thus allowing seven degrees-of-freedom motion.

1-3: the IKK and MARS driving simulators

Around the same time, the Swedish National Road and Transport Research Institute, VTI, were unveiling their first driving simulator. It consisted of a 120° visual system and a three degree of freedom motion system capable of ±24°pitch, ±24° roll and with a lateral displacement of 7m. The motion system could achieve a maximum acceleration of 0.4g. The simulator was re-developed in the late 1980s to allow a higher payload and again in 2004 with the addition of an improved linear drive to the lateral sled and an ability to orient the vehicle cab either longitudinally or laterally along the sled (Nordmark, Janson, Palmkvist & Sehammar, 2004). VTI continues to be a leader in the field, with a fourth driving simulator currently under development in Gothenburg.

Figure 1-4: the three VTI driving simulators

Spurred on by their European rivals, Daimler-Benz commissioned their first simulator in 1985 located at the Berlin-Marienfeld research centre (Drosdol & Panik, 1985), the first to use a hexapod motionbase. For many years this simulator was considered a world leader, further improved in the mid 1990s

when a seventh linear lateral motion over a 10m long track was introduced (Käding & Hoffmeyer, 1995). In fact, throughout the 1990s, many other automotive manufacturers such as Mazda (Suetomi, Horiguchi, Okamoto & Hata, 1990), General Motors (Bertollini, Johnston, Kuiper, Kukulam, Kulczycka & Thomas, 1994), Ford (Greenberg & Park, 1994), Renault (Reymond & Kemeny, 2000) and BMW all jumped on the bandwagon and built interactive simulation facilities with full motion systems.

Over the same period, several national research institutions also began to develop their own, smaller-scale, facilities. In 1990, work began on the Japanese Automobile Research Institution simulator that became operational in 1995 (Soma, Hiramatsu, Satoh & Uno, 1996). The facility was the first Japanese simulator with the capability of six degree-of-freedom motion. Meanwhile, the U.K.'s Transport Research Laboratory (TRL) moved from their 1979, non-interactive (film-based) British Leyland Mini simulator (Watts & Quimby, 1979) to a fully interactive three degree of freedom, limited-motion, wide-field of view facility in 1995 (Duncan, 1995). Updated to a Honda Civic cab in 2001, the TRL car simulator was joined in 2004 with a hexapod-based truck simulator, creating the U.K.'s first driving simulation centre with multiple vehicles. Around this time, other national research institutions also started to exploit the emergence of "off-the-shelf" driving simulator software platforms and fixed-base facilities were commissioned in Norway (SINTEF), France (INRETS) and the Netherlands (TNO).

Figure 1-5: the TRL and JARI driving simulators

A multitude of university-based facilities also began to materialise during the 1990s, the most advanced of which was arguably the University of Iowa Driving Simulator (IDS), which became operational in 1994 (Freeman, Watson, Papelis, Lin, Tayyab, Romano & Kuhl, 1995). The simulator utilised a decommissioned Boeing 737 flight simulator hexapod motion system, the vehicle cab was a Ford Taurus Sedan and the visualisation system, fixed to the motion platform, projected over 140°. This development led in turn to the unveiling in 2001 of the National Advanced Driving Simulator (NADS), which until 2007 when Japanese car giant Toyota extended the design, was most the expansive (and expensive) driving simulator ever assembled. Four different and exchangeable vehicle-cabs can be mounted inside a 7.3m diameter dome located on a pioneering motion platform: a large amplitude, hexapod motion subsystem with a two-axis sled allowing just under 19m of horizontal longitudinal and lateral travel plus an ability to rotate in yaw 330° using a turntable located above the hexapod. At the time, it was the first nine degree-of-freedom system ever attempted. NADS continues to operate as the most advanced driving simulator in a publically-funded research establishment.

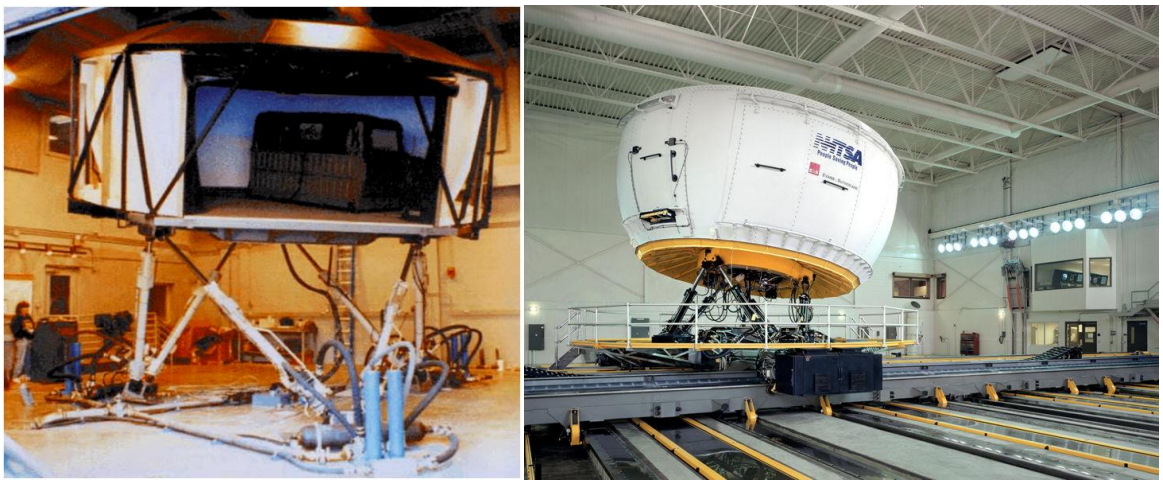

Figure 1-6: the Iowa Driving Simulator and eventual offspring, the National Advanced Driving Simulator

Through the early 21st century, the performance of electrically-driven motion systems gradually became equivalent to that previously associated with hydraulic systems. This launched a new, more cost-effective era of motion platform such that many more driving simulators were able to exploit extensive

horizontal motion. The first was Renault, with the flamboyantly titled ULTIMATE, a three channel, forward field of view of 150° with an overall payload of 1 tonne. The sled allowed 7m of lateral and longitudinal of effective travel in addition to that available through its 500mm actuator-length hexapod (Dagdelen, Reymond, Kemeny, Bordier & Maïzi, 2004). Three years later both the University of Leeds Driving Simulator (Jamson, Horrobin & Auckland, 2007) and PSA Peugeot-Citroen's SHERPA2 (Chapron & Colinot, 2007) utilised a similar motion system with increased payload (2.5t), but reduced available horizontal stroke (5m). The fourth VTI simulator will also use the same system.

Figure 1-7: Renault's ULTIMATE, University of Leeds and SHERPA2 driving simulators

Around the same time, two new facilities arrived on the scene, both with novel conceptual and structural designs of their motion systems. Near Hanover, the Institute of Transportation Studies at the German Aerospace Centre plumped for a large "inverted" hexapod in the DLR driving simulator (Suikat, 2005). The design offered similar motion capabilities to a more traditional hexapod, but the simulator cabin hung down in between the actuators, hinged at their upper rim. The main advantage to this design was that the rotation point, and hence the "feel" of the motion system, could be positioned more closely to the head of the driver than would be possible in a standard hexapod without the sacrifice of any motion system performance.

Across the border in the Netherlands, a revolutionary motion platform design was unveiled at TNO Safety and Security in DESDEMONA (DESoriëntatie DEMONstrator Amst). Its gimballed cab allowed unlimited rotation in all three orthogonal axes fixed on a 2m vertical linear track. This whole structure moved along a 4m radius centrifuge arm, which revolved at up to 155°/s, sustaining

accelerations in the cab up to an incredible 1g. Although initially designed as a disorientation trainer for military flight applications, the cab can resemble a small driving cockpit with a single seat and narrow field of view. The ability of DESDEMONA to sustain lateral acceleration whilst maintaining an expansive yaw rate has been shown to benefit driving applications involving aggressive manoeuvres (Valente Pais, Wentink, van Paassen & Mulder, 2009).

Figure 1-8: the "inverted" hexapod DLR simulator and centrifuge-style DESDEMONA

This decade ends with the recent arrival of the world's most costly and advanced driving simulator to date. Heavily influenced by the design of NADS, the gargantuan Toyota driving simulator at the Higashi-Fuji Technical Centre is almost identical to its American cousin, except that its two-axis sled allows an increased travel of 25m laterally and 35m longitudinally.

Figure 1-9: the world's largest driving simulation facility, the Toyota Driving Simulator

This section has outlined the major milestones along the path of driving simulator development. Now, as much as ever before, great debate rages within the driving simulator community as to whether such hugely expensive facilities are truly worth their outlay. One argument is that a simulator's fidelity and hence its value as a research tool is inherently related to its ability to create a realistic representation of driving, which in turn is likely to induce realistic driver performance. The greater a facility's development cost, the more likely it is to employ cutting-edge technology in its endeavour for such realism. However, even with such significant numbers of research driving simulators now active worldwide and with a vested interest for those facilities to demonstrate their worth, the validation literature is hardly filled with an overabundance of peer-reviewed articles. The following section, however, briefly examines what evidence does exist on how the characteristics of the sub-systems affect simulator validity in terms of driver behaviour.

1.4. Key sub-systems and their affect on driving simulator validity

In a driving simulator, there are three main modalities through which drivers sense their movement within the virtual environment: stimulation of the visual system, the vestibular system and via auditory information (Kemeny & Panerai, 2003). It has for some time been commonly regarded that the visual, and to a lesser extent the vestibular feedback, are the most important with regard to the perception of vection. Only more recently has the accuracy of audio rendering been shown to influence such vection (although its effect is much weaker and typically only occurs in between 25% and 60% of people (Sakamoto, Osada, Suzuki & Gyoba, 2004). A combination of all three modalities is more influential than the sum of the individual modalities (Väljamäe, Larson, Västfjäll & Kleiner, 2006).

1.4.1. Effects of the visual system

Under natural conditions, visual cues provide a significant contribution to allow an observer to form a perception of their environment space. However, under simulated conditions, the inherently inferior display characteristics (e.g. image resolution, update frequency and field of view) bring about a reduction in the quality of these cues. A driver's use of these cues is important for the estimation of:

- Vehicle speed.
- Distance to objects.
- Vehicle heading and lateral control.

Early work in visual perception (Gibson, 1950) suggests that drivers' visual perception of space is based on disparity and optic flow. Disparity refers to the relative lateral displacement of the retinal images in the left and right eyes of the same object in space. It is an effective binocular cue to depth at short distances. Optic flow, on the other hand, describes the dynamic pattern of retinal motion that our brains use to decipher an apparent visual motion. In driving, both are thought to play dominant roles both in the control of heading (Lappe, Bremmer & van den Berg, 1999) and in collision detection (Lee, 1976).

Binocular cues are not typically present in driving simulators since to achieve this acceptably requires either stereo projection or the use of Head-Mounted Displays. Whilst it is generally accepted that the effectiveness of binocular convergence as a cue to absolute distance is limited to a few metres (van Hofsten, 1976), the effectiveness of binocular disparity has been judged to be up to 30m (Loomis & Knapp, 1999). Given that the majority of objects within a driving environment are positioned beyond this range, disparity is normally less important to the qualities of a driving simulator display system than optic flow.

The evaluation of vehicle speed and the estimation of inter-vehicle distance are essential skills in safe and controlled driving. Manoeuvres such as overtaking and collision avoidance require such abilities. In a driving simulator, these skills require the accurate representation of self-motion from both optic

flow and egocentric direction – the direction of an object in space relative to the observer (Gogel & Tietz, 1979). Optic flow can give information about either absolute speed or distance and also exploited to compare relative spatial intervals, central to the accurate estimation of time-to-contact (Lee, 1976; Loomis, 2010). A significant number of studies into speed perception have shown that observers tend to underestimate their velocity in simulated environments (Alicandri, Roberts & Walker, 1986; Riesmersma, van der Horst & Hoekstra, 1990; Harms, 1993; Duncan, 1995; Groeger, Blana, Carsten & Jamson, 1999). This effect is also sensitive to image contrast (Blakemore & Snowdon, 1999), the amount of texture (Blakemore & Snowdon, 2000), projector brightness (Takeuchi & De, 2000) and the overall field of view (Jamson, 2000).

Distance estimation is also based on a number of reliable cues, such as optic flow (Bremmer & Lappe, 1999), disparity (Howard & Rogers, 1995) and motion parallax (Rogers & Graham, 1979). Motion parallax describes the differential motion of pairs of points as a result of their different depths relative to the fixation point and to the motion of the observer. It provides robust estimates of absolute egocentric distance when combined with additional visual information describing an observer's self-motion. In a driving simulator study, it was shown that the central nervous system is able to combine these two cues to calibrate the retinal image motion and infer absolute distance just as efficiently in a virtual environment as it does under natural conditions (Panerai, Cornilleau-Peres & Droulez, 2002).

It has also been demonstrated that both optic flow and motion parallax are crucial for correct interpretation of heading and its control (Crowell, Banks, Shenoy & Andersen, 1998). However, it is important to note that during curve negotiation, drivers tend to fixate points along their path (Land & Lee, 1994). These active gaze strategies play an important role in heading control (Land & Horwood, 1995). However, more recent studies have proposed that accurate heading control can be achieved through a combination of optic flow *and* visual egocentric cues (Wann & Land, 2000). This was demonstrated experimentally

by Harris & Bonas (2002) in a study of human walking. When road markings were apparent, visual egocentric cues alone provided enough information to allow walkers to maintain accurate heading control. However, performance did not degrade when the markings were missing. It was concluded that in this case an optic flow strategy was dominant.

1.4.2. Effects of the motion system

Due to its significance in this work, motion cueing is afforded a more significant review in Chapter 2. However, generally its influence on driving simulator validity has been positively demonstrated.

In a stationary observer, vection usually takes several seconds to establish itself (Melcher & Henn, 1981). The latency of this vection can be reduced by the addition of inertial motion cues (Groen, Howard & Cheung, 1999). Furthermore, from a steady condition of stabilised speed and lane position, drivers experiencing a disturbance to such conditions exhibit a significantly shorter response time in simulators with motion as opposed to without (Wierwille, Casali & Repa, 1983).

Greater variation in lane position has been observed in drivers of fixed-base simulators compared to those experiencing similar but real-life conditions (Harms, 1993; Duncan, 1995; Blana & Golias, 2002). The addition of motion cues reduces this variation (Alm, 1995; van Winsum & Godthelp, 1996; Reymond, Kemeny, Droulez & Berthoz, 2001; Greenberg, Artz and Cathey, 2002). Moreover, drivers perform wider turns when lateral cues are present compared to those when only visual information is available (Siegler, Reymond, Kemeny & Berthoz, 2001).

1.4.3. Effects of the sound system

Compared to the visual inducement of self-motion, audio cues are much less compelling. Auditory vection is influenced by the realism of the acoustic simulation and the number of sound sources (Larson, Väljamäe, Västfjäll &

Kleiner, 2004; Riecke, Schulte-Pelkum, Caniard & Bülthoff, 2005). The accurate spatialisation of sound-emitting objects within the virtual environment further benefits the process (Riecke, Väljamäe & Schulte-Pelkum, 2009).

Sound cues are so frequently represented in driving simulation that unearthing a driving simulator without the provision of a sound system would be quite a discovery. However, the effect of audio cues on the fidelity of simulator driver behaviour in comparison to real conditions has not been shown so clearly. McLane and Wierwille (1975) investigated the effects of presence or absence of speed-related sounds and vibrations in a driving simulator. Results indicated that the performance measures of yaw, lateral and velocity deviation were significantly affected by the deletion of vibration. The authors reported that the existence of audio had no significant effect on either driving speed or lane control. However, they acknowledged that the audio rendering had the advantage that irrelevant sounds emanating from the various simulator sub-systems were effectively masked, improving the simulator's face validity. Similarly, some twenty years later, Davis and Green (1995) confirmed the lack of an effect of sound in a simple fixed-base simulator, demonstrated by unchanged drivers' rating of realism with and without audio cues, a result replicated by Capustiac, Hesse, Schramm & Banabic (2010).

1.5. Thesis outline

Following on from this introduction and statement of research objectives, Chapter 2 delves deeply into the perceptual theory leading to the design and development of modern motion cueing. It also looks at the implementation of a range of motion drive algorithms, the signal processing that filters the vehicle motion before commands are made of the motion system to simulate this motion. The strategy and implementation of various algorithms is discussed, with their deployment in the field of driving simulation given particular focus. Previously published literature is also addressed, culminating in the justification of the selection of one algorithm for further investigation. Chapter 3 describes the dynamic characteristics of the simulator used during the study and how the

driver's vehicle handling results in the motion cues demanded and subsequently manipulated in the three-staged experimental design outlined in Chapter 4. The three stages are described separately in Chapters 5, 6 and 7, before Chapter 8 discusses the main impact of the findings. This discussion focuses on the scope of the research, its limitations and caveats, implications for the design and evaluation of motion cueing in research driving simulation and the potential for further work.

CHAPTER 2

MOTION CUEING

Visual cues play an important role in the perception of self-motion and the estimation of an observer's position within a 3-D environment. However, human visual motion perception is tuned to velocity rather than acceleration (Brandt, Koenig & Dichgans, 1973). Thus fixed-base driving simulators, heavily reliant on the quality of their visual system for the perception of accurate speed cues, are best suited to conditions that remain relatively constant. Disturbances away from this steady-state are more quickly recognised by the vestibular system, a sensory organ enclosed in a fluid-filled cavity within the inner ear (Figure 2-1), than the visual system (Young, Dichgans, Murphy & Brandt, 1973). Hence, the specific forces from a range of acceleration cues can be recreated in the simulation by the utilisation of a device designed to mimic such forces: the motion system.

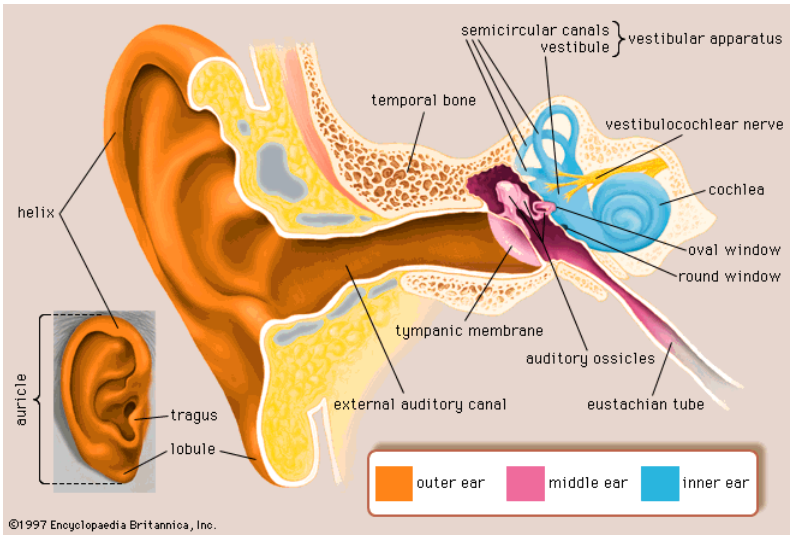

Figure 2-1: location of the vestibular system (reproduced from Encyclopaedia Britannica)

Within the vestibular system, the utricle and saccule are small sacs containing minute sensitive hairs which in combination make up the otolith organs. When the head tilts relative to gravity or is accelerated, the hairs are deflected and the nerve fibres transmit the perception of acceleration to the central nervous system. The otoliths perform identically either due to linear acceleration or tilt. Hence, assuming that the position of the visual display to an observer remains unchanged, a motion system exploits this ambiguity to create the perception of linear acceleration by simply changing their tilt angle with respect to the gravitational vector through the observer (Figure 2-2).

The other main functioning organs within the vestibular system are the semi-circular canals. These consist of three-fluid filled circular ducts, fixed approximately in the three main orthogonal planes. The base of each duct is enlarged forming the ampulla. Within the ampulla, a gelatinous valve known as the cupula stretches from its base, the crista, to its roof. When the observer undergoes an angular acceleration, the momentum of the fluid causes a pressure differential over the cupula. The resulting distortion of the cupula elicits movement of the hair cells of the crista and the perception of angular acceleration is carried by the nerve fibres (Figure 2-2). Within the realm of the simulation of motion cues, a fuller description as to why the otoliths are sensitive to the roll angle while the semicircular canal organs are sensitive to roll acceleration is available in Vander, Sherman & Luciano (1975).

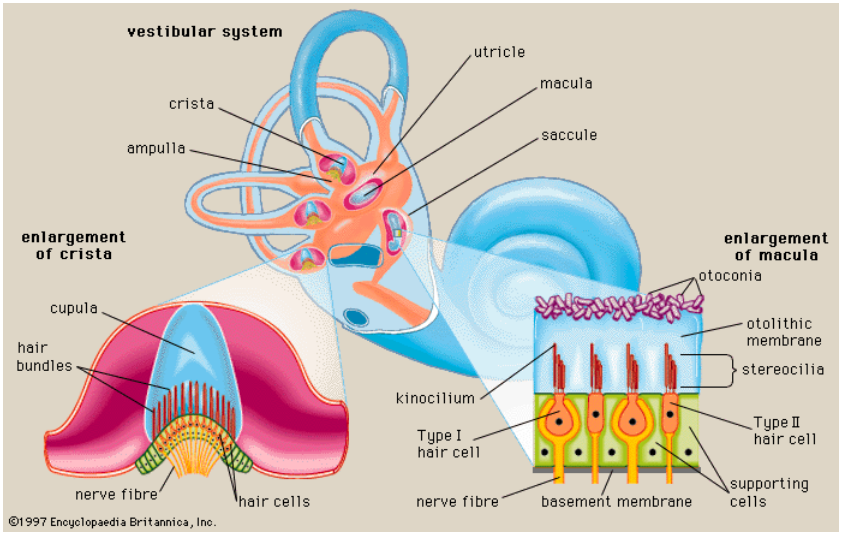

Figure 2-2: the otoliths and semi-circular canal organs within the vestibular system (reproduced from Encyclopaedia Britannica)

2.1. Motion Drive Algorithm

In an ideal world, a simulator would faithfully reproduce the complete range of dynamic cues acting on the driver emanating from the linear and angular accelerations experienced during the manoeuvring of the vehicle. Furthermore, this would be done in a straight 1:1 manner, such that the acceleration felt in reality would exactly match that in the simulator. However, to simulate typical vehicle handling in such a fashion demands a dynamic representation of motion that far exceeds the limited displacement capability of a conventional motion system workspace. In other words, short-lived accelerations at the onset of a

manoeuvre can be reproduced quite accurately, whilst sustained cues cannot. Hence another technique must be employed to satisfactorily simulate a long-lived acceleration cue. To achieve this, the Motion Drive Algorithm (MDA) filters the vehicle motion before signals are sent to the motion system.

Only the high-frequency components (onset cue) of the translational and rotational accelerations are reproduced by a corresponding acceleration of the motion system. The low-frequency components (sustained cue) are recreated using tilt co-ordination. As the motion system is tilted, so long as this tilt occurs below the threshold of perception of the semi-circular canals and thus there is no impression of angular motion, the behaviour of the otoliths gives the sense of a sustained linear acceleration to the driver. A simultaneous presentation of the corresponding situation in the virtual environment through the display system makes it impossible for the observer to determine whether the perception of linear acceleration arises from tilt or translation (Berthoz & Droulez, 1982) and minimises any delays in the perception of vection (Groen, Howard & Cheung, 1999). The accepted human thresholds of angular motion perception that can be detected by the semi-circular canals are about 3°/s in terms of angular velocity and 0.3°/s^2 in terms of angular acceleration (Groen & Bles, 2004).

2.2. Classical motion drive algorithm

Of the MDAs (or filters) in use today, particularly within the domain of flight simulation, the classical filter is the most wide-spread (Colombet, Dagdelen, Reymond, Pere, Merienne & Kemeny, 2008). It is most applicable to the range of six-axis motion platforms, known as Stewart platforms or hexapods. These possess six independently actuated legs, where the actuator length can be changed rapidly to vary the platform's position and attitude (Figure 2-3). The Stewart platform allows movement in all six degrees-of-freedom of the Cartesian inertial frame:

- ***surge*** (forward and backward translation along its x-axis
- ***sway*** (sideways translation along its y-axis
- ***heave*** (vertical translation alongs its z-axis)

- ***pitch*** (tilting rotation around the y-axis)
- ***roll*** (tilting rotation around the x-axis)
- ***yaw*** (horizontal rotation around the z-axis)

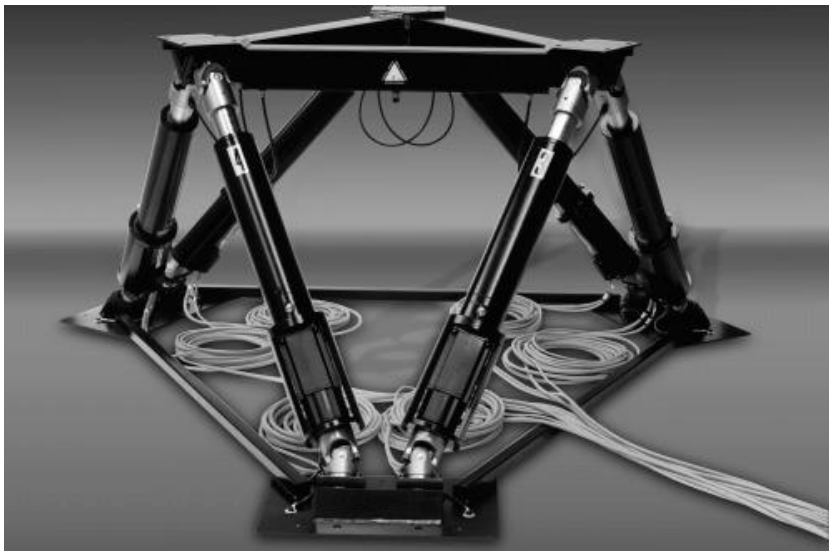

Figure 2-3: typical hexapod motion platform (image courtesy of Bosch Rexroth B.V.)

Basic research undertaken at the University of Toronto in the mid 1980s (Reid & Nahon, 1985; Reid & Nahon, 1986a; Reid & Nahon, 1986b) underpins current understanding and utilisation of the classical algorithm (Nahon & Reid, 1990).

In the example of driving simulation, the classical filter works primarily on the six orthogonal accelerations generated from the vehicle dynamics model. These are the three linear accelerations of longitudinal acceleration (braking/accelerating), lateral acceleration (cornering) and the vertical acceleration (road roughness and bumps). These are supplemented by the three angular accelerations of pitch (suspension effects of braking/accelerating), roll (suspension effects of handling) and yaw (actual yawing of the vehicle in a turn). To be more accurate, the input to the classical MDA for the linear accelerations is actually the specific force, a description of the linear acceleration with respect to the normal acceleration felt through gravity.

The output of the classical filter describes the desired attitude that the motion platform should adopt, known as the set point. However, in reality, the inertia

and mechanical dynamics of the motion platform will delay arrival at the set-point. The higher the bandwidth of the motion system, the smaller these delays are. A typical hexapod bandwidth would be in the order of 5-10Hz.

The horizontal plane specific forces arrive from the vehicle dynamics in the time domain, the signals changing their value continually over the period of the simulation. The main function of the classical filter (Figure 2-4) is to split these time-driven specific forces into the frequency domain, such that their magnitude is described over a range of frequencies that the motion system can realistically achieve.

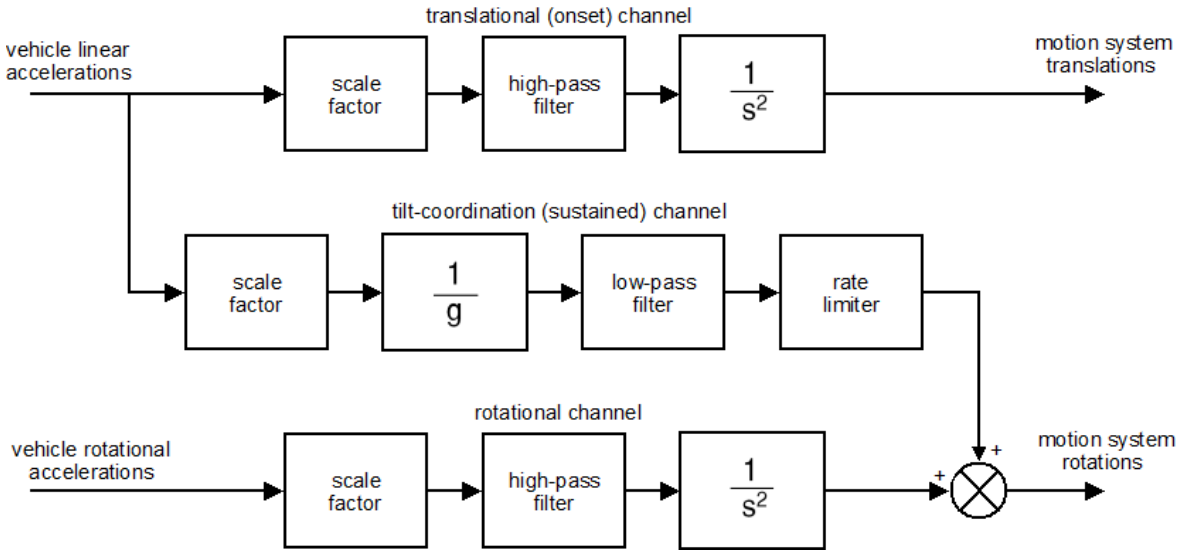

Figure 2-4: classical motion drive algorithm

For an example, let us take the case of a vehicle manoeuvring at speed through a long-sweeping curve. In this situation, the driver would primarily sense the translational lateral acceleration acting on the vehicle along with the rotational acceleration associated with the body roll. The high-frequency component of this translational acceleration (the onset cue) is acquired by passing the input signal through a high-pass filter. This is then double integrated to create a corresponding, short-lived, translation in sway of the motion system. The main role of the high-pass filter is to ensure that the sway remains within the physical capabilities of the motion system. After the onset cue, the motion platform gently translates back to its initial position. This is known as *washout*

and readies the simulator to undertake another translational onset cue, should that be required. By its nature, washout creates simulator motion in the opposite direction to that expected, and so, in order to reduce false cues, does so at a rate below perceptual threshold, readily accepted at around 0.01g (Grant & Reid, 1997).

To simulate the manoeuvre through the translational channel alone would result solely in the fast sway motion, followed by the slow washout motion; just a short but accurate onset cue would be felt. To allow for a realistic simulation of both the onset and the sustained lateral acceleration felt throughout the curve, a method know as *tilt-coordination* is employed. First the translational input is divided by the acceleration due to gravity. This calculates the angle through which the motion platform must be rotated to obtain the component of the gravity vector that equals the desired specific force. This calculation actually gives the tangent of the angle. However, for the small angles in question, this is approximately equal to the angle itself. The low frequency component of the linear acceleration is achieved through a low-pass filter and then the corresponding roll of the motion platform is limited to ensure that the tilt (roll in this case) occurs below the perceptual thresholds of 3°/s and 0.3°/s^2 (Groen and Bles, 2004), in order to “fool” the vestibular system into the perception of sustained lateral acceleration.

The motion system also rotates to mimic the rotational acceleration that the driver would perceive through body pitch roll, determined by the suspension characteristics of the driven vehicle. Like linear acceleration, this rotational acceleration is also high-pass filtered to ensure that its representation exists within the available motion envelope. However, since the acceleration is only short-lived with body roll quickly developing as the vehicle enters the curve, high-pass filtering alone is sufficient as the major components of the cue exist in the high frequency range. The motion platform adopts this roll angle in addition to that commanded by tilt-coordination.

The final element to the classical filter is the ability to reduce the acceleration output actually represented by the motion system in relation to the input from the vehicle dynamics model through a scale-factor. Whilst undergoing linear accelerations, humans find estimating the absolute magnitude of those accelerations far more challenging than successfully accessing their relative difference (Berthoz & Droulez, 1982). Furthermore, motion platform demands which cause an actuator to reach its position limit result in unacceptable discontinuities in the motion representation, felt by the driver as a jolt as the smooth actuator movement abruptly comes to an end. By reducing the scale-factor of a particular channel, the classical MDA can be tuned for the worst-case scenario, such that the maximum acceleration to be simulated falls within the motion platform's displacement limits. However, in such a case only a fraction of the acceleration commanded by the vehicle dynamics model is actually achieved.

In practice, constraints in the design of a hexapod result in interaction of its available modes of motion. For example, significant actuator stroke is required by the demands of pure simulator yaw; this minimises the available stroke required to achieve demanded excursions in roll or pitch. Hence, in a fully interactive (rather than pre-scripted, such as the case of a entertainment simulator) the simulation engineer is obliged to select even more conservative channel scale-factors for the classical filter.

2.2.1. Development of the classical algorithm

The classical filter was born during the early development of six degree-of-freedom flight simulators at NASA Ames Research Centre (Conrad & Schmidt, 1969). The early MDA filtered aircraft accelerations, but only rendered the onset cues existing in the high-frequency domain. A few years later, tilt-coordination improved the algorithm (Conrad, Schmidt & Douvillier, 1973). However, the maximum physical displacement of these early hexapods was extremely limited, leading to a highly conservative, worst-case tuning. Parrish, Dieudonne, Bowles & Martin (1975) had an ingenious solution to this problem, introducing an

adaptive strategy. The new algorithm was derived from the classical filter and still operated in the frequency domain, but at each computational time-step adjusted the filter settings in an attempt to minimise a cost function. The cost was weighted to trade-off the demands of faithful specific force rendering and the limitations of platform displacement.

The advantage of the adaptive algorithm was clear: false cues associated with maximum actuator extension could be nullified and a smooth simulation could be guaranteed. However, the constantly changing nature of the adaptive algorithm brought with it the drawback of the loss of homogenous motion sensation. Since the handling of the simulator by the pilot caused the simulator's position starting to constantly change, the available motion envelope for a given flight manoeuvre could never be guaranteed. Hence, consistent pilot input to the control column could result in varying behaviour of the simulator. This led to concerns over the efficacy of motion in training and a pilot's ability to invariably recognise hazardous situations associated with disturbances away from controlled flight (e.g. engine failure, autopilot failure), particularly in the critical phases of approach and landing (Gundry, 1976).

Further developments of the algorithm applied linear optimal control techniques that minimised a cost function that also predicted a model of the human vestibular system (Sivan, Ish-shalom & Huang, 1982). The linear motion perception model had been proposed by Hosman & van der Vaart (1981). The work was ground-breaking in that it freely acknowledged the imperfect cues that are produced by the motion system. The intention was to design a MDA that resulted in pilot behaviour in the simulator that tallied with reality, rather than one that simply attempted to achieve matching acceleration cues. However innovative, the MDA had the significant disadvantage that the tuning of the weights in the cost function was subjective and time-consuming. Furthermore, experiments by Reid & Nahon (1985) showed that even if the cost function weights were justifiably selected, the optimal algorithm fared no better in terms of pilot performance and subjective fidelity than the basic classical algorithm of Conrad et al. (1973).

Whilst optimal control and the development of perception/controller models remains an on-going area of research, Reid & Nahon's (1985) work culminated in the definition of the classical filter in its most widely utilised form today (Nahon & Reid, 1990). Its behaviour is discussed in more detail in the following sections.

2.2.2. Response of the classical filter to sustained linear acceleration

In the following sections, the classical filter is considered in its most widely utilised form (Nahon & Reid, 1990), introduced previously in Figure 2-4.

2.2.2.1. Time domain

Due to rate-limiting of the tilt-coordination channel, the typical response of the classical filter to a sustained linear acceleration shows a defined "sag" in the acceleration perceived by the driver. An example of such sag is shown in Figure 2-5. In the example, the first graph shows the vehicle undergoing a step change in linear acceleration of $1m/s^2$. The corresponding response of the translational and tilt-coordination channels are shown in the second graph. The onset cue is strong, but the perceived acceleration is short-lived as the actuators of the hexapod quickly reach their full extension and the washout smoothly takes the translation back to the motion platform's starting position. Meanwhile, rotation of the motion platform gradually reaches an angle sufficient to achieve the same perceived acceleration through tilt-coordination. The combination of these channels provides the overall perceived acceleration shown in the third graph.

By modifying the scale-factors, cut-off frequencies and damping ratios of the high-pass and low-pass filter of the classical MDA (described in more detail in the following sections), the simulation engineer can alter the response of the motion system in both the translational and tilt-coordination channels. However, to reduce the sag by quickening the response of the tilt-coordination channel requires the development of tilt at a rate above perceptual threshold. Hence, when using the classical filter, the simulator engineer always has the trade-off

between a response which may be perceived as prompt but with too much tilt, or a response which is lagged but with unnoticeable tilt.

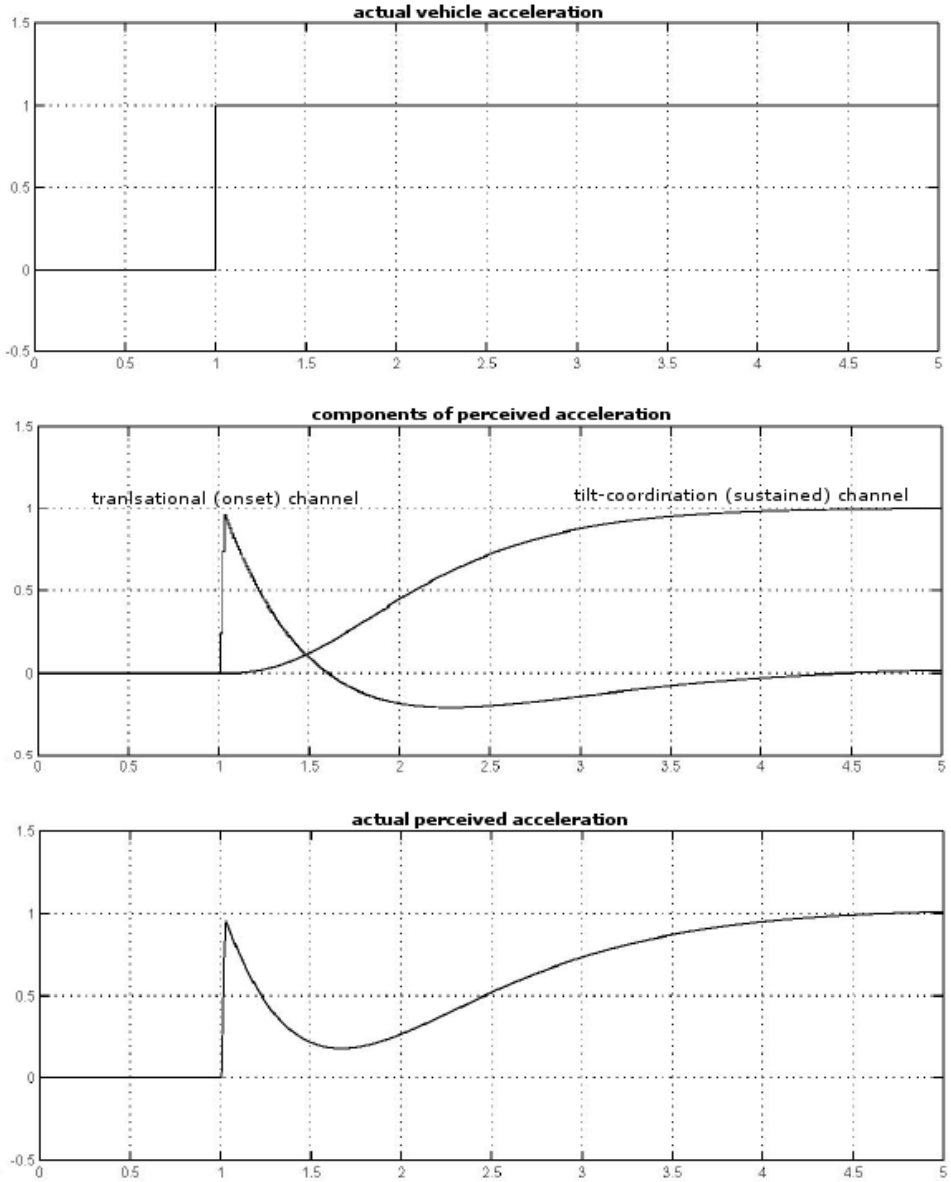

Figure 2-5: typical response of the classical filter to a step-input linear acceleration

2.2.2.2. Frequency domain

The previous technique describes the relationship between the input (demanded acceleration from the vehicle dynamics model) and output (total apparent acceleration felt through the motion platform) of the classical MDA for a single specific input in the time domain: the inputs and outputs of the system

are each described as functions of time. An alternative and more wide-ranging way to illustrate the behaviour of the classical filter, the system performance, is in the frequency domain. In essence, the higher the frequency of input, the higher the rate of change of that input with respect to time.

System performance in the frequency domain is achieved mathematically by employing a *Laplace transform*. The Laplace transform is a transformation of system performance, where the same inputs and outputs are functions of angular frequency rather than time. The result of the transformation gives the *transfer function* of the system, a mathematical or functional description of the relationship between the input and output of the system, simplifying the analysis of the behaviour of the system.

A *Bode plot* illustrates the transfer function graphically. It is a combination of a Bode *magnitude* (usually expressed as gain in dB) and a Bode *phase* (usually expressed as degrees of phase shift) plotted against angular frequency. The Bode magnitude describes the relationship between the system's input and output, the amplitude ratio, on a logarithmic scale. The gain in dB, or power, is 20 times the common logarithm of the amplitude ratio such that a negative dB value implies that output is smaller than the input and vice-versa. The Bode phase portrays to what degree the output will be phase-shifted away from the input. A negative Bode phase implies a phase lag of the output in relation to the input, whilst a positive value indicates a phase lead. Either way, the timing of the output is shifted from the timing of the input. Further reading on linear, time-invariant system theory can be found in Porat (1996).

A Bode plot, depicting the transfer function of the classic filter's response to the vehicle undergoing a step change in linear acceleration of $1 m/s^2$, can be seen in Figure 2-6. The Bode magnitude (dB gain) suggests that the amplitude of the output acceleration of the MDA almost identically matches the input acceleration, except for the hatched region between 0.02Hz and 0.7Hz. Considering the lateral case, this suggests that for a sinusoidal steering input in

this range achieving a peak lateral acceleration of 1m/s^2, the actual perceived lateral acceleration felt by the driver would be significantly lower.

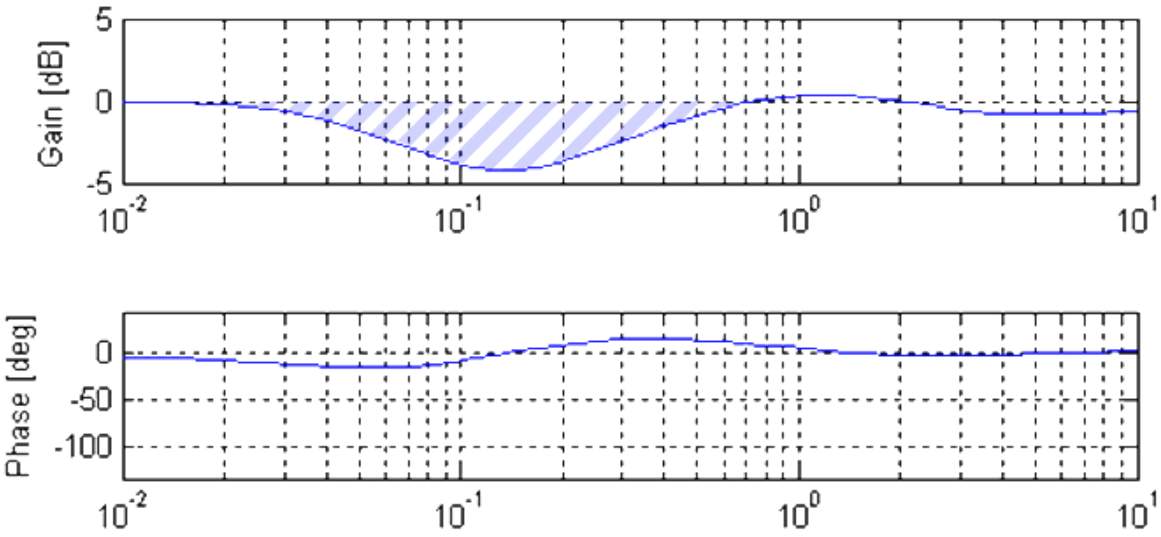

Figure 2-6: Bode plot of the transfer function of typical classical filter response to linear acceleration

Modifying the parameters (scale-factors, cut-off frequencies and damping ratios) of the high-pass and low-pass filters of the classical MDA (described in more detail in the following sections 2.2.4 and 2.2.5) results in a transfer function that, except in the case of very low accelerations or very small filter scale-factors, it almost impossible to flatten. Hence whilst the simulation engineer can alter response of the motion system in both the translational and tilt-coordination channels independently, to reduce the sag (flatten the transfer function) by quickening the response of the tilt-coordination channel requires the development of tilt at a rate above perceptual thresholds. Hence, when using the classical filter, the simulator engineer is faced with the difficulties of finding an optimal solution between a platform response which is may be perceived as prompt but with too much tilt (often perceived in driving as a soft suspension allowing excessive body roll), or a response which feels lagged but without detectable tilt.

2.2.3. Motion reference point

The motion reference point (MRP) denotes the point in space at which the platform translations and rotations are centred. Analogous to the design eye-point at which optimal viewing of a display system is achieved, in effect it is the point at which the perceived acceleration is ideally felt. For a conventional hexapod system, although the location of the MRP can be varied, it is typically specified by manufacturers with respect to the geometry of the motion platform. Most commonly, it is defined as the centroid of the two triangles formed at the upper joint rotation points (Figure 2-7).

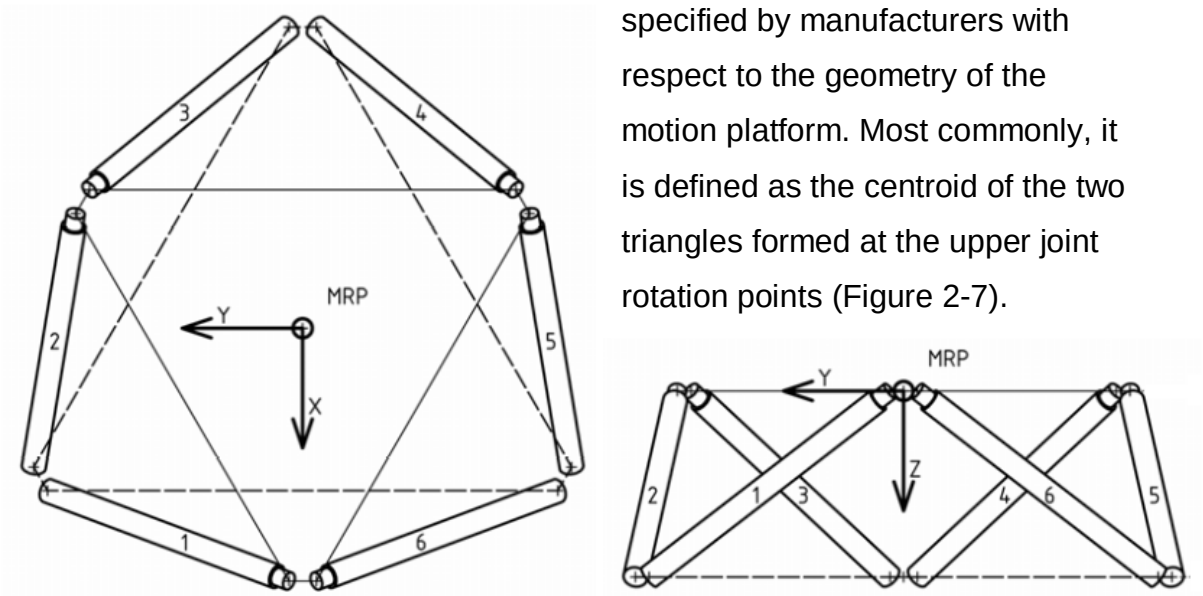

Figure 2-7: motion reference point of typical hexapod (image reproduced courtesy of Bosch Rexroth B.V.)

Since the vestibular system is located in the inner-ear, the ideal location for the MRP should actually be centred on the head of the observer (Reid & Nahon, 1985). However, due to the geometric constraints of the hexapod, moving the MRP vertically upwards to this point requires significantly greater actuator strokes in order to achieve the same degree of tilt. But leaving the MRP at the upper joint rotation points in order to maximise the angular displacement capability causes a cue conflict (Figure 2-8). In a conventional hexapod design, using tilt-coordination to create the impression of forwards linear longitudinal acceleration (Figure 2-8, large black arrow) causes a pitching up of the driver at the MRP (Figure 2-8, double green arrow). However, such pitch also creates a tilting velocity and acceleration in the direction contrary to the desired cue (Figure 2-8, small red arrows) which becomes greater towards the head as the rotation arm increases.

Fischer & Werneke's (2008) study using the DLR driving simulator showed a subjective preference for a higher MRP (fewer false cues). However the geometry of the simulator's motion platform was an inverted hexapod, where the cab hangs below the main platform. Contrary to a traditional six degree of freedom motion platform, the inverted hexapod allows the MRP to be located above the driver's head without any loss of platform angular displacement. Hence, yet another compromise is faced by the simulation engineer who must decide, for a standard hexapod, whether the false cue or the loss of angular displacement capability is the lesser of two evils. This dilemma is not shared by the engineers at DLR, but who are faced with a more expensive motion system that requires a significantly larger foot-print.

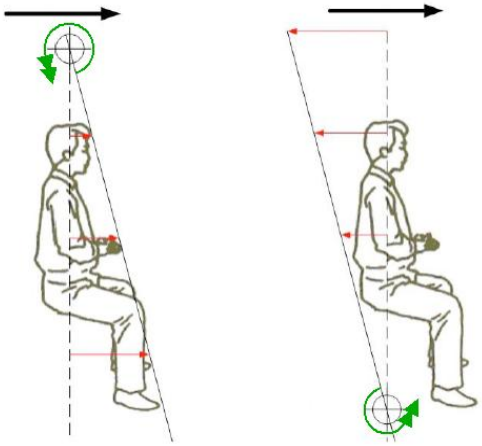

Figure 2-8: MRP above the drivers head (left) or below (right) (modified from Fischer & Werneke, 2008)

2.2.4. Influence of the translational (onset) channel

Whilst Figure 2-4 gives an overview of the key elements in the classical filter, a more detailed block diagram of the translational (onset) channel is given below in Figure 2-9. For linear accelerations associated with longitudinal (braking/accelerating) behaviour of the vehicle, the resulting motion system translations are in surge. For linear accelerations associated with lateral (cornering) behaviour of the vehicle, resulting motion system translations are in sway.

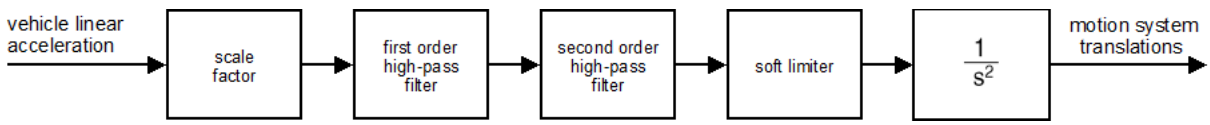

Figure 2-9: detailed translational (onset) channel of classical MDA

First, the linear acceleration emanating from the vehicle dynamics model is multiplied by the scale-factor of the translational channel in order to ensure that the motion system remains within its operational limits, i.e. the" worst-case" tuning described in section 2.2. Next, the signal is passed through a first order high-pass filter (onset filter), its cut-off frequency removing the low frequency components of the signal and ensuring that only the initial onset cue is handled. The washout movement returning the motion platform to its neutral position is managed by a second order high-pass filter (washout filter). In addition to having another, higher cut-off frequency, this filter also has a value for damping ratio associated with it. Next, the output is soft-limited which, if required, further minimises the false cues associated with full actuator extension, before being double integrated in order to demand a set-point from each of the six actuators.

2.2.4.1. First-order high-pass – Onset filter

Figure 2-10 shows the influence of the onset filter on both the perceived acceleration associated with the onset cue and the corresponding translational excursion of the motion platform to a step change in linear acceleration of 1m/s^2. The onset filter has only one parameter: the cut-off frequency. Reducing the cut-off frequency sustains the cue for a longer duration but this rapidly and significantly increases the required excursion.

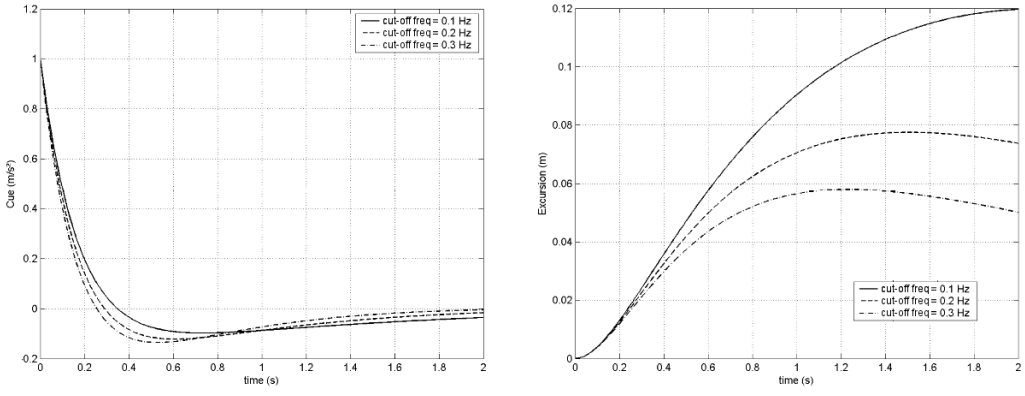

Figure 2-10: influence of the onset (first order high-pass) filter on pecieved cue and platform excursion

Given an appropriately sized motion envelope, using a unity scale-factor where the onset acceleration of the motion platform directly matches that of the input

may seem an intuitive choice. However, there is evidence that the selection of high scale-factors can lead to the perception of unrealistically strong motion cues. In a study undertaken by Groen, Valenti Clari & Hosman (2001), a group of seven F16 pilots participated as passive observers during a simulated take-off run in the National Simulation Facility of the National Aerospace Laboratory in Amsterdam. The acceleration profile corresponded to a static takeoff where the pilot applies takeoff thrust before releasing the brakes. The magnitude of the longitudinal acceleration was constant at 0.35g, representative for a medium-sized civil aircraft. Whilst the scale-factors of the translational (surge) and tilt-coordination channel (pitch) were systematically varied, the cut-off frequency of the onset filter was correspondingly adjusted such that the linear travel of the motion platform in response to the acceleration cue remained constant at 1.3m. Based on their subjective response, the range of realistic motion parameters was centred around a scale-factor as low as 0.2 for the onset filter. Unity scale-factors were unanimously rejected as too powerful. A consistent scaling of motion was recommended due to the tendency of the pilots to overestimate physical motion relative to the corresponding vection perceived visually through the simulator's display system.

Of course, in reality, motion scale-factors always equal one so the question arises as to why physical motion is overestimated with respect to simulated visual motion? Groen et al. (2001) suggest a theory that the visual-vestibular discrepancy is actually a result of an underestimation of visual cues but manifested as an over-estimation of vestibular cues. Their argument is supported by several laboratory studies:

- actual self-motion results in a greater threshold for visual motion perception (Wertheim, 1994).
- actual self-motion is consistently over-estimated with respect to visual motion (Harris, Jenkin and Zikovitz, 2000)
- observers tend to underestimate their velocity in simulated environments (Howarth, 1998).

Grant and Haycock (2008) propose a more straight-forward solution, blaming a distortion of jerk (rate of change of linear acceleration) resulting from both the increased stiffness associated simplifications of typical vehicle dynamics and mathematical output of a high-pass filter in response to a step input. Both give rise to a level of jerk much higher in the simulator compared to a real road vehicle. Given that human observers are sensitive not only to linear acceleration, but also its first derivative (Hosman & Stasson, 1999), unity onset scale-factors therefore result in motion that is perceived as too strong.

To achieve an acceptable perception of motion within the constraints of a typical motion platform, the onset filter scale-factor is often set at a value around 0.7 (Reid & Nahon, 1988). Grant, Blommer, Artz & Greenberg (2009) even observed accurate lane keeping and acceptable subjective ratings to a range of slalom steering manoeuvres undertaken by drivers of Ford's VIRTTEX simulator with a classical MDA onset filter scale-factor of 0.5. The manoeuvre used in this experiment was a double lane change demarcated by a set of orange cones. However, decreasing the scale-factor still further to 0.3 resulted in a significant deterioration of driver performance and an accompanying worsening of subjective motion assessment. Schroeder, Chung & Hess (2000) investigated onset scale-factor in a sample of helicopter pilots attempting to control their altitude between two points 32 feet (9.75m) apart. One-to-one vertical motion was possible since the study utilised the large amplitude vertical motion capability of the NASA Ames Vertical Motion Simulator. The authors achieved improved performance and better accepted motion perception with an onset scale-factor of 0.5 than with unity, a result they attributed to the reduction in the filter's scale-factor reducing its phase error.

2.2.4.2. Second order high-pass – Washout filter

The washout filter, designed to slowly return the motion platform to its neutral position is a second order high-pass filter. It has two parameters: the cut-off - frequency and the damping ratio. Figure 2-11 and Figure 2-12 show the influence of both the cut-off frequency and damping ratio of the washout filter on the corresponding translational excursion of the motion platform to a step

change in linear acceleration of 1m/s^2. As for the first-order onset filter, reducing the cut-off frequency sustains the cue for a longer duration, but this rapidly and significantly increases the required excursion. Decreasing the damping ratio minimises the effect of the washout filter, sustaining the cue for longer. Since washout creates simulator motion in the opposite direction to that expected, in order to reduce false cues, suitably low damping is used. However, low damping ratios rapidly increase the excursion of the motion platform and hence risk alternative false cues from the jolt of maximum actuator displacement.

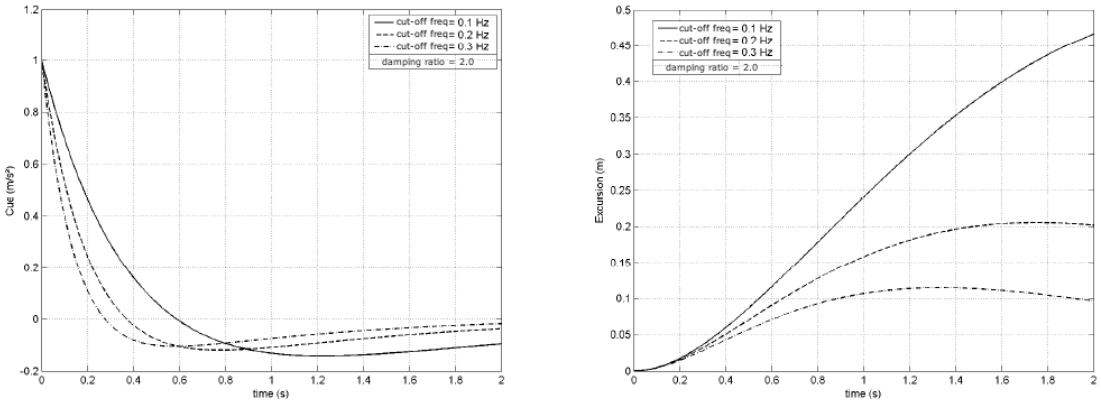

Figure 2-11: influence of cut-off frequency of washout (second order high-pass) filter on peceived cue and platform excursion

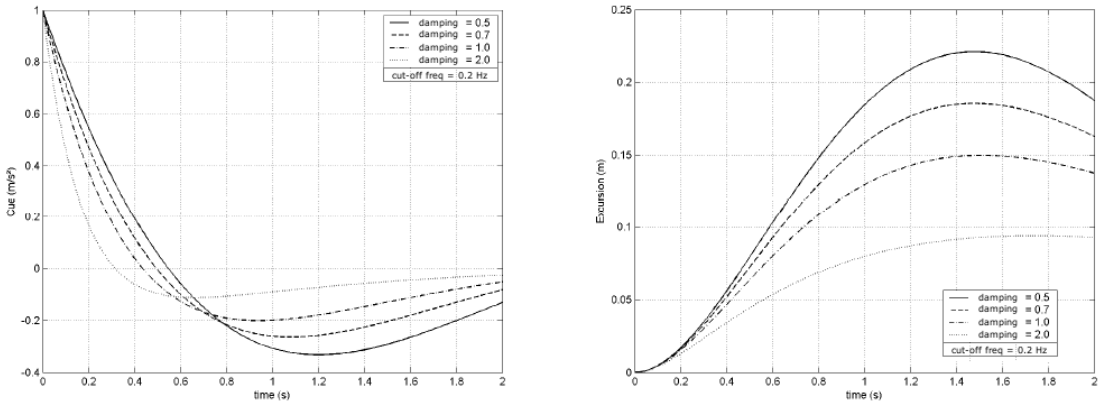

Figure 2-12: influence of damping ratio of washout filter on peceived cue and platform excursion

Washout relies on a limitation of the vestibular system. Laboratory studies reported by Benson (1990) indicate that, in a dark environment and with the absence of visual cues, translational movements of short duration (10s or less) are unlikely to be detected if the change in linear acceleration is less than 0.05m/s^2. For prolonged stimuli exceeding 15s, this threshold value increases to

0.1m/s^2. The perceptual threshold of vertical acceleration is higher at 0.35m/s^2. Benson also observed that motion stimuli many times greater than the minimal levels of perception go unnoticed if the observer is busy with additional workload, such as those associated with the demands of flying or driving. The addition of visual cues, even when not associated with the motion cues, increases this threshold still further (Berthoz, Pavard & Young, 1975). Hence, with the combination of operator workload and corresponding visual and long-duration motion cues typically provided in a simulator, the washout limit for translational motion is readily accepted at around 0.01g (Grant & Reid, 1997).

2.2.5. Influence of the rotational (tilt-coordination) filter

The layout of the classical MDA's tilt-coordination filter, commanding rotations of the motion platform, is shown in Figure 2-4. For linear accelerations associated with longitudinal (braking/accelerating) behaviour of a vehicle, the resulting rotations are in pitch. For linear accelerations associated with lateral (cornering) behaviour of the vehicle, resulting motion system rotations are in roll.

As for the onset filter, first the linear acceleration emanating from the vehicle dynamics model is multiplied by the scale-factor of the tilt-coordination channel. Subsequently, the signal is passed through a second order low-pass filter (tilt-coordination filter) and rate-limiter resulting in the rotational displacement of the motion platform.

Linear acceleration creates an illusory sensation of tilt (Clark & Graybiel, 1966). The tilt-coordination filter relies on the physiological parallel also being true. Indeed, it has been shown that horizontal linear acceleration induces ocular torsion (Lichtenberg, Young & Arrot, 1982), a response which also occurs when the head is tilted. The rate-limiter ensures the output of the low pass filter develops slowly enough to occur below the perceptual thresholds of 3°/s and 0.3°/s^2 (Groen and Bles, 2004), but resulting in the sag in perceived

acceleration shown earlier in both the time (Figure 2-5) and frequency (Figure 2-6) domains.

Figure 2-13 shows the influence of the tilt-coordination filter on the perceived acceleration associated with the tilt-coordination cue and the corresponding rotational displacement of the motion platform to a step change in linear acceleration of 1m/s^2. The tilt-coordination filter has only two parameters: the cut-off frequency and the damping ratio. The cut-off frequency removes the high frequency components already handled by the onset filter and the damping ratio reducing the effect of output signal overshoot. Increasing the cut-off frequency and lowering the damping ratio quicken the tilt of the motion platform.

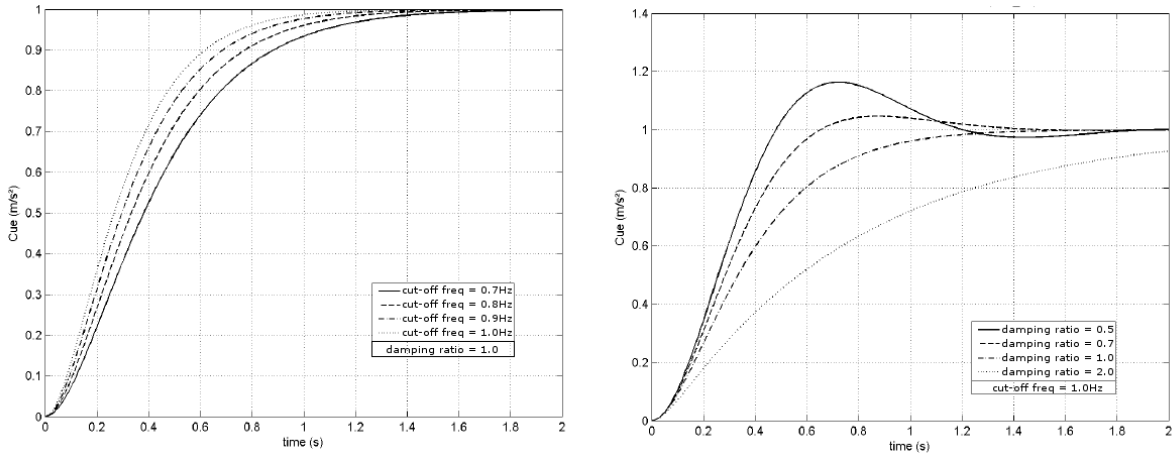

Figure 2-13: influence of tilt-coordination filter on perceived cue (platform angular displacement)

2.2.6. Specific force error and angular rate error trade-off

The difficulty in achieving a smooth transition between motion platform translation (onset filter) and rotation (tilt-coordination filter) and the associated flatness of the transfer function (Figure 2-6) can be also described mathematically as a balance between the specific force (perceived acceleration with respect to gravity) error and the tilt velocity error (Pouliot, Gosselin & Nahon, 1998). If the tilt-coordination is not rate-limited, increasing the cut-off frequency of its low-pass filter reduces the specific force error as the tilt will build up more quickly. This will, however, lead to an increase in tilt velocity error as the angular velocity felt by the observer greatly exceeds that of the

suspension of the driven vehicle, hence the simulation engineer's trade-off described in section 2.2.2.2: the prompt/over-tilt response against the lagged/correct-tilt.

The trade-off between specific force errors and angular velocity errors has vexed researchers for some time, especially in the flight simulation domain (e.g. Hosman & van der Vaart, 1981), but often with task-dependent results. In their helicopter bob up/down simulator motion study with pilots undergoing a tracking task of achieving a varying target height, Schroeder et al. (2000) suggested that, within limits, flattening the transfer function through lowering high-pass onset filter cut-off frequency had a greater impact in terms of a degradation in tracking performance than through reducing the onset scale-factor. Similarly, in an evaluation of perceived motion during a take-off run, Groen et al. (2001) concluded that the high correlation of perceived discontinuity and perceived magnitude of surge motion indicates that pilots tolerate variations in filter natural frequency less than they do variations in filter scale-factor. For this particular task, downscaling the specific force is suggested to be the most desirable of the two.

Similar task dependencies exist within the realm of driving simulation. To date, few studies have specifically evaluated the specific force / angular velocity error trade-off. During the development of the DLR driving simulator's MDA, Fischer & Werneke (2008) had drivers undertake a series of emergency stops (full brake pedal depression) with tilt-coordination either limited at the accepted perceptual thresholds of 3°/s and 0.3°/s^2 (Groen & Bles, 2004) or unlimited. In the limited case, specific force error is low but pitch velocity error is high. In the unlimited condition, the opposite is true. Whilst observing that a higher location of the motion reference point did play a minor role in improving the subjective rating of realism of the sustained period of braking, a clear preference was shown in the ratings of both the magnitude and timing of the deceleration in the unlimited condition. The conclusion was drawn recommending minimising the specific force error at the expense of increased pitch rate error.

The opposite conclusion was reached in a study using Ford's VIRRTEX simulator with drivers tasked with a series of lane changes on a straight, two-lane carriageway (Grant et al., 2009). In the experiment, the classical MDA was compared with four different parameter sets, varying the cut-off frequency and damping ratio of the onset, washout and tilt-coordination filters. Two parameter sets were selected that balanced specific force and roll rate errors, with one specifically optimised for the lane change task in question. Of the other two parameter sets, one had a reduced specific force error at the expense of roll rate error whilst the final set sacrificed specific force error for reduced roll rate error.

Fischer & Werneke (2008) had compared subjective preference by allowing drivers to rate the magnitude and timing of perceived cue on a scale between 1 and 15 (1 - too low/too slow; 8 - correct; 15 - too high/too fast). Such a technique suffers from a problem first highlighted by Thurstone (1927) that when a discriminating variate is involved, perceivable and linear differences must exist among the items presented for comparison. Furthermore, the analysis of variance technique, used to scrutinise the subjective rating, assumes a normal variation in that observed data. Could it be reasonably assumed that the DLR simulator drivers gave consistent and linear ratings on such a scale? Grant et al. (2009) plumped for a more robust technique, using a two-alternative forced-choice method, analysed using a paired comparison (Kendall & Babington-Smith, 1940) and maximum likelihood estimation of the preference probabilities (Bradley & Terry, 1954).

In addition to comparing subjective preference, Grant et al.'s (2009) study also evaluated driver performance whilst performing the lane change task by undertaking a repeated-measures analysis of variance on the root mean square of steering wheel angle. Making the very reasonable assumption that a lower value indicated better driving performance through a smoother execution of the manoeuvre with fewer steering corrections, their final conclusions were as wide-ranging as they were enlightening. First, across the varying parameter sets, steering performance was more consistent and hence the statistical analysis

had more power relative to the subjective paired comparison data. Furthermore, the rank ordering of the parameter sets was supported, although to varying degrees of power, by both the objective and subjective data. Finally, and perhaps most crucially, improved driver performance and subjective rating was achieved through reducing the roll rate error at the expense of specific force error.

When considering a technique involving fast tilting (see section 2.4.5), Fischer, Lorenz, Wildfeuer & Oeltze (2008) examined subjective assessment on a more mundane driving task, the approach to and the negotiation of a roundabout. This task demanded significantly less specific force than the emergency stop manoeuvre of Fisher & Werneke (2008), in which participants were instructed to stop as quickly as possible after the presentation of a commanding auditory stimulus. Although a higher-tilt rate had no effect on task performance, the resulting low specific force error/high roll rate error was reported to be significantly more preferable than the alternate slow tilting condition, associated with a high specific force error but low roll rate error.

On the surface, these studies do differ considerably in their conclusion. However, it should be remembered that the characteristics of the driving tasks and hence demands of the motion platform did vary considerably from one investigation to the other. The long duration of the emergency braking manoeuvre in Fisher & Werneke (2008) gives it a significant component in the low frequency range that necessitates ample tilt-coordination. Maybe the expectations of drivers to feel this deceleration quickly, strongly and continuously predisposed them to the unlimited tilt rate condition – the lesser of two evils? By comparison, Grant et al. (2009) did consistently rate-limit motion platform roll throughout each of the parameter sets under evaluation. But the lane change manoeuvre had a comparably larger high-frequency component, demanding a lateral acceleration cue that lasted for only one second. Furthermore, it was an elongated sine wave in nature as the cue naturally changed direction as the lane change manoeuvre reached the midway point. In assessing the trade-off between specific force and roll rate errors, maybe

drivers are actually judging the credibility of different portions of the cue: its onset rather than its sustainability. The underlying significance is that it appears to be the demands of the specific driving task at the time that should define the cueing technique and consequently its acceptance.

This argument is strengthened by a study undertaken at the Motion Lab of the Max Planck Institute for Biological Cybernetics in Germany. Berger, Schulte-Pelkum & Bülthoff (2010) employed a hexapod motion platform equipped with a projection screen to display a range of linear longitudinal accelerations to participants. Their task was not to control the performance of the simulator, but to rate the "believability" of the acceleration cues presented as they "moved" through a randomly textured ground plane populated to the left and right with life-size images of people, designed to maximise visual vection through familiar size cues. For each presentation, the visual scene faded in as forward acceleration was increased from zero to its peak value over 4s. This was followed by a further 2s of constant acceleration before the visual image was faded out. The visual scene corresponded with brief movements of the motion platform in surge and backward tilt. Amongst other independent variables considered, this surge motion and tilt rate was manipulated. Peak acceleration ranged from 0 to 1.5m/s^2.

The main conclusion reached was the most believable simulation occurred when the visual acceleration was combined with a corresponding backward tilt of the platform that changed the observer's gravitational vector consistently with the acceleration. Most importantly, this was observed even when the platform tilt rate was above the vestibular threshold. However, this important finding needs to be mitigated with the limitations of the study: falling into the same pitfall as Fischer & Werneke (2008), Berger et al (2010) rated believability on a continuous scale of 256 separate steps. It is doubtful that a human observer can maintain a consistent and accurate rating in a linear fashion on such a scale. Although the authors did report significant individual differences in perception, they failed to perform any test of within-participant rating consistency when presented with matching visual and tilt conditions. Strong

consistency would have provided a more solid case to justify their assumption of a linear believability scale.

Given the task was to rate believability based on the consistency of the motion cue and the visual stimulus, the authors were “surprised” to observe that ratings were significantly correlated with acceleration, such that higher accelerations were rated as more believable than lower ones. Although they did acknowledge that the higher accelerations were more likely to induce a more compelling feeling of self-motion, it does raise the question about whether the participants were fully able to rate the quality rather than the quantity of the motion. Such difficulties would therefore lead towards a better rating of the super-threshold conditions due to their immensity rather than their accuracy. That individuals were passive observers rather than actively participating in an interactive simulation is likely to have confounded the results still further by masking the effects of the actual controllability of the higher tilt rate conditions. However, all of this said, the study did, at least, once again raise a question mark over the need to limit tilt rate in the simulation of motion.

2.3. Assessment of motion cueing fidelity

Even if happy in the selection of the classical MDA as the most appropriate motion filter, the simulation engineer is still faced with the daunting task of selecting the ideal set of parameters to “tune” the motion system to achieve the highest level of fidelity for the driving task in question. The previous section has touched on a number of recent studies that have employed varying methods to assess motion fidelity, in particular addressing the thorny issue of how best to optimise the perception of low frequency acceleration cues through tilt coordination. However, such attempts are not new and, for the most part, the literature is broadly populated with studies that have investigated the perceived quality of motion either through an objective or subjective methodology. Each method has its own pros and cons.

When employing a subjective methodology (e.g. Bürki-Cohen, Sparko & Go, 2007), the simulator engineer will setup the simulation to achieve a specific task – Bürki-Cohen et al. (2007) selecting manoeuvres commonly assessed in the type-rating of a pilot on a specific aircraft, such as flight preparation, take-offs, flight manoeuvres, missed approaches and landings. For each, the performance of simulation is assessed by the comments of an expert, in this case a test pilot highly familiar with operation and performance characteristics of the specific aircraft. Based on the comments of the test-pilot, the simulator engineer will then tune the operation of the simulator by adjusting the parameter set available in the MDA until an acceptable rating is achieved. A subjective method is simple to administer and also benefits from the human observer being the ultimate judge of simulation accuracy. What better way can there be to assess whether the human observer can be deceived to perceive self-motion than by addressing that question to the observer? However, the technique is fraught with the difficulties of human individual differences – one test pilot may perceive good motion that which another may not necessarily concur. Furthermore, following on from the criticism of Berger et al.'s (2010) study, ratings of perception may not be consistent within individuals even when the same visual and motion conditions are presented.

The converse to subjective assessment is objective assessment. Here, an off-line assessment of cueing fidelity is made, based on known models of human perception and task performance (e.g. Padfield & White, 2005). Whilst a more robust and repeatable methodology, it is only as reliable as the model of the human operator, models which tend to be both complex and difficult to prove over the full range of tasks that may be required of the simulator.

2.3.1. Objective assessment

2.3.1.1. Models of human perception and behaviour

The first stage of an appropriate objective assessment is the development of the perceptual model. Such work builds on the Rasumussen's (1983) well-accepted model characterising human performance (Figure 2-14). The highest

level is knowledge-based behaviour, where the goal has to be “explicitly formulated” based on an analysis of the nature of the problem and the overall aim. Essentially, the human relies on the development of a mental model of a number of potential strategies and the subsequent selection of the most appropriate action based on knowledge of the situation. Examples of knowledge-based behaviours are problem solving and fault diagnosis which may not have been specifically trained for.

The next level of complexity is rule-based behaviour controlled by the middle level of the processing hierarchy. It is characterised as consisting of “a sequence of subroutines in a familiar work situation”, where task execution relies on previously stored rules or procedures. Rule-based behaviours depend primarily on feedforward control, for example, the requirement to stop at a red traffic light.

Rasmussen (1983) describes the simplest form of behaviour as skill-based. It is controlled from the lowest level of the cognitive processing hierarchy, and may be characterised as “smooth, automated and highly integrated” taking place “without conscious attention or control”. To extend the driving analogy, skill-based behaviours include the ability to actually operate the vehicle through the use of its driver controls.

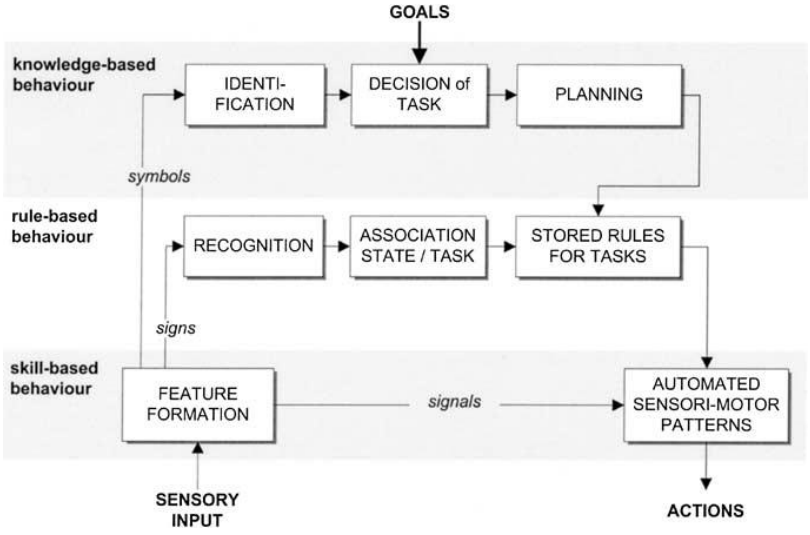

Figure 2-14: Rasmussen's (1983) model of human behaviour

It is at the skill-based level that the impact of simulator fidelity can be most easily felt: the requirement to re-create visual and vestibular cues for operators to effectively control the simulator in the same way as they would the real vehicle. To maintain such control, the operator must be able to manipulate

information in the virtual environment as they would in reality. There is a need to transmit information from the simulation to instruct the operator on what needs to be done – feedforward information. An example is an accurate representation of the red light informing the simulator driver to stop. Subsequently, feedback information provides the operator with information about how things are progressing: in our example, a managed application of the brake in order to regulate an appropriate stopping point. Rasmussen's (1983) model is predominantly feedforward, sensory inputs dictating subsequent actions. Hence to objectively assess the appropriateness of perception within the simulator, additional focus needed to be committed towards the feedback element describing the actual control of the vehicle to accurately achieve the skill-based behaviour based on a perception of its behaviour within the virtual environment.

Lee & Bussolari (1989) applied linear optimal control in an attempt to design a MDA that minimised a cost function that included the sensed motion error as predicted by a model of the vestibular system (Young, 1969). This rudimentary model was further developed by Hess & Malsbury (1991), but when this model was analysed by Schroeder (1999), whilst it did predict general trends of changes in helicopter pilot behaviour as adjustments were made to the parameters of the MDA, it did not do so with sufficient accuracy to fully justify its value as an off-line tuning method.

Hosman & Stassen (1999) made use of experimental observations to establish which sensory inputs a human operator exploits in closed-loop feedback control (Wickens & Flach, 1988). The model suggests that central visual (foveal), peripheral visual and vestibular feedback all play a vital role in the successful completion of both tracking (target following) and disturbance tasks (Figure 2-16). In both, the human operator attempts

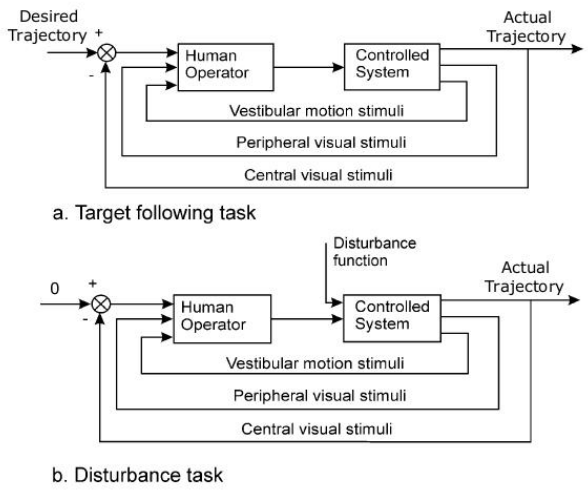

Figure 2-15: closed-loop visual/vestibular control feedback loop (Hosman & Stassen, 1999)

to nullify the perceived error. Hosman & Stassen (1999) went on to use their model to optimise motion platform washout filters by basing their modification on pilots' visual-vestibular perception and corresponding control of aircraft motion. The same technique was also successfully employed by Advani, Hosman & Haeck (2002) in the development of the motion cueing algorithm for a simulation of the Wright Flyer: a development to celebrate the centenary of the Wilbur and Orville's pioneering heavier-than-air flight and to demonstrate the immense difficulties in controlling an aircraft exhibiting such unstable flight characteristics.

In the driving example, the tracking task (Figure 2-16a) describes required maintenance of the vehicle's operation both longitudinally and laterally. A driver may wish to maintain what is perceived as a safe speed: here, by accelerating or braking the error between the desired and actual speed is minimised. Similarly, car following behaviour can be described: the error being the difference between the desired and actual headway. Finally, lane keeping is a tracking task where the driver inputs control to the steering to minimise the error between desired and actual lane position. In the manually controlled tracking task, only the central visual system is used to detect the error, whereas the peripheral visual and vestibular systems are used to detect the response of the vehicle in the driver's attempt to minimise the error.

In the case of a manually controlled disturbance task (Figure 2-16b), the input signal is zero. In the driving example, this may be a case where the vehicle is in a controlled state of operation (e.g. cruise) and is acted on by an outside disturbance, such as a wind gust, tyre blowout or other vehicle subsystem failure. In this case, both the vestibular and the visual system play a role in detecting the disturbance as well as the response of the vehicle in the driver's attempt to correct.

The promise of human perceptual models is great and efforts are on-going to further refine their accuracy, for example by the inclusion of proprioceptive perceptual models accounting for the effects of task interference, degraded

motion and visual cues, vehicle modelling errors, differing levels of pilot control aggressiveness and pilot skill level (Hess & Marchesi, 2009). However, as yet limitations in the models mean that they cannot always fully predict the effect of either motion scaling or parameter selection on operator performance a-priori. Given that answers to these questions are ones at the heart of the simulation engineer, subjective, human-in-the-loop investigations can often provide the most reliable method to assess motion cueing fidelity.

2.3.1.2. Analysis of frequency response

By describing the perception of the operator as a transfer function, descriptive perception models clearly have the potential to describe the effect of modifications to the MDA's filter parameter settings on predicted operator performance. The filter parameters settings have their own dynamic characteristics and such characteristics may be accompanied by potential negative effects, for example by a large phase lag, particularly around the natural frequency of critical operator/vehicle operation, around 0.2-0.8Hz for airline pilots (McRuer & Jex, 1967). An alternative to the introduction of a perception model is a more straightforward off-line assessment of the cueing algorithm in the frequency domain alone. This was touched on in section 2.2.2.2, but deserves a fuller discussion here.

Figure 2-17 shows a Bode plot describing the transfer function of a second-order complementary filter, the filter on which the classical MDA is based. The red dashed line shows the typical frequency response of the high-pass filter (onset), in this specific case with a cut-off frequency of 0.5Hz. The upper plot essentially describes the magnitude of the output compared to the input, showing the system's magnitude gain in dB (the gain in dB is 20 x log{amplitude gain} where the amplitude gain is the ratio of the amplitudes of the output and input signals). The high-pass filter passes high-frequency signals, but as frequency decreases it starts to attenuate the signal. By the cut-off frequency, the signal has been attenuated by half (3dB). The lower plot shows the phase-lead of the output signal compared to the input. As the frequency decreases, the phase lead increases until it reaches 90° at the filter's cut-off frequency.

The green dashed line shows the typical frequency response of the low-pass filter (tilt coordination), here with a cut-off frequency of 1.0Hz. Low-frequency signals are passed without any reduction in amplitude, but as frequency increases the filter starts to attenuate the signal. By the cut-off frequency, the signal has been attenuated by half (3dB). As the frequency increases, the phase lag increases until it reaches 90° at the filter's cut-off frequency.

The black solid line shows the combination of the high-pass and low-pass filters: the complementary filter. When the frequency of the input is low, the low-pass filter dominates, the high-pass filter attenuating the input significantly. The output closely matches the input in terms of both magnitude and phase. Conversely, when the frequency of the input is high, the high-pass filter dominates, the low-pass filter attenuating the input significantly. Again, the magnitude gain is close to unity and the input and output signals are in phase. When the frequency resides between these two extremes, the combined performance of both filters results in an output that does not totally match the input in either magnitude or phase. In terms of magnitude, the worst performance of this complementary filter occurs with an input signal of around 0.6Hz. Here the magnitude gain is as low as -20dB, i.e. the amplitude of the output is only 10% of the input. In terms of the signals being most out of phase with one another, this occurs at 0.5Hz, where the lag is around 60° (or 333ms at this frequency). However, the range of frequencies providing poor performance (say 0.3Hz-1.1Hz) is limited in comparison to the wide range of frequencies where filter performance is better. Unfortunately, however, in terms of flight simulation, this band tends to include the natural frequency of critical pilot/aircraft interaction operation suggested by McRuer & Jex (1967).

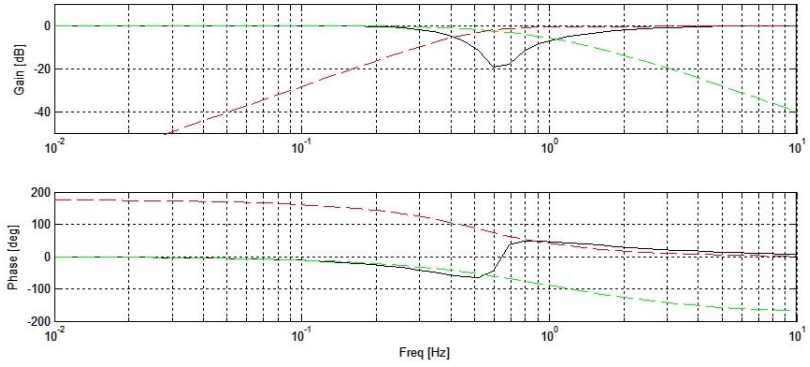

Figure 2-17: Bode plot describing frequency response of a typical complementary filter

In terms of the response of the classical MDA to linear acceleration, perception of acceleration is based on the magnitude gain of the signal at a particular frequency. The controllability of the simulation is dictated by the minimisation of any phase lag or lead. Ideally, the transfer function would be flattened in both magnitude gain and phase. However, attempting to achieve this by decreasing the high-pass onset filter cut-off frequency results in huge displacements of the motion system, way beyond the capabilities of a standard hexapod. Alternatively, flattening by increasing the low-pass tilt-coordination filter results in rapid tilting, way beyond perceptual thresholds. And so the simulation engineer is left with the customary dilemma at this critical frequency: whether to accept motion cues that are distorted in both magnitude gain or phase, or to artificially reduce the input with a scale-factor resulting in a more accurate, but significantly attenuated, simulation of motion. Nevertheless, by keeping the frequency response as flat as possible through rapid tilting, an invaluable assessment of MDA performance is provided and forms best practice in the off-line, coarse tuning of a flight simulator motion system (Reid & Nahon, 1986b).

2.3.1.3. Analysis at critical frequency

Whilst not yet proven in the driving domain, MDA performance at critical frequencies eliciting most appropriate pilot response has long been employed in flight simulators based on experimental evidence. Many studies have concentrated on the rotational behaviour of the aircraft and how the corresponding high-pass rotational filter of the classical MDA should be optimised (e.g. Jex, Magdaleno & Junker, 1978; Shirachi & Shirley, 1981). However, a car does not roll, pitch or yaw like an aircraft during its manoeuvring. In a driving simulator, roll and pitch are used to simulate sustained linear acceleration, rather than to resemble the rotational motion of the aircraft. Hence, it is the studies that have examined translational motion that more closely resemble the driving condition.

The effects of vertical motion on the ability of helicopter pilots to achieve a tracking and disturbance rejection task, one where the impact of the disturbance

has to be minimised, was studied by Bray (1985) in the world's biggest flight simulator, the large amplitude Vertical Motion Simulator at NASA Ames Research Center. Having manipulated high-pass filter cut-off frequency, Bray (1985) suggested that the phase-fidelity should be accurate down to 1.0-1.5 rad/s (0.16-0.24Hz). Fidelity was somewhat arbitrarily defined as the simulation motion cue having a phase error of less than 20° relative to the helicopter's vehicle dynamics model.

Based on evidence that the semi-circular canals have the highest magnitude gain around a frequency of 1 rad/s (0.16Hz) and therefore are most sensitive to perceived acceleration (van Egmond, Groen & Jongkees, 1949), Sinacori (1977) postulated from "intuition" that this should be the critical frequency when assessing the performance of the MDA in relation to motion fidelity. Based on limited evidence observed in a similar helicopter study, Sinacori's postulated validation criteria for both specific force and angular rate are shown in Figure 2-18. The x-axis "gain" is the scale-factor used in relating the desired acceleration output of the motion system to the actual input acceleration from the helicopter's dynamic model. The y-axis "phase distortion" is the phase difference between the input and output. Sinacorri's criteria show three levels of motion fidelity: high, medium, and low with definitions given at the bottom of Figure 2-18. As expected, high motion fidelity is associated with high scale-factor and low phase distortion, and low motion fidelity is associated with low scale-factor and high phase distortion. Schroeder et al. (2000) later comprehensively validated Sinacori's criteria.

Whilst certainly valuable to the driving simulation engineer, Schroeder et al.'s (2000) validation only provides half the answer. Its coarse indication of fidelity is only applicable to a very simple MDA consisting of a second-order filter with its output in motion platform translation. There is no published evidence to suggest that a similar critical frequency analysis additionally exists for the tilt-coordination filter associated with the classical MDA. Further, the addition of the tilt-coordination filter significantly changes the MDA's frequency response from the translation-only filter used to define the Sinacori/Schroeder fidelity

boundaries. Hence, whilst a critical frequency response can be employed to suggest the validity of the onset filter of the classical algorithm, whether to tune tilt-coordination similarly remains a matter of speculation.

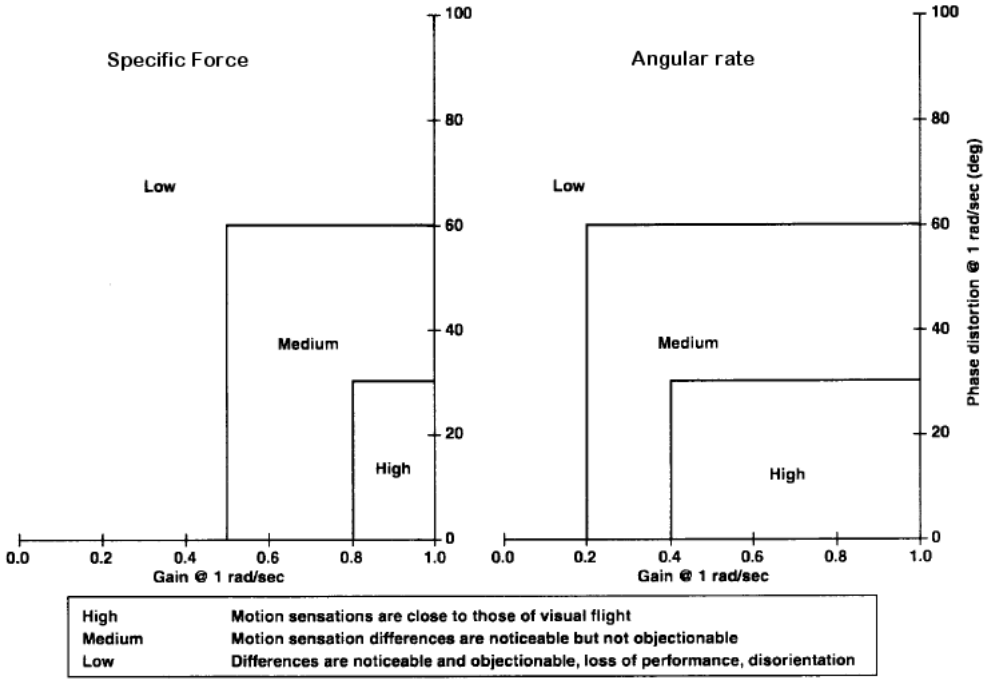

Figure 2-18: Sinacori/Schroeder motion fidelity criterion (from Schroeder, 1999)

2.3.2. Subjective assessment

Section 2.3.1 outlines some of the noble attempts to predict the validity of motion cueing in the domain of flight simulation, approaches that have not yet been applied to driving simulation. Given that a human observer exists in both, it is reasonable to expect a strong transfer for the results from one domain to the other. However, these off-line methods have substantial inadequacies. Hence, whilst limited to the specific control task demanded of the pilot or driver, human-in-the-loop investigation often becomes the most straightforward and consistent method to assess the fidelity of the simulation of motion.

Several studies investigating pilot performance and/or preference in flight simulators have already been introduced when describing the effects of the onset and tilt coordination filters of the classical algorithm (e.g. Reid & Nahon, 1988; Groen et al., 2001). Recently, as the development of driving simulators

has progressed, additional subjective assessments of motion fidelity have started to emerge in this domain. Reymond & Kemeny (2000) presented the development of the first motion driving simulator developed at Renault's Research and Development Turbocentre. The simulator cab was mounted on a small hexapod allowing some motion, but the projection system was fixed to the lab floor. Although a dynamic point-of-view compensation was performed by the image generator software module in order to maintain stable visual references relative to the cab during platform movements, the ability of the motion platform to sustain linear accelerations through tilt co-ordination was limited. Nevertheless, the benefits of even small amplitude motion was suggested through a non-linear modification to the classical MDA that minimised the "sag" typically observed with step changes in desired acceleration. However, no statistical evidence was offered to support the case for the non-linear filter. Anecdotal evidence from "several professional test drivers" who assessed the non-linear filter against the classical filter "deemed it superior".

One year later, Reymond, Kemeny, Droulez & Berthoz (2001) did offer some statistical evidence when comparing drivers' cornering behaviour with and without motion cues in comparison to that observed on a test-track in an instrumented vehicle. Participants were tasked in both environments with negotiating a range of curves in both their "normal" and "fast" driving styles. The inclusion of even the limited motion cues available had a significant effect in lowering the maximum lateral acceleration achieved in "normal" driving. The reduction was even greater in the "fast" driving style. The authors interpreted the addition of motion cues as directly responsible for this closer resemblance of curve negotiation to reality through the reduction in steering variability. However, the study is limited as it only compares motion with no motion. They made no attempt to quantify the quality of the motion with the validity of the simulation nor any attempt to optimise this motion in any way. Furthermore, only seven drivers participated in the study, leaving a sizeable question-mark over the statistical power of the study.

The most significant and robust subjective assessment of the classical MDA in driving was the previously reported paired comparison, lane-change study of Grant et al. (2009). The main aim of the study was to investigate an alternative algorithm, designed around the lane-change task. However, by maintaining a constant scale-factor of 0.5 and consistently rate-limiting the output of the tilt-coordination filter throughout, the study thoroughly compared a combination of complementary classical filters by modifications to the high-pass and low-pass cut-off frequencies only. It has already been noted that results indicated both a preference for and improved driving performance with a filter that reduced roll rate error at the expense of specific force error. However, since it was not relevant to the lane change task under scrutiny, the various parameter sets did not differ significantly in tilt performance in the simulation of sustained lateral acceleration, as had the emergency stop scenario employed by Fischer & Werneke (2008).

Flattening the classical MDA transfer function is possible through the application of scale-factors significantly reducing the output required of the motion platform. However, increasing the cut-off frequency of the low-pass filter and not constraining the resultant more rapid, super-threshold tilt, has the same effect. Both Fischer & Werneke (2008) and Berger et al. (2010) would suggest such a strategy. However, both their experimental designs required participants to maintain a consistent and repeatable judgement of motion perception that is both unrealistic and unreasonable. In the realm of driving simulation, a robust and broad subjective comparison of techniques to flatten the transfer function either by filter modification or by scale-factor does not yet exist.

2.4. Alternative algorithms for driving simulation

The fact that vehicle motions generally far exceed realistic motion system excursion limits drove Conrad et al.'s (1973) development of the classical MDA as a complementary filter. The authors' novel solution was the best available compromise, accepting the fact that simulation motion can only ever partially agree with reality. However, since this time, researchers have striven to adjust

and modify the classical algorithm in order to maximise this agreement. This has resulted in a number of alternative MDAs that have continually attempted to squeeze ever more realistic motion given consistently contradictory objectives: maximising the perception of acceleration with a device that has physical constraints and limited acceleration capabilities.

2.4.1. Adaptive algorithm

The adaptive algorithm of Parrish et al. (1975), modifying the time-invariant parameters of the classical algorithm to filter settings that are constantly adjusted to minimise a cost-function based on vehicle and simulator states, has already been introduced. In the context of driving simulation, the adaptive algorithm allows manoeuvres that require substantial motion cues, such as heavy braking, to be heavily filtered. On the other hand, more modest manoeuvres, such as a gentle lane change or speed management as a result of car following, are lightly filtered.

The cost-function of the adaptive algorithm has penalties on the required motion state, motion cueing errors and the distance of the adaptive parameters from their nominal values. Traditionally, the motion states are described in the Cartesian inertial frame, resulting in each of the six degrees-of-freedom being stated explicitly. However, the geometric design of the hexapod results in a strong coupling between degrees of freedom: maximum displacement in one degree of freedom implies a reduced capacity in the other five. Hence the description of the motion state and associated workspace becomes highly complex, where the availability of each degree of freedom becomes a function of the other five. These complications have resulted in the adaptive algorithm not being widely exploited in driving. Furthermore, it can be prone to instabilities and become under-damped for some large inputs (Nahon, Reid & Kirdeikis, 1992).

Grant & Nasri (2005) presented an alternative version of the adaptive algorithm, more appropriately designed for use in driving simulation. Whilst in

the Cartesian frame the hexapod is coupled, each of the six individual actuators are free to move to their own individual limit independently and hence are completely uncoupled. By limiting the cost-function on motion state in terms of actuator space rather the previously considered Cartesian space, Grant & Naseri (2005) were able to develop the Actuator State Based Algorithm (ASBA) which avoided actuator limits more successfully and demonstrated improved stability.

Colombet et al. (2008) compared the performance of the classical algorithm with the ASBA. Over a five minute driving period, participants were required to maintain a constant distance to a lead vehicle that was displaying a varying speed profile. The authors concluded that the effect of cueing algorithm design on drivers tracking performance was not significant, based on both subjective ratings and observed variations between lead and simulator vehicle speeds. They went on to suggest that the classical and adaptive algorithms generate equivalent acceleration perception. However, only seven drivers took part and no statistical analysis was presented to support the case. Furthermore, the simulator used was the Renault CARDS simulator, employing a motion system with limited actuator displacement. This would have resulted in a realisation of the adaptive algorithm that would not have differed overly in terms of actuator displacement from the implementation of the classical algorithm. Rather than the classical and adaptive algorithms generating equivalent *perception* of acceleration it is highly likely that, in this case, they actually generated the equivalent *acceleration*.

Nevertheless, the complexity, unstable characteristics and non-linear features of the adaptive algorithm have made its use extremely rare in driving simulators worldwide.

2.4.2. Optimal control algorithm

Optimal control deals with the problem of finding a control law for a given *system* such that a certain *optimality* criterion is achieved. Within the context of

flight simulation, it has become a natural extension of the adaptive algorithm. Given the underlying question of how best to provide motion cues in order to maximise the correspondence between pilot behaviour in the simulator and in reality, the system is the motion platform and the optimality criterion is the behavioural equivalence. Just as the adaptive algorithm continually adapts the parameters of the high-pass and low-pass filters of the MDA to minimise a cost-function, so does the optimal control algorithm. Both result in non-linear algorithms with the resultant draw-backs discussed in the previous section. However, as introduced in section 2.2.1, optimal control algorithms exist that minimise a cost-function based not only on motion state and motion cueing errors, but also taking into account a linear motion perception model (Sivan et al., 1982) and the acceptability of these errors to the pilot (Lee & Bussolari, 1989).

The optimal control algorithm is yet to be deployed in driving simulation, predominantly due to a lack of appropriate physiologically-sound human models of perception in driving. The development of such models is highly complex, and it is questionable as to whether this effort is justifiable given the significant disadvantage that tuning the weights of the cost-function remains highly subjective and time-consuming, even when simplified for real-time applications (Telban, Cardullo & Houck, 2002). Furthermore, in flight, the algorithm showed no significant improvement in pilot performance and only a small, and statistically untested, improvement in handling quality ratings (Guo, Cardullo, Telban, Houck & Kelly, 2003) when compared to the adaptive algorithm.

2.4.3. Predictive strategy

A novel solution to avoid the physical limits of the motion platform is to employ a MDA based on Model Predictive Control (MPC) strategy. Dagdelen, Reymond, Kemeny, Bordier & Maïzi (2009) first employed this technique in the Renault ULTIMATE Driving Simulator. By applying MPC, platform limitations are respected due to its capability of dealing with multivariable, constrained optimisation problems. In effect, the reference signals (input accelerations) are

predicted into the future and matched closely with a corresponding motion of the platform until it reaches its physical limits. False cues are avoided as much as possible by a smooth platform deceleration as the physical limits are reached.

Whilst certainly innovative, the application described by Dagdelen et al. (2009) acts only in translation. No tilt-coordination was attempted. Admittedly, the MPC algorithm is less likely to reach the physical limits of the system than a classical MDA acting only in translation, but even with the benefit of the large translation capabilities of the ULTIMATE, the accelerations can only still be felt by the driver for a very short duration. Nevertheless, the Renault test drivers polled did “prefer simulation strategies with the predictive strategy to the classical strategy”, but no statistical evidence supported the claim.

MPC strategy need not be limited in this manner. Leal-Loureiro (2009) used such a technique in the small hexapod of the Chalmers Driving Simulator, adding additional constraints of washout and a driver perception model. Results showed a proven benefit of MPC strategy over classical cueing for the driving tasks simulated. However, those tasks were limited predominantly to high frequency manoeuvres, ones which by their nature would bias preference.

Whilst promising, motion cueing techniques using MPC strategy are still in their infancy and need significant refining. The benefit that the technique currently offers over the much more widely understood classical MDA is questionable.

2.4.4. Lane position algorithm

The classical MDA splits the longitudinal and lateral specific forces in the frequency domain with high-pass and low-pass filtering. In contrast, the lane-position algorithm (LPA) splits the specific force into that based on the movement of the vehicle within its lane and that due to curve negotiation.

The LPA was initially developed for use in the first VTI driving simulator (Nordmark, Lidström & Palmkvist, 1984). It is best deployed in motion systems with a substantial capacity in translational displacement due to the fact that lane position is scaled before directly driving a lateral motion of the simulator. With prior knowledge of the width of the available carriageway and assuming that the driver remains within this lane boundary, the position of the motion system in sway can be matched directly to that of the driven vehicle. This unfiltered motion therefore results in a motion of the simulator almost identical to that of the driven vehicle providing highly correlated, if scaled, motion cues.

The main drawback of the LPA is that the lateral specific force due to roadway curvature still has to be reproduced through tilt-coordination. Hence, it suffers from the same shortcomings as the classical algorithm. Only if the driving task involves relatively high-frequency lane change manoeuvres on a straight or gently curving road, does the main benefit of the LPA come to the fore. Furthermore, there is no analogy of lane position in the longitudinal plane; hence the LPA can only handle lateral specific forces. Longitudinal specific forces must be managed by an alternative algorithm, typically the classical MDA.

2.4.5. Fast tilt-coordination algorithm

The difficulties in achieving accurate perceived acceleration in driving through tilt-coordination rate limited to perceptual thresholds have already been discussed. The fast tilt-coordination algorithm (FTC), initially employed at the DLR driving simulator, provides a novel, yet simple solution to the problem: ignore the perceptual thresholds (Fischer, Lorenz, Wildfeuer & Oeltze, 2008).

The FTC algorithm is essentially identical to the classical algorithm. By ignoring the perceptual thresholds of tilt and allowing a much faster development of tilt angle, the acceleration cue is handled almost entirely through the low-frequency tilt-coordination filter. In response to a step input of specific force, the inherent danger of this approach is that the early stages of

the cue are now significant to both the high-frequency onset *and* low-frequency filters in combination. Hence, the onset of the step becomes too large in relation to its eventual steady-state and the magnitude of the Bode plot becomes hard to flatten. The FTC algorithm alleviates this problem by allowing the high-pass filter to still characterise the lion's share of the onset cue. Only the remnant (the desired specific force minus that already achieved through the high-pass onset filter) is passed through the low-pass filter.

The FTC was evaluated both longitudinally and laterally by Fischer, Lorenz, Wildfeuer & Oeltze (2008) in comparison to the classical algorithm, both with a motion reference point located at the driver's head. A statistical analysis was undertaken on participants' subjective assessment of and on their driving task performance with both algorithms. The task was to proceed towards a roundabout intersection via a straight approach, negotiate ¾ of the roundabout before exiting right at the third available exit of the four-armed intersection. For the longitudinal task of braking from 50kph on the approach, no subjective preference could be shown for either algorithm. However, the lateral task of negotiating the roundabout did demonstrate a significant preference for the FTC. Task performance did not differ significantly with either algorithm.

2.4.6. Spherical washout algorithm

The arrival of DESDEMONA at TNO in 2006 provided a ground-breaking motion platform. The small simulator cab is suspended in a freely-rotating gimbal system allowing unlimited rotation in all three orthogonal axes. It can also move 2m vertically along a heave axis and 8m horizontally along a linear arm. The linear arm can spin around a central yaw axis to achieve sustained centripetal acceleration. Unique to DESDEMONA's capabilities is the ability to combine onset cueing (like a hexapod) with high-acceleration sustained accelerations, more akin to a dynamic flight simulation.

Whilst achievable, the application of the classical filter in DESDEMONA has a number of disadvantages:

- the available motion envelope would be unnecessarily limited.
- the benefits of using centripetal acceleration rather than tilt-coordination to simulate sustained specific forces would not be achieved.
- the classical algorithm is based on a Cartesian frame of reference whilst the inherent kinematics of DESDEMONA are Polar.

To make better use of the cylindrical motion envelope available, a dedicated algorithm was developed: the Spherical Washout Algorithm, SWA (Wetink, Bles, Hosman & Mayrhofer, 2005). Instead of directly high-pass filtering the longitudinal and lateral specific forces through a high-pass onset filter, they are first transformed to radial and tangential acceleration in the polar frame. Only the resulting commands of cabin radius, cabin yaw angle and the central yaw rate are subsequently high-pass filtered. The SWA significantly enlarges the motion space, since the simulator washes out towards a certain base radius and not towards a fixed neutral position, as is the case for the classical algorithm. In addition, sustained specific forces can be simulated using a combination of tilt and (predominantly) centripetal acceleration.

In driving, low speed curve negotiation typically results in yaw motion and lateral acceleration that are strongly coupled. Yet the geometrical design of the standard hexapod makes it difficult to achieve both simultaneously without the danger of actuators quickly reaching their limit of extension before the required acceleration cues are reached. Valente Pais, Wentink, van Paassen & Mulder, (2009) used just such a scenario to assess the SWA against its classical cousin. Both algorithms were implemented in DESDEMONA with the driving task being the negotiation of two differing-radius, 90°, left-hand turns separated by 150m-long straight segments. Subjective assessments were made for accelerating and braking between the curves as well as during both the curve entrance and exit. Regrettably, no differences in driving task performance were evaluated. The SWA was preferred to the classical algorithm for overall “ease of driving” and when leaving the curves. The effect size, however, was not substantial. Nevertheless, the authors did acknowledge that they would have expected a stronger effect had a more rigorous driving task been chosen.

2.5. Chapter summary

A common feature of both the classical MDA and its alternatives is that they employ some sort of scaling or filtering to allow a realistic rendering of vehicle motion within the physical constraints of the motion platform at hand. This filtering results in a set of parameters that can be tuned to minimise the error between the vehicle and simulator motion. This chapter has set out the development of the classical algorithm and some of its alternatives within the realms of its origin, flight simulation, and its subsequent applications with the domain of driving simulation. Several studies have been presented that demonstrate the benefit of one algorithm over another in the accurate modelling of motion, but each has focussed on a specific driving manoeuvre.

However, at the control level, typical driving manoeuvres vary wildly within both the time and frequency domains. Table 2-1shows figures derived from in-vehicle tests undertaken by Rover (Jackson, Crick, White & Shuttleworth, 1999) and Renault (Reymond & Kemeny, 2000). The tests were performed to assess the requirements and applicability of automotive simulation in the vehicle design process, particularly for ride and handling simulation. The Rover report concluded that, of the 19 manoeuvres typically performed during their handling tests, only five could not be performed to what they deemed an acceptable level of fidelity in a typical hexapod motion system: lift-off (engine braking), brake or accelerate mid-bend, chicane and slalom. It was suggested that a larger linear displacement would be necessary to execute torque steer acceleration from rest and high speed straight line braking, along with both single-lane and expansive lane change.

Such a broad range of predominant frequencies places a great burden on a particular cueing algorithm as it includes some of the most poorly represented frequencies (e.g. the hatched area of Figure 2-6). Let us put it another way, for example, in the lateral direction. The dominant characteristic of a long sweeping curve lies in the low frequency range (<0.1Hz) and therefore, for a hexapod, regardless of MDA, is handled predominantly by tilt-coordination. A rapid lane change or swerve around a hazardous object exists in a much higher frequency

range (>1Hz), better managed by more expansive onset cueing typified by the lane position algorithm (Nordmark et al., 1984). The typically lower dominant frequency range in braking compared to steering, hence its particular reliance on tilt-coordination, also demonstrates one of the reasons why its representation remains such a cardinal challenge in driving simulation (Boer, Kuge & Yamamura, 2001)

degree of freedom	acceleration limit	dominant frequency range	vehicle motion
longitudinal	-6m/s^2 to +4m/s^2	0 to 0.1Hz	accelerating, braking
lateral	-7m/s^2 to +7m/s^2	0 to 1Hz	cornering
vertical	-8m/s^2 to +11m/s^2	0 to 0.5Hz & 1 to 2Hz	suspension (road surface)
roll	±320°/s^2	>3Hz	suspension (cornering)
pitch	±360°/s^2	>3Hz	suspension (braking/accelerating)
yaw	±45°/s^2	0 to 4Hz	steering

Table 2-1: typical vehicle manoeuvres (from Jackson, Crick, White & Shuttleworth, 1999)

And therein lies the nub. Typical, run-of-the-mill driving is a much more challenging environment for motion cueing compared to commercial flight simulation. Longitudinally, acceleration or deceleration is not limited to a specific portion of the journey, i.e. take-off and landing. Laterally, turns are more frequent and are uncoordinated, with car occupants feeling a specific lateral force in every bend or swerve, unlike the changing of direction in a commercial airliner. Rotationally, suspension characteristics need to be handled over a broad range of frequencies. For specific individual driving manoeuvres, the perception of acceleration cues presented via the classical filter can be marginally superseded by alternative algorithms. However, it is its flexibility, simplicity and, above all, its elegance that makes it the most applicable to cope with the expansive and varied nature of driving. How best to optimise the classical algorithm for this diverse nature of driving tasks forms the basis of the presented range of studies, the experimental design of which are outlined in chapter 4. The next chapter introduces the University of Leeds Driving Simulator, the facility used throughout the experimental stage.

CHAPTER 3

THE UNIVERSITY OF LEEDS DRIVING SIMULATOR

The main apparatus used in this study was the University of Leeds Driving Simulator (UoLDS). Operational since early 2007, UoLDS is the second generation of driving simulators developed at the University.

Between 1994 and 2005, the original Leeds Advanced Driving Simulator (LADS) became an essential element in much of the driver behaviour and transport safety research work carried out at the University prior to its decommissioning in October 2005. The facility (Figure 3-1) was based on a complete Rover 216GTi with all of its basic controls and dashboard instrumentation still fully operational. On a 2.5 m radius, cylindrical screen in front of the driver, a real-time, fully textured and anti-aliased, 3-D graphical scene of the virtual world was projected. This scene was generated by a SGI Onyx^2 Infinite Reality^2 graphical workstation. The projection system consisted of five forward channels, the images edge-blended to provide a near seamless total horizontal field of view of 230°. A rear view (60°) was back projected onto a screen behind the car to provide an image seen through the vehicle's rear view mirror. Realistic sounds of engine and other noises were generated by a Roland sound sampler and two speakers mounted close to each forward road wheel. Although the simulator was fixed-base, feedback was given by steering torque at the steering wheel. Data were collected at 60 Hz and included information of the behaviour of the driver (i.e. driver controls), that

Figure 3-1: the original Leeds Advanced Driving Simulator

of the car (position, speed, accelerations, etc.) and other autonomous vehicles in the scene (e.g. identity, position and speed).

The re-development of the LADS, culminating in the construction of the UoLDS was made possible thanks to investment from HEFCE's Science Research Investment Fund, and took place throughout 2005 and most of 2006. The core software was maintained, but was re-written to exploit a PC-based network as opposed to LADS's increasingly antiquated SGI workstation. All other components of the LADS were completely replaced and the simulator relocated during the UoLDS development, culminating in the realisation of the simulator used in the present study (Figure 3-2).

Figure 3-2: the existing University of Leeds Driving Simulator

3.1. General characteristics

Currently, UoLDS's vehicle cab is based around a 2005 Jaguar S-type, with all of its driver controls fully operational. The vehicle's internal Control Area Network (CAN) is used to transmit driver control information between the Jaguar and one of the network of eight Linux-based PCs that manage the overall simulation (Figure 3-3). This '*cab control*' PC receives data via an on-board CAN card and transmits it over Ethernet to '*vehicle dynamics*', which runs the vehicle model, described in more detail in section 3.3. The vehicle model returns data via *cab control* to command feedback so that the driver seated in the cab feels (steering torque and brake pedal feel), sees (dashboard instrumentation) and hears (80W 4.1 sound system provides audio cues of engine, transmission and environmental noise) an appropriate simulation of the driving environment.

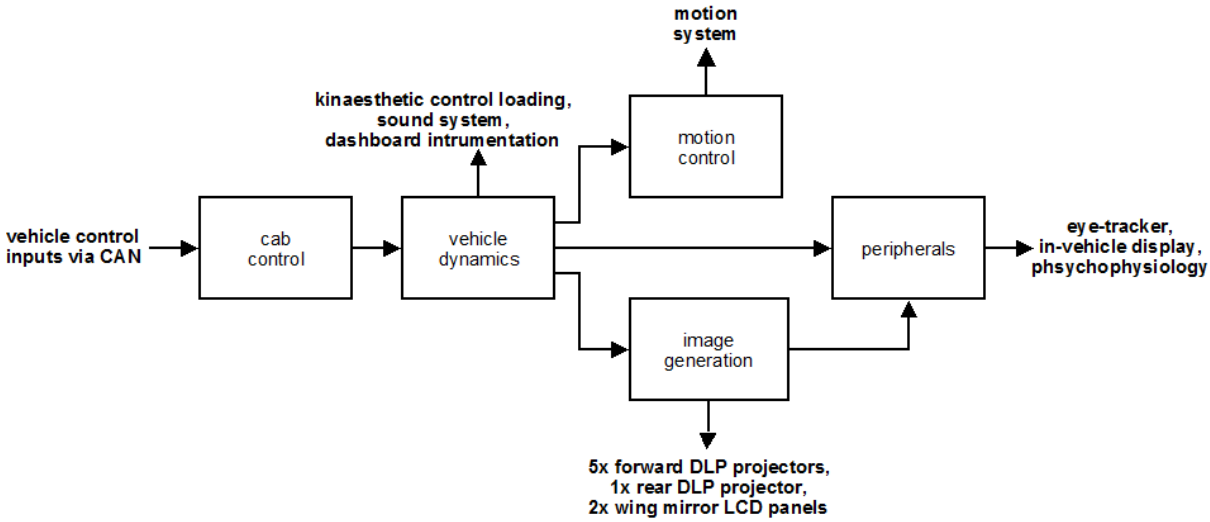

Figure 3-3: UoLDS PC network

The Jaguar is housed within a 4m diameter, composite, spherical projection dome. A real-time, fully textured 3-D graphical scene of the virtual world is presented over eight visual channels. Six of these channels are front projected onto the inner surface of the dome using six 3D-Percpetion HMR-15 DLP projectors. These channels are generated by three further dedicated *'image generation'* PCs on the local network, each housing a single nVidia FX4500G graphics card. Each PC is used to render two of the six projected channels at 60 frames per second and at a resolution of 1024x768. The PCs are frame-locked to avoid any "tearing" of the visual image and the composite image is corrected and colour balanced using the on-board electronics of the HMR-15s. The total horizontal field of view of the front projection system is 250°; the vertical field of view is 45°. The rear channel (40°) is viewed only through the vehicle's rear view mirror. The display resolution of all channels is 4.1 arcmin per pixel. Two further *image generation* PCs, each hosting a single nVidia FX3000 card are used to generate the two rearward displays seen in the vehicle's wing mirrors. Each physical mirror has been modified to house a 7" Lilliput wide-angled LCD panel, achieving a resolution of 800x480 pixels.

The simulator incorporates an eight degree-of-freedom motion system, described in more detail in section 3.4. A hexapod motion platform, carrying the 2.5t payload of the dome and vehicle cab combination allows limited motion in all six orthogonal degrees-of-freedom of the Cartesian inertial frame.

Additionally, the platform is mounted on a railed sled that allows a further 5m of effective travel in sway and surge. The performance of the motion system is controlled by an additional *'motion control'* PC running a version of real-time Linux. This ensures the timely arrival, over Ethernet, of the driven vehicle's calculated linear and rotational accelerations and velocities, transmitted from *vehicle dynamics*.

Additional peripheral PCs can be added to the network as required, for example to control in-vehicle tasks, allow the collection of driver psychphysiological data or to facilitate use of UoLDS's Seeing Machines faceLAB eye-tracker.

3.2. Dynamic characteristics

It is, of course, important to convey the general characteristics of the UoLDS to best comprehend the three-staged experimental plan detailed in the next chapter. However, most of the these characteristics, such as the vehicle cab / kinaesthetic control loading, the projection / image generation system and the sound system were not modified or manipulated in any way. It was only UoLDS's dynamic character that was the focus of this thesis: the performance of the simulator's vehicle dynamic model and, in particular, the subsequent behaviour of its motion system. Hence, this chapter focuses particularly on a detailed description on how these characteristics were developed specifically to support the experimental plan.

Accurate dynamic modelling is fundamental to a faithful representation of the driving experience. This modelling, leading in turn to an authentic dynamic performance of the motion system, is critical in the development of the perception of motion felt by the participants in the simulator during the experimental stages.

3.3. Vehicle dynamics

The vehicle dynamics is a software package developed to simulate the behaviour of a typical four-wheeled saloon car in response to the steering, brake, accelerator and transmission inputs of the driver. Originally developed to support LADS and its manual-transmission Rover 216 cab, it was substantially modified during the development of UoLDS to mimic the automatic-transmission Jaguar S-type. It produces, in real-time, the inputs required to drive the simulator's dashboard display, kinaesthetic control loading on the steering and foot brake, information regarding engine speed, load and rotational speed used by the sound system and the driver's eye point in the virtual environment utilised by the display system. Most importantly, however, it calculates the six linear and rotational accelerations and velocities used by the motion system. The accuracy of the vehicle dynamics, based predominantly on Segel (1956), Nordmark (1984) and Sayers & Han (1996), is vital to controllability and realism of the overall simulation. To describe the equations of motion, a vehicle-fixed set of body axes were defined according to the Society of Automotive Engineers convention (SAE, 2008) shown in Figure 3-4.

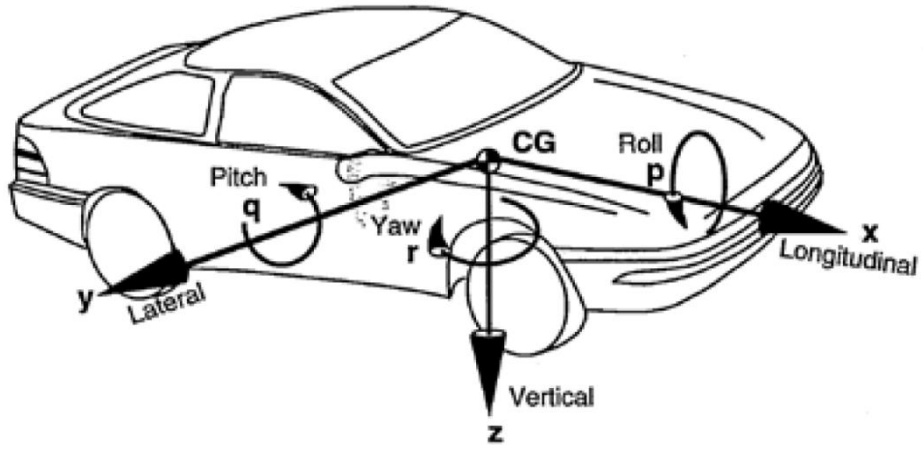

Figure 3-4: SAE J670 vehicle axis system

Equations of motion, based on Newtonian dynamics were developed for both a longitudinal and lateral model of the vehicle. Prior to real-time deployment in the overall simulator, the dynamics model was developed in MATLAB/Simulink. Figure 3-5 shows a high-level description of this model.

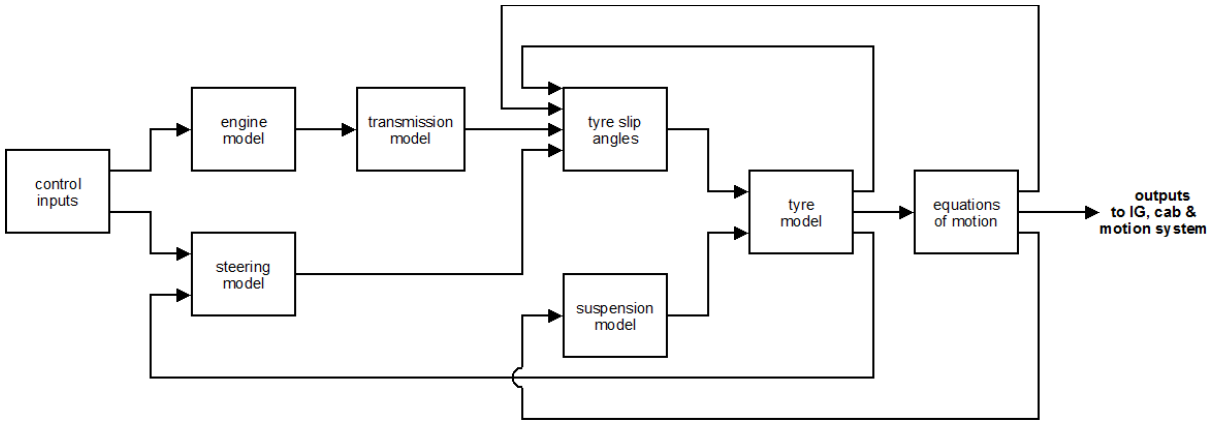

Figure 3-5: vehicle dynamics model

3.3.1. Longitudinal model

The longitudinal model describes the translational motion of the vehicle in the x and z axes along with rotational motion around the y axis in pitch. It characterises the behaviour of the vehicle in performance and ride.

3.3.1.1. Control inputs

Three longitudinal control inputs are available to the driver: accelerator position, brake pedal effort and the mode selection of the automatic transmission. These are measured at 240Hz and delivered to the vehicle dynamics model within the simulator's PC network by *cab control*.

3.3.1.2. Engine model

The Jaguar AJ25 that powers the S-type is a 201hp 2.5l V6 petrol engine. It is modelled using a quasi-static engine map supplied by Jaguar Land Rover. The engine map results in a look-up table that estimates engine torque resulting from a particular accelerator position input and engine speed. The torque curve can be seen in Figure 3-6. It is assumed that all of the torque developed by the engine is absorbed by the torque convertor of the transmission.

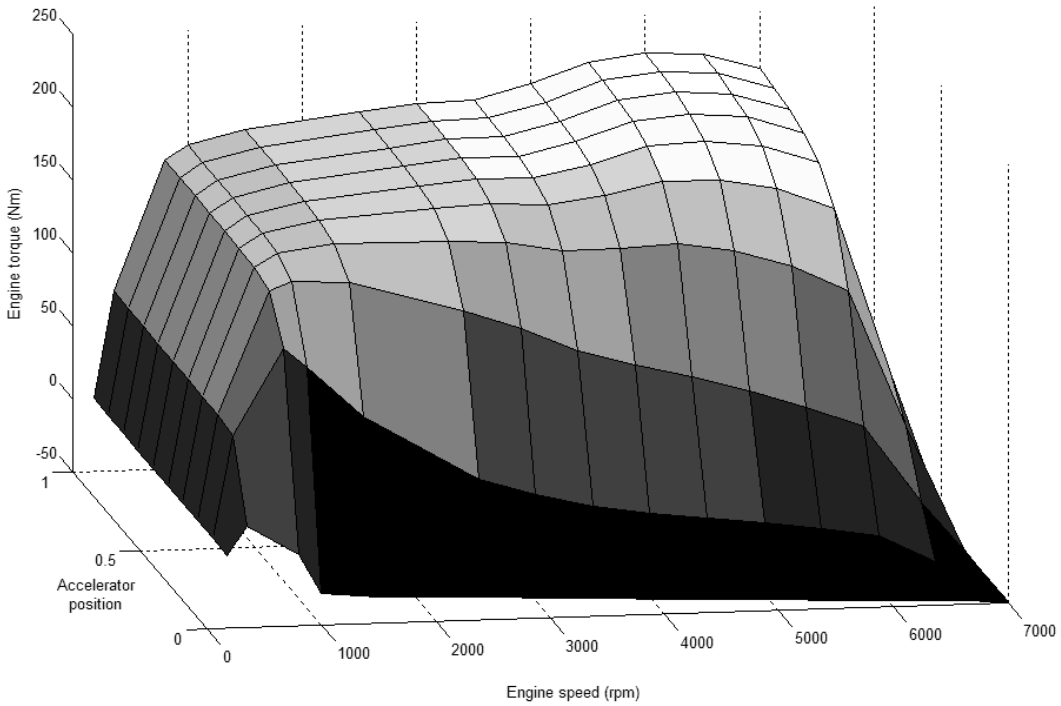

Figure 3-6: engine map for the Jaguar AJ25 2.5l V6 petrol engine

3.3.1.3. Transmission model

The transmission model consists of sub-models mimicking the behaviour of the torque converter, the gearbox and the differential. Its implementation within the simulator is based on Salaani & Heydinger (1998).

The torque converter takes the place of a mechanical clutch. It is a fluid coupling, hydraulically connecting the engine to the transmission through the impeller, stator and turbine. Each are modelled individually with the impeller receiving the torque from the engine model, the stator amplifying the torque input to the turbine at the expense of speed and the turbine torque acting as the torque input to the gearbox. No power losses in the fluid coupling of the torque converter are modelled.

The gearbox also magnifies the torque delivered to the differential at the expense of speed, this reduction in speed proportional to the gear selected. Gear shifting logic, supplied by Jaguar Land Rover employs a look-up table to select a driving gear based on accelerator position, current gear selection,

engine speed. The gear ratios of the Jaguar's five forward gears were also supplied. Finally, using parameters taken from both Jaguar Land Rover and from Salaani & Heydinger (1998), the tractive torque delivered to each of the front wheels is estimated by further increases through the differential and final drive.

3.3.1.4. Longitudinal slip

In order to calculate longitudinal slip angle for each of the four tyres within the longitudinal vehicle model, it is important to develop the forces and moments acting at each wheel to develop the torque balance. Figure 3-7 shows the free-body diagram for each wheel.

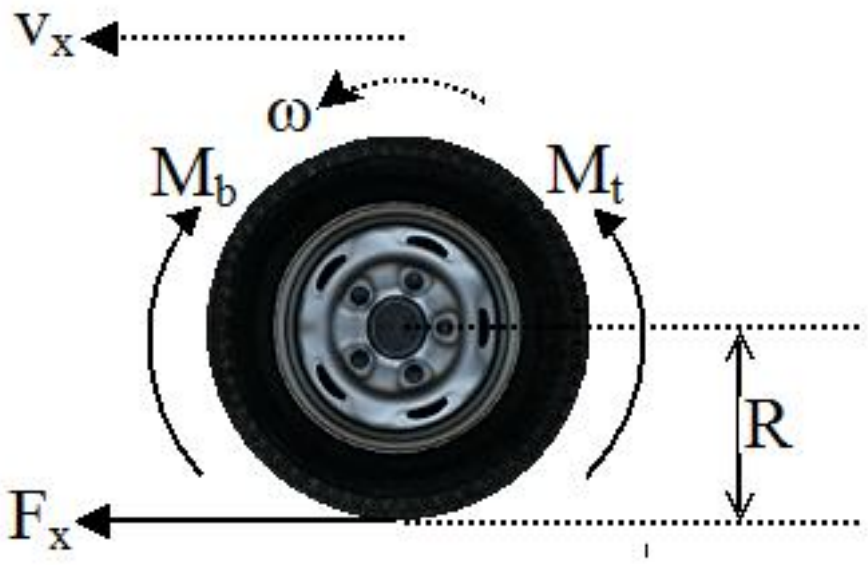

Figure 3-7: free body diagram of the moments acting at each wheel

The wheel is moving from right to left with a longitudinal velocity of the vehicle of v_x. The tractive torque acting at the wheel from the transmission model is given by M_t and the braking torque, estimated as a function of the brake pedal effort of the driver with the brake gain and balance of front to rear braking of the S-type supplied by Jaguar Land Rover. The longitudinal tyre force, developed from the later tyre model is denoted by F_x and the rolling radius of the wheel is given by R.

The angular velocity of the wheel, ω, is calculated from the differential equation describing the torque balance:

$$\dot{\omega} = \frac{M_t - M_b - F_x R}{I_w}$$

where I_w is the polar moment of inertia of the spinning wheel.

The longitudinal tyre slip (κ) required by the tyre model to calculate the longitudinal force acting at each wheel. It is normally defined as:

$$\kappa = \frac{\omega}{\omega_0}$$

where ω_0 is the zero-slip angular velocity of the wheel:

$$\omega_0 = \frac{v_x}{R}$$

However, since the longitudinal speed finds itself in the denominator of the longitudinal slip, its calculation at low or zero forward speeds of the vehicle leads to numerical instability. Hence, longitudinal slip was determined using a method developed by Bernard & Clover (1995), who derived a set of differential equations for longitudinal slip which are numerically well behaved, with some damping, at all speeds.

3.3.1.5. Longitudinal suspension model

During braking and acceleration, the load transfer of the sprung mass (the portion of the vehicle's total mass that is supported above the suspension) is the measurable change of load borne by front and rear wheels. In order to manage the vertical loads at each wheel (F_z), this load transfer is managed by the suspension system. The suspension model assumes a simple spring/damper system with values for the front and rear spring stiffnesses (K_f and K_r) along with the front and rear shock absorber damping ratios (C_f and C_r) taken from Jaguar Land Rover data.

Figure 3-8 shows the suspension model used in the longitudinal vehicle model that, given parameters such as centre of gravity height (h), cg to front wheel contact (L_f) and cg to rear wheel contact (L_r), allows the computation of

sprung mass pitch angle (θ) and the front and rear vertical tyre loads (F_{zf} and F_{zr}).

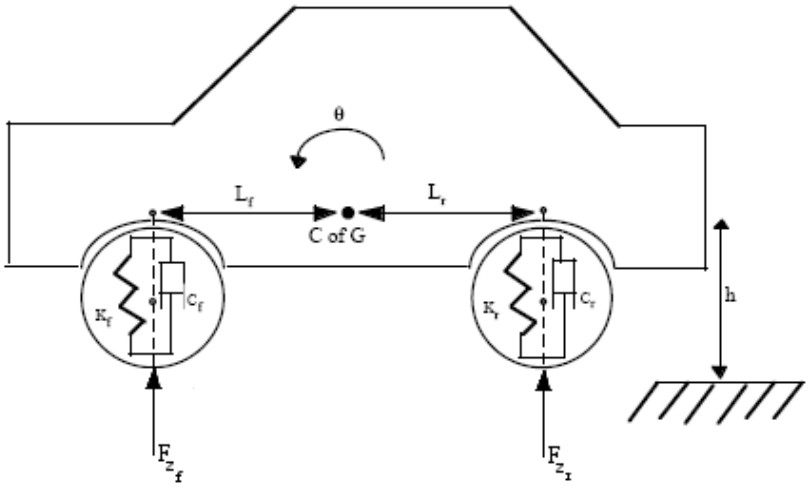

Figure 3-8: longitudinal suspension model

3.3.1.6. Longitudinal tyre model

The primary forces acting on the vehicle are developed at the four pneumatic tyre contact patches. Calculating these shear forces arising between the tyre and the ground is fundamental to the modelling of the stability, control and guidance of the vehicle. SAE J670 (SAE, 2008) also defines a tyre axis set representing the forces and moments acting on the tyre, shown in Figure 3-9. In the longitudinal plane, the tractive tyre force (F_x), the tyre vertical load (F_z) and the rolling resistance moment (M_y) are estimated.

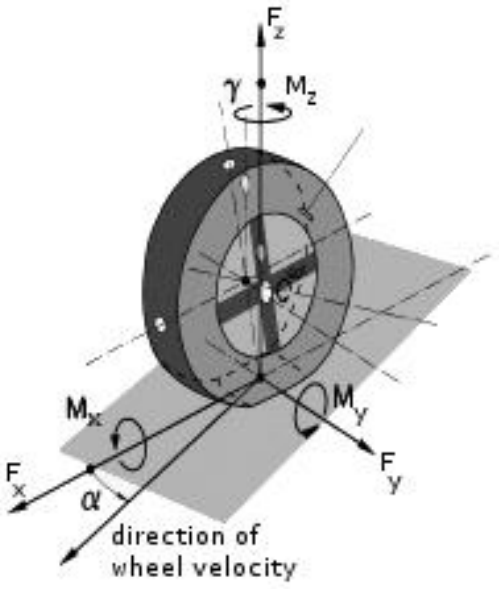

Figure 3-9: SAE J670 tyre axis system

The vehicle dynamics employs a version of the widely-employed Magic Formula tyre model (Pacejka & Besselink, 1997). The model is a parametric method that characterises each tyre using 120 parameters and 20 scaling factors, employing experimental data to best fit the model to the empirical evidence. As the recording of these coefficients is expensive and often confidential, obtaining the coefficients from tyre manufacturers is notoriously difficult. Hence the tyres are not specific to the S-type and are modelled on parameters and scaling factors for a generic saloon tyre presented in Pacejka (2005).

The results of the tyre model presenting the normalised longitudinal force (F_x/F_z) can been seen in Figure 3-10. The model requires knowledge of the tyre's longitudinal slip, its lateral slip angle (α, presented in section 3.3.2.3) and its vertical load (F_z) in order to estimate the longitudinal or tractive tyre force (F_x). For small levels of longitudinal slip, longitudinal force increases linearly with increasing slip. However, as the wheel starts to slip either due to excessive acceleration (positive slip) or lock-up due to disproportionate braking (negative slip), then the ability of the tyre to maintain force starts to diminish in a non-linear fashion upto full slipping. The addition of lateral slip from vehicle handling further reduces the tyre's ability to develop longitudinal force.

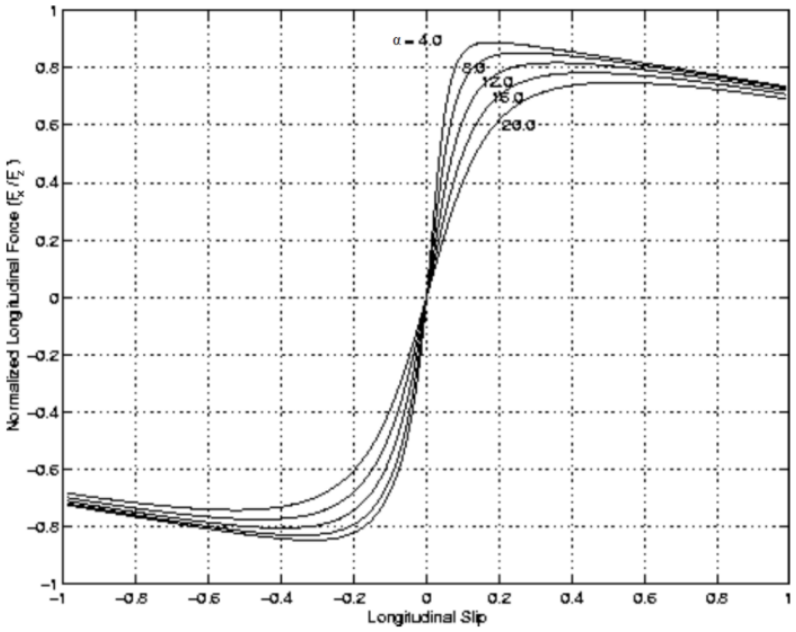

Figure 3-10: normalised longitudinal force as a function of longitudinal and lateral slip angle (from Pacejka, 2002)

3.3.1.7. Equations of motion

The equations of motion are based on Newtonian dynamic analysis, applied to both translational and rotational systems. The derivation of such equations can be found in a plethora of textbooks related to dynamic systems, such as Den Hartog (1961). In the longitudinal direction, the calculated tyre forces, along with other longitudinal forces such as the vehicle aerodynamic drag and tyre rolling resistance equations are summed. Newton's Second Law defines that the sum of these forces is equal to the product of its mass and acceleration in the longitudinal plane. A similar analysis in the vertical plane allows the heave of the vehicle to be calculated. This analysis results in a pair of ordinary differential equations which are solved using a fourth-order Runge-Kutta (RK4) numerical integration technique (e.g. see Forsythe, Malcolm & Moler, 1977).

In order to calculate the rotational pitch angle of the vehicles' sprung mass, Newton's Second Law of rotational dynamics is employed. The sum of moments acting around the vehicle's lateral y axis is equal to the product of the rotational moment of inertia of the sprung mass and the rotational pitch acceleration. The resultant differential equation is also solved using RK4 to evaluate body pitch.

A set of Direction Cosine Matrices, representing the quaternion of the vehicle's Euler rotations, translate the motion of the vehicle with respect to its SAE J670 body-fixed vehicle axis system to a set of earth-fixed planar axes, used by the visualisation system to display the position of the vehicle in the virtual environment (e.g. see Goldstein, 1980).

3.3.2. Lateral model

With reference to Figure 3-4, the lateral model of the vehicle is related to translational motion in the lateral y axis along with rotational motion around the x axis in roll and around the z axis in yaw. It characterises the behaviour of the vehicle in handling, stability and control.

3.3.2.1. Control inputs

The single lateral control input available to the driver is steering angle. As for the longitudinal control inputs, this is recorded at 240Hz and delivered to the vehicle dynamics model within the simulator's PC network by *cab control*.

3.3.2.2. Steering model

A rack-and-pinion steering system, along with the power steering assistance, was implemented in the simulator from an internal Jaguar Land Rover report (Burchill, 2003). Figure 3-11 shows a schematic of this model.

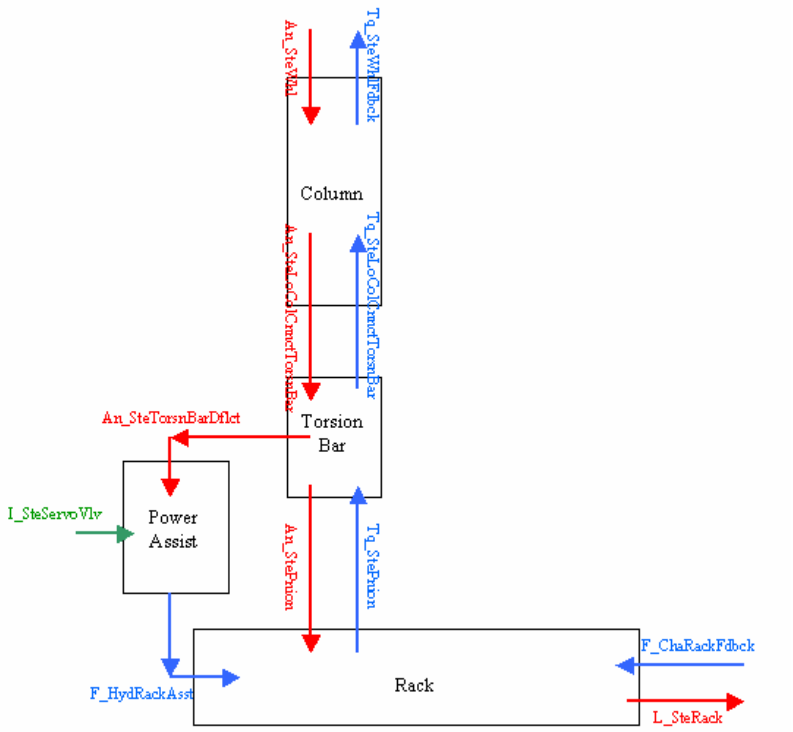

Figure 3-11: rack and pinion steering system with power assist (from Burchill, 2003)

The steering wheel angle held by the simulator driver (*An_SteWhl*) is used as the angular input to the top of the steering column. The column is modelled as a second order, spring-damper system whose output, the angle of lower column at the interface with the torsion bar (*An_SteLoColCnnctTorsnBar*), is fed into another second order spring-damper mimicking the torsion bar. The output from the torsion bar model is the steering pinion angle (*An_StePinion*) and the deflection of torsion bar (*An_SteTorsnBarDflct*). Using a look-up table describing the relationship between pinion position and gear ratio, the rack

travel (*L_SteRack*) and hence the steered angle of each front wheel is calculated.

In order to simulate steering feel, the steering model is also responsible for evaluating the torque feedback at the steering wheel (*Tq_SteWhlFdback*). This value is used to command the TRW-Conekt Active Steering Wheel System motor that is directly linked to the physical steering wheel in the simulator cab. The complete set of tyre forces and aligning moments resulting from the tyre model (see sections 3.3.1.6 and 3.3.2.5) are assembled as the force felt by the steering rack (*F_ChaRackFdck*) using a model developed by Salaani, Heydinger & Grygier (2002). The power steering model culminates in the assist force felt by the steering rack (*F_HydRackAssist*), counteracting the force on the rack from the chassis and hence reducing the steering torque felt by the driver.

3.3.2.3. Lateral slip

In vehicle handling, particularly at high speeds, the turning movement of the vehicle generates a lateral acceleration and hence a sideslip velocity. This sideslip deflects the tread of the tyre that is in contact with the ground and allows the tyre to develop a lateral force to counteract the lateral acceleration (Figure 3-12). Due to the elasticity of the tyre, the tread will distort developing the lateral slip angle (α), the angle between the tread in the contact patch and the direction the wheel is turned. An alternative definition, according to SAE J670, is the angle between the rolling tyre's direction of travel and the direction in which it is side-slipping, the direction of travel of the centre of the contact patch.

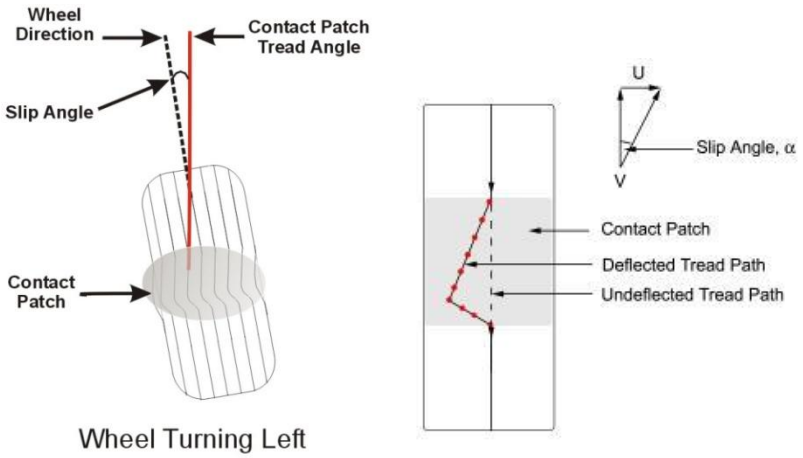

Figure 3-12: tyre lateral slip angle (from Gillespie, 1992)

3.3.2.4. Lateral suspension model

A change in lateral acceleration will cause a shift in load from the tyres on the inside of the turn to those on the outside. Load transfer can significantly reduce the vertical force on the inside tyres and hence their ability to develop a lateral force due to their respective slip angles. This can significantly affect handling in terms of under or over-steer.

Within the vehicle model, the lateral suspension model corresponds to the longitudinal suspension attempting to manage tyre vertical load (F_z). It is also modelled as a spring-damper system with identical spring stiffnesses and shock absorber damping ratios as in the longitudinal plane. With knowledge of the height of the roll centres of the front and rear suspension, provided for the S-type by Jaguar Land Rover data, along with F_z the suspension model results in the body roll angle (ϕ).

3.3.2.5. Lateral tyre model

The Magic Formula tyre model (Pacejka & Besselink, 1997) with the parameter set given in Pacejka (2005) is also used in the lateral plane. With reference to the SAE J670 tyre axis set (Figure 3-9), the lateral tyre model is predominantly responsible for calculation of each tyre's lateral or cornering force (F_y) and aligning moment (M_z), the moment arising from the tyre's natural tendency to self-straighten. In addition the less significant overturning moment (M_x) is also estimated.

The tyre's inclination angle (γ), modelled from Jaguar Land Rover data in the form of a look-up table related to suspension movement, also has an influence on the on the overall lateral tyre force and moments and is included within the Magic Formula model.

The results of the tyre model presenting the normalised lateral force (F_y/F_z) can been seen in Figure 3-13. The model uses the longitudinal slip (κ), the lateral tyre slip angle and the tyre vertical load (F_z) in order to estimate the

lateral force (F_y). The vast majority of vehicle handling results in small lateral slip angles, where the lateral force tend to increase linearly with increasing slip. The gradient of the model in this region defines the tyre's *cornering stiffness*. As vehicle handling becomes more extreme and lateral slip angle increases, the ability of the tyre to maintain cornering force becomes non-linear and gradually diminishes upto full slipping. The addition of longitudinal slip from braking and accelerating further reduces the tyre's ability to develop lateral force. This describes the perils of braking hard in a tight bend and the potential to lose control of a vehicle, especially one with a tendency to over-steer. As braking intensifies and a tyre's longitudinal slip increases, the cornering forces required from the tyres to counteract the vehicle's lateral acceleration become insufficient.

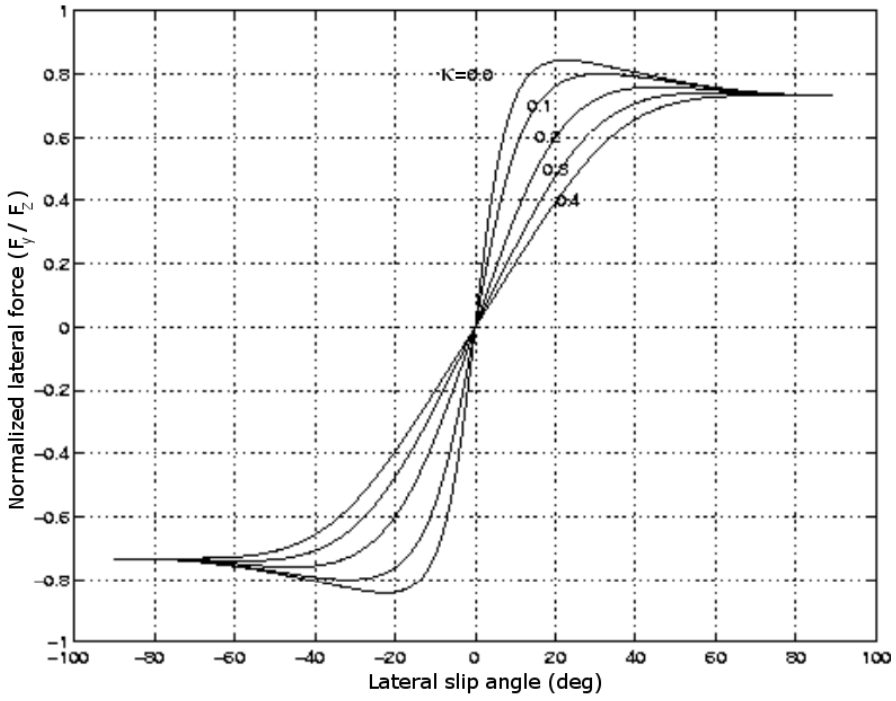

Figure 3-13: normalised lateral force as a function of longitudinal and lateral slip angle (from Pacejka, 2002)

3.3.2.6. Equations of motion

Just as in the longitudinal direction, the calculated tyre forces, along with other lateral forces such as those associated with road elevation are summed and Newton's Second Law applied to calculate the acceleration of the vehicle in

its lateral y axis. Similarly, the sum of the moments acting around the vehicle's longitudinal x axis are summed to calculate the rotational yaw (heading) angle of the complete vehicle and the roll angle of the sprung mass. A further set of Direction Cosine Matrices transform the motion of the vehicle with respect to its SAE J670 body-fixed vehicle axis system to the set of earth-fixed planar axes used by the visualisation system.

3.4. Motion system

The motion system was designed, manufactured and installed by Dutch company Rexroth Hydraudyne B.V. Systems & Engineering, a wholly owned subsidiary of the Bosch Group. The electrically-driven, synergistic EMotion-2500-8DOF-500-MK1-XY consists of a typical six degree-of-freedom (DoF) *hexapod* built upon a two DoF *XY-table*. Similar systems exist at several driving simulator facilities worldwide. Renault's ULTIMATE in Paris and PSA Peugeot-Citroen's SHERPA2 in Versailles are currently in operation. Three more are under development at the University of Stuttgart, Tongji University in Shanghai and VTI's new Simulator IV, currently under construction in Gothenburg.

3.4.1. Motion system dynamic characteristics

A schematic drawing and the dynamic characteristics of the motion system are shown in Figure 3-14. The performance of the system was undertaken with the fully installed payload during the final acceptance tests on the complete simulator system. The driver's seat was removed and a rigid framework installed to allow the fixing of three Crossbow CXL linear accelerometers and a single Columbia SR-100FR rotational accelerometer at the driver's head position. A Tektronix TDS3014B digital storage oscilloscope recorded the information from the accelerometers (Bosch Rexroth-Hydraudyne, 2006).

The bandwidth of the system describes its ability of the motion system to achieve a particular acceleration (output) compared to the desired input. The -3dB bandwidth is the frequency at which the magnitude of the output has

reduced to 70.8% (1/√2) of the input. The 90° phase lag bandwidth is the frequency at which the output lags the input by such an angle.

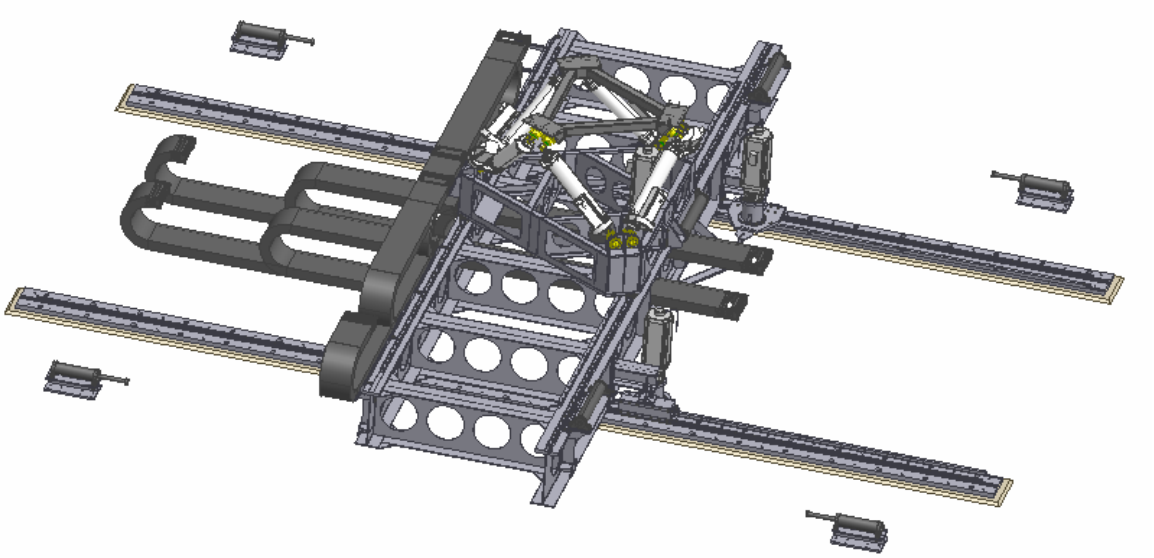

		excursion	velocity	acceleration	bandwidth (-3dB magnitude)	bandwidth (90° phase lag)
hexapod	*Surge*	-408 / +307 mm	±0.82 m/s	±6.6 m/s²	5.9 Hz	7.8 Hz
	Sway	-318 / +318 mm	±0.82 m/s	±6.9 m/s²	5.3 Hz	7.2 Hz
	Heave	-261 / +240 mm	±0.62 m/s	±6.2 m/s²	9.0 Hz	9.5 Hz
	Roll	±21°	±41.3 °/s	±321 °/ s²	7.8 Hz	5.7 Hz
	Pitch	-20° / +22°	±40.7 °/s	±310 °/s²	9.5 Hz	6.1 Hz
	Yaw	±23°	±53.3 °/s	±362 °/ s²	8.1 Hz	6.2 Hz
XY- table	*Surge*	+2610 / -2590 mm	±2.1 m/s	±5.1 m/s²	5.6 Hz	5.3 Hz
	Sway	±2500 mm	±3.1 m/s	±5.4 m/s²	5.2 Hz	7.1 Hz

Figure 3-14: dynamic characteristics of the eight degrees-of-freedom of the EMotion-2500-8DOF-500-MK1-XY motion system

The mass of the payload (2500kg), the hexapod (1500kg) y-sled (1000kg) and x-sled (5000kg) leads to a sizeable moving mass and subsequent inertia of the motion system. The frequency response of the system, particularly critical in XY-table surge given its significant inertia, indicates a minimum bandwidth over 5Hz. This suggests that the motion system can comfortably achieve input frequencies 3Hz and less with virtually no attenuation of the input signal (which would result in a lower than expected perceived acceleration) or phase lag (which would result in a delay in the expected perceived acceleration leading to controllability issues). This unfiltered dynamic range encapsulates the vast majority of typical driving tasks. Furthermore, it matches the maximum bandwidth of the vestibular system of upto 5Hz (Berthoz, 2000).

3.4.2. Implementation of the Classical Motion Drive Algorithm

The previous section has outlined the capability of the motion system alone to achieve the unfiltered dynamic range required in routine driving. However, in order to keep the movement of the motion system within its physical limits, the input signal (acceleration) is filtered in each degree-of-freedom through implementation of the Motion Drive Algorithm (MDA). It is the performance of this filter that adds significant signal attenuation and phase lag. Hence, in order to optimise the experience of driving the simulator in terms of the magnitude of the perceived acceleration along with the timeliness of its arrival, there is a requirement to tune the MDA to the specific driving tasks required of the simulator.

The classical MDA, as outlined in Chapter 2, is employed in the UoLDS and was manipulated in the three stages of experimental work presented in Chapter 4. The algorithm requires the timely arrival from the vehicle dynamics model of the following data with respect to the vehicle's SAE J670 body-fixed axis set and in the S.I. units stated:

- Three linear accelerations
  - $\mathbf{A_x}$ longitudinal (x axis – braking/accelerating, m/s^2)
  - $\mathbf{A_y}$ lateral (y axis – cornering. m/s^2)
  - $\mathbf{A_z}$ vertical (z axis – road roughness, m/s^2)
- Three rotational accelerations
  - $\dot{\mathbf{p}}$ roll (acceleration around the x axis – cornering, rad/s^2)
  - $\dot{\mathbf{q}}$ pitch (acceleration around the y axis – braking/accelerating, rad/s^2)
  - $\dot{\mathbf{r}}$ yaw (acceleration around the y axis – heading change, rad/s^2)
- Two rotational angles
  - $\boldsymbol{\phi}$ roll angle (rad)
  - $\boldsymbol{\theta}$ pitch angle (rad)

Yaw angle is not included in the Classical MDA since it involves no change to the gravitational vector of the driver, hence cannot be felt (as opposed to yaw

acceleration). The visual system alone is sufficient to indicate the heading of the vehicle.

The latency of the real-time connection between *dynamics* and *motion control* ensures that the arrival of this data is not significantly delayed. Testing of this connection during the commissioning of the simulator indicated the average time delay between the sending of dynamic data and its use by the MDA to be less than 0.5ms.

The full block diagram of the implementation of the classical MDA in the UoLDS can be found in Figure 3-15, controlling the movement of the hexapod in translation and rotation along with the XY-table in translation. The first stage of signal processing is the protection of the input accelerations. Input protection fulfils two main aims. First, it restricts the acceleration that the motion system will attempt to mimic with a soft-limiter, which smoothly restricts the input signal to an upper and lower limit by using an upper and lower breakpoint. Signals which rise above the upper breakpoint are asymptotically reduced so as never to exceed the upper limit. Correspondingly, those that fall below the lower breakpoint are constrained within the lower limit. Since the MDA has been tuned to a specific maximum acceleration in each degree of freedom, this feature is used to smoothly prevent the motion system from reaching its excursion limits from larger than expected manoeuvres.

The other aim of input protection is to prevent the motion system from attempting to simulate excessively high input frequencies. These may result from mathematical irregularities within the vehicle dynamic model providing the inputs or from errors within the model itself. In practice, once soft-limited, the input signal is passed through a low-pass filter with a cut-off frequency just beyond the normal dynamic operating range of the car model (20Hz was used for all six acceleration inputs).

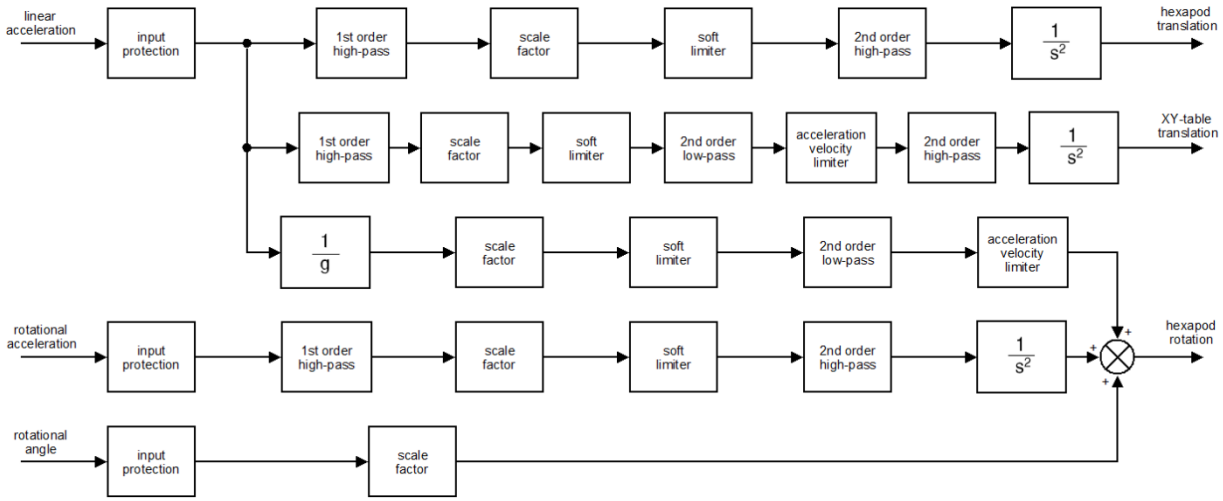

Figure 3-15: classical MDA implementation

3.4.2.1. Hexapod translation

Let us first consider the processing of the input signal (linear acceleration) resulting in a translational movement of the hexapod. For longitudinal vehicle motion, the inputs are A_x resulting in surge motion and A_z resulting in heave motion. For lateral vehicle motion, the input is A_y and produces sway motion.

First, the protected input signal is passed through a first-order high-pass filter: only its cut-off frequency can be manipulated. The filter removes the static component from the input signal and is primarily responsible for the initial translational onset cue. Reducing the cut-off frequency results in a more dynamic and longer lasting cue that, in turn, requires an increased excursion of the hexapod.

After high-pass filtering the input is scaled before it is limited using a soft-limiter with identical functionality as for input protection. Both of these blocks act, if necessary, to restrict the overall surge and sway.

Next, the signal is passed through a second-order high-pass filter: its cut-off frequency and damping ratio are available for modification. This filter smoothly controls the washout behaviour of the hexapod such that, after onset, it smoothly returns to its starting position. Reducing the cut-off frequency and

increasing the damping ratio result in a protracted washout. However, it is the congruent nature of the two high-pass filters that manage collectively the overall translational movement of the hexapod.

The final stage of the process is double integration of the scaled and filtered acceleration input, resulting in the actual position demand of the hexapod in translation.

3.4.2.2. XY-table translation

The XY-table allows additional capacity of the motion system in surge and sway, allowing increased translational movement than would be possible through the hexapod alone. Again, the input signal of A_x, A_y or A_z is first-order high-pass filtered before it is scaled and soft-limited. This stage is primarily responsible for the onset cue of the XY-table.

Washout behaviour of the XY-table is a little more complicated. The input signal is passed through a second-order low-pass filter where both the filter's cut-off frequency and damping ratio can be adjusted. The combination of this filter with the subsequent second-order high-pass filter results in a band-pass filter that is predominantly accountable for the washout. The filter parameters are selected such that the band-pass filter prevents input frequencies that are too low to permit effective hexapod translation but too high to be successfully achieved through tilt-coordination and its resultant hexapod rotation. Just as for hexapod translation, the combination of parameters in the high-pass and band-pass filters handle the overall translational movement of the XY-table. In a well-tuned system, the hexapod and XY-table combinatory filters need to be harmonious in the frequencies allowed through each.

The final stage of the process is double integration of the scaled and filtered acceleration input, resulting in the actual position demand of the XY-table in translation.

3.4.2.3. Hexapod rotation

Hexapod rotation results from three input sources, linear vehicle acceleration, rotational vehicle acceleration and rotational vehicle angle.

For linear vehicle accelerations, the inputs A_x and A_y result in a corresponding pitch and roll of the hexapod in order to achieve the low frequency component of the input signal through tilt-coordination. Clearly, a manipulation of the gravitational vector cannot achieve any low frequency component of A_z, hence this signal is not passed through the tilt-coordination filter. First the protected input signal is divided by g, the acceleration due to gravity, which results in the angle required of tilt-coordination (small angle approximation of the tangent). The desired angle is then scaled and soft-limited before passing through a second-order low-pass filter: both its cut-off frequency and damping ratio can be varied. Increasing the cut-off frequency results in the hexapod adopting the desired tilt angle more rapidly. The overshoot/undershoot of the tilt angle can be controlled through its damping. Finally, both the angular acceleration and velocity of the tilt is limited through a hard limiter. The limiter caps demanded tilt acceleration and velocity, the constraints normally being linked to perceptual thresholds.

The high-frequency components of vehicle roll, pitch and yaw acceleration also result in hexapod rotation. These rotational acceleration signals are processed in the same way as the linear accelerations, filtered through both a first-order high-pass primarily responsible for onset and a second-order high-pass filter largely influencing washout behaviour.

The final source of hexapod tilt is through a matching of the vehicle body (sprung mass) pitch and roll. These signals, once input-protected and scaled are passed directly to the hexapod.

All three channels demanding hexapod rotation act in combination. Hence, careful tuning of the system in tilt, using all the parameters available for modification in the classical MDA, is required to prevent each actuator's position

limit being reached. Furthermore, a hexapod by its nature suffers from a certain degree of cross-axis coupling: hexapod movement in one degree of freedom limits the amount of actuator stroke available to achieve motions in the other five degrees of freedom. Hence careful selection of the thresholds for each channel's soft-limiters or small modification to the filter's cut-off frequencies are required to ensure that false cues through actuator positioning limiting are not encountered.

3.5. Chapter summary

This chapter has described the general characteristics of the apparatus used in the three-staged experimental plan, the University of Leeds Driving Simulator. It has also illustrated, through a description of the vehicle dynamics model, how the driver's handling of the simulator results in the translational accelerations, rotational accelerations and rotational angles achieved by the motion system.

In general, the dynamic and interactive nature of driving simulation makes motion system tuning, through selection of the available parameters in the chosen MDA, a challenging assignment. However, within the three-staged experimental plan, the driving tasks and subsequent vehicle manoeuvres were precisely defined and choreographed. These resultant and recurring demands allowed a tuning of the motion system that could ensure a repeatable experience for participants across the range of motion cueing conditions examined. The specific driving tasks and corresponding dynamic performance of the simulator are outlined along with the experimental design in the following chapter.

CHAPTER 4

EXPERIMENTAL DESIGN

Chapter 2 argued the case for substantiating the classical Motion Drive Algorithm (MDA) as the most well-understood, flexible and elegant solution to cope with the expansive and varied nature of driving. This line of reasoning forms the main justification for its selection in the three-staged experimental design presented here. But like virtually all of the alternative motion filters outlined in section 2.4, it suffers from the difficulties associated with tilt-coordination. In tilt-coordination, the low-frequency, sustained specific force is achieved by a proportional tilt of the motion platform. However to remain sub-threshold the commanded motion platform tilt rate is low. Hence, after the high-frequency onset cue has subsided, there is a sag in the perceived specific force witnessed by the driver. Moreover, as the demanded specific force quickly disappears at the end of a particular driving manoeuvre, platform tilt lags behind resulting in a false cue. The consequence is the typical trade-off between specific force and tilt rate errors.

This trade-off is also heavily influenced by the duration, magnitude and timing of the complementary high-frequency onset cue, established by motion platform translation. First, there is the selection of the cut-off frequency of the first-order high-pass filter. A low value will sustain the onset cue for a longer duration and with reduced magnitude and phase errors, but demands significantly more excursion in translation. Scaling the specific force demand will limit this movement, hence, the second influence becomes the choice of this scale-factor. Thirdly, the available motion envelope can be increased with the extra translational capacity of an XY-table. Finally, washout behaviour, typified by the cut-off frequency and damping ratio of the second-order high-pass filter is also significant; it acts to resist translational movement, attempting always to return the motion platform to a fixed position.

Once the classical MDA has been parameterised, its performance must be considered. Objective assessment techniques through the development of pilot models in order to predict the validity of motion cueing in flight simulation were summarised in section 2.3.1. Although the progression of corresponding car-driver models is a focus of contemporary research (e.g. Guo, Ding, Zhang, Lu & Wang, 2004) the author is not aware of any such models that are comparable in terms of their development of the transfer functions describing a driver's perceptual response to typical driving tasks. Hence, whilst acknowledging that it will be limited to the specific driving tasks selected, a subjective, human-in-the-loop assessment methodology is proposed.

The fundamental aim of the study was to investigate how best to manage the trade-off between specific force and tilt rate errors in order to achieve the best possible classical motion cueing in a research driving simulator. The influence of both the MDA and the characteristics of the motion platform which it commands were considered. The quality of the motion cues actually perceived by drivers, the resulting impact of this perception of motion on driver's ability to undertake conventional driving tasks and the subsequent validity of the simulator in terms of driver behaviour were all taken into account.

The experimental design was influenced by the choice of the most suitable and applicable statistical techniques, discussed later in this chapter. It was broken down into three main stages, each aimed at assessing and optimising the classical algorithm for a range of driving tasks and subsequent vehicle handling manoeuvres. Through a *Just Noticeable Difference* procedure, Stage 1 examined the maximum perceptible scale-factors of both pure translational and rotational motion platform movement. It was undertaken for longitudinal and lateral, low and high-frequency driving manoeuvres involving steering or braking/accelerating.

With knowledge of the maximum perceptible scale-factor, Stage 2 made use of maximally-scaled motion without needless platform excursion. Using a *Paired Comparison*, it examined of the effects of relocating Motion Reference Point

(MRP, see section 2.2.3) and the specific force/tilt rate trade-off for the most extreme motion demands realistically required. MRP location is important to the application of the classical algorithm in driving due to the geometry of a standard hexapod. Moving the MRP higher (closer to the driver's vestibular organs) limits the maximum tilt angle available by requiring additional actuator extension to achieve that tilt. Consequently, the maximum specific force available through tilt-coordination is significantly decreased, restricting the simulator's capabilities.

With a suitable MRP location, Stage 3 investigated the specific force/tilt rate trade-off more deeply. The classical MDA was tuned with eight different parameter sets (the available settings within the classical MDA). Each parameter set was designed to manipulate specific force scale-factor, tilt-coordination behaviour and XY-table availability as three independent, experimental factors. Again using a Paired Comparison technique for both longitudinal and lateral driving tasks, the study considered ratings of perceived realism and the accuracy of driving task performance. The effect of the three experimental factors on these subjective and objective measures was assessed.

4.1. Assessment of dynamic simulator performance

The three-staged experimental plan demanded accurate control of the experimental factors manipulated within its design, each potentially influencing the perception of motion and subsequent behaviour of participant drivers. Hence, an assessment method was required to measure dynamic simulator performance. Initially, a confident validation of the vehicle dynamics model had to be made since its fidelity is intrinsically linked to the accuracy of the resultant motion cueing. Furthermore, the MDA's scaling and filtering of the vehicle model outputs, along with the dynamic capabilities of the motion system itself, additionally influence the overall perception of motion. Therefore, these too were required to be recorded and assessed.

4.1.1. Vehicle dynamics model

Unfortunately, it was not possible to validate the vehicle dynamics model against any real-world data. Therefore its evaluation had to be made against an alternative model, previously authenticated against such real world data. For this, v4.51 of the vehicle dynamics software package CarSim was used. CarSim is a product of the Mechanical Simulation Corporation, founded in 1996 as a spin-off company from the University of Michigan Transportation Research Institute (UMTRI). From the late 1960s, UMTRI pioneered early vehicle dynamics and modelling work, culminating eventually in the development of AUTOSIM, software that describes the equations of motion for models of vehicles and vehicle components (Sayers, 1993). AUTOSIM, itself validated against real-world data (Sayers & Riley, 1996), was later commercialised to become CarSim. Its real-time version is currently used in many driving simulators worldwide, including the Toyota and DLR facilities as well as the driving simulator module of TNO's DESDEMONA.

Where compatable, the parameters describing the driven vehicle and used in the UoLDS dynamic model were matched in the CarSim model. Unfortunately, two drawbacks to v4.51 did limit the entirety of this parameter-entry process. Most significantly, the CarSim v4.51 tyre model did not correspond to the entire range of the Pacejka Magic Formula coefficients used in the UoLDS tyre model. Instead, a series of data points had to be taken from the UoLDS Pacejka data to create plots of normalised tyre forces and moments in CarSim, similar to those shown in Figure 3-10 and Figure 3-13. Whilst this technique did not allow the Pacejka calculations to be performed at each time step, as in the UoLDS vehicle dynamics model, it did provide a reasonable approximation to the full Pacejka tyre model used. Secondly, CarSim did not include any powertrain modelling capabilities, rendering impossible any assessment of the model's capacity to handle accelerator control inputs. However, confidence in UoLDS's powertrain model was gained from an evaluation of straight-line acceleration from rest, performed during the simulator's post-installation acceptance tests (Bosch Rexroth-Hydraudyne, 2006). These had shown good correspondence

to available Jaguar Land Rover data in terms of speed-time histories and overall top speed.

4.1.2. Motion system

The linear and rotational accelerometers, used during the post-installation acceptance tests of the motion system, were supplied at the time by Bosch Rexroth-Hydraudyne and were not available for the present study. However, the Emotion-2500-8DOF-500-MK1-XY motion system does have a capability to infer platform position in its managed eight degrees-of-freedom via an internal position-sensing mechanism. The technique, known as Inverse Actuator Extension Transformation (IAET), converts the actual actuator positions to the corresponding motion platform position in all eight of its degrees-of-freedom. By double differentiating the IAET position of the hexapod and combining them with the IAET position of the XY-table, it is possible to infer the overall perceived translational and rotational accelerations, as would have been recorded by an accelerometer. The motion system's "disklogger" records IAET position at 100Hz.

The differential calculations transforming position to velocity and subsequently acceleration include a small denominator (time step). Furthermore, they are performed on recorded data partial to small discrepancies. Hence the calculated signal of "perceived" acceleration, also recorded by the disklogger, is somewhat afflicted by noise. Whilst this noise leads to a more variable signal than the output of an accelerometer, the process is cheap and straight-forward. Most importantly, it provides an adequate method of inferring the specific force perceived by participant drivers.

4.1.3. Motion Drive Algorithm

To facilitate the appraisal of the classical algorithm in the experimental design, a model of the MDA was developed using a pair of complementary packages available from the MathWorks software suite. MathWorks' MATLAB is

a high-level computing language for algorithm development, data analysis and numerical computation. It is particularly useful for applications involving signal processing and control system design. The add-on toolbox Simulink is integrated with MATLAB, providing an interactive graphical interface that facilitates the rapid development of MATLAB models and the visualisation of their output.

Figure 4-1 shows the MATLAB/Simulink model of the major component filters of the classical algorithm for the input of demanded linear acceleration. The model is split into three channels representing the resultant positional commands of the MDA on the complete motion system, namely hexapod translation, hexapod rotation and XY-table translation. The combination of all three channels forms the overall specific force output, eventually witnessed by the driver once the motion platform has adopted these positional commands. Hexapod translation is modelled through the middle channel, representing its first-order high-pass (*HP1_ms*) and second-order high-pass (*HP2_ms*) filters. Hexapod rotation, characterised in the lower channel, is limited to its second-order low-pass filter (*LP2_ms*). The band-pass filter controlling XY-table translation is illustrated in the upper channel by its first-order high-pass (*HP1_xy*) and second-order high-pass (*HP2_xy*) filters along with its second-order low-pass filter (*LP2_xy*).

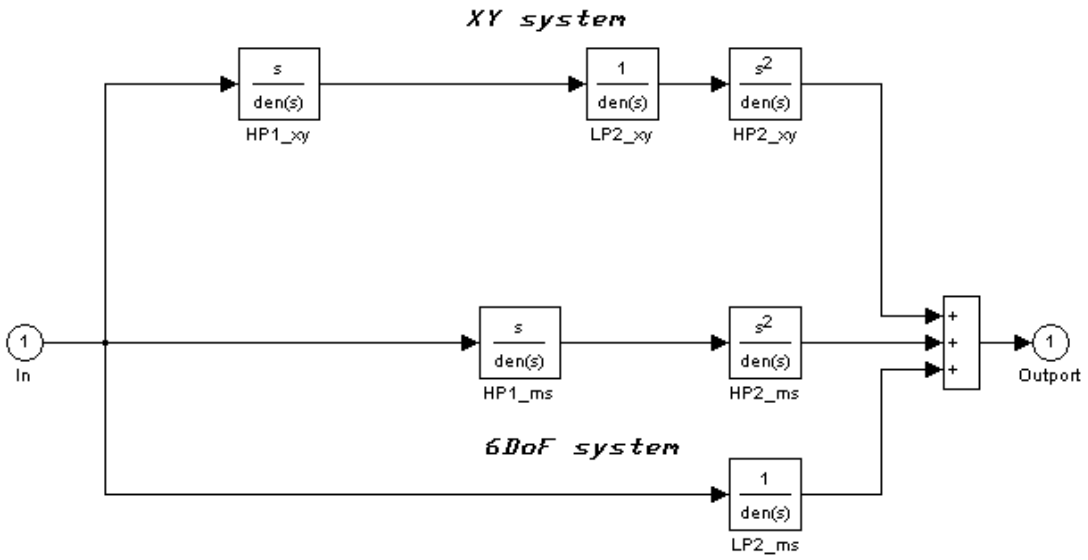

Figure 4-1: MATLAB/Simulink model of the classical MDA for linear acceleration

The MATLAB/Simulink model allowed the visualisation of the MDA commands to be expressed in terms of the acceleration, velocity and displacement of the overall motion platform in all three degrees-of-freedom involved[1]. Additionally, the transfer function of the MDA could be described in the frequency domain, depicted as a Bode plot. Finally, a time history of demanded input and the commanded specific force output could be plotted.

The MATLAB/Simulink model proved invaluable when tuning the classical algorithm in order to account for the permutations of the independent experimental factors under investigation. The tuning process involved defining thirteen specific values as set of parameters forming a single parameter set, as outlined in Table 4-1.

Table 4-1: the thirteen values defined in a single parameter set

parameters		hexapod translation	hexapod tilt	XY-table translation
scale-factor		value	value	value
HP1	cut-off	frequency	N/A	frequency
HP2	cut-off	frequency	N/A	frequency
	damping	ratio	N/A	ratio
LP2	cut-off	N/A	frequency	frequency
	damping	N/A	ratio	ratio

4.1.4. Validated channels

The specific driving tasks requiring longitudinal and lateral vehicle control, designed in each stage of the experimental design, are detailed later within their respective chapters. For each of these tasks, UoLDS vehicle dynamics model output, CarSim equivalent, commanded motion cueing (predicated by the MATLAB/Simulink model) and the actual perceived acceleration achieved by the motion platform (recorded by its disklogger) were assessed.

[1] For linear longitudinal acceleration: hexapod surge, XY-table surge and hexapod pitch. For linear lateral acceleration: hexapod sway, XY-table sway and hexapod roll.

Since all driving manoeuvres took place on a flat road surface, with the exception of road roughness which was simulated as a special effect[2], no vertical linear acceleration of the vehicle was possible. Hence, for longitudinal tasks, the fidelity of motion cueing was evaluated only in linear longitudinal acceleration (A_x) and rotational pitch acceleration ($\dot{q}$). For lateral tasks, linear lateral acceleration (A_y), rotational roll acceleration ($\dot{p}$) and rotational yaw acceleration ($\dot{r}$) were assessed.

In terms of vehicle model equivalence, one issue was the fact that CarSim v4.51 does not allow the output of any vehicle rotational accelerations. However, their integrals of rotational rate and rotational angle can be gathered. Thus, for longitudinal tasks, the two vehicle models' estimation of pitch rate (q) and pitch angle (θ) were contrasted. Laterally, this comparison was made for the respective outputs of roll rate (p), yaw rate (r) and roll angle (ϕ).

4.2. Experimental techniques

4.2.1. Just Noticeable Difference

The design of Stage 1 was based on an application of the Just Noticeable Difference (JND) method, a technique devised in the 19th century by one of the founding fathers of experimental psychophysics, Ernst Weber. JND allows the measurement of the *difference threshold*, the minimum amount by which stimulus intensity must be changed in order to produce a noticeable variation in the sensory experience. Weber's law, later refined to become the Weber–Fechner law (see Adler, Howes *&* Boring, 1966), states that the ratio between the just noticeable difference in stimulus intensity and the reference stimulus intensity is a constant. Adler et al. (1966) describe an early Weber experiment, where the weight that a blindfolded participant was holding was gradually increased. The participant was informed to respond on first perception of the

[2] Based on real road data, the motion computer continuously computes the sum of twenty sine waves characterised by frequency and amplitude. The result is a "turbulent" motion in heave, related to forward speed, resembling the vehicle travelling over an asphalt road surface.

increase. Weber observed that the just noticeable difference in weight was proportional to the starting value of the weight. For some time, the technique has been applied to research into sensory perception (e.g. Wald, 1945).

The merit of JND has also been demonstrated in simulation by its application in visual-vestibular sensory perception. For example, Grant & Lee (2007) used the technique to estimate motion-visual phase error detection in a moving-base flight simulator. In a simulator, the transport delays inherent to the image generation and motion systems do not necessarily match, the latter being eminently modifiable through the MDA. By manipulating the coherence of visual and motion cues across a range of input frequencies, Grant & Lee (2007) discovered that the average phase error detection threshold depends predominantly on the scale-factor of the motion and frequency of its input. They used these findings to suggest first and second-order high-pass cut-off frequencies for onset cueing to ensure that motion-visual phase error is kept below perceptual limits.

Due to human individual differences, there is no absolute detection threshold. Perceptual threshold is therefore most appropriately expressed as the *probability of detection*. This is best described by a psychometric function with respect to the amplitude of the signal being detected. The Levitt procedure allows an accurate estimate of a single point on the psychometric probability of detection curve (Levitt, 1971).

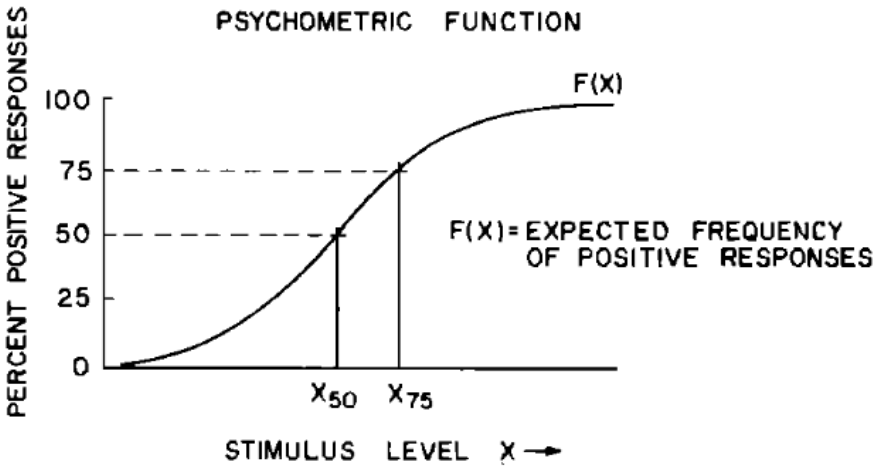

Figure 4-2: psychometric function of stimulus level and detection likelihood (from Levitt, 1971)

In Levitt's *method of limits*, a stimulus having a high probability of detection is presented to an observer. If the stimulus is perceived, it is reduced in intensity for the next trial. If another positive response is obtained, the stimulus level is again reduced by the same amount (the step size). This procedure is continued until the stimulus can no longer be sensed. The mean of the last two stimulus levels (the smallest stimulus detected and the subsequent one undetectable) is used as an estimate of the 50% detection probability (X_{50}, Figure 4-2).

A more accurate, yet still efficient way of estimating the X_{50} is by the *1 up / 1 down* or *staircase* method. It is similar to the method of limits in that the stimulus level is decreased after a positive response (or vice versa), but the test is not terminated after the first reversal: when the stimulus is changed from decreasing to increasing, or vice versa. Levitt (1971) recommends to continue testing until at least six reversals before taking a mean of the stimulus magnitude at each reversal as the observer's 50% detection threshold.

A higher probability level can be determined by modifying the response sequence to *1up / 2 down.* In this procedure, two consecutive positive responses have to be made before the stimulus level is reduced. However, just one negative response leads to an increase in stimulus level. The probability level now increases from P[x]=0.5 to $P[x]=0.5^{1/2}$, i.e. 71%. Likewise, a *1 up / 3 down* technique estimates the 79% level ($P[x]=0.5^{1/3}$) and a *1 up / 4 down* technique estimates the 84% level ($P[x]=0.5^{1/4}$). The procedure can be further optimised by reducing the step size after each reversal.

4.2.2. Paired Comparison

Stages 2 and 3 evaluated the effects of varying motion cueing on participant's perception of realism and driving performance in relation to specific vehicle handling tasks. The qualitative nature of forming such a subjective opinion and the inherent difficulty in maintaining a linear scale, forced the use of a *Paired Comparison* as the most robust method to facilitate the comparative judgments.

In a paired comparison, objects are presented in pairs to one or more judges, who are obliged to choose between the two based on pre-defined criteria. In its simplest form, a paired comparison profits from its reduction of the area of possible disagreement between judges to an absolute minimum. If more than two objects exist, the pairs can be ordered in such a way that each judge pronounces a verdict on every possible combination; this is known as a *balanced design*. The technique is commonly employed when objects can only be compared in a highly subjective fashion.

Based on the pioneering psychophysical theory developed by Ernst Weber and Gustav Fechner, American psychophysician Louis Thurstone introduced the first scientific realisation of the paired comparison, known at the time as the "law of comparative judgement" (Thurstone, 1927). In more modern parlance, the term "law" is more appropriately replaced by "model". Thurstone's model allowed the establishment of a relationship between objects with no clear, physical method of contrast, such as attitudes, opinions or moral judgments. When clear perceptible differences exist between the objects, the law of comparative judgement allows their representation on an arbitrary, non-linear, inter-interval scale. The technique supersedes a simple ranking of the objects when both a fine judgement between objects is required and the comparison between them needs to be free of extraneous influences caused by the presence of other objects.

Ranking is a data transformation in which numerical or ordinal values are replaced by their rank. For example, the ordinal data hot, cold and warm become ranks 3, 1 and 2. A rank test is an extension of a paired comparison that allows an analysis of any observable differences between the objects. If a judge is able to legitimately compare several objects at the same time, non-parametric statistical techniques exist such as the Wilcoxon rank-sum test for equal sample sizes (Wilcoxon, 1945), or the Mann-Whitney-Wilcoxon (Mann-Whitney U test) for arbitrary sample sizes (Mann & Whitney, 1947).

A rank test is typically quicker to administer than a paired comparison since there is no requirement to rank objects against one another as individual pairs, but rather as a complete group. It also removes the tedium that may be associated when a judge is required to contrast a multitude of pairs. The technique requires the judge to consider each condition against its rivals simultaneously so that the context for the ranking can be provided. Clearly, this is impossible when considering observers in a driving simulator assessing the realism of perceptible motion cues: each observer would have to be in multiple simulators concurrently.

Nevertheless, ranking perceived realism would be an option if judges were able to retain each motion cueing condition in short-term memory until all had been presented. However, results of comparable studies using tactile stimulation suggest that short-term memory is partially based on a continuing "trace" of the original sensation, known as sensory memory, decaying over a period of about 5s – 10s after the stimulus is experienced (Davidson, 1972). The dynamic and inertial characteristics of typical motion systems often prevent the presentation of stimuli from being managed within such a short time frame. Such trace-fading could equally be an argument not to support paired comparisons in the assessment of motion cueing fidelity either, since the same working memory issues remain. However, the technique is preferable since the ranking of objects in which differences are either small or highly subjective is notoriously difficult for judges to make (David, 1988).

Sinclair & Burton (1996) attempted to quantify human short-term-memory decay functions for delayed vibrotactile discriminations. In their experiment, participants witnessed stimuli of varying frequency through a vibrating pad applied to the index finger. Two successive stimuli were presented containing a higher or lower frequency separated by delay periods of between 0.5s – 30s. After each pair of stimuli, participants were required to detect, randomly, either the higher or lower frequency. Whilst, as expected, performance did decrease as a function of delay when that delay exceeded 5s – 10s, participants were still able to positively discriminate stimuli even upto 30s apart. The authors

suggested their findings indicated that short-term tactile memory depends on more than a just a sensory trace persisting for some 5s – 10s. After this period, they proposed that another mechanism, possibly involving some recoding of sensory information, supersedes the weakening sensory "image", making a longer retention of the stimulus characteristic possible. If extendable to vestibular as opposed to tactile stimulation, this would justify the use of paired comparisons when comparing the fidelity of motion cueing with paired conditions presented in excess of 5s – 10s apart.

Indeed, paired comparisons have been utilised successfully to compare the motion cueing for both flight simulation (Reid & Nahon, 1985) and driving simulation (Grant, Blommer, Artz & Greenberg, 2009) in just such extended stimulus delay conditions. Furthermore, the technique has also been used in distinguishing between examination content and performance standards (Sinclair & Burton, 1996). In this context, performance standards relate to where the grade boundaries should be set on a particular assessment – how many marks are 'good enough' for a script to be worthy of a particular grade. In assessing standards in this manner, judges were required to read and mark two scripts before making a comparison as to which of the pair was superior. Holding the assessment of each script in working memory required many times the stimulus interval used by either Reid & Nahon (1985) or Grant et al. (2009).

4.2.2.1. Consistency testing

Kendall & Babington-Smith (1940) extended Thurstone's (1927) work to develop a non-parametric method of calculating an individual judges' *coefficient of consistency*. To illustrate this, let us consider three objects, A, B and C, that are to be judged in a paired comparison. Clearly three pairs are required: A v B, B v C and A v C. If A is preferred to B and B is preferred to C, it would be expected that A also be preferred to C. Kendall & Babington-Smith termed this a *consistent triad*. When more than three objects are judged, it is possible to calculate the number of consistent triads as a proportion of the total number of triads that exist: an individual judge's *coefficient of consistency*. An analysis of coefficient of consistence permits an internal test of reliability of an individual's

subjective ratings, an acceptable criteria used previously by Grant el al. (2009) in their assessment of varying motion cueing during double lane change manoeuvres.

Judges may demonstrate low consistency for one of two reasons: either the individual judge does not possess the inherent ability to discriminate between the objects or those objects do not differ from one another above a distinguishable threshold. In order to discriminate between these two possibilities, Kendall & Babington-Smith also introduced the *coefficient of agreement* when more than one judge is involved in the assessments. For a specific pair undergoing comparison, the number of times that one object is preferred over its rival can be calculated. Totalling the actual number of these preferences as a proportion of the total number possible gives the coefficient of agreement across the judges.

Kendall & Babington-Smith point out that it is possible for judges to display high agreement, but be similarly inconsistent. Conversely, a lack of agreement does not necessarily imply inconsistency. When there is low agreement between the judges and a large proportion also demonstrate inconsistency, it can be surmised that the objects do not differ to a recognisable degree. Similarly, for low agreement but now with only a small number of judges showing inconsistence, those individuals can reasonably be suspected of an inability to satisfactorily execute the classification task. In such circumstances, they can be rejected from the analysis. Conversely, for high agreement, it would be expected that most inconsistencies be confined to particular objects, and in a reliable manner across all of the judging panel.

Where Kendall & Babington-Smith's method becomes so beneficial is in their proof that coefficient of agreement can be tested, non-parametrically, for statistical significance, the null hypothesis being that judges allocate their preferences at random. The number of agreements can be formulated as an approximate χ^2 distribution with a degree-of-freedom related to the number of objects and judges.

4.2.2.2. Bradley-Terry model

Whilst the contribution of Thurstone allowed the relative scaling of objects and Kendall & Babington-Smith's efforts added a statistical test of their differences, both methods were further improved by the introduction of the Bradley-Terry linear model (Bradley & Terry, 1952). The model provides another ability to express the relationship between objects, but crucially, now on a linear scale. If the observed data fit the model well, it therefore becomes possible to express quantitative information of individual objects in comparison to one another, but in a more convenient mathematical fashion.

The Bradley-Terry linear model states that the probability that object i is preferred to object j (π_{ij}) is related to the overall preference probabilities for object i (π_i) and object j (π_j) by

$$\pi_{ij} = \frac{\pi_{\mathrm{i}}}{\pi_{\mathrm{i}} + \pi_{\mathrm{j}}}$$

with the constraint that

$$\sum \pi_i = 1$$

Based on the observed π_i, the Bradley-Terry linear model makes a Maximum Likelihood Estimation of the object's preference probability, p_i. This allows a calculation of its "merit" (V_i) on the now possible linear scale using an approach first introduced by Noether (1960).

$$V_i = \log_e(p_i) - \left\{\frac{1}{t}\sum_{i=1}^{t} \log_e(p_i)\right\}$$

where t is the number of objects, given the restriction of the arbitrary linear scale

$$\sum_{i=1}^{t} V_i = 0$$

A test of fit of the Bradley-Terry model is possible using Likelihood Ratio Theory. By applying a monotonic function, Bradley & Terry (1952) prove that the overall probability distribution (B_1) can be found from

$$B_1 = n\sum_{i<j}\log_{10}(p_i + p_j) - \sum_{i=1}^{t} a_i \log_{10}(p_1)$$

where

n is the number of judges multiplied by the number of repetitions of each paired comparison per judge, and

a_i is the total number of times that object i was preferred.

The importance of the probability distribution becomes clear as Bradley & Terry go on to show that the fidelity of their linear model can be expressed from the result of

$$nt(t-1)\log_e(2) - 2B_1\log_e(10)$$

which is distributed approximately as χ^2 with $t-1$ degrees of freedom. By undertaking this test against a standard χ^2 distribution, an acceptance of the null hypothesis indicates a satisfactory linear model.

Active during a period prior to the advent of personal computers, Bradley & Terry were forced to torturously number-crunch their models by hand. Hence, for ease of application, they tabulated p_i to two decimal places for small numbers of objects and paired comparison repetitions per judge (Bradley & Terry, 1952). However, for larger numbers of participants, repetitions or objects, numerical calculations based on the proofs outlined above had to, and still must, be employed. However, in such calculations, $\sum p_i$ does not always compute to 1, as should clearly be the case. Therefore, Dykstra (1956) offered an empirical correction factor replacing p_i in the calculation of B_1 with $p_i - k_i$, where

$$k_i = \frac{\left[\frac{\mathrm{R(t-1)} - N^2}{\mathrm{t}}\right] + \mathrm{a_i[n(t-1) - a_i]}}{\mathrm{R(t-1)} - N^2 + \sum\{\mathrm{a_i[n(t-1) - a_i]}\}}\left[\left(\sum\{\mathrm{p_i}\} - 1\right)\right]$$

and $R = \sum {a_i}^2$

and $N = \frac{1}{2}nt(t-1)$

The implementation of the Bradley-Terry model in Stages 2 and 3 was achieved by manually developed formulae, facilitated by spreadsheets developed using Microsoft Excel.

4.2.2.3. Balanced paired comparison design

A paired comparison is most efficient when all judges rate objects in all combinations, known as a fully balanced design. However, even with such a design, it is possible for judges to experience order effects, where their perceptions change either due to familiarity or over time. Similarly, carry-over effects are possible where perceptions are potentially altered due to preceding objects. In order to limit these effects, counter-balancing the order of objects presented to judges for rating must be carefully controlled.

Russell (1980) studied paired comparison designs that balance such effects either exactly or approximately. He noted an exact balance, hence the complete elimination of any carry-over effects, is possible when the number of objects is a power of 2 (Russell's counterbalancing is shown in Table 4-2 for eight objects). An additional benefit is that Russell's design can be ordered in a manner to ensure a balanced sequence of objects can be achieved in terms of their order of presentation to individual judges.

Table 4-2: Russell's Galois field theory for balanced pair presentation (Russell, 1980)

A v D	B v E	C v H	F v G
A v E	B v D	C v F	G v H
A v F	B v H	C v E	D v G
A v G	B v C	D v F	E v H
A v H	B v F	C v D	E v G
A v B	C v G	D v E	F v H
A v C	B v G	D v H	E v F

For approximate balance in designs containing less than eight objects, any table entry that exceeds the dimension of the design is simply ignored; e.g. all entries containing ‘H’ for a seven-object design.

4.3. Statistical techniques

4.3.1. Analysis of variance

Within Stage 1, the maximum perceptible scale-factor across the participant sample was subject to statistical analysis. Furthermore, Stages 2 and 3 also evaluated a number of driving behaviour metrics as an objective measure of driving task performance. In both cases, *Analysis of Variance* (ANOVA) with repeated-measures was selected as the most appropriate manner to assess objective performance whilst experiencing the varying motion cueing conditions. This technique is summarised here.

The origins of ANOVA lie in the t-test, a statistical technique introduced in the early 20th century by William Gosset under the pseudonym “Student” (Student, 1908). Student’s t-test provides an exact test for the equality of the means of two normally distributed groups with unknown, but equal, variances. Gosset extended his t-test with the development of ANOVA, applicable to the assessment of more than two groups. It manages this by partitioning the observed variance within each group and comparing it to the overall variance of the combined population. The result is the *F* statistic, the ratio of the variance of the group means and the mean of the within-group variances. From the F statistic, the probability of obtaining this result is given by the *p* value; in other words, the statistical significance. Undertaking multiple t-tests to achieve the same goal would result in an increased likelihood of a type I error: the false-positive rejection of the null hypothesis (equal populations) when it is actually true.

Whereas the *p* value judges the reliability of the relationship between independent and dependent variables, the *effect size* assess the strength of

that relationship. ANOVA also allows a measurement of the effect size, presented here as a partial η^2: the proportion of total variation attributable to the particular group.

Fundamental to ANOVA are the definitions of *independent* and *dependent variables*. The *independent variable* represents the groups or *factors* that are manipulated experimentally into their various levels. The *dependent variable* describes the observed data that result from the manipulations of the independent variable.

In a *single-factor* ANOVA, one independent variable is manipulated, the key result being the *main effect* of the manipulation on the dependent variable in terms of statistical significance. A *multi-factorial* ANOVA allows the assessment of the main effect of a series of unrelated independent variables. In addition, the significance of the *interaction* of the independent variables can also be estimated. Finally, in a *repeated-measures* ANOVA, the dependent variable is observed in a sample participating in every possible permutation of the independent variable(s). Whilst susceptible to carry-over and order effects, a repeated-measure ANOVA provides the ultimate in matching, as each participant effectively acts as their own baseline, hence minimising the systematic variance arising from the individual differences of the participants.

ANOVA makes certain assumptions on the structure of the evaluated populations that are fundamental to its correct application. First, independent variables must be consistent and unrelated from one another. Next, the dependent variables observed during each manipulation of the independent variable(s) must be normally distributed. Finally, independent variables must demonstrate *homogeneity*; in other words, the dependent variables observed during each manipulation of the independent variable(s) must be equal in their variance.

Throughout Stages 2 and 3, multi-factorial, repeated-measures ANOVA were used. These were performed using v16.0 of IBM's SPSS statistical analysis

software. Results of the repeated-measures ANOVA were considered signifcant if the probability of the null hypothesis, i.e. no relationship between groups, was 5% or less.

4.3.2. Paired comparison non-parametric test of equality

Within Stages 2 and 3, the subjective data were reduced to the overall rating scores for each motion cueing condition throughout the paired comparison. This allowed a test of equality in order to assess the significance of any variation in those scores. The method is analogous to the F-statistic in ANOVA. The null hypothesis under test is, for all i upto t:

$$H_0'\colon\ \pi_i = {}^1\!/_2$$

In the equation below, D_n varies as a χ^2 distribution with $t-1$ degrees of freedom:

$$D_n = 4\left[\sum_{i=1}^{t} a_i^2 - \frac{1}{4}tn^2(t-1)^2\right]\Big/nt$$

where $\sum a_i^2$ is the sum of the squares of the scores.

At a particular confidence level, H'_o is rejected if the value of D_n exceeds or equals the corresponding critical value.

The above test is comparable to discovering the existence of a main effect in any particular experimental factor. The post-hoc test, which determines to what extent the levels of that factor differ from one another, is obtained from a Least Significance Difference of the overall rating scores. For a two-sided test at a particular significance level , the critical value (m_{crit}) by which scores must differ by is given in:

$$m_{crit} = Z_{crit}\sqrt{({}^1\!/_2\, nt^2)}$$

where Z_{crit} is the Z-score for the percentile point of the significance level in question. If necessary, m_{crit} is rounded up to the next available integer.

4.4. Chapter summary

This chapter has outlined the fundamental design of the three-staged experimental plan. Its complementary nature has been highlighted in that the main results from each stage feed into the one that follows. The maximum perceptible scale-factors in motion platform movement both in translation and tilt, to be gleaned during Stage 1, will allow Stage 2 to examine of the effects of relocating Motion Reference Point and the specific force/tilt rate trade-off for maximally-scaled motion. Using the most appropriate MRP, Stage 3 will be able to investigate the specific force/tilt rate trade-off more deeply through manipulate specific force scale-factor, tilt-coordination behaviour and XY-table availability as three independent, experimental factors. During the stages, the assessment of both subjective perception of motion and objective driver performance will be supported.

This chapter has also introduced the method by which the dynamic characteristics of the vehicle model and motion system combination will be measured. This will confirm that the actual performance of the simulator matches that required by the experimental design.

Finally, the statistical techniques at the heart of the experimental design were presented. Their accurate and appropriate application is fundamental in ensuring that meaningful and substantive conclusions can be drawn from the observations made during each experimental stage.

The participants, procedures and results of each stage follow, each being afforded its own chapter.

CHAPTER 5

EXPERIMENTAL STAGE 1: JUST NOTICEABLE DIFFERENCE – THE MAXIMUM PERCEPTIBLE SCALE-FACTORS IN MOTION PLATFORM TRANSLATION AND TILT

In order to help flatten the transfer function of the perceived linear or rotational acceleration felt by the occupant of a moving simulator, most applications typically undertake a scaling of the respective input signals. The scale-factor (or gain[3]) is a constant by which the input signal is multiplied. Section 2.2.4.1 outlines some of the published literature regarding input scaling, with scale-factors between 0.5 to 0.7 commonly employed. Such values are considered sufficient to allow an accurate perception of acceleration without it being characterised as overly strong or amplifying the inevitable magnitude and phase errors introduced by the Motion Drive Algorithm (c.f. Reid & Nahon, 1988; Groen, Valenti Clari & Hosman, 2001; Grant & Haycock, 2008; Grant, Blommer, Artz & Greenberg, 2009). Accelerations in all six degrees-of-freedom are scaled individually and can differ. This is particularly necessary if platform limits dictate (e.g. Schroeder, 1999).

The performance of an MDA to an acceleration input in each of the three linear and rotational vehicle degrees-of-freedom is characterised most easily in the frequency domain. The resultant transfer function is commonly illustrated by a Bode plot, the magnitude describing the system gain and the phase depicting the timing of the output with respect to the input (see section 2.2.2.2). In terms of driving simulation, the system gain effectively describes the *magnitude of the perceived acceleration*: the extent to which the simulator achieves the required acceleration demand. The *controllability* of the simulator, on the other hand, is a

[3] This common terminology is avoided to minimise confusion with the Bode magnitude (usually expressed as *gain* in dB) describing the amplitude ratio of input and output signals.

direct result of the phase error between demanded and perceived accelerations. For a particular frequency of input, the mismatch can be expressed in units of time. Phase error affects the overall transport delay or latency of a driving simulator motion. Such latencies lead to handling difficulties (Reid & Nahon, 1988) and can contribute towards simulator sickness (see Stanney, Mourant & Kennedy, 1998, for a review).

Simulator sickness is a condition where a person exhibits vertigo and/or nausea on exposure to a virtual environment, symptoms similar to a car passenger suffering from motion sickness. Whilst clearly a major issue in the design and development of driving simulators, its effect is often physiological, specific to the individual experiencing the virtual environment. Potentially, it is also influenced by the duration of exposure (Kennedy, Lane, Lilienthal, Berbaum & Hettinger, 1992). In this work, there was no available mechanism to assess simulator sickness as a useful dependent variable within the time frame that participant's experienced any of the various motion cueing conditions. Since associating any symptoms of simulator sickness to a specific experimental condition was therefore impossible, it was not considered.

In assessing only the maximum perceptible scale-factor, Stage 1 simply considers motion system gain. Participant drivers were not required to actively handle the simulator through the vehicle controls, simply to ride as observers to a pre-scripted series of control inputs. Dynamically, the performance of the simulator, including the update of the visual scene, was as though drivers had made those control inputs. The phase lag associated with motion filtering and the consequent issues of simulator controllability of the simulator was considered later in Stages 2 and 3.

The output of specific force can be independently scaled in both of the resultant translational or rotational displacements of the motion platform. Whilst the same scaling is commonly used in both channels, there is an argument for differing scale-factors to be beneficial in the overall perception of motion. In their study of perceived linear acceleration during a simulated take-off run, Groen et

al. (2001) suggested that for “realistic motion” a very low translational scale-factor of 0.2 best complimented the greater value of 0.6 selected for tilt-coordination. For this reason, Stage 1 was split into two phases; the first investigated maximum perceptible scale-factor error for motion platform translation (or more accurately the maximum perceptible scale-factor closest to unity). A second, complimentary phase deciphered the equivalent for platform tilt.

Stage 1, therefore, required four driving scenarios, designed to assess the maximum perceptible scale-factor for platform translation and tilt for both longitudinal and lateral vehicle manoeuvres. Each trial consisted of a scenario pair, one for which motion was scaled and one for which it was unscaled (unity scale-factor), the order of which being presented randomly. Participants were required to indicate for which of the scenario pair they felt motion had been unscaled.

A Levitt 1 up / 3 down procedure was used to estimate the maximum perceptible scale-factor using a Just Noticeable Difference technique. The stimulus, therefore, was the error between the scaled and unscaled, “ideal” motion cue. Thus the perceptual threshold measured was the minimum error that could be sensed at the 79% probability level (see section 4.2.1).

As the fundamental aim was to determine the maximum perceptible scale-factors (closest to unity), only the specific force generated by linear acceleration was simulated by platform movement. Providing the additional dynamic inputs mimicking vehicle rotational acceleration would have necessitated an additional assessment as to their individual impact on scale-factor perceivability and therefore overcomplicated the experimental design for Stage 1.

5.1. Method

5.1.1. Scaling of motion platform displacement in translation

For platform translation, the simulation of linear acceleration was realised through raw, unfiltered cueing, using surge and sway generated only by the XY-table. Naturally, the greater the scale-factor, the larger the XY-table displacement required. Two scenarios were designed at a driver control input frequency of 1.35rad/s (0.215Hz) in order to achieve a similar frequency demand of the XY-table motion. Comfortably inside the bandwidth of both XY-table surge and sway, the acceptance tests of the motion system undertaken at the simulator's commissioning stage indicated no appreciable signal attenuation (>-0.1dB gain) or phase error (<3°) at this frequency (Bosch Rexroth-Hydraudyne, 2006).

The value of 1.35rad/s was selected to be close to the 1rad/s "critical" frequency suggested by the Sinacori / Schroeder motion fidelity criterion (see section 2.3.1.3) whilst allowing the scenario to be achieved unfiltered and unscaled within the excursion limits of UoLDS's XY-table.

5.1.1.1. Longitudinal translation driving scenario

The longitudinal translation scenario involved braking and accelerating during car following (Figure 5-1). The participant was seated in the vehicle cab viewing the visual scene as normal, but the display showed full white. Over a 1s period, the scene was faded-in to present a typical rural road with the participant "driving" at the speed limit of 60mph (96kph). A pre-scripted accelerator position input of 9.4% maintained the trimmed speed for the automatically selected fifth gear. Another vehicle, also travelling at 60mph was situated in front at a distance headway of 25m. After 10s the lead vehicle first slowed then sped up, its linear acceleration following one cycle of a continuous sine function. The peak of the sine wave was ±1.5m/s^2 at the selected frequency of 1.35rad/s (0.215Hz) implying a time period of 4.65s.

Figure 5-1: screenshot taken from the longitudinal translation scenario

Simultaneously, pre-scripted vehicle control inputs were made on behalf of the driver (Figure 5-2). First, whilst maintaining the 9.4% accelerator input, a 1.35rad/s sinusoidal brake pedal effort was made for the first half of the sine-wave (2.325s), reaching a peak of 38N and achieving a similar braking performance to the lead vehicle during this period. Once brake pedal effort had returned to zero, the accelerating half of the sine wave was achieved with an additional peak accelerator position amplitude of 38% (combined total 47.4%), returning to the residual 9.4% after the remaining 2.325s of the sine wave. After 7.85s back at constant speed and still car following, the visual scene faded- out to white concluding the 22.5s scenario.

Participants were instructed that their vehicle would behave in the same way as the lead vehicle. As it slowed, its brakelights illuminated. The main aim of the lead vehicle was to allow participants to form a concept of how the pre-scripted driving controls were handling their vehicle. To them, the scenario appeared as though they had gently applied the brakes in an attempt to keep a constant gap to the lead vehicle, before accelerating to close the gap and maintain a constant following distance to the lead vehicle. The speedometer in the simulator cab displayed the gentle speed reduction of approximately 5mph followed by its return to 60mph.

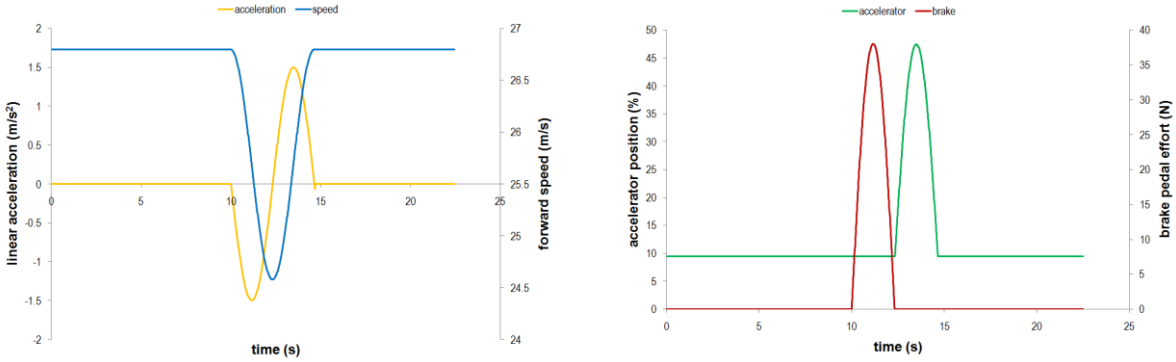

Figure 5-2: lead vehicle behaviour (left) & pre-scripted longitudinal translation control inputs (right)

The response of the UoLDS vehicle dynamics model as a result of the longitudinal pre-scripted control inputs was assessed against corresponding CarSim output (Figure 5-3). CarSim's lack of powertrain model prevented its assessment in the accelerating phase of the scenario. In the decelerating phase, the left-hand plot shows a close correspondence in linear deceleration modelled by UoLDS and CarSim. However, there is a small spike evident around 12.4s as the brake is released and the accelerator applied. This is mostly likely due to a modelled free-play: neither acceleration demand nor brake pressure are developed for light pedal applications. In normal operation when the driver applies the pedal inputs, these thresholds prevent measurement noise on the inputs signals activating the accelerator or brake. The pre-scripted controls used the same thresholds.

The right-hand plot of Figure 5-3 shows a reasonably accurate response of the model also in pitch rate and pitch angle. Whilst pitch rate and angle are marginally lagged in the UoLDS model compared to CarSim, it could be concluded with reasonable confidence that the models performed in a agreeably similar fashion during the longitudinal translation driving scenario.

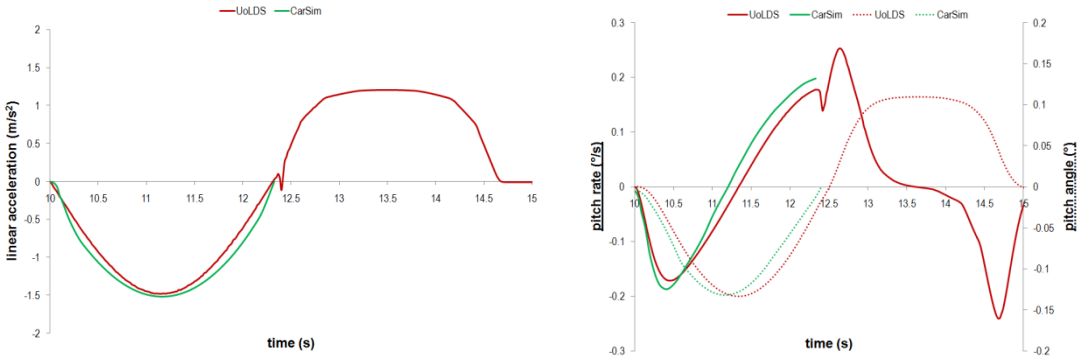

Figure 5-3: UoLDS & CarSim vehicle dynamics outputs: right, linear longitudinal acceleration; left, pitch rate (solid) and pitch angle (dashed)

Figure 5-4 shows the perceived linear longitudinal acceleration recorded by the (noisy) disklogger. The demand of the UoLDS vehicle dynamics model (A_x) is, as expected, closely matched through the unfiltered XY-table surge.

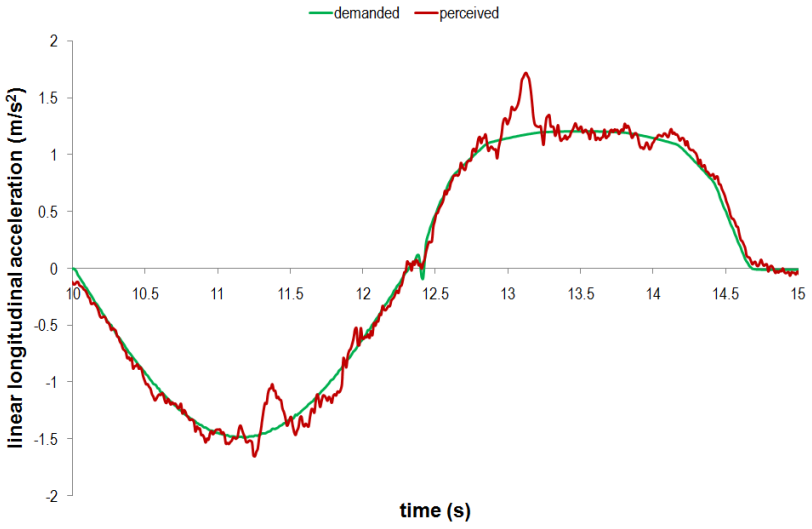

Figure 5-4: demanded & perceived linear longitudinal acceleration

5.1.1.2. Lateral translation driving scenario

The achievement of unfiltered and unscaled motion within the excursion limits of UoLDS's XY-table, close to the Sinacori / Schroeder motion fidelity criterion, was equally desirable to assess the scale-factor for lateral translational platform excursion in sway. Hence, its scenario was also designed at the same driver control input frequency (steering) of 1.35rad/s (0.215Hz). Again, this demand fell well within the bandwidth of XY sway with no appreciable signal attenuation (>-0.1dB gain) or phase error (<3°) at this frequency.

The lateral translation scenario involved steering through a short chicane, delineated by cones in a wide test-track environment (Figure 5-5). Again the scene was faded-in with the participant "driving" at a constant 60mph with a pre-scripted accelerator position input of 9.4% maintaining the trimmed speed.

Figure 5-5: screenshot taken from the lateral translation scenario

Again, participants were instructed that pre-scripted vehicle control inputs would be made on their behalf that allowed the vehicle to follow the short, S-shaped chicane (Figure 5-6, left). After 10s of constant forward speed, one cycle of a continuous sinusoidal steering wheel input was made at 1.35rad/s. The amplitude of the sine steer was 6.6°, designed to achieve a peak linear lateral acceleration of ±1.5m/s^2 from the vehicle model. After the 4.85s time period of the steering cycle, the input returned to zero for another 7.85s before the visual scene faded-out to white, concluding the 22.5s scenario.

The response of the UoLDS vehicle dynamics model as a result of the sine-steer was assessed against corresponding CarSim output. Figure 5-6 (right) shows that the models display a close correlation in lateral acceleration, with the CarSim output marginally leading its UoLDS equivalent.

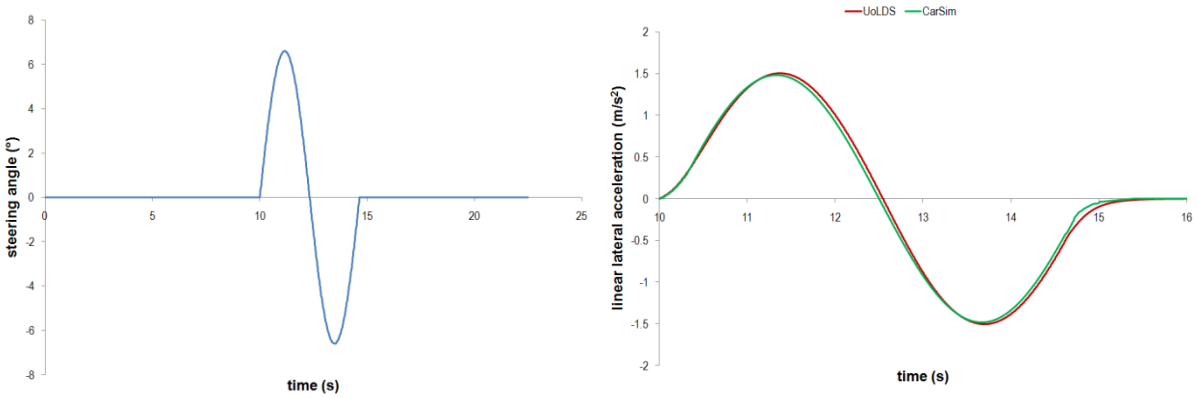

Figure 5-6: pre-scripted lateral control inputs (left) & UoLDS / CarSim vehicle dynamics outputs for linear lateral acceleration (right)

Figure 5-7 shows the response of the UoLDS model for the two lateral rotational motions: roll and yaw. Whilst in each degree-of-freedom, angular rate and angle both display a marginally smaller magnitude and somewhat lagged when compared to the CarSim model, the relatively close correspondence gives sufficient confidence in the ability of the UoLDS model to accurately simulate both the linear and rotational behaviours demanded by the lateral translation driving scenario.

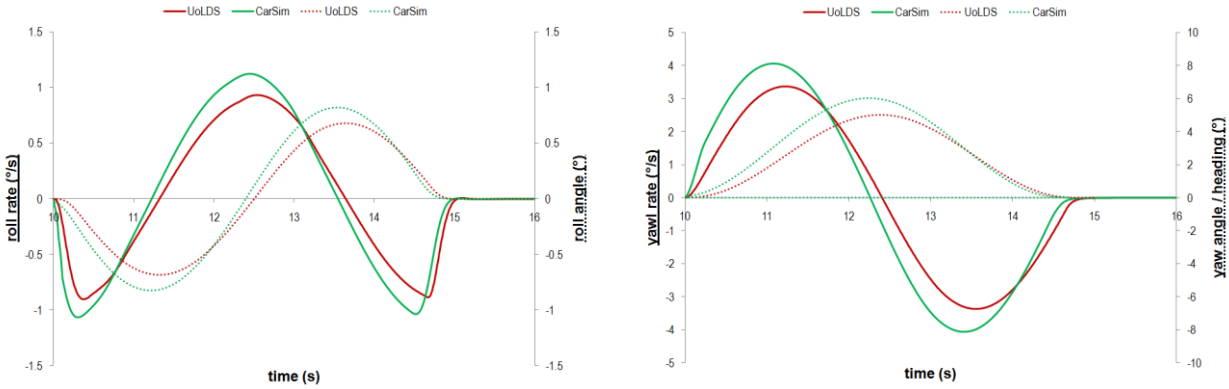

Figure 5-7: UoLDS / CarSim outputs for lateral rotation: left, roll rate (solid) & roll angle (dashed); right, yaw rate (solid) & yaw or heading angle (dashed)

Figure 5-8 shows the perceived linear lateral acceleration felt by the participant driver, recorded by the disklogger. Although the disklogger output is more noisy when compared to its estimate of linear longitudinal acceleration, the demand of the UoLDS vehicle dynamics model (A_y) is closely matched through the unfiltered XY-table sway.

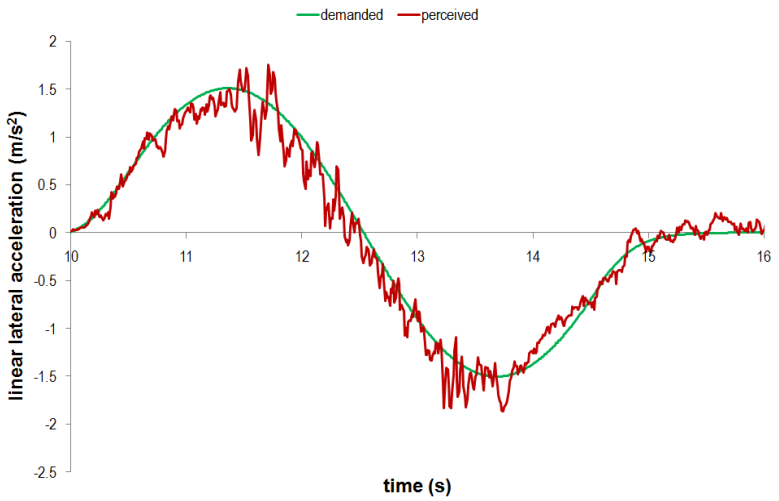

Figure 5-8: demanded & perceived linear lateral acceleration through platform translation

5.1.2. Scaling of motion platform displacement in tilt

For the assessment of the maximum perceptible scale-factor in platform rotation, the simulation of linear acceleration was realised entirely through tilt-coordination, the input signal merely being low-pass filtered to command a corresponding platform angular position. Unsurprisingly, the greater the scale-factor in question, the larger the tilt displacement required.

In order for this tilt-coordination to remain below perceptual thresholds, the longitudinal and lateral driving scenarios were designed at a much lower control input frequency than for the previous assessment of translational scale-factor. The lower input frequency ensured that, even with a unity scaling, the specific force built up sufficiently slowly to demand only an imperceptibly low tilt acceleration and rate. This was managed by the selection of the cut-off frequency (1.5Hz) and damping ratio (1.0) of the low-pass filter. For the selected control input frequency, the filter demonstrated no appreciable modification of the input in terms of the magnitude or phase of its output. Hence, motion was effectively unfiltered, to all intents and purposes specific force demand directly affecting tilt angle.

5.1.2.1. Longitudinal tilt driving scenario

Similarly to motion platform translation, the longitudinal tilt scenario involved braking and accelerating during car following. Again, the visual scene was faded-in over a 1s period to present a typical rural road with the participant "driving" at the speed limit of 60mph (96kph). The lead vehicle, also travelling at 60mph, was situated at a distance headway of 25m. After 10s, once more the linear acceleration of lead vehicle followed one cycle of a continuous sine wave with a peak of ±1.5m/s^2. However, this time it did so at the lower frequency of 0.333rad/s (0.0531Hz): a time period of 18.85s.

The simultaneous, pre-scripted vehicle control inputs (Figure 5-9) first maintained the 9.4% trimmed-speed accelerator input, followed by a 0.333rad/s sinusoidal brake pedal effort (40N peak) for the first half of the sine-wave. During this period, a similar braking performance to the lead vehicle was achieved. Once brake pedal effort had returned to zero, the accelerating half of the sine wave was achieved with an additional peak accelerator position amplitude of 30% (combined total 39.4%), returning to the residual 9.4% after the remaining 9.425s of the sine wave. After a further 6.15s, the visual scene faded-out concluding the 35s scenario.

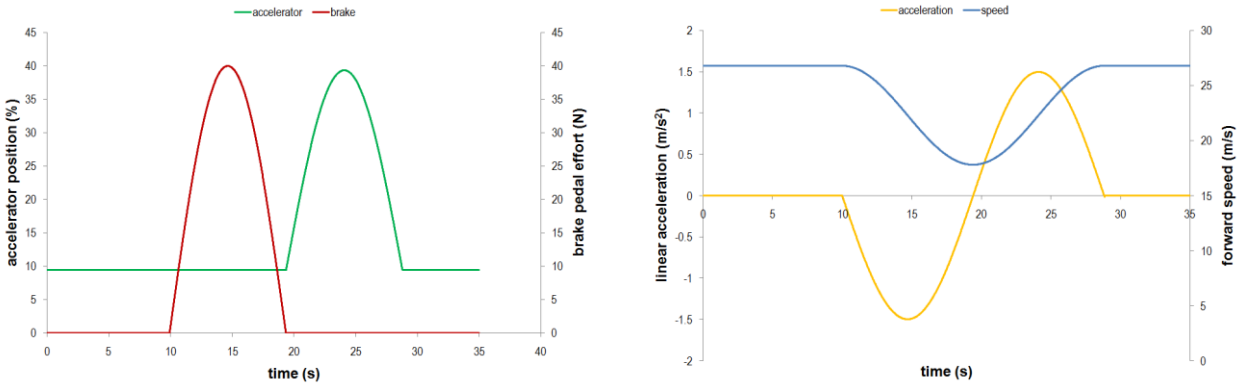

Figure 5-9: lead vehicle behaviour (left) & pre-scripted longitudinal tilt control inputs (right)

Again, CarSim's lack of powertrain model prevented a complete comparison with the UoLDS vehicle dynamics model as a result of the longitudinal pre-scripted control inputs. However, this was undertaken for the decelerating phase of the scenario. The left-hand plot of Figure 5-10 shows a good likeness

in linear deceleration modelled by both UoLDS and CarSim. The lower frequency application of pedal effort leads to a near eradication of the previously observed negative-to-positive acceleration spike of the translational longitudinal scenario. The right-hand plot of Figure 5-10 shows a similarly respectable correlation of modelled pitch rate and pitch angle and a confidence in the accuracy of the UoLDS model for the designed lateral tilt driving scenario.

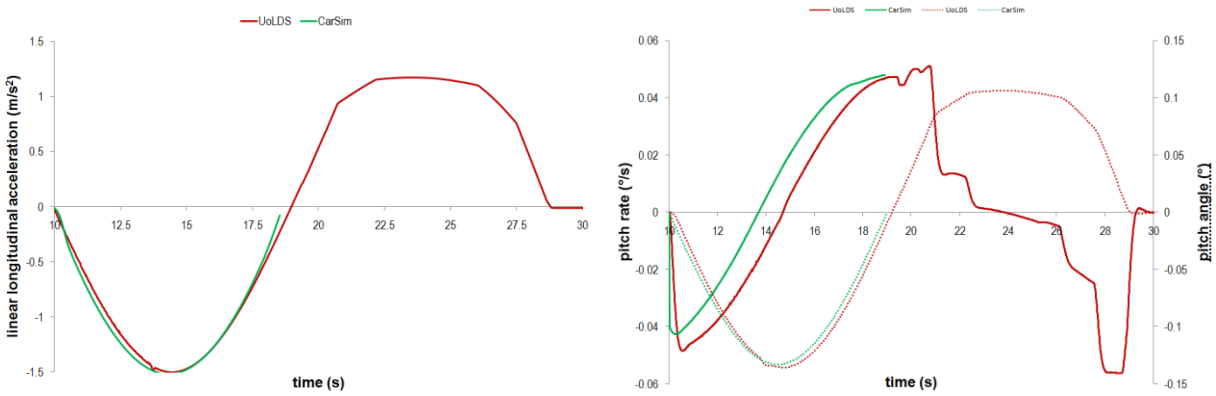

Figure 5-10: UoLDS & CarSim vehicle dynamics outputs: left, linear longitudinal acceleration; right, pitch rate (solid) and pitch angle (dashed)

Figure 5-11 shows the disklogger-recorded linear longitudinal acceleration perceived by the participant driver through tilt-coordination. The demand of the UoLDS vehicle dynamics model (A_x) is closely matched through the motion platform pitch of tilt-coordination.

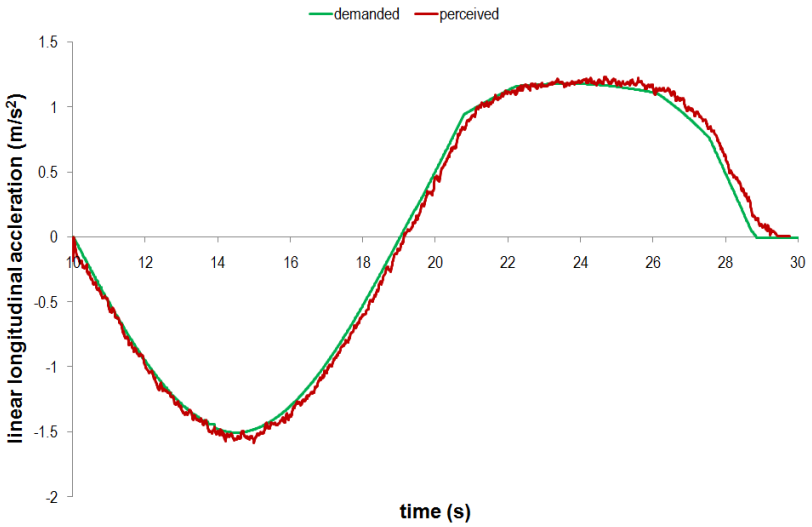

Figure 5-11: demanded & perceived linear longitudinal acceleration

5.1.2.2. Lateral tilt driving scenario

A similar, slowly-developing motion platform rotation, but this time in roll, was also required to assess the scale-factor for lateral platform tilt. Hence, its scenario was also designed at the same driver control input frequency (steering) of 0.333rad/s. Like its lateral translation equivalent, the lateral tilt scenario involved a steering through a section of virtual test-track marked out by cones. However, the lower control input frequency called for a much longer, sweeping S-shaped curve as opposed to the short chicane.

Again, participants were instructed that pre-scripted vehicle control inputs would be made on their behalf that allowed the vehicle to follow the long, S-shaped curve (Figure 5-12, left). The scene was faded-in with the participant "driving" at a constant 60mph, a pre-scripted accelerator position input of 9.4% maintaining the trimmed speed. After 10s at constant forward speed, one cycle of a continuous sinusoidal steering wheel input was made at 0.33rad/s. The amplitude of the sine steer was 6.35° to achieve the designed peak linear lateral acceleration of ±1.5m/s^2. After the 18.85s time period of the steering cycle, the input returned to zero for another 6.15s before the visual scene faded-out to white denoting the end of the 35s scenario.

Figure 5-12 (right) shows a solid parallel in lateral acceleration modelled by the UoLDS vehicle dynamics as a result of the sine-steer, tested against the corresponding CarSim output. Once again, the CarSim output marginally leads its UoLDS equivalent.

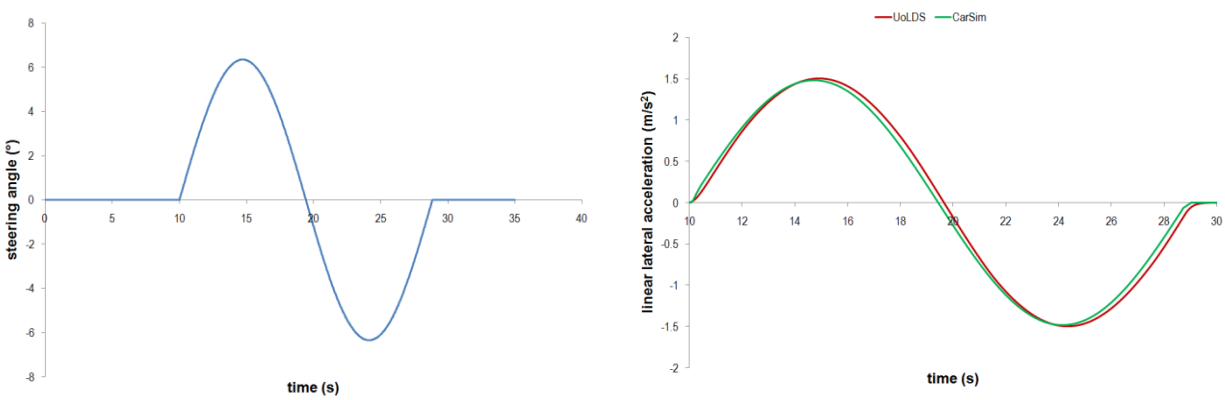

Figure 5-12: pre-scripted lateral control inputs (left) & UoLDS / CarSim vehicle dynamics outputs for linear lateral acceleration (right)

The response of the UoLDS model in roll and yaw is illustrated in Figure 5-13. In each degree-of-freedom, both angular rate and angle remain marginally smaller and slightly more lagged than those estimated by the CarSim model. Nevertheless, the extent of the differences remain slight.

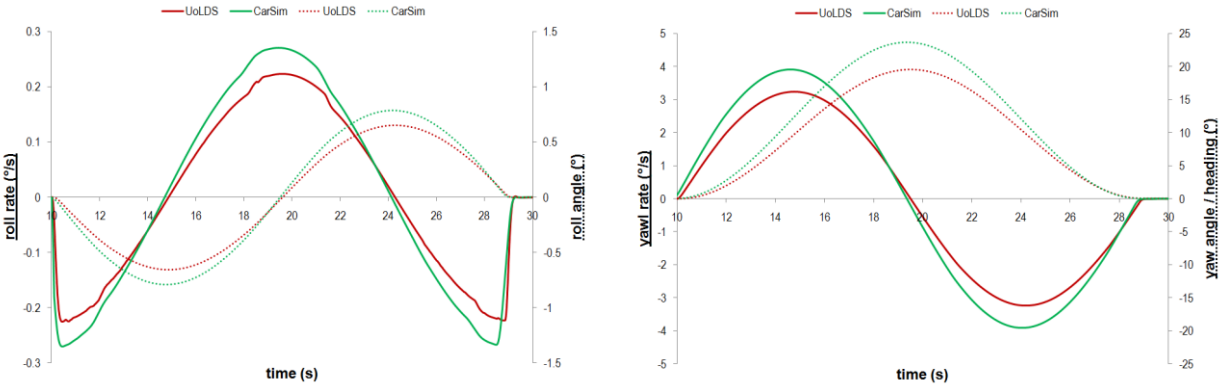

Figure 5-13: UoLDS / CarSim outputs for lateral rotation: left, roll rate (solid) & roll angle (dashed); right, yaw rate (solid) & yaw or heading angle (dashed)

Finally, the perceived linear lateral acceleration felt by the participant driver during the manoeuvre is demonstrated in Figure 5-14, more than adequately matching the UoLDS vehicle dynamics model requirement (A_y).

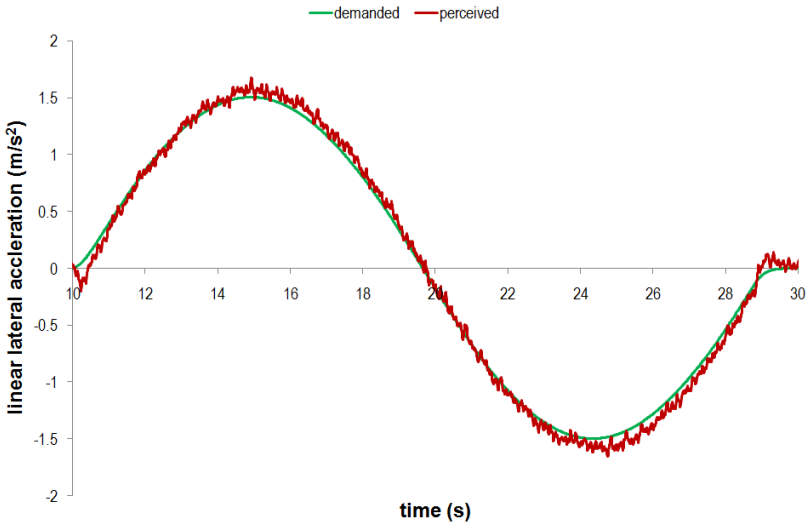

Figure 5-14: demanded & perceived linear lateral acceleration through platform translation

5.2. Participants

Twenty drivers were recruited for Stage 1 with experience provisos that each had to have held a valid U.K. driving licence for at least five years and were currently driving at least 5000 miles (8000km) per annum. Seven of the sample were female. The demographics of the participants is shown in Table 5-1. Payments of £20 were made for participation in Stage 1.

Table 5-1: participant demographics

	age (♂/♀)	years licensed (♂/♀)	annual mileage (♂/♀)
mean	37.1 / 36.6	17.7 / 17.4	8846 / 9286
standard deviation	10.2 / 7.4	11.0 / 7.3	2968 / 1496

5.3. Procedure

Stage 1 was scheduled over two separate, one-hour visits to the simulator. Each visit was split into two sessions. Each session was limited to the experience of either motion platform translation or tilt, with half of the participant sample undertaking translation first and vice versa. Within each visit, the order in which longitudinal or lateral scenarios were presented was also balanced.

On arrival at the simulator participants were briefed on the requirements of the study, their ethical rights, risks and safety measures. On completion of informed consent, they were escorted into the simulator and seated in its vehicle cab with the image generation system showing a full white display. The escorting researcher verbally repeated the characteristics of the requisite driving scenario, emphasising the non-driving nature of the task. Although this implied that no specific practice sessions were required, the researcher did allow a visual demonstration of the scenario, indicating what vehicle controls would have been required had they not been pre-scripted; this was performed without the motion system active. Once the participant fully understood the nature of the study and especially the obligation to indentify the unscaled motion condition within a scenario pair, the researcher departed, leaving the

participant alone in the simulator throughout the session. Once successful intercom communication between researcher and participant had been established, the motion system was activated and the session began.

The appearance of scaled and unscaled motion within a scenario pair was ordered randomly. The initial scale-factor was 0.5. In order to speed up convergence, a slightly modified version of the Levitt procedure was used such that each time the scaled motion was correctly identified, scale-factor was increased by a step size of 0.1. Once the first error was made, the step size was halved and the scale-factor reduced by 0.05. This was the point of the first reversal, where the direction of scale-factor modification changed sense. At this moment, standard Levitt 1 up / 3 down was used such that three consecutively correct responses had to be achieved before any further reductions in scale-factor were made. Any error led to an decrease in scale-factor by the 0.05 step size. The session was terminated after six reversals or thirty scenario pairs, whichever occurred first. The participant's threshold in motion scaling was estimated by taking the mean value of the third and subsequent reversals. An example of the procedure is shown in Figure 5-15, in this case resulting in an estimated scale-factor threshold of 0.91 (the mean of 0.95, 0.9, 0.95 & 0.85)

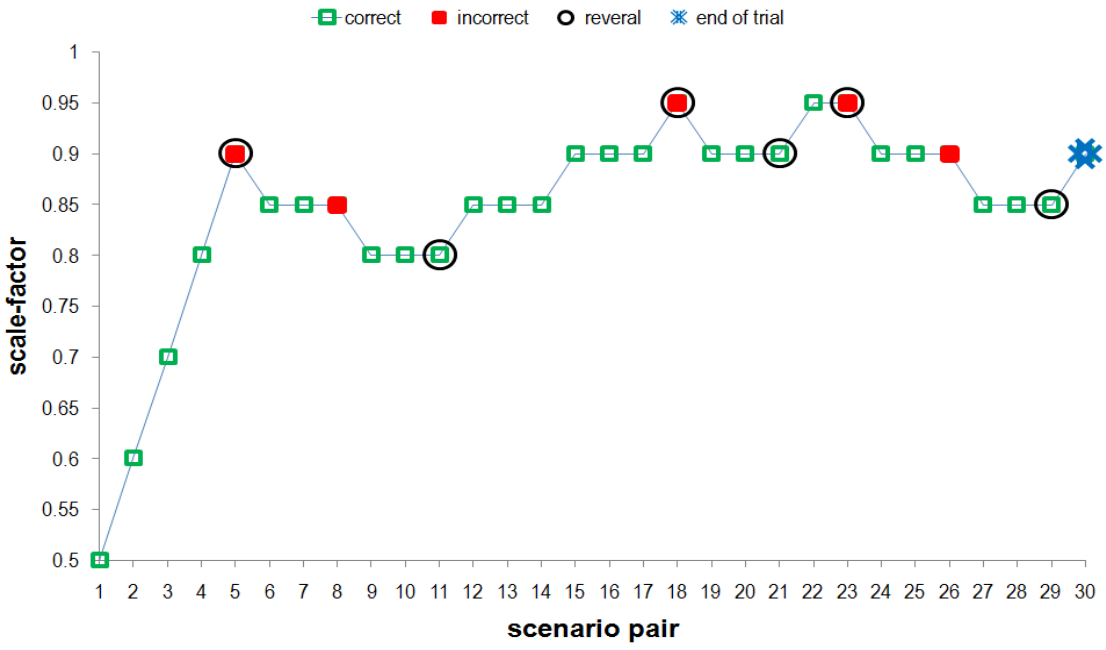

Figure 5-15: example of Levitt 1 up / 3 down Just Noticeable Difference procedure

After a short break away from the simulator, the second session was carried out with participants undertaking the corresponding longitudinal/lateral translation/tilt JND task. After the two one-hour visits required for Stage 1, all four were sessions were completed.

5.4. Results

A repeated-measures ANOVA was undertaken, for two independent variables, each of two levels: Motion System Movement (translation / tilt) and Movement Modality (longitudinal / lateral). The assumptions of ANOVA were not violated in any way, with the resulting maximum perceptible scale-factor threshold (79% detection likelihood) shown in Figure 5-16. The error bars show the 95% confidence intervals of the means displayed.

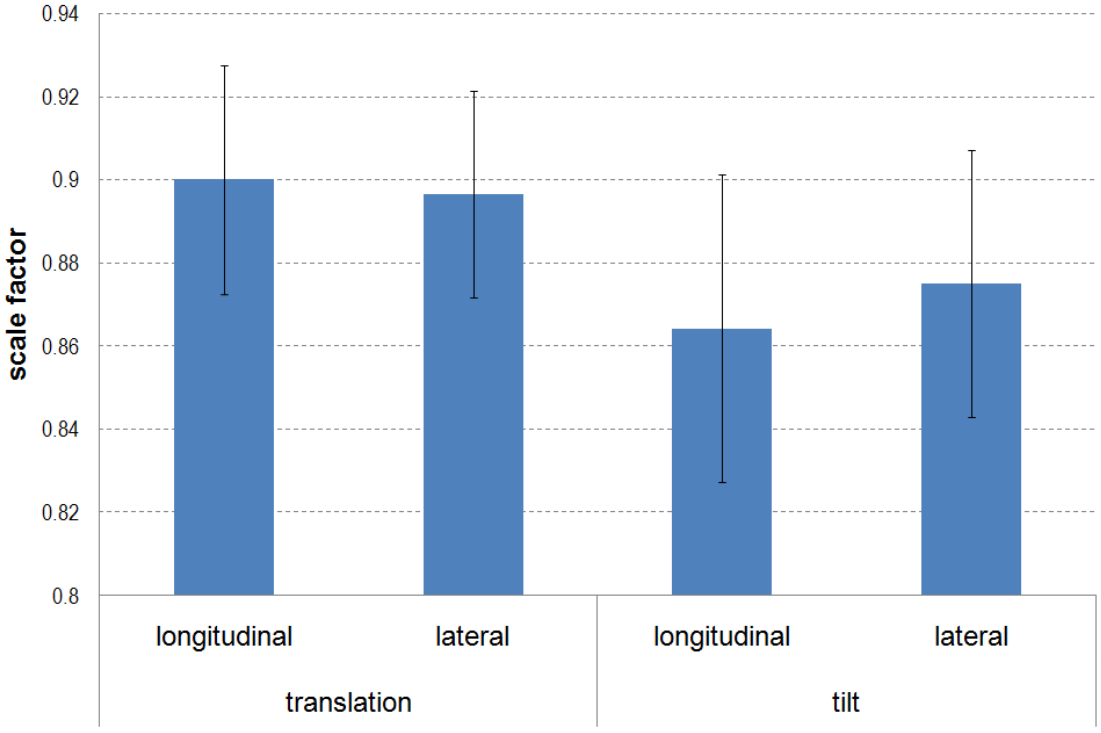

Figure 5-16: maximum perceptible scale-factors for motion system movements in translation & tilt for longitudinal & lateral driving scenarios (error bars 95% C.I.)

Maximum perceptible scale factors were significantly higher in translation that in tilt, $F_{(1,19)}=4.56$, $p=.046$, $\eta^2=.20$ However, there was no significant effect of driving scenario ($F_{(1,19)}=0.098$) nor was there any significant interaction of

motion system movement and scenario ($F_{(1,19)}$=0.198). Hence, for the consideration of maximally-scaled motion conditions in the upcoming experimental investigations of Stage 2 and Stage 3, the same scale-factors were used for both longitudinal and lateral motion, the mean of their respective values to two significaint figures: 0.9 for motion platform translation movements and 0.87 for platform tilt.

5.5. Chapter summary

The chapter justifies the first step in the optimisation of the classical algorithm for research driving simulation: the selection of the overall specific force scale-factor. Through the choice of a pair of pre-scripted driving scenarios and validating the dynamic performance of the simulator to these longitudinal and lateral scenarios, a Just Noticeable Difference experiment was designed and undertaken to evaluate the maximum perceptible scale factors in motion platform translation and tilt. Twenty drivers took part, with results indicating that motion scaling is more noticeable in translational platform movements compared to those involving tilt. The effect size was moderate.

A discussion of the significance of this result is made in conjunction with the rest of the experimental design in Chapter 8. Until then, let us concern ourselves with its impact on the three-staged experimental plan. The main aim of Stage 1 was to inform Stage 2 and facilitate the siting of Motion Reference Point. Due to the lack of any main effect in the modality of the driving task or any interaction of the independent factors, the following scale-factors were carried through to Stage 2 for both lateral and longitudinal scenarios:

- Translation: 0.90
- Tilt: 0.87

CHAPTER 6

EXPERIMENTAL STAGE 2: PAIRED COMPARISON – THE EFFECTS OF MOTION REFERENCE POINT AND TILT RATE ON DRIVERS' TASK PERCEPTION AND PERFORMANCE

By taking into account only the maximum perceptible scale-factor, Stage 1 simply considered the perception of motion through Bode gain: the relationship between the magnitude of the demanded acceleration and the achieved specific force. Stage 2 considered the second vital element in motion cueing, controllability of the simulator resulting from the implementation of its MDA and the consequential filtering of the input acceleration signal. This filtering leads to a phase difference between the demanded and achieved specific forces. Large phase errors result in a significant time delay between the expected and perceived specific forces, rendering the closed-loop driver control process difficult to manage (Reid & Nahon, 1988). Hence rather than riding as observers to a pre-scripted series of control inputs, Stage 2 closed the driver control feedback loop as participants now took on the role of interactive simulator drivers .

Motion cueing in Stage 2 was achieved using the classical algorithm. To begin the process of its optimisation in driving simulation, the overall scale-factors used were based on the maximum perceptible gleaned from Stage 1. This ensured that precious actuator stroke was not unnecessarily utilised in order to produce needlessly high specific forces through overly-scaled motion.

Two independent experimental factors were manipulated in Stage 2: MRP location and the maximum tilt rate achieved during tilt-coordination. MRP location is important to the application of the classical algorithm in driving due to the geometry of a standard hexapod. Theoretically, moving the MRP upwards,

closer to the driver's vestibular system[4], results in a more accurate perception of specific force derived from platform tilt, free of any false translational cues (see section 2.2.3). However, the achievement of a particular tilt angle subsequently requires significantly longer actuator extensions than for a MRP located closer to the upper joint rotation points of the hexapod. Since actuator stroke is limited, MRP location constrains the maximum tilt angle possible and effectively the maximum linear acceleration achievable for driving manoeuvres in the simulator.

Manipulation of the second experimental factor, maximum allowable tilt rate, allowed a simple comparison of the specific force / tilt rate error trade-off. Whilst it is acknowledged that this trade-off is influenced by other concerns such as scale-factor, onset filter performance and available platform translational displacement, at this stage these were held constant prior to their deeper investigation during Stage 3.

6.1. Method

The two independent experimental factors each had two levels:

- *MRP-Location*
  - low (MRP level with hexapod upper rotation datum (see Figure 2-7)
  - high (MRP level with driver's eye-point in the simulator, 1.1m above datum)
- *Maximum-Tilt-Rate*
  - low (0.05rad/s, 2.86°/s)
  - high (0.15rad/s, 8.59°/s)

The four resulting motion cueing conditions were assessed both subjectively through a paired comparison and objectively by an analysis of driver performance measures. Hence, two specifically designed driving scenarios had

[4] Pinpointing a specific location of the vestibular system is in itself difficult, but MRP is typically located to coincide with the driver's head and the design eye-point of the complete simulator.

to be developed, requiring both longitudinal and lateral control of the vehicle, that were sufficiently manageable to allow predictable and repeatable demands on motion cueing whilst allowing a continuous determination of task accomplishment against well-understood vehicle handling criteria. Furthermore, the scenarios had to appear natural and familiar to the participant driver. For these reasons, scenarios analogous to a tracking task were designed that mimicked common driving situations.

6.1.1. Longitudinal scenario

Given that the highest of the two levels of MRP-Location was 1.1m above the motion platform datum, the maximum possible roll and pitch angles achievable by UoLDS's motion system were subsequently limited to just under ±12° (0.209rad). Hence, any driving manoeuvre requiring a corresponding maximum sustained specific force through tilt-coordination could not exceed approximately 0.2g. To allow for extra hexapod actuator excursion in the handling of rotational accelerations by the motion system during the manoeuvre, the driving scenario was further limited to a linear acceleration of 0.15g. Longitudinally, a scenario was developed that required this value in braking by a near step-input of brake activation and resulting deceleration of the simulator vehicle. Laterally, the scenario required a similar acceleration in cornering through a near step-input of steering angle.

6.1.1.1. Longitudinal driving task

The common longitudinal driving situation chosen was braking at a set of traffic-lights. Car following on the approach to the traffic-lights was exploited in order to sufficiently control the degree of braking required.

The participant was seated in the vehicle cab viewing the visual scene as normal, but with the display showing full white. Once both the simulator operator and the participant were ready, the visual scene was faded-in to present a typical two-lane urban road (Figure 6-1) with the participant "driving" at the speed limit of 40mph (64kph). A speed controller maintained this forward speed

regardless of the driver's accelerator input. Another vehicle, also travelling at 40mph was located in front at a distance headway of 17.8m (time headway of 1s). Both vehicles were heading towards a signalised intersection, the state of the traffic-lights always being visible to the simulator driver beyond the low-profile lead vehicle. After 7s at constant speed, the traffic-lights changed from green to amber; 3s later they turned to red. As this moment, the lead vehicle underwent a step deceleration of 1.5m/s^2 in response to the red light and its brakelights illuminated.

Figure 6-1: screenshot taken from the longitudinal paired comparison scenario

Since the parameters of the motion system had to be changed between trials, a process that took approximately 10s, the simulator operator had to indicate to the participant that the next trial was set. At this point, participants were instructed over the simulator's intercom to initiate the scenario when ready by depressing the accelerator pedal. Although they had steering control throughout, they were not informed that, at this stage of the scenario, they did not have full control of the vehicle and were unaware of the operation of the speed controller. During their pre-study briefing, they had been informed that the lead vehicle would decelerate the moment the traffic-light changed to red and at this point to "brake as smoothly as possible, maintaining a constant distance to the car in front". Whilst the driving task was to keep the distance gap stable, in effect it also became matching the step change in deceleration of the lead vehicle, guaranteeing (as much as possible in an interactive simulation)

that the specific force demand of the motion system was equivalent between scenarios. Performance in the tracking task of maintaining distance headway could also be assessed.

After 6.5s on red and with the lead vehicle gradually slowing to 18.2mph (29.3kph), the traffic-lights changed to red/amber and 2s later to green. This was to ensure that a full stop was never required given the difficulties in tilt-coordination that would have arisen from the need to quickly eradicate the developed pitch angle of the motion system. Participants were informed that their task was only to distance match while the lead vehicle was braking. Their task was over once the traffic-lights returned to red/amber. 5s later the visual scene faded-out, returning to full white as the scenario concluded.

This driving situation was presented twice, forming a scenario pair, each trial with a different permutation of MRP-Location and Maximum-Tilt-Rate in order to allow the paired comparison to be made. Participants had been briefed that during each pair the motion system would behave differently. At this point of the trial they were asked “compared to real driving, was the simulation of motion more accurate in the first or second presentation of the scenario pair?” The question had been introduced during their pre-experiment briefing, when they were also told that the visual scene would reinforce the illusion, but that it was important to answer based on their perceived realism, rather than their success in the tracking task of keeping a constant distance headway.

6.1.1.2. Motion system tuning

In order to achieve the two levels of Maximum-Tilt Rate, two different parameter sets of the classical algorithm were drawn up. Labelled $Tilt_{hi}$ for the high Maximum-Tilt-Rate and $Tilt_{lo}$ for the low Maximum-Tilt-Rate, the two parameter sets for the longitudinal driving task are shown in Table 6-1 and Table 6-2. They were obtained by trial and error as a result of objective, off-line tuning through an analysis of the MATLAB/Simulink model of the classical algorithm. Tuning was an iterative process involving two fundamental stages in both the frequency and time domains. No additional parameter sets were

required for the two levels of MRP height (MRP_{hi} and MRP_{lo}) since the demands of the MDA were identical in both situations.

During off-line tuning, the input to the MATLAB/Simulink classical MDA model was the demanded linear acceleration, resulting from the behaviour of the driver in terms of brake pedal application. This was approximated by a model of an "idealised" driver achieving a peak and unvarying braking response sinusoidally over a 250ms period from the start of brake activation. The idealised driver model demanded a peak MDA input acceleration of 1.35m/s^2 (the task-demanded 1.5m/s^2 multiplied by the 0.90 longitudinal scale-factor).

The two levels of Maximum-Tilt-Rate were achieved through varying the cut-off frequency of the second-order low-pass tilt-coordination filter rather than by any non-linear rate-limiting of the filter's output. This ensured a smooth tilt acceleration, free of any jerks caused by rate-limiting. Although only tilt rate was specifically manipulated in the experimental design, tilt acceleration also has perceptible threshold limits and must also be considered in the development of sub-threshold tilt-coordination, especially important in the $Tilt_{lo}$ condition.

First, the filter's damping ratio was set to 1.0, to achieve critically damped motion platform rotation. Next, its cut-off frequency was modified to achieve the maximum desired tilt rate. Other values in the parameter set were then adjusted in order to flatten, as best as possible, the transfer function of the MATLAB/Simulink classical MDA model in the frequency domain. For $Tilt_{hi}$ the output specific force developed much quicker due to the more rapid tilt-coordination. Hence, there was less demand on hexapod and XY-table translation, these parameters being adjusted accordingly to moderate onset cueing. However for $Tilt_{lo}$, onset cueing and resulting platform translation in both degrees-of-freedom had to be maximised to counteract the slow build-up of tilt.

Once the flattest transfer function had been achieved, an assessment was then made of the linear acceleration demand and the specific force achieved by the algorithm as a time history, adjusting the parameter set as required. The

iterative tuning process, assessing off-line the classical MDA performance in both frequency and time domains was continued until the best possible parameter set was achieved.

Table 6-1: the parameter set selected for the condition of high Maximum-Tilt-Rate

$Tilt_{hi}$ parameters		hexapod surge	hexapod pitch	XY-table surge
scale-factor		0.6	0.87	1.1
HP1	cut-off	0.09Hz	N/A	0.001Hz
HP2	cut-off	0.81Hz	N/A	0.12Hz
	damping	1.0	N/A	1.0
LP2	cut-off	N/A	0.48Hz	4.1Hz
	damping	N/A	1.0	1.0

Table 6-2: the parameter set selected for the condition of low Maximum-Tilt-Rate

$Tilt_{lo}$ parameters		hexapod surge	hexapod pitch	XY-table surge
scale-factor		0.6	0.87	1.5
HP1	cut-off	0.08Hz	N/A	0.08Hz
HP2	cut-off	0.35Hz	N/A	0.35Hz
	damping	1.0	N/A	1.0
LP2	cut-off	N/A	0.16Hz	N/A
	damping	N/A	1.0	N/A

The time-consuming tuning process ensured the best available quality of motion cueing for each level of Maximum-Tilt-Rate within the physical constraints of the motion system. However, to ensure that an over-zealous driver response would not jeopardise these excursion limits, the soft-limiters for all three degrees-of-freedom of motion platform movement (see Figure 3-15) were set as shown in Table 6-3. This did limit the specific force that could be felt by the driver for larger brake inputs, but was a necessary evil to make sure the motion system movement avoided unnecessary false cues.

Table 6-3: soft-limiter breakpoints & thresholds protecting motion system excursion

degree-of-freedom	lower breakpoint	lower limit
hexapod surge	-1.8m/s^2	-1.9m/s^2
hexapod pitch	-0.183rad (10.51°) {≡1.8m/s^2}	-0.194rad (11.10°) {≡1.9m/s^2}
XY-table surge	-1.8m/s^2	-1.9m/s^2

The figures below visualise the MATLAB/Simulink classical MDA model in response to longitudinal manoeuvre handled by the idealised driver model. Figure 6-2 illustrates the parameter set associated with $Tilt_{hi}$, whereas Figure 6-3 relates to $Tilt_{lo}$. On the left-hand side of the images, the upper trio of plots (labelled *LP_6DOF*) show the classical MDA demand in hexapod pitch, the middle row (labelled *HP_6DOF*) express the output in hexapod surge and the final three (labelled *XY*) reveal XY-table surge. The columns from left to right show acceleration, velocity and displacement in the three degrees-of-freedom. The right-hand side of the figures show system response. The upper two plots illustrate the Bode plot in the frequency domain whilst the lower one depicts the time history of the input and output of the classical MDA.

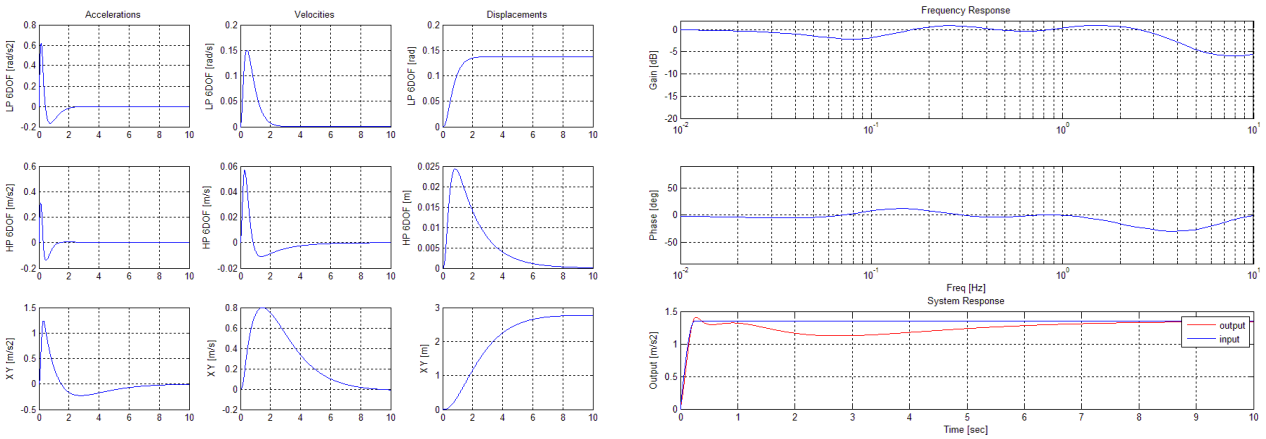

Figure 6-2: classical MDA response for the condition of high Maximum Tilt Rate ($Tilt_{hi}$)

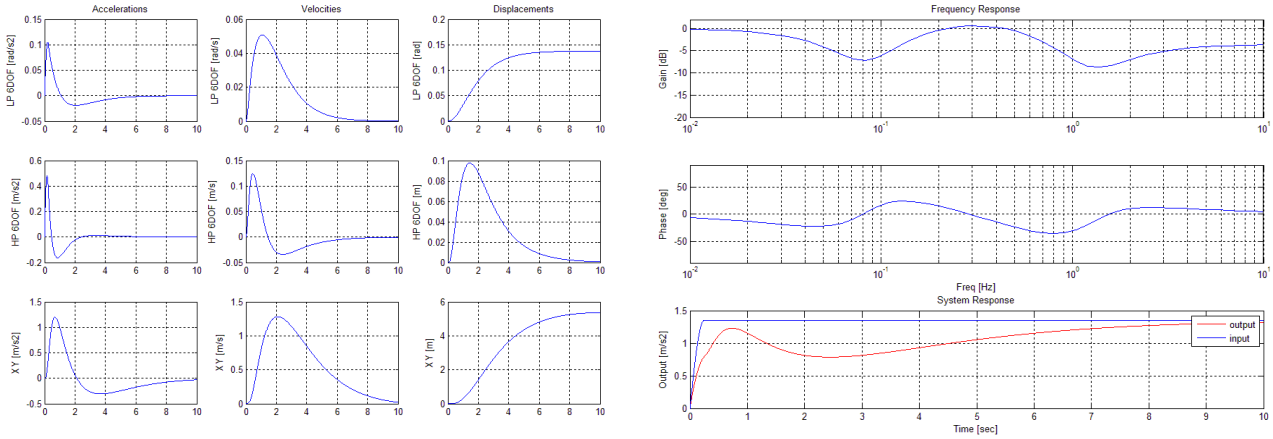

Figure 6-3: classical MDA response for the condition of low Maximum-Tilt-Rate ($Tilt_{lo}$)

The output of $Tilt_{hi}$ portrays the result of minimising specific force error at the expense of pitch rate error. The outcome of rapidly developing pitch angle is a

rather flat transfer function and close correspondence of input and output that, on paper at least, appears superior to the more sluggish efforts of $Tilt_{lo}$. However, $Tilt_{lo}$ adheres to the perceptual thresholds commonly used in tilt-coordination that, in theory, should result in a more acceptable, if delayed, perception of motion to the participant. It does moderate its poor frequency response by the use of additional hexapod and XY-table surge, the latter up to the maximum 5m available in the UoLDS. However, even this extra surge cannot make up for the slow onset of tilt without significant sag in the perceived acceleration throughout the full duration of the manoeuvre.

For each parameter set, high frequency rotational hexapod movement, simulating the vehicle's pitch acceleration during braking, was held constant. This motion was tuned to maximise the perception of motion without the additional pitch angle of the hexapod endangering a position limit. The first and second-order high-pass filter settings selected are outlined in Table 6-4 below.

Table 6-4: first and second-order high-pass filter settings for pitch acceleration input

pitch acceleration parameters		hexapod pitch
scale-factor		0.9
HP1	cut-off	0.001Hz
HP2	cut-off	0.012Hz
	damping	1.0

To have manipulated the performance of the classical MDA to an input rotational acceleration in pitch, as well as the longitudinal linear acceleration, would have seriously over-complicated the experimental design. Furthermore, aside from the initial onset of braking, its impact on the simulation of motion for the remainder of the driving task was minimal. Modelled as a result of the braking response of the idealised driver, the MDA output in pitch acceleration demand and the subsequent perceived rotational acceleration of the hexapod, recorded by its disklogger, are shown in Figure 6-4. The initial spike is from the settling down of the speed controller. The braking manoeuvre is initiated around 13s into the trial. The immediacy of the perceived pitch acceleration is good, but the filtering does tend to sustain the signal for a slightly longer period than required.

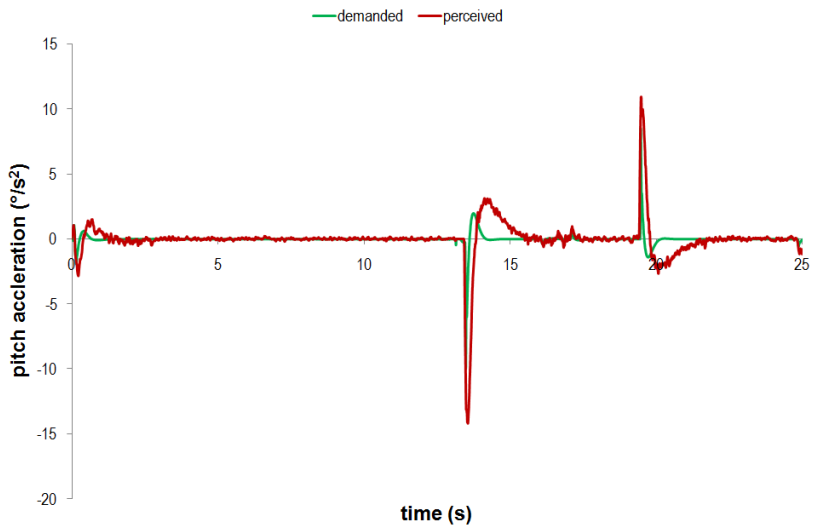

Figure 6-4: performance of the motion system to pitch acceleration demanded by the braking response of the idealised driver model

6.1.1.3. Subjective and objective driving measures

At first, participant's subjective assessment of motion cueing realism was analysed using the non-parametric methods of paired comparison described in Chapter 4. Subsequently, the observed preference data were assembled parametrically using the Bradley-Terry linear model.

Subjective ratings of the quality of motion perception are clearly of interest in order to optimise available motion cueing. Arguably, of greater importance to simulator validity is the predictable behaviour of the driver in the simulator. The longitudinal driving scenario allowed the assessment of driver performance in relation to the specific tracking task. Two measures defined longitudinal task performance:

- Standard deviation of linear longitudinal acceleration (*sd_long_acc*)
- Standard deviation of distance headway (*sd_hwd*)

For *sd_long_acc*, a low value was interpreted to indicate that a smooth deceleration was achieved, in line with the task demand of matching the lead vehicle's constant rate of change of speed. A low value of *sd_hwd* was similarly construed; limited variation in inter-vehicle distance suggests that the task was performed accurately. These data were analysed by ANOVA.

6.1.2. Lateral scenario

Laterally, the controllable driving situation selected was the negotiation of a circular curve requiring a near step-input of steering angle, undeniably a natural and familiar driving task. The curve radius (737.4m) and entry speed (74.4mph) were such that a 1.5m/s^2 linear lateral acceleration would be developed during the handling task. Its tracking element was the stipulation for accurate maintenance of the centre of the driving lane.

6.1.2.1. Lateral driving task

Once motion system parameters had been selected and the participant had indicated their readiness by depressing the accelerator pedal, the visual scene was faded-in to present a typical three-lane motorway (Figure 6-5) with the participant located in the centre of the left-most lane. In order to manage forward speed throughout the 12.7s straight approach to the upcoming left-hand curve and to guarantee that the required lateral acceleration would be achieved during its negotiation, a speed controller maintained the forward speed regardless of the driver's accelerator input. Participants had been briefed to steer the curve "as smoothly as possible, keeping as close as you can to the middle of the lane that you are in".

Figure 6-5: screenshot taken from the lateral paired comparison scenario

Again, this driving situation was presented twice, forming a scenario pair, each trial with a different permutation of MRP-Location and Maximum-Tilt-Rate. As for the longitudinal scenario, after each scenario pair participants were asked to rate which was perceived as the more accurate in terms of the simulation of motion. The same warning was given to base their answers only on perception and not tracking task success.

6.1.2.2. Motion system tuning

For the off-line assessments, the same idealised driver model was used, achieving a peak and stabilised steering response sinusoidally over a 250ms period. The model once again demanded a peak MDA input linear acceleration of 1.35m/s^2 (the task-demanded 1.5m/s^2 multiplied by the 0.9 lateral scale-factor). The symmetrical nature of the UoLDS motion system allowed identical parameters sets for $Tilt_{hi}$ and $Tilt_{lo}$ used for the longitudinal motion platform movements to be redeployed laterally. However, the specific force output of the MDA now obviously demanded hexapod sway, hexapod roll and XY-table sway. The same soft-limiter breakpoints and thresholds protecting motion system excursion were employed as for longitudinal platform movements.

Again, the high frequency rotational hexapod movements, this time simulating the vehicle's roll and yaw accelerations during steering, were not manipulated. Tuning was carried out to maximise motion without risking position limits, the filter settings chosen are shown in Table 6-5.

Table 6-5: first and second-order high-pass filter settings for roll & yaw acceleration

rotational acceleration parameters		hexapod roll	hexapod yaw
scale-factor		0.9	0.9
HP1	cut-off	0.001Hz	0.001Hz
HP2	cut-off	0.012Hz	0.06Hz
	damping	1.0	1.0

Once more, the MDA output of pitch and yaw accelerations were modelled as a result of the response of the idealised driver model. These demands and the

subsequent perceived rotational acceleration of the hexapod, recorded by its disklogger, are shown in Figure 6-6. The left-hand plot shows a good cueing of roll acceleration in the magnitude and timing of its onset, but as the idealised model reaches a steady-state in braking (after ~13s) and on brake release (~20s), there is some delay in the perceived signal reaching zero as quickly as the demand. The timing of yaw acceleration is more accurate, but the output signal does suffer from some attenuation. Whilst tuned as best as possible, the impact of these variations between demanded and perceived rotational accelerations is probably limited since these characteristics of cueing were consistent between trials.

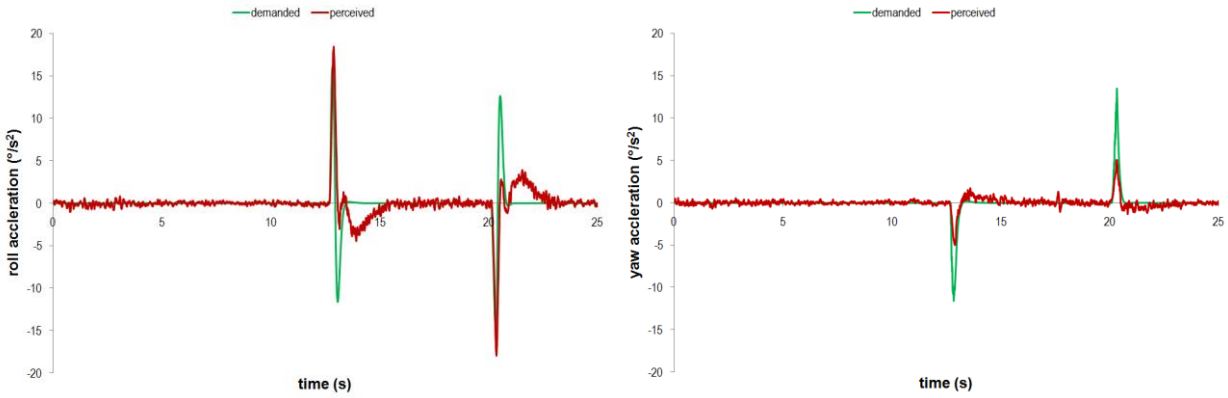

Figure 6-6: performance of the motion system to roll & yaw accelerations demanded by the steering response of the idealised driver model

6.1.2.3. Driving measures

The analysis of participant's subjective assessment of motion cueing realism was identical to that undertaken for the longitudinal driving scenario. Driver performance in relation to the specific lateral tracking task was assessed with three behavioural metrics:

- Standard deviation of linear lateral acceleration (*sd_lat_acc*)
- Standard deviation of lane position (*sd_lp*)
- Minimum time to line crossing (*u_ttlc*)

For *sd_lat_acc*, a low value was taken to indicate that smooth cornering was achieved, in line with the task demand of following the centre of a constant

radius curve at a stable speed. A low value of *sd_lp* was similarly interpreted; limited variation in lane position suggesting accurate task performance.

Time to line crossing (TtLC) is defined as the time to cross either lane boundary with any of the wheels of the vehicle, given its instantaneous path. As the vehicle approaches the edge or centre line of the road, TtLC decreases. TtLC reflects a driver's steering strategy (Godthelp and Konnings, 1981). Contrary to *sd_lat_acc* and *sd_lp*, a high value of u_ttlc indicates good lane tracking and that no lane encroachments are imminent.

6.2. Participants

In an effort to maintain consistency in the ratings offered by the randomly-selected sample, it was the intention that those who took part in Stage 1 would also participate in Stage 2. However, only eighteen of the twenty drivers did so. Both withdrawals (P15, ♂, 44.7yrs and P20, ♀, 41.1yrs) were due to issues of participant availability and the limited data collection epoch available prevented any replacements. Payments of £10 were made for participation.

6.3. Procedure

Stage 2 was scheduled for a single, one-hour visit to the simulator. Each visit was split into two sessions, limited to the experience of either longitudinal or lateral driving tasks. One half of the participant sample undertook braking first with the other half's initial session involving steering.

On arrival at the simulator, participants were briefed on the requirements of Stage 2 and reminded of ethical rights, risks and safety measures. Once again, they were escorted into the simulator and seated in its vehicle cab with the image generation system showing a full white display. The escorting researcher repeated the characteristics of the requisite driving scenario, emphasising the requirements of the task in terms of driver performance. With the motion system

inactive, the researcher allowed two practice trials of the 25s scenario in order to familiarise the participant with the nature and requirements of the driving task. Once the researcher had departed and the motion system was functional, eight more practice sessions were completed, using each of the four conditions of MRP-Location and Maximum-Tilt-Rate twice. This ensured that no particular motion cueing condition became the perceived norm. Furthermore, the order of presentation of motion in practice sessions was balanced within and across participants in a Latin Square.

After the practice session, scenario pairs were presented so that participants could make their paired comparisons of motion cueing based on the question "was the simulation of motion more accurate in the first or second presentation of the scenario pair?". With four cases, six pairs were necessary[5]. The order of the motion condition was balanced for order and carry-over effects across participants as best as possible according to Russell (1980) (Table 6-6).

Table 6-6: semi-balanced motion cueing order for Stage 2

		scenario pair						
		1	2	3	4	5	6	
participant ID	1 / 13	A v D	B v C	D v B	C v A	D v C	B v A	A = $Tilt_{hi}$ MRP_{hi}
	2 / 14	C v D	A v C	B v D	C v B	D v A	A v B	B = $Tilt_{hi}$ MRP_{lo}
	3 / 15	B v D	C v B	D v A	A v B	C v D	A v C	C = $Tilt_{lo}$ MRP_{hi}
	4 / 16	D v C	B v A	A v D	B v C	D v B	C v A	D = $Tilt_{lo}$ MRP_{lo}
	5 / 17	D v A	A v B	C v D	A v C	B v D	C v B	
	6 / 18	D v B	C v A	D v C	B v A	A v D	B v C	
	7 / 19	C v D	A v C	B v D	C v B	D v A	A v B	
	8 / 20	A v D	B v C	D v B	C v A	D v C	B v A	
	9	D v C	B v A	A v D	B v C	D v B	C v A	
	10	D v A	A v B	C v D	A v C	B v D	C v B	
	11	D v B	C v A	D v C	B v A	A v D	B v C	
	12	B v D	C v B	D v A	A v B	C v D	A v C	

[5] If *n* stimuli are compared, $\frac{n(n-1)}{2}$ pairs of stimuli must be presented in a balanced design.

Once the preferences for the six scenario pairs were given and the driving data recorded, following a short break, the second session was carried out with participants undertaking the corresponding longitudinal/lateral scenario.

6.4. Results

Results are presented separately for the longitudinal and lateral driving tasks. For each, both the subjective ratings of motion cueing condition realism and particular driving task performance were assessed. The subjective data were analysed through a Least Significance Difference of the overall rating scores for each motion cueing condition in order to assess the significance of the variation in those scores. In addition, the intra-participant coefficient of consistency was also calculated. The objective data, on the other hand, were analysed through a repeated-measures ANOVA for the driver metrics in question. During the paired comparison, each motion cueing condition was experienced on three separate occasions. The mean of these three was taken as the participant's overall performance for the metric under evaluation.

6.4.1. Longitudinal driving task

6.4.1.1. Subjective measures

The number of times each motion cueing condition was rated as more realistic than a rival in a paired scenario in shown in Figure 6-7.

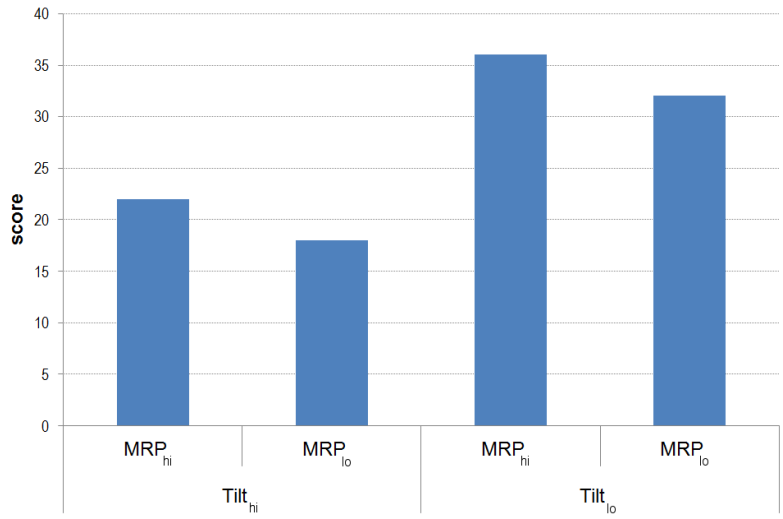

Figure 6-7: score (total number of times rated more realistic than a rival condition)

At the 95% confidence level, Least Significance Difference method suggests that a significant difference between motion condition scores occurs when the critical score difference (m_{crit}) is

$$m_{crit} = Z_{crit}\sqrt{(1/2\, nt^2)} = 1.96\sqrt{1296} \approx 13$$

shows in tabular format where this difference was achieved and hence the motion conditions that varied significantly.

Table 6-7: Least Significant Difference test of scores (significant or non-significant)

	$Tilt_{hi}\ MRP_{hi}$	$Tilt_{hi}\ MRP_{lo}$	$Tilt_{lo}\ MRP_{hi}$	$Tilt_{lo}\ MRP_{lo}$
$Tilt_{hi}\ MRP_{hi}$		n.s.	sig.	n.s.
$Tilt_{hi}\ MRP_{lo}$			sig.	sig.
$Tilt_{lo}\ MRP_{hi}$				n.s.
$Tilt_{lo}\ MRP_{lo}$				

Due to the small number of conditions, only three triads existed. Hence, each participant's coefficient of consistency could only possible equal 0, ½ or 1. Results are shown in Figure 6-8. Six participants demonstrated no consistent triads whilst the remainder were fully consistent. None were removed from the forthcoming development of the Bradley-Terry linear model of subjective data.

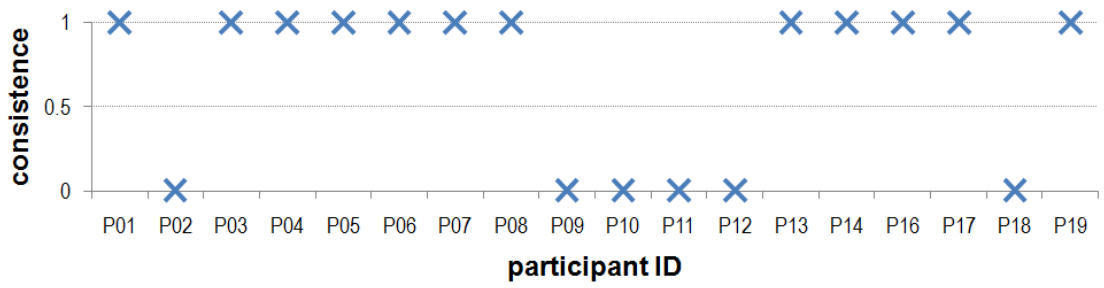

Figure 6-8: inter-participant consistency of ratings

The Bradley-Terry model allowed an assessment of the Noether "merit" value of the four motion cueing conditions on a scale between -1 and +1(Figure 6-9). A test of fit using Maximum Likelihood Ratio theory showed a satisfactory linear model (p=.52).

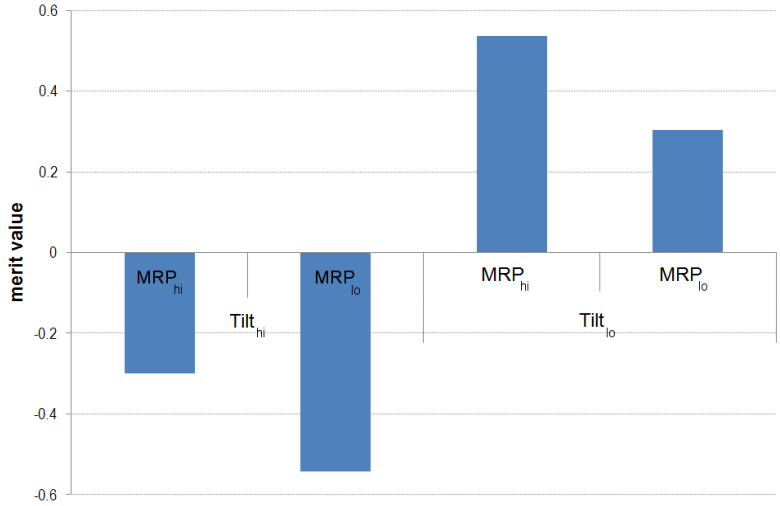

Figure 6-9: merit value of motion cueing conditions

In summary, for Maximum-Tilt-Rate the subjective data indicated that a slow tilt was considered more realistic than a more rapid one. However, there was no suggestion that participants had any preference for, or maybe any awareness of, a shifting in MRP-Location.

6.4.1.2. Objective measures

A repeated-measures ANOVA was carried out for the task performance related dependent variables of standard deviation of longitudinal acceleration (Figure 6-10) and standard deviation of distance headway (Figure 6-11). The error bars show the 95% confidence intervals of the means displayed. Both were normally distributed according to Kolmogorov-Smirnov tests of normality.

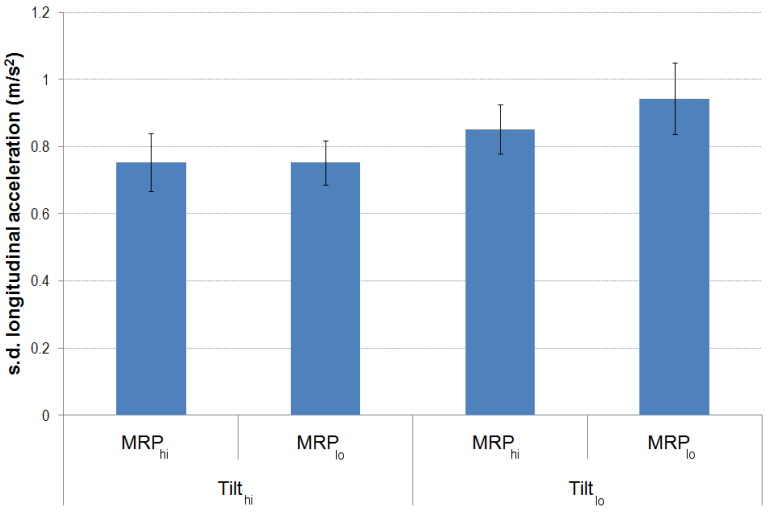

Figure 6-10: standard deviation of longitudinal linear acceleration (error bars 95% C.I.)

There was a very strong main effect of Maximum-Tilt-Rate with significantly poorer task performance demonstrated when tilt rate was slow (*sd_long_acc* = 0.897m/s^2) rather than more rapid (*sd_long_acc* = 0.792m/s^2); $F_{(1,17)}$=17.0, *p*<.001, η^2=.50. There was also a reasonable main effect of MRP-Location with better performance exhibited when the MRP was in the higher (*sd_long_acc* = 0.802 m/s^2) rather than the lower position (*sd_long_acc* = 0.847 m/s^2); $F_{(1,17)}$=4.89, *p*=.041, η^2=.22. No interaction was evident; $F_{(1,17)}$=2.11.

In terms of the variation of inter-vehicle distance, there was a reasonably strong main effect of Maximum-Tilt-Rate with, once again, significantly poorer task performance demonstrated when tilt rate was slow (*sd_hwd* = 1.46m) rather than more rapid (*sd_hwd* = 1.08m); $F_{(1,17)}$=8.03, *p*=.011, η^2=.32. For this metric, there was no main effect of MRP-Location ($F_{(1,17)}$=0.044) nor interaction ($F_{(1,17)}$=1.80).

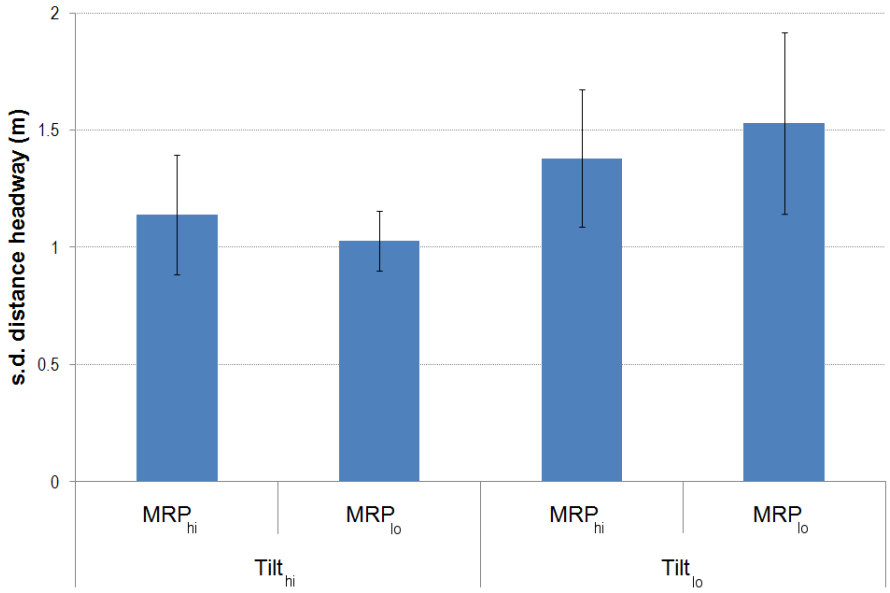

Figure 6-11: standard deviation of distance headway (error bars 95% C.I.)

In contrast to the subjective data, for Maximum-Tilt-Rate both behavioural metrics revealed convincingly that more accurate task performance was achieved in conditions of rapid tilt rather than one that developed more slowly. Drivers also demonstrated smoother braking, in accordance with the task demands, when the MRP-Location was situated closer to their vestibular organs, rather than when it was positioned at the motion platform datum.

6.4.2. Lateral driving task

6.4.2.1. Subjective measures

For the task of lane position maintenance at speed on a motorway, the number of times each motion cueing condition was rated as more realistic than a rival in the paired scenarios in shown in Figure 6-12.

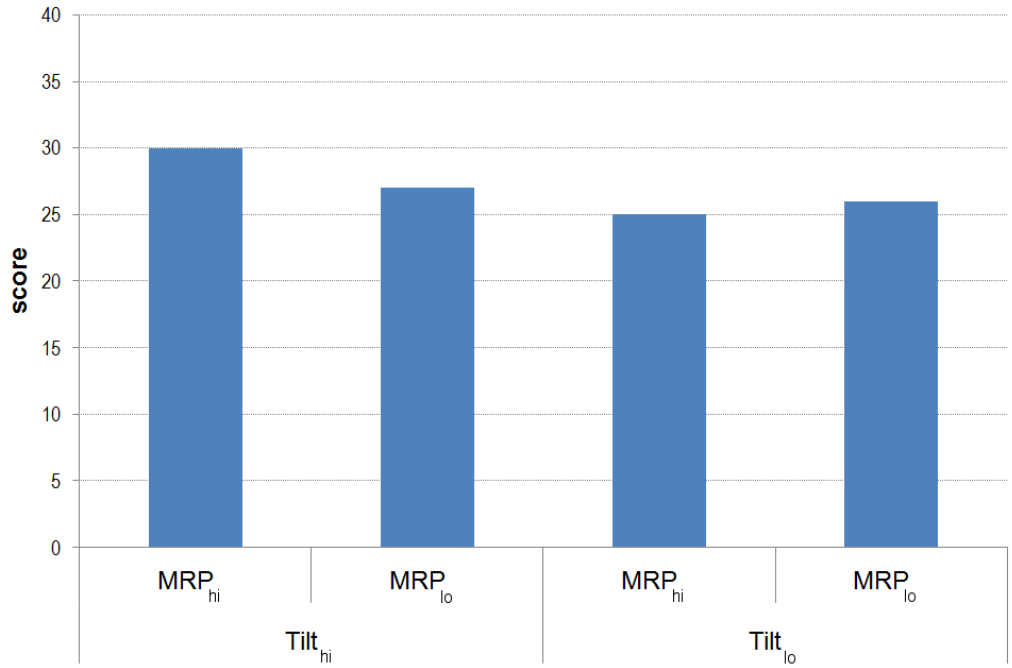

Figure 6-12: score (total number of times rated more realistic than a rival condition)

Since neither the confidence level, the number of conditions, nor the number of judges changed from the longitudinal task, m_{crit} remained at the previously calculated value of 13, much greater than any of the score differences in Figure 6-12. Hence, in terms of perceived realism, there was no significant preference for any of the motion cueing conditions.

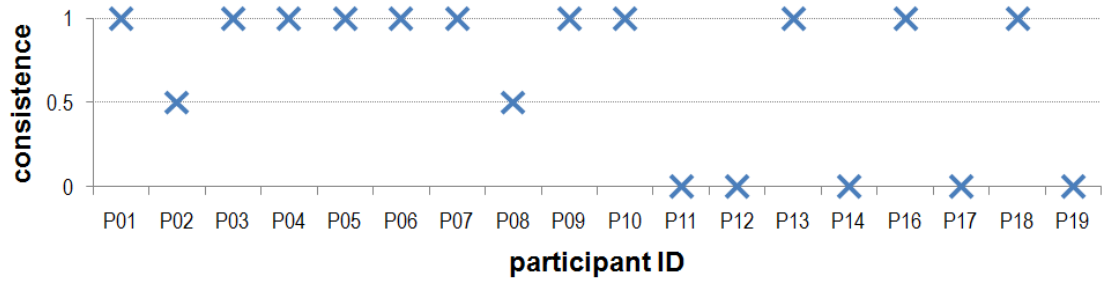

Figure 6-13: participant consistency

In terms of consistency (Figure 6-13), three participants demonstrated no consistent triads, two were 50% consistent, whilst the remainder were fully reliable in their ratings. Again, none were removed from the Bradley-Terry linear model of subjective data (satisfactory test of fit: p=.64) culminating in the Noether merit value (Figure 6-14).

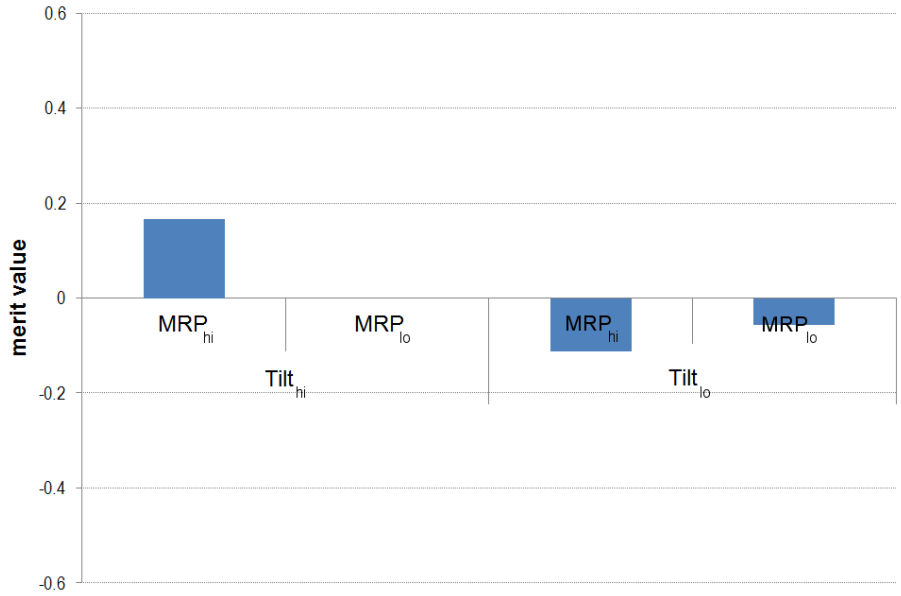

Figure 6-14: merit value of motion cueing conditions

Contrary to the longitudinal braking task, when participants were faced with curve negotiation, neither Maximum-Tilt-Rate nor MRP-Location appeared to have any influence over perceived motion cueing realism.

6.4.2.2. Objective measures

A repeated-measures ANOVA was carried out for the task performance related dependent variables of standard deviation of lateral acceleration (Figure 6-15), standard deviation of lane position and minimum headway. The error bars show the 95% confidence intervals of the means displayed. All motion cueing conditions in all three metrics were normally distributed according to Kolmogorov-Smirnov tests of normality.

With regard to standard deviation of lateral acceleration, there was a marginal (borderline but non-significant at 95%) effect of Maximum-Tilt-Rate

with task performance degraded very slightly when tilt rate was slow (*sd_lat_acc* = 0.448m/s^2) rather than more rapid (*sd_lat_acc* = 0.430m/s^2); $F_{(1,17)}$=3.94, *p*=.064, η^2=.19. There was no effect of MRP-Location ($F_{(1,17)}$=0.480) and most definitely no interaction ($F_{(1,17)}$=0.002).

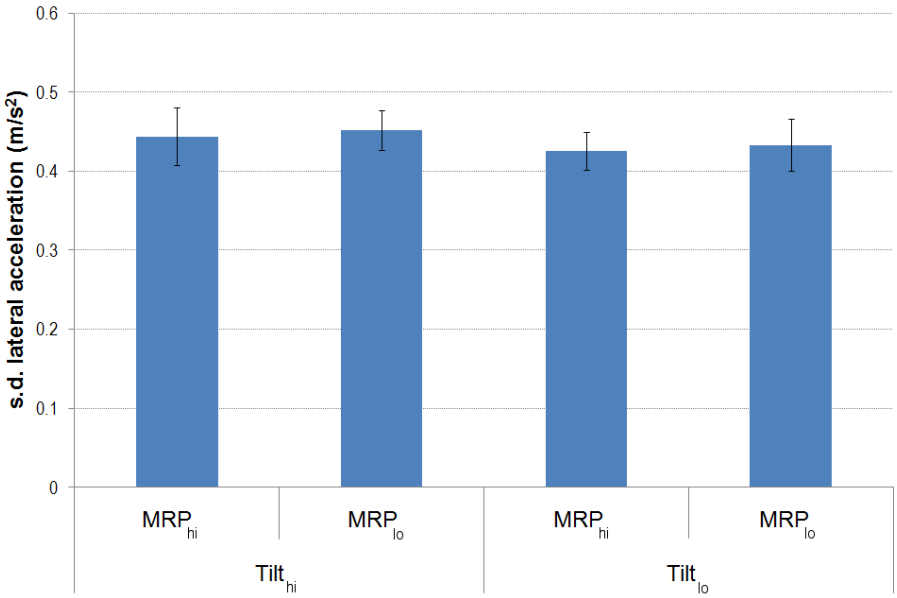

Figure 6-15: standard deviation of lateral linear acceleration (error bars 95% C.I.)

shows the results for the task metrics of standard deviation of lane position (*sd_lp*) and minimum time-to-line-crossing (*u_ttlc*). There was no proven effect of Maximum-Tilt-Rate ($F_{(1,17)}$=0.831) and MRP-Location ($F_{(1,17)}$=0.343) on *sd_lp*. However, there was a significant effect of Maximum-Tilt-Rate on *u_ttlc*, such that lane encroachments were more likely when tilt rate was slow (*u_ttlc* = 1.01s) rather than more rapid (*u_ttlc* = 1.04s); $F_{(1,17)}$=9.09, *p*=.008, η^2=.35.

Table 6-8: standard deviation of lane position (*sd_lp*) & min time-to-line-crossing (*u_ttlc*)

	$Tilt_{hi}$		$Tilt_{lo}$	
	MRP_{hi}	MRP_{lo}	MRP_{hi}	MRP_{lo}
sd_lp (m)	0.154	0.141	0.150	0.170
u_ttlc (s)	1.03	1.05	1.01	1.02

In contrast to the longitudinal braking task, lateral task performance was hardly affected by either Maximum-Tilt-Rate or MRP-Location; only for minimum time-to-line-crossing was any significant difference observed. For this metric,

participants demonstrated an inferior steering performance by coming significantly closer to lane encroachments when experiencing conditions of slow tilt rather than one that developed more rapidly.

6.5. Chapter summary

Every motion system has its own physical displacements limits defined by the constraints of its individual actuators and the movement they are able to afford. Through the use of maximum perceptible scale-factors to achieve maximally-scaled motion without any unnecessary depletion of precious actuator extension, this chapter describes the attempts made in Stage 2 to address the next step in the optimisation of the classical MDA for use in driving simulation: Motion Reference Point location. The study employed MRP-Location as one of two factors in a repeated-measures experimental design, the other independent variable being the manipulation of platform tilt rate in the perceptual trade-off of specific force and tilt rate errors.

The permutation of two levels in each of MRP-Location and Maximum-Tilt-Rate necessitated four different conditions of motion cueing resulting in two different classical MDA parameter sets. The corresponding motion cueing was experienced by participants undertaking two familiar, unexceptional driving tasks in braking and steering. The parameter sets were each tuned to achieve their best possible off-line optimisation of predicted perceived motion during driving task performance. Eighteen drivers took part, with both their subjective assessments of motion cueing realism and objective task performance analysed in a Paired Comparison.

The significance of these results varied considerably depending on the modality of the driving task in question. In braking, whilst participants expressed no preference for a MRP location close to the head, such placement of the MRP did result in marginally better longitudinal task performance. During the same manoeuvres, they also consistently and strongly favoured the development of slow tilt over one that arose more rapidly. However, the fondness for a slow tilt

rate was not borne out by the performance metrics, which indicated, conversely, that the driving task was achieved more accurately in rapid-tilt motion cueing conditions. The lateral task did not show such substantial differences. Participants demonstrated no partiality to any of the motion cueing conditions and only for a single performance measure, minimum time-to-line-crossing, was anything approaching a robust effect unearthed. That result confirmed high Maximum-Tilt-Rate as the most likely to produce more accurate steering performance although its impact was far from substantial in terms of the proportion of that improvement.

A fuller discussion of the significance of Stage 2 results with regard to the rest of the experimental design is made in Chapter 8. But, based predominantly on the longitudinal performance data, a decision was made to fix MRP location at 1.1m above the platform datum level. The scene was now set for the most comprehensive evaluation of the three-staged experimental plan, Stage 3's three-factor optimisation of the perceptual trade-off of specific force and tilt rate errors, the account of which follows in the next chapter.

CHAPTER 7

EXPERIMENTAL STAGE 3: PAIRED COMPARISON – THE EFFECTS OF OVERALL SCALE-FACTOR, TILT RATE AND EXTENDED MOTION PLATFORM DISPLACEMENT ON DRIVERS' PERCEPTION AND TASK PERFORMANCE

With the maximum perceptible scale-factor and most suitable MRP location established, it was now possible to make a more thorough evaluation of the perceptual trade-off of specific force and tilt rate errors. Arguably, motion platform tilt rate, manipulated through the classical MDA's filtering of low frequency specific force input, has the greatest impact on this trade-off due to its significant effect on the speed with which tilt-coordination is developed. However, overall scale-factor also plays a significant role, since its scaling of the desired output reduces specific force error; effectively, less demand is easier to achieve. In a series of laboratory-based studies, perceived self-motion was considered most realistic when motion cues were attenuated from corresponding visual cues by up to two-thirds (Mesland, 1998). In flight simulation, such an approach has also been shown to benefit the perception of longitudinal acceleration during a take-off run (Groen et al., 2001), although scale-factors of between 0.5 and 0.7 are more commonly employed (see Schroeder, 1999, for a review). Conversely, more recent studies undertaken both in driving simulation (Fischer & Werneke, 2008) and those analogous to it (Berger et al., 2010) have suggested that high scale-factors are best employed.

In addition to scale-factor and tilt-coordination, the accuracy and longevity of the onset cue, handled by the classical algorithm high-frequency channel, also significantly affects specific force / tilt rate error. By sustaining the onset cue for

a longer period, less specific force sag is perceptible. This can only be achieved by increasing the available displacement of the motion system in translation. Hence, the final piece in the classical MDA jigsaw is best found from an optimisation of all three of these factors. In combination they characterise the behaviour of the motion system and the inherent role that the classical algorithm plays in driving simulation. This motivation drove the fundamental aim of Stage 3: the appropriate combination of scale-factor, tilt rate and platform translational capacity. In all cases, the onset cue was always realised to some extent through hexapod translation; however, for platform translational capacity, the extra surge and sway provided by UoLDS's XY-table was either exploited or not.

7.1. Method

The resulting three independent experimental factors under manipulation each had two levels:

- *XY*
    - on (XY-table in use)
    - off (XY-table not in use)
- *Maximum-Tilt-Rate*
    - low (0.05rad/s, 2.86°/s)
    - high (0.15rad/s, 8.59°/s)
- *Scale-Factor*
    - Low (0.50)
    - High (0.87)

The rationale for the selection of XY was made at the start of this chapter. Maximum-Tilt-Rate was considered for a second time due to potential interactions with the third independent variable, Scale-Factor, and its associated ability to reduce specific force errors by limiting the demand. The resulting eight conditions of motion cueing are represented throughout this chapter by the abbreviations defined in Table 7-1.

Table 7-1: motion cueing condition abbreviations

abbreviation	XY	Max.-Tilt-Rate	Scale-Factor
$XY_{on}Tilt_{hi}SF_{hi}$	on	high	high
$XY_{on}Tilt_{hi}SF_{lo}$	on	high	low
$XY_{on}Tilt_{lo}SF_{hi}$	on	low	high
$XY_{on}Tilt_{lo}SF_{lo}$	on	low	low
$XY_{off}Tilt_{hi}SF_{hi}$	off	high	high
$XY_{off}Tilt_{hi}SF_{lo}$	off	high	low
$XY_{off}Tilt_{lo}SF_{hi}$	off	low	high
$XY_{off}Tilt_{lo}SF_{lo}$	off	low	low

As in Stage 2, the motion cueing conditions were assessed subjectively through a paired comparison and objectively by an analysis of driver performance measures. The same longitudinal and lateral driving tasks were also employed. The MRP was located 1.1m above the platform datum level in line with the findings of Stage 2.

7.1.1. Motion system tuning

To achieve the required motion cueing conditions, eight different parameter sets of the classical algorithm were defined. These were tuned using the MATLAB/Simulink classical MDA model and the same idealised driver model as in Stage 2. Hence, each parameter set was optimised for best performance given the constraints of the independent variable manipulations The symmetrical nature of the UoLDS motion system allowed identical parameters sets to be utilised for both longitudinal and lateral motion platform movement.

7.1.1.1. *Parameter set for $XY_{on}Tilt_{hi}SF_{hi}$*

The Parameter set for $XY_{on}Tilt_{hi}SF_{hi}$ was typified by a low specific force error achieved through compromising tilt rate error. As a result, the Bode plot shows a relatively flat transfer function as the output specific force is achieved quickly through a combination of rapid tilt and strong onset cueing, requiring a XY-table displacement of almost 3m in the process.

$XY_{on}Tilt_{hi}SF_{hi}$ parameters		hexapod translation	hexapod rotation	XY-table translation
scale-factor		0.6	0.87	1.1
HP1	cut-off	0.09Hz	N/A	0.001Hz
HP2	cut-off	0.79Hz	N/A	0.12Hz
	damping	1.0	N/A	1.0
LP2	cut-off	N/A	0.48Hz	4.1Hz
	damping	N/A	1.0	1.0

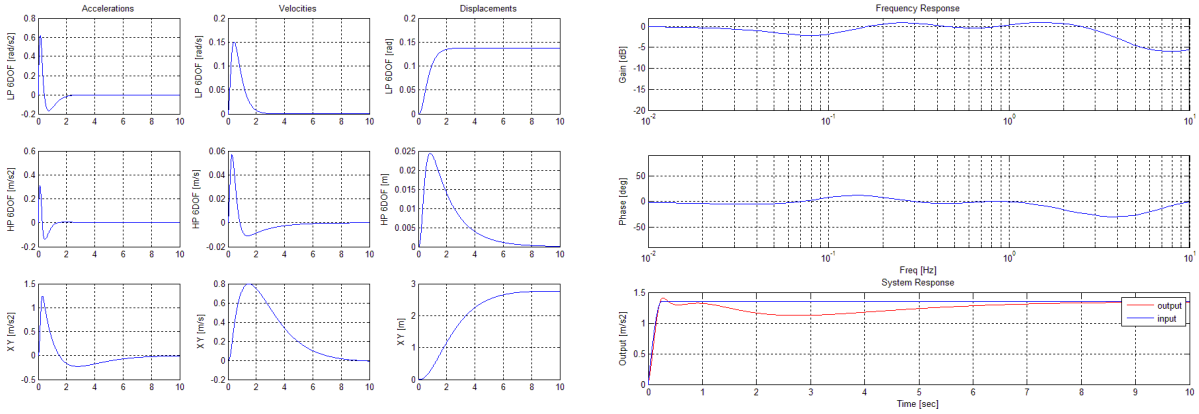

7.1.1.2. Parameter set for $XY_{on}Tilt_{hi}SF_{lo}$

$XY_{on}Tilt_{hi}SF_{lo}$ showed a more rapid conversion to the required steady-state conditions than when a higher scale factor was used. As a result of this reduced specific force error, its Bode plot is flatter.

$XY_{on}Tilt_{hi}SF_{lo}$ parameters		hexapod translation	hexapod rotation	XY-table translation
scale-factor		0.6	0.5	0.35
HP1	cut-off	0.09Hz	N/A	0.001Hz
HP2	cut-off	0.79Hz	N/A	0.12Hz
	damping	1.0	N/A	1.0
LP2	cut-off	N/A	0.89Hz	4.1Hz
	damping	N/A	1.0	1.0

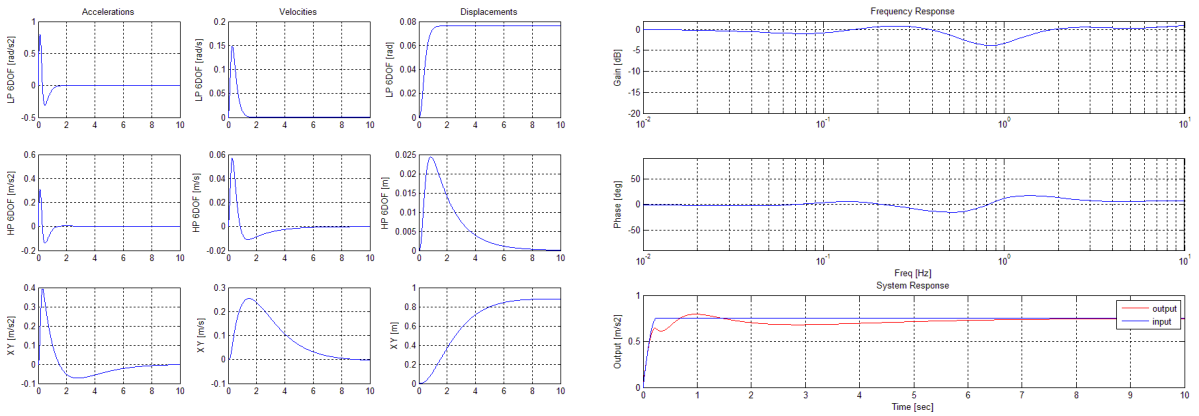

7.1.1.3. Parameter set for $XY_{on}Tilt_{lo}SF_{hi}$

The response of $XY_{on}Tilt_{lo}SF_{hi}$ demonstrated the typical sag associated with slowly developing tilt-coordination. Its Bode plot shows significant gain and phase errors around the 0.07Hz and 1Hz input frequencies and the underlying specific force takes quite some time to build up. These errors were mitigated as much as possible by the use of the maximum 5m available XY-table excursion.

$XY_{on}Tilt_{lo}SF_{hi}$ parameters		hexapod translation	hexapod rotation	XY-table translation
scale-factor		0.6	0.87	1.5
HP1	cut-off	0.09Hz	N/A	0.001Hz
HP2	cut-off	0.35Hz	N/A	0.10Hz
	damping	1.0	N/A	1.0
LP2	cut-off	N/A	0.16Hz	0.80Hz
	damping	N/A	1.0	1.0

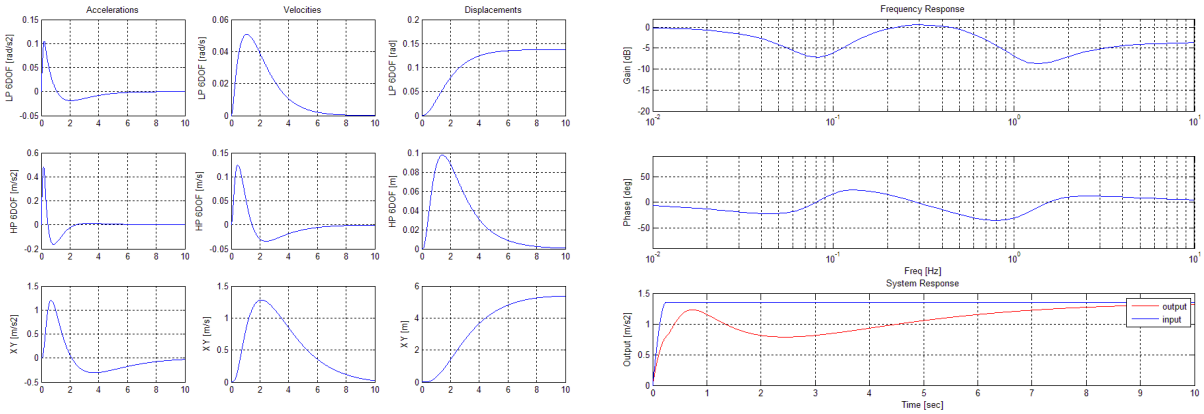

7.1.1.4. Parameter set for $XY_{on}Tilt_{lo}SF_{lo}$

In comparison to its highly scaled equivalent, $XY_{on}Tilt_{lo}SF_{lo}$ boasts a better frequency response due to the reduced specific force demanded. Apart from increased sag, its response does not differ all that much from the corresponding high tilt rate condition $XY_{on}Tilt_{hi}SF_{lo}$ due to the impact of the XY-table.

$XY_{on}Tilt_{lo}SF_{lo}$ parameters		hexapod translation	hexapod rotation	XY-table translation
scale-factor		0.6	0.5	0.85
HP1	cut-off	0.09Hz	N/A	0.001Hz
HP2	cut-off	0.35Hz	N/A	0.11Hz
	damping	1.0	N/A	1.0
LP2	cut-off	N/A	0.28Hz	1.04Hz
	damping	N/A	1.0	1.0

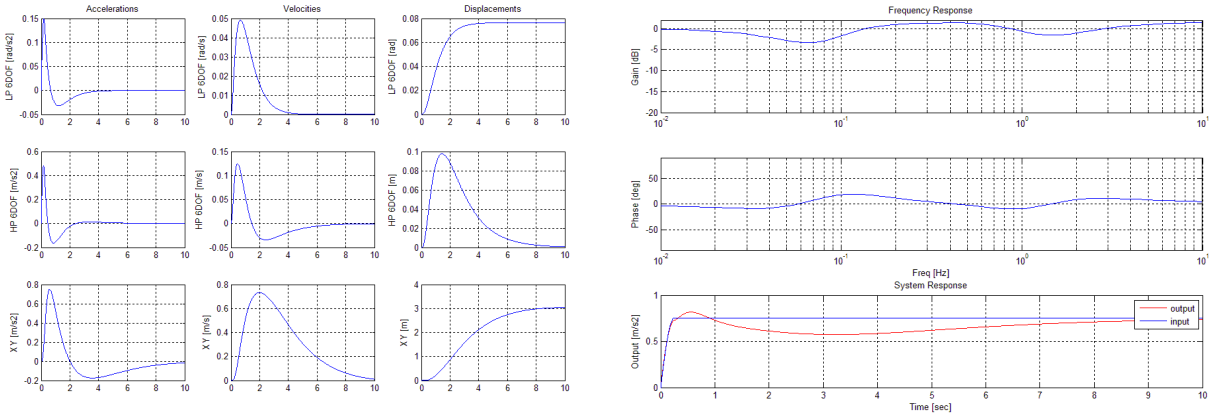

7.1.1.5. Parameter set for $XY_{off}Tilt_{hi}SF_{hi}$

The impact of no additional translational capacity afforded by the XY table is immediately apparent for $XY_{off}Tilt_{hi}SF_{hi}$. Even though hexapod translation has been maximised, the Bode plot shows a considerable attenuation and phase lag around the 0.5Hz region. This is characterised in the time history by a specific force that takes around 2s to reach the desired level, despite the high tilt rate.

$XY_{off}Tilt_{hi}SF_{hi}$ parameters		hexapod translation	hexapod rotation	XY-table translation
scale-factor		0.6	0.87	0.0
HP1	cut-off	0.09Hz	N/A	N/A
HP2	cut-off	0.35Hz	N/A	N/A
	damping	1.0	N/A	N/A
LP2	cut-off	N/A	0.48Hz	N/A
	damping	N/A	1.0	N/A

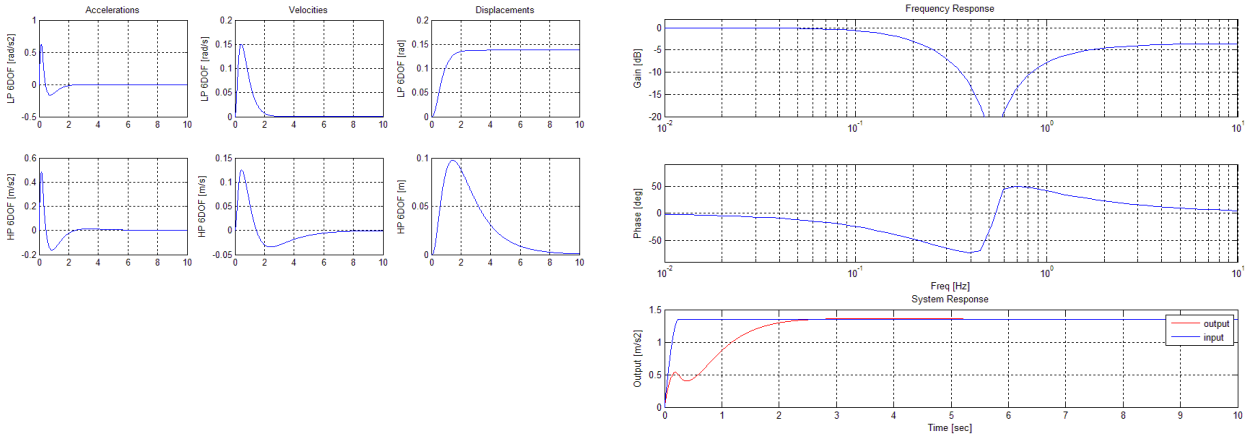

7.1.1.6. Parameter set for $XY_{off}Tilt_{hi}SF_{lo}$

For $XY_{off}Tilt_{hi}SF_{lo}$, lowering the scale factor does mitigate somewhat the poor frequency response associated with no XY-table movement, personified by a much flatter Bode plot. However, in terms of onset cueing, it does not differ at all from its highly scaled cousin $XY_{off}Tilt_{hi}SF_{hi}$.

$XY_{off}Tilt_{hi}SF_{lo}$ parameters		**hexapod translation**	**hexapod rotation**	**XY-table translation**
scale-factor		0.6	0.5	0.0
HP1	cut-off	0.09Hz	N/A	N/A
HP2	cut-off	0.35Hz	N/A	N/A
	damping	1.0	N/A	N/A
LP2	cut-off	N/A	0.89Hz	N/A
	damping	N/A	1.0	N/A

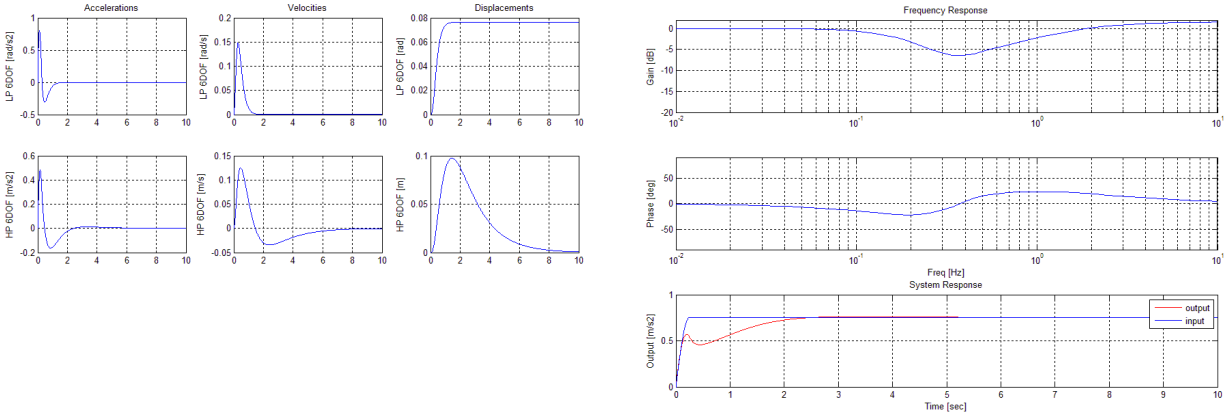

7.1.1.7. Parameter set for $XY_{off}Tilt_{lo}SF_{hi}$

$XY_{off}Tilt_{lo}SF_{hi}$ is epitomised by one of the least flat frequency response of all eight of the motion cueing conditions, suggesting awkward motion cueing at best. Limited translation and slow tilt combine to result in a very laboured development of specific force.

$XY_{off}Tilt_{lo}SF_{hi}$ parameters		**hexapod translation**	**hexapod rotation**	**XY-table translation**
scale-factor		0.6	0.87	0.0
HP1	cut-off	0.09Hz	N/A	N/A
HP2	cut-off	0.35Hz	N/A	N/A
	damping	1.0	N/A	N/A
LP2	cut-off	N/A	0.16Hz	N/A
	damping	N/A	1.0	N/A

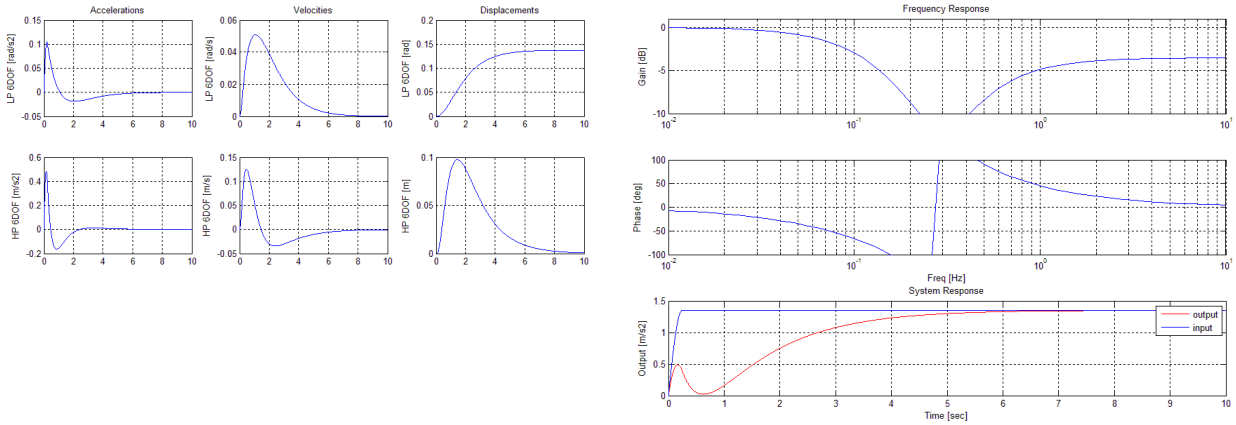

7.1.1.8. Parameter set for $XY_{off}Tilt_{lo}SF_{lo}$

In terms of its off-line assessment, the unfortunate frequency response of $XY_{off}Tilt_{lo}SF_{hi}$ is marginally enhanced by a reduced scale-factor. That said, there is still a significant sag in the perceived specific force, although the reduced demand does allow the output to reach the input somewhat more promptly.

$XY_{off}Tilt_{lo}SF_{lo}$ parameters		hexapod translation	hexapod rotation	XY-table translation
scale-factor		0.6	0.5	0.0
HP1	cut-off	0.09Hz	N/A	N/A
HP2	cut-off	0.35Hz	N/A	N/A
	damping	1.0	N/A	N/A
LP2	cut-off	N/A	0.28Hz	N/A
	damping	N/A	1.0	N/A

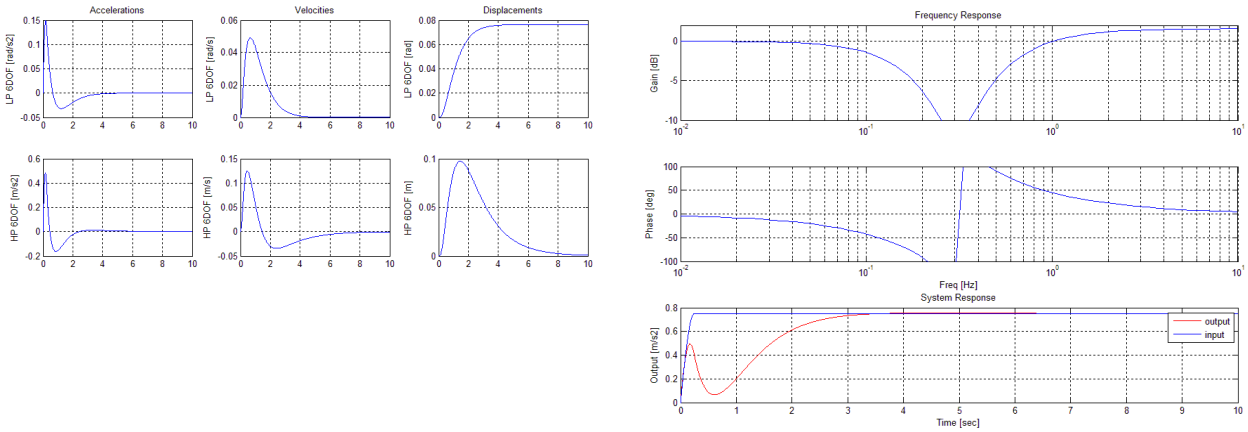

7.2. Participants

The same eighteen drivers who took part in Stage 2 also formed the population sample for Stage 3. Due to the increased duration of the study (see next section), payments of £20 were made for participation.

7.3. Procedure

Stage 3 involved two one-hour sessions, limited to the experience of either longitudinal or lateral driving tasks. One half of the participant sample undertook braking first with the other half's initial session involving steering.

On arrival at the simulator, participants did not receive a formal written briefing since their requirements were identical to Stage 2. However, when seated in the simulator, the researcher did allow one motionless practice scenario to provide a re-familiarisation with the driving task. This was supplemented by four further practice trials in four of the eight motion cueing conditions, different from one another and allocated at random.

After the practice session, the experimental paired scenarios began in one of four pre-defined sequences outlining the order of presentation of the various motion cueing conditions. A central, single sequence was exactly balanced for order and carry-over effects according to Russell's balanced paired comparison design (1980). This was reversed for a second ordering. Finally, a third and fourth sequence were found by alternating the order of presentation of a condition within a specific scenario pair (Table 7-2). Table 7-2 also demonstrates how, for each participant, these four sequences were presented for each modality of the two driving tasks. The result was the quasi-counterbalancing of the motion cueing conditions witnessed during Stage 3.

The large number of scenario pairs resulted in a one-hour experimental session. Hence, to alleviate participant fatigue and boredom, a short break was allowed at the half-way stage, after the presentation of scenario pair 14.

Table 7-2: quasi-counterbalanced motion cueing condition presentation order

		motion cueing condition order sequence				
		I	II	III	IV	
scenario pair	1	A v D	F v E	E v F	D v A	A = $XY_{on}Tilt_{hi}SF_{hi}$
	2	B v E	H v D	D v H	E v B	*B* = $XY_{on}Tilt_{hi}SF_{lo}$
	3	C v H	B v G	G v B	H v C	*C* = $XY_{on}Tilt_{lo}SF_{hi}$
	4	F v G	C v A	A v C	G v F	*D* = $XY_{on}Tilt_{lo}SF_{lo}$
	5	E v A	F v H	H v F	A v E	*E* = $XY_{off}Tilt_{hi}SF_{hi}$
	6	D v B	D v E	E v D	B v D	*F* = $XY_{off}Tilt_{hi}SF_{lo}$
	7	F v C	C v G	G v C	C v F	*G* = $XY_{off}Tilt_{lo}SF_{hi}$
	8	H v G	A v B	B v A	G v H	*H* = $XY_{off}Tilt_{lo}SF_{lo}$
	9	A v F	G v E	E v G	F v A	
	10	H v B	D v C	C v D	B v H	
	11	C v E	F v B	B v F	E v C	
	12	D v G	H v A	A v H	G v D	
	13	G v A	E v H	H v E	A v G	
	14	C v B	D v F	F v D	B v C	
	15	F v D	B v C	C v B	D v F	
	16	H v E	A v G	G v A	E v H	
	17	A v H	G v D	D v G	H v A	
	18	B v F	E v C	C v E	F v B	
	19	C v D	B v H	H v B	D v C	
	20	E v G	F v A	A v F	G v E	
	21	B v A	G v H	H v G	A v B	
	22	G v C	C v F	F v C	C v G	
	23	E v D	B v D	D v B	D v E	
	24	H v F	A v E	E v A	F v H	
	25	A v C	G v F	F v G	C v A	
	26	G v B	H v C	C v H	B v G	
	27	D v H	E v B	B v E	H v D	
	28	E v F	D v A	A v D	F v E	

		first session	second session
participant. ID	P1 / P5 / P9 / P13 / P17	longitudinal I	lateral II
	P2 / P6 / P10 / P14 / P18	lateral I	longitudinal II
	P3 / P7 / P11 / P19	longitudinal III	lateral IV
	P4 / P8 / P12 / P16	lateral III	longitudinal IV

7.4. Results

Results are presented separately for the longitudinal and lateral driving tasks. As in Stage 2, the subjective data were analysed through a Least Significance Difference of the overall ratings and the objective data by repeated-measures ANOVA. The mean of all seven experiences of each motion cueing condition was taken as the participant's metric of task performance for each dependent variable under evaluation.

7.4.1. Longitudinal driving task

7.4.1.1. Subjective measures

The number of times each motion cueing condition was rated as more realistic than a rival in a paired scenario is illustrated in Figure 7-1.

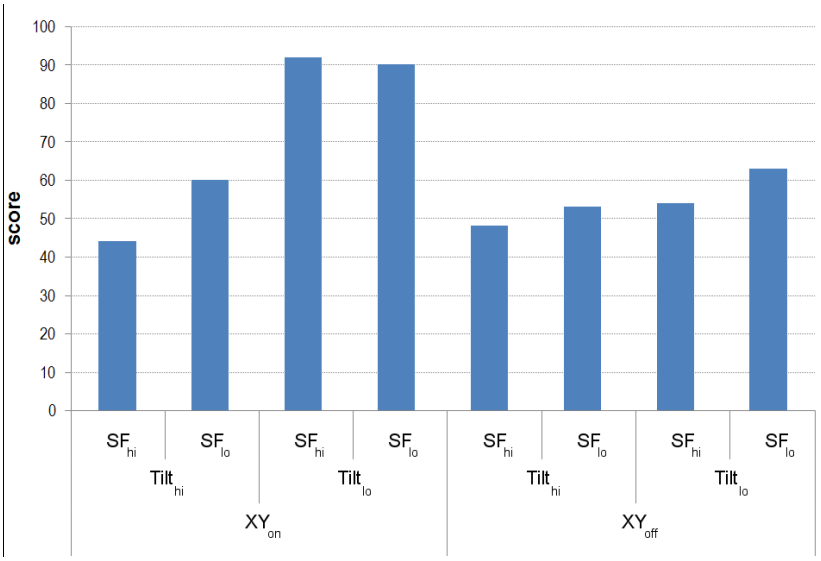

Figure 7-1: motion cueing score (total number of times rated over a rival condition)

At the 95% confidence level, Least Significance Difference method suggests that the critical score difference (m_{crit}) is

$$m_{crit} = Z_{crit}\sqrt{(1/2\, nt^2)} = 1.96\sqrt{2592} \approx 17$$

The columns and rows of Table 7-3 represent the eight differing motion cueing conditions. The relationship between any two can be found from the corresponding column/row entry. Significant differences were achieved when the difference in condition score equalled or exceeded the m_{crit} value.

Table 7-3: Least Significant Difference test of scores (n.s. or sig. at 95% confidence level)

			XY_{on}				XY_{off}			
			$Tilt_{hi}$		$Tilt_{lo}$		$Tilt_{hi}$		$Tilt_{lo}$	
			SF_{hi}	SF_{lo}	SF_{hi}	SF_{lo}	SF_{hi}	SF_{lo}	SF_{hi}	SF_{lo}
XY_{on}	$Tilt_{hi}$	SF_{hi}		n.s.	sig.	sig.	n.s.	n.s.	n.s.	sig.
		SF_{lo}			sig.	sig.	n.s.	n.s.	n.s.	n.s.
	$Tilt_{lo}$	SF_{hi}				n.s.	sig.	sig.	sig.	sig.
		SF_{lo}					sig.	sig.	sig.	sig.
XY_{off}	$Tilt_{hi}$	SF_{hi}						n.s.	n.s.	n.s.
		SF_{lo}							n.s.	n.s.
	$Tilt_{lo}$	SF_{hi}								n.s.
		SF_{lo}								

On average, participants demonstrated a very reasonable 59.4% consistency in their rating of motion cueing condition realism, illustrated individually in Figure 7-2. Four participants (P6, P8, P10 and P18) found the task particularly tricky, only managing a reliability of around 15%. They were not, however, excluded from the analysis.

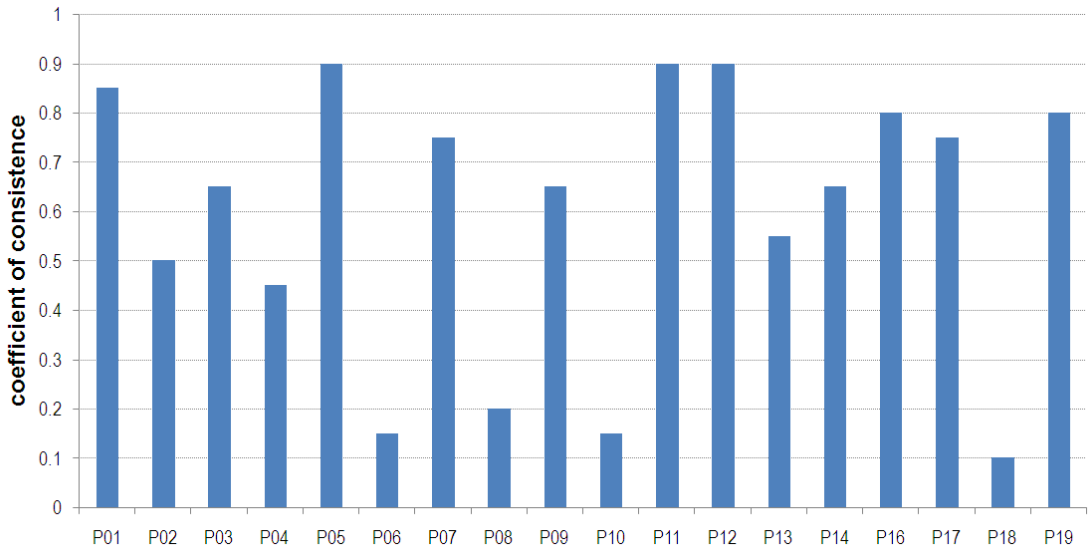

Figure 7-2: inter-participant consistency of ratings

Fitting a Bradley-Terry linear model to the subjective ratings revealed that the null hypothesis indicating an equality of objects could be rejected with a high degree of confidence (p=1.39x10^{-11}). An application of Maximum Likelihood Ratio theory demonstrated a satisfactory test of fit the model using (p=.37). The resulting assessment of the Noether merit value for each of the eight motion cueing conditions, on a linear scale between -1 and +1, is illustrated in Figure 7-3.

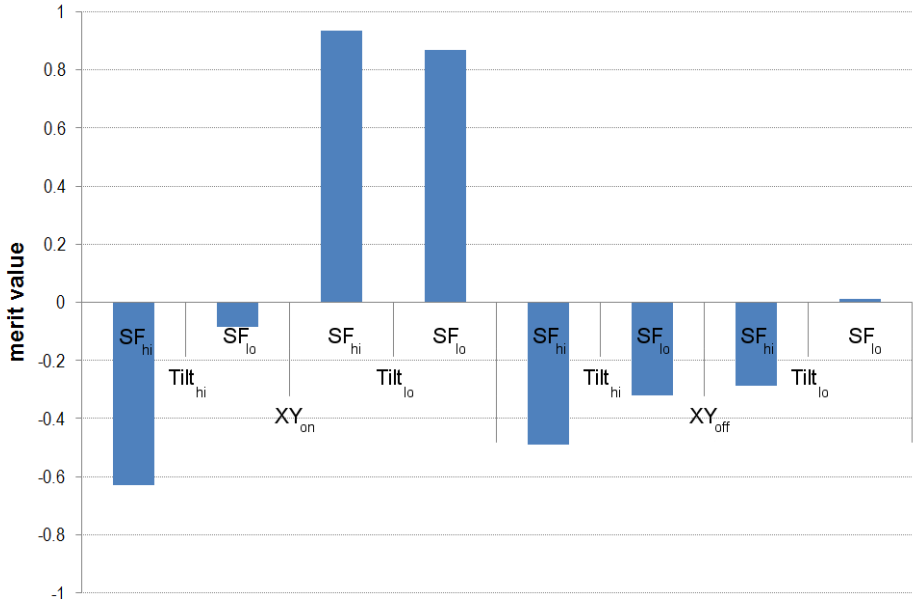

Figure 7-3: merit value of motion cueing conditions

Overall, the subjective data indicated a strong preference, in terms of more realistic motion cues, for the low Maximum-Tilt-Rate than a more rapid development of tilt angle. However, this was the case only when the slow tilt was supplemented by extended motion platform translation, made available by the XY-table. In the other six motion conditions, there was a general inclination towards the lower of the two Scale-Factors, but this effect never reached statistical significance at the 95% confidence level.

7.4.1.2. Objective measures

A repeated-measures ANOVA was carried out for the task performance related dependent variables of standard deviation of longitudinal acceleration (Figure 7-4) and standard deviation of distance headway (Figure 7-5). The error

bars show the 95% confidence intervals of the means displayed. Both were normally distributed according to Kolmogorov-Smirnov tests of normality.

Regarding driving task success as inversely proportional to the variability of longitudinal acceleration (*sd_long_acc*), there were very strong main effects for all three experimental factors. First, performance was superior when extended translational movement was available during the onset cue (0.758m/s^2), compared to when the XY-table was not active (0.876m/s^2); $F_{(1,17)}$=25.6, p<.001, η^2=.60. There was also less variation in braking when tilt rate was rapid (0.756m/s^2) rather than more slow (0.879m/s^2); $F_{(1,17)}$=47.2, p<.001, η^2=.74. Finally, there was also a considerable benefit of reducing the specific force demand, smoother braking being demonstrated when the motion was unscaled (0.791m/s^2) compared to scaled (0.843m/s^2); $F_{(1,17)}$=18.2, p<.001, η^2=.52.

In addition to the main effects, there was also a significant interaction of Maximum-Tilt-Rate and Scale-Factor. When tilt-coordination was slow, task performance was similar with unscaled (0.878m/s^2) and scaled motion (0.881m/s^2). However, as tilt rate increased, braking performance was more inconsistent with a scale-factor of 0.5 (0.806m/s^2) rather than in conditions of no effective scaling (0.704m/s^2); $F_{(1,17)}$=5.86, p=.030, η^2=.25.

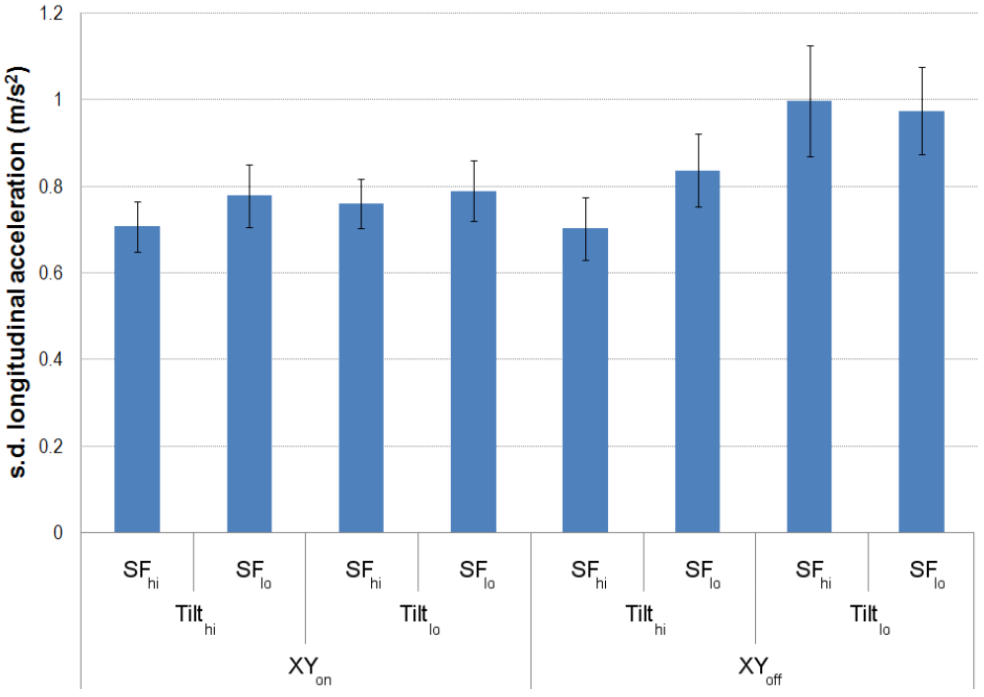

Figure 7-4: standard deviation of longitudinal linear acceleration (error bars 95% C.I.)

All three factors were again heavily implicated in the successful undertaking of the braking task when it was considered in terms of the variation of following distance (*sd_hwd*). Performance was enhanced when the XY-table was active (1.73m), compared to when it was not (1.97m); $F_{(1,17)}$=17.0, p<.001, η^2=.50. Braking was also less varied with rapid tilt (1.67m) compared to slow tilt (2.03m); $F_{(1,17)}$=16.2, p<.001, η^2=.49. Finally, the observed main effect of Scale-Factor was also considerable: braking was more uniform when the scale-factor was high (1.60m) than when the output specific force was reduced by 50% from its input (2.10m); $F_{(1,17)}$=57.0, p<.001, η^2=.77.

Along with the main effects, there was a significant interaction, however this time for Maximum-Tilt-Rate and XY. The deterioration in performance associated with a reduction in tilt rate was far more substantial when the XY-table was not operational (from 1.71m to 2.23m) compared to when it was active (from 1.63m to 1.83m); $F_{(1,17)}$=6.27, p=.023, η^2=.27.

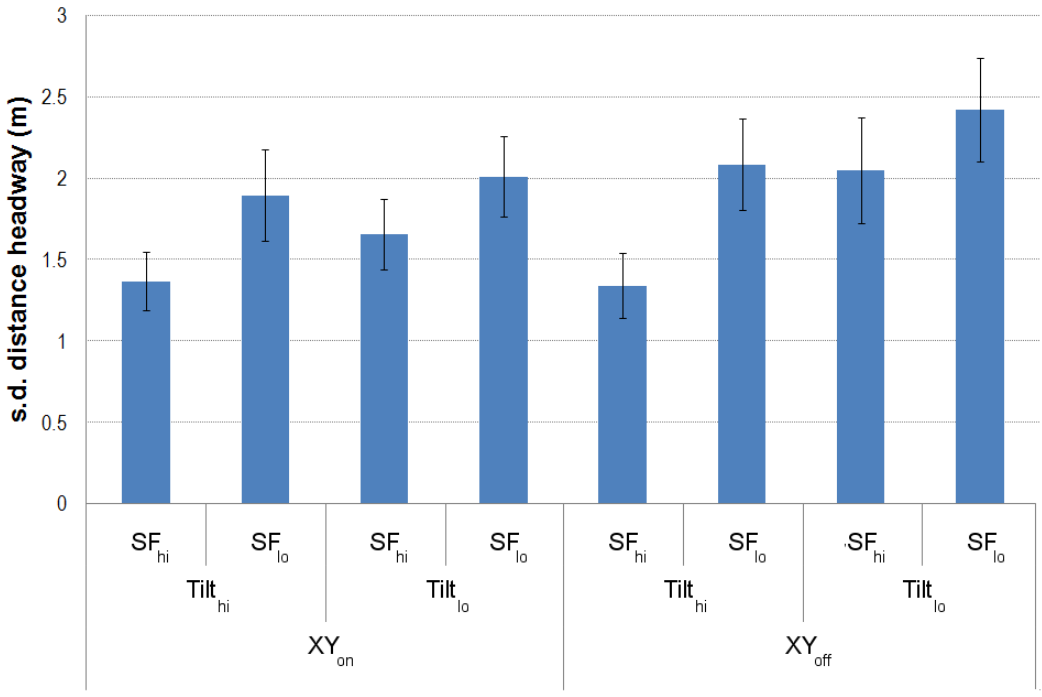

Figure 7-5: standard deviation of distance headway (error bars 95% C.I.)

In summary, the behavioural results observed during the longitudinal task contrasted with the subjective ratings of perceived realism. In accordance with the task demands, drivers demonstrated smoother braking and less variation in following distance when experiencing conditions of rapid tilt rate rather than when tilt developed at the accepted thresholds of tilt perception. Additionally, both behavioural metrics revealed a more accurate performance when participants felt extended transitional motion, afforded by the increased displacement capacity of the XY-table. Finally, motion cues that were effectively unscaled (Scale-Factor fixed at the maximum threshold of perceptibility observed during Stage 1) also resulted in superior braking task performance. The size of these main effects of all three factors on both dependent variables were highly convincing.

The interactions of Maximum-Tilt-Rate also proved to be reasonably strong. When tilt rate was low, braking was equally smooth regardless of the Scale-Factor selected. Increasing tilt rate to a value well above perceptual threshold generally improved performance, but by a greater degree when the Scale-Factor was also high. Similarly, Maximum-Tilt-Rate interacted significantly with XY for both measures of longitudinal task performance. When the onset motion cues experienced during braking were enhanced by the extra translational capacity of the XY-table, variations in Maximum-Tilt-Rate had little impact on the task. However, without the benefits of extended motion, braking task performance became worse as tilt rate was reduced from high to low.

7.4.2. Lateral driving task

7.4.2.1. Subjective measures

For the experience of motion cues during the lateral steering task of maintaining lane position at speed, the number of times each motion cueing condition was rated as more realistic than a rival during the paired scenarios is shown in Figure 7-6.

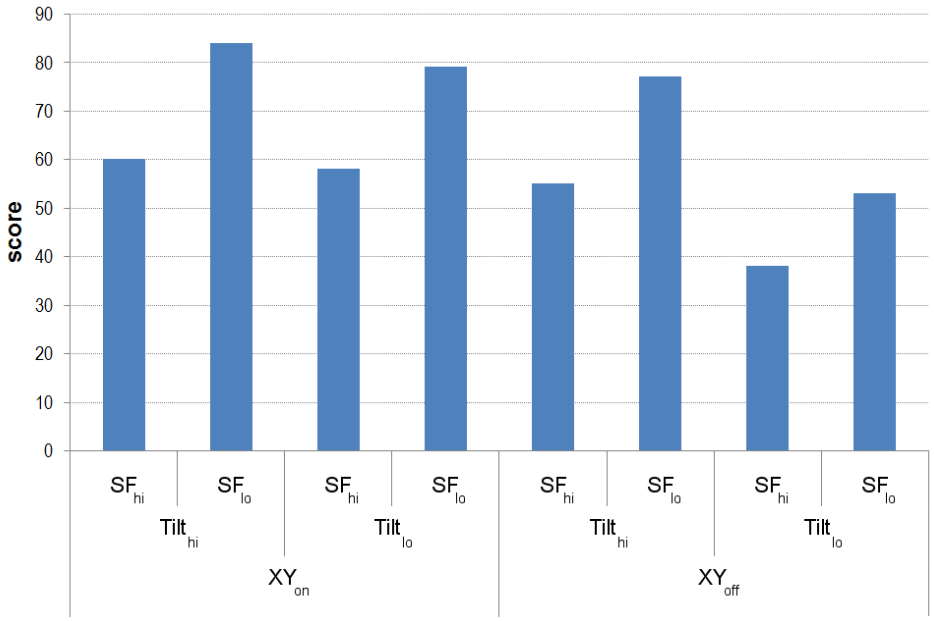

Figure 7-6: motion cueing score (total number of times rated over a rival condition)

Since neither confidence level, number of conditions nor number of judges changed from the longitudinal task, m_{crit} remained at the previously calculated value of 17 for significant score difference at 95% confidence (Table 7-4).

Table 7-4: Least Significant Difference test of scores (n.s. or sig. at 95% confidence level)

			XY_{on}				XY_{off}			
			$Tilt_{hi}$		$Tilt_{lo}$		$Tilt_{hi}$		$Tilt_{lo}$	
			SF_{hi}	SF_{lo}	SF_{hi}	SF_{lo}	SF_{hi}	SF_{lo}	SF_{hi}	SF_{lo}
XY_{on}	$Tilt_{hi}$	SF_{hi}		sig.	n.s.	sig.	n.s.	sig.	sig.	n.s.
		SF_{lo}			sig.	n.s.	sig.	n.s.	sig.	sig.
	$Tilt_{lo}$	SF_{hi}				sig.	n.s.	sig.	sig.	n.s.
		SF_{lo}					sig.	n.s.	sig.	sig.
XY_{off}	$Tilt_{hi}$	SF_{hi}						sig.	sig.	n.s.
		SF_{lo}							sig.	sig.
	$Tilt_{lo}$	SF_{hi}								n.s.
		SF_{lo}								

On average, participants demonstrated 55.8% consistency in their ratings of motion cueing condition realism, illustrated individually in Figure 7-7. The overall sample is reasonably consistent and none were removed from the analysis.

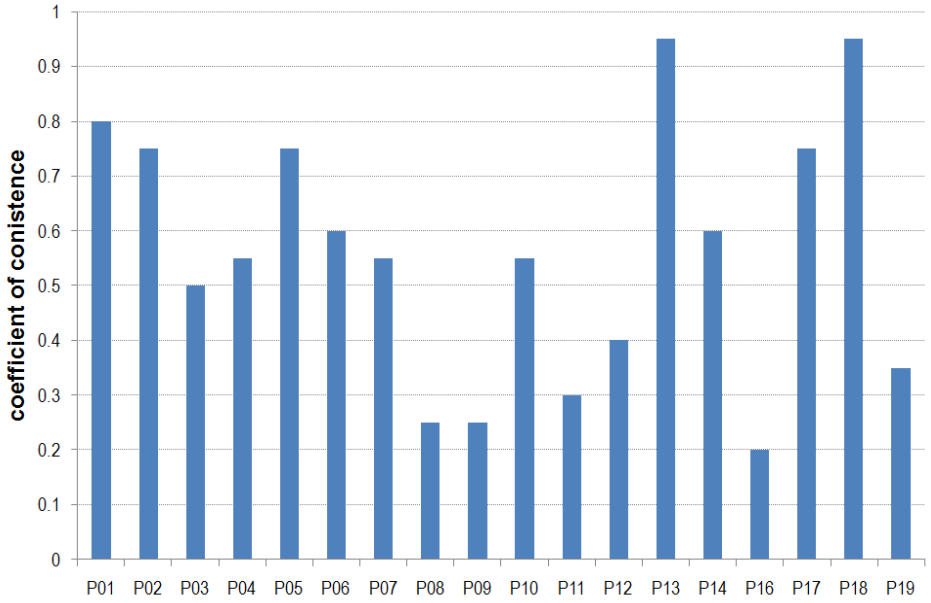

Figure 7-7: inter-participant consistency of ratings for lateral task

A Bradley-Terry model of the subjective data revealed that the variations made to the parameters sets of the eight motion cueing conditions did impact significantly perceived realism; p=1.93x10^{-8}. The model fitted the observed data reliably (p=.85) and allowed an assessment of the Noether merit value of the four motion cueing conditions illustrated in Figure 7-8.

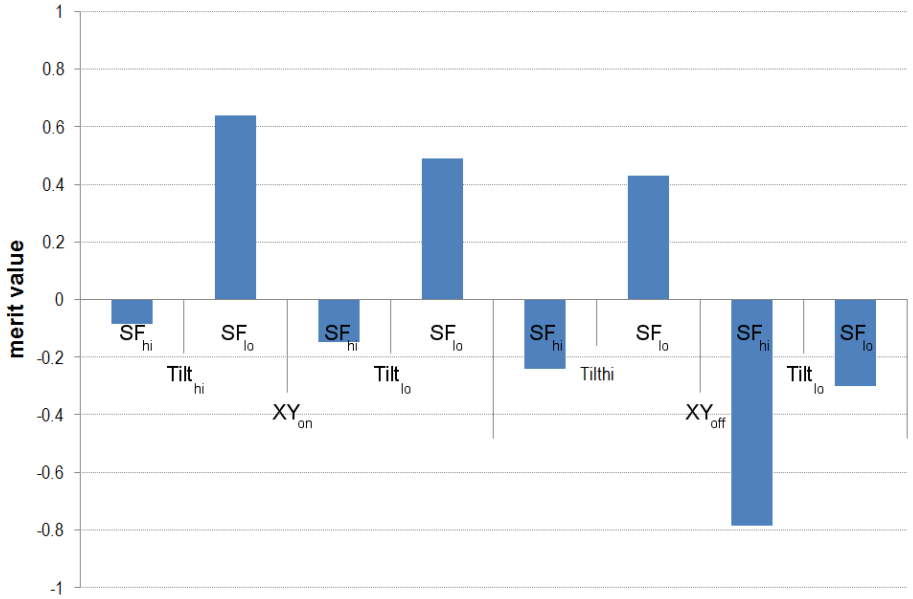

Figure 7-8: merit value of motion cueing conditions

On the whole, for the lane keeping task, the consistent subjective data indicated a strong preference in terms of perceived realism for motion cues scaled by 50%, especially when supplemented by the extended motion platform translation capabilities afforded by the XY-table. However, for the handling manoeuvres required, Maximum-Tilt-Rate had no impact on participant ratings.

7.4.2.2. Objective measures

A repeated-measures ANOVA was carried out for the dependent variables related to lateral task performance, namely standard deviation of lateral acceleration (Figure 7-9), standard deviation of lane position (Figure 7-10) and minimum time-to-line-crossing (Figure 7-11). All three metrics for each condition were normally distributed according to Kolmogorov-Smirnov tests of normality.

With regard to standard deviation of lateral acceleration (*sd_lat*), there was a very marginal main effect of XY, with task performance very slightly improved when the XY-table was operating (0.447m/s^2) rather than inoperative (0.465m/s^2); $F_{(1,17)}$=4.20, p=.056, η^2=.20. However, there was a stronger effect of Maximum-Tilt-Rate. When tilt rate was slow, participants displayed increased variation in lateral acceleration (0.462m/s^2) rather than when a more rapid tilt was experienced (0.450m/s^2); $F_{(1,17)}$=6.64, p=.020, η^2=.28. There was no effect of Scale-Factor ($F_{(1,17)}$=1.52) nor any significant interactions.

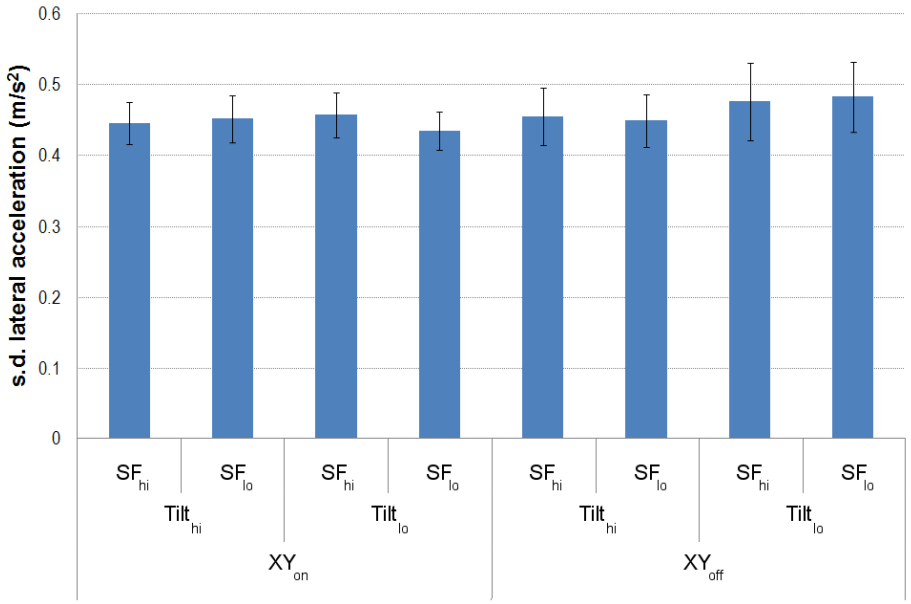

Figure 7-9: standard deviation of lateral linear acceleration (error bars 95% C.I.)

Figure 7-10 illustrates the strong main effect of XY observed on standard deviation of lane position (*sd_lp*). Steering performance was significantly more accurate, demonstrated by a reduced variation in lane position when the XY-table was active (0.162m) compared to when it was inactive (0.183m); $F_{(1,17)}$=17.3, p<.001, η^2=.51. No main effects of either Maximum-Tilt-Rate ($F_{(1,17)}$=1.90) or Scale-Factor ($F_{(1,17)}$=3.79) were apparent.

One of the major findings of Stage 3 was the noteable significant interaction of XY and Maximum-Tilt-Rate for *sd_lp*. With the XY-table in operation, task performance differed little as tilt rate was reduced from high to low (from 0.164m to 0.160m). However, without any additional sway motion, a reduction in tilt rate resulted in a marked performance degradation (from 0.173m to 0.193m).

A similar interaction was also observed between XY and Scale-Factor. When XY-table sway was available, a reduction in scale-factor had little impact on participant's ability to execute the task (from 0.162m to 0.163m). Conversely, without such platform movement, lane tracking became more varied with unscaled motion as opposed to that scaled by 50% (from 0.190m to 0.176m).

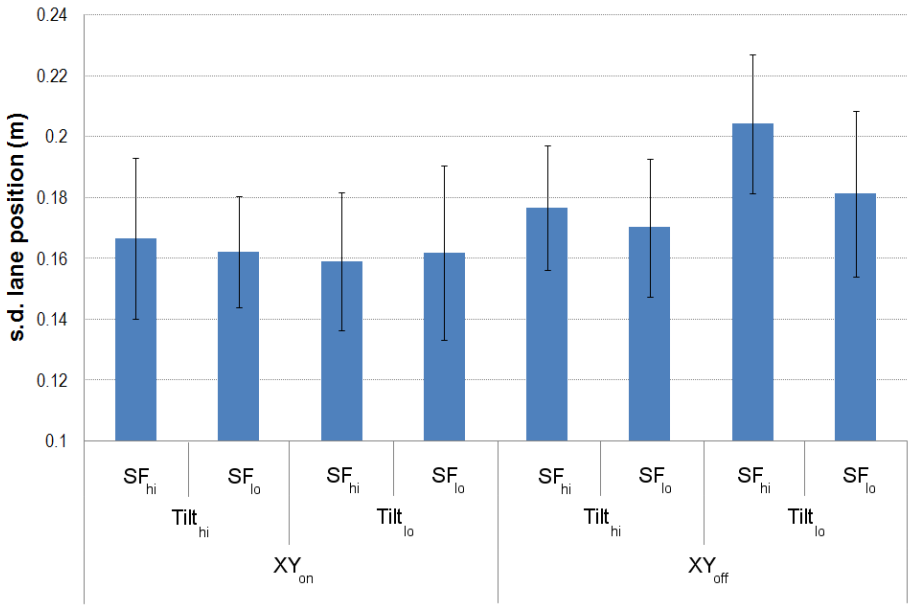

Figure 7-10: standard deviation of lane position (error bars 95% C.I.)

In contrast to lane position variability, when assessing lane keeping performance in terms of the minimum time to line crossing (*u_tlc*) achieved

during curve negotiation, a very strong main effect of Scale-Factor was observed (Figure 7-11). On average, a superior steering task was executed, illustrated by a reduced proximity to lane boundaries, when the motion cues were effectively unscaled (1.07s) as opposed to reduced by a factor of one-half (1.01s); $F_{(1,17)}$=95.3, p<.001, η^2=.85.

Observations more harmonious with those made for lane position variability were substantiated by two significant interactions of Scale-Factor with both XY ($F_{(1,17)}$=5.24, p=.035, η^2=.24) and Maximum-Tilt-Rate ($F_{(1,17)}$=8.59, p=.009, η^2=.34). Reducing Scale-Factor from high to low had a greater impact on the potential for lane excursions when extra motion platform surge was utilised (from 1.08s to 1.01s) than when the XY-table was not functioning (from 1.07s to 1.02s). A similar reduction in Scale-Factor from high to low had a larger influence on task performance in slow tilt conditions (from 1.08s to 1.01s) than during a platform tilt above the normally accepted perceptual threshold (from 1.06s to 1.02s).

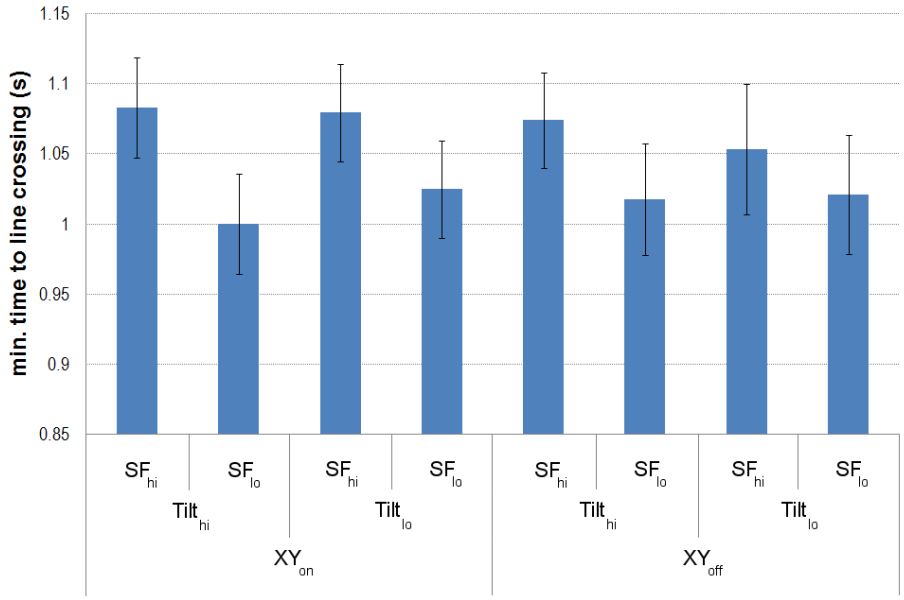

Figure 7-11: minimum time-to-line-crossing (error bars 95% C.I.)

In the main, the lateral task performance measures did show a pretty consistent picture of the effects of the various motion cueing parameter sets on steering task accomplishment. However, in contrast to the longitudinal task metrics, they did not all exhibit statistical significance simultaneously.

When tilt rate was rapid, considerably higher than the perceptual threshold condition, participants did display improved task performance. However, this result was discernible only through a reduction in the variation of lateral acceleration; the effect was not detectable by an assessment of either lane position variation or minimum time-to-line-crossing during the negotiation of the curve. Similarly, extra motion platform sway did benefit precise steering as measured by lane position variation, a finding also not duplicated in either of the other two metrics. Finally, minimum time-to-line-crossing alone illustrated any adverse effects of motion scaling on task accuracy.

The significant interactions observed in the data were also strong, but more persistent across two of the three dependent variables involved. Most notably, for lane position variation, the availability of XY-table sway and Maximum-Tilt-Rate interacted. With the XY-table in operation, task performance differed little as tilt rate was increased from sub to super-threshold. However, without any additional sway motion, the already degraded performance became worse still with reducing tilt rate. A comparable interaction was also observed between XY and Scale-Factor. When XY-table sway was available, a reduction in scale-factor had little impact on participant's ability to accurately execute the task. Without such platform movement lane tracking was worse, poorer still with unscaled motion as opposed to when it was scaled. Equivalent interactions of XY and Maximum-Tilt-Rate and XY and Scale-Factor were observed when assessing lateral task performance in terms of the proximity of lane excursions, measured by minimum time-to-line-crossing.

7.5. Chapter summary

With inputs from Stages 1 and 2, this chapter has described the investigation undertaken during Stage 3 to optimise the specific force / tilt rate error trade-off through the manipulation of three elements critical to the implementation of the classical MDA and its application in a research driving simulator. The permutation of two levels in each of XY-table availability, Maximum-Tilt-Rate and Scale-Factor necessitated eight different conditions of motion cueing and

classical MDA parameter sets. As in Stage 2, these conditions were experienced by participants undertaking two typical driving tasks in both braking and steering, each with explicit performance requirements. The parameter sets were tuned to achieve their best possible off-line optimisation of perceived motion during driving task performance. Eighteen drivers took part in a paired comparison design, with both their subjective assessments of motion cueing realism and objective task performance analysed.

As in Stage 2, the significance of the findings were much stronger for braking than they were for steering. Moreover, once again consistent with Stage 2 results, the motion cueing conditions that were perceived as the most realistic did not always correspond to those that afforded the best task performance. For the longitudinal task, a keen preference was expressed for low platform tilt rates, especially when supplemented by the additional surge of the XY-table. While the extra surge was not only considered more lifelike, it also resulted in a more precise braking. However, whereas a slow tilt in pitch was deemed a more credible low-frequency deceleration cue, a fast tilt actually resulted in more precise braking as the lead vehicle slowed for the traffic-lights. Finally, participant realism ratings were unaffected by varying Scale-Factor, but enhanced braking performance was observed when motion was effectively unscaled.

The longitudinal task also demonstrated significant interactions of Maximum-Tilt-Rate with Scale-Factor and XY. Whilst a rapid tilt rate resulted in braking performance that was more precise, under these conditions it was unaffected either by significant changes in either tilt rate or scale-factor. Only when tilt was low did performance suffer and to a greater extent for considerably scaled motion or motion that did not benefit from extensive surge.

When considering the lateral curve negotiation task, participants' inclination did shift towards those motion cues that were scaled down from the perceptual maximum, but this predilection was not borne out by a corresponding improvement in task accuracy. This was also true for Maximum-Tilt-Rate, where

a low tilt rate was once again considered more lifelike but a fast tilt resulted in a more precise steering.

Several interactions involving XY-table availability were also observed. Provided that sizeable sway was available through XY platform displacement, task performance, when assessed by lane position variation and minimum time-to-line-crossing, was unaffected by substantial changes in either Scale-Factor or Maximum-Tilt-Rate. However, without such platform translation, a reduction in either Scale-Factor or Maximum-Tilt-Rate resulted in significantly degraded lane tracking performance.

A fuller discussion of the main impact of these findings follows in Chapter 8. It includes the relationship and relevance of Stage 3 to the other two experimental stages, the study limitations and potential for further work, along with implications for the design and evaluation strategies of motion systems within research driving simulation.

CHAPTER 8

DISCUSSION

8.1. Scope

In car driving, vehicle handling is predominantly a perceptual task (Gibson & Crooks, 1938). Furthermore, there are three main modalities on which drivers depend to accurately perceive self-motion within a virtual environment: visual cues, proprioceptive cues and auditory cues (Kemeny & Panerai, 2003). Therefore, to create a compelling simulation of driving, these stimuli must be reproduced faithfully, such that accurate estimations of distance, speed and acceleration can be made. The extent and accuracy with which the simulator excites these sensory modalities, is inherently linked to its validity (Blaauw, 1982). Rolfe, Hammerton-Frase, Poulter & Smith (1970) define validity in this context as “the ability of a simulator to elicit from the operator some sort of response that he would make in a real situation”.

This definition, however, is extremely broad. Whilst utterly reasonable and rational, it is not specific to the multitude of various tasks that are constantly demanded of the driver to maintain safe and controlled operation of the vehicle. More practically, validity can only be defined specifically relative to the individual driving tasks that, in combination, add up to the overall driving exercise (Allen, Mitchell, Stein & Hogue, 1991). But to identify a suitably wide-ranging taxonomy of such tasks in order to, in turn, define an acceptable driving simulator operational range, is an exceptionally demanding challenge.

Hence, the research presented here focussed on a single, but key sensory modality, and its influence on driving simulator validity: namely the perception of motion through the vestibular channel, stimulated by dynamic cues produced through the exploitation of a motion system. Primarily, this modality was selected due its importance to the quality of driving simulation (e.g. Reymond, Kemeny, Droulez & Berthoz, 2001; Greenberg, Artz & Cathey, 2002). However,

an additional motivation was the relatively limited consideration that motion cueing has received from the driving simulator community to date, in contrast to the far more comprehensive attentions of those researchers involved in flight simulation (see Allerton, 2009, for a review).

A second consideration was the development and selection of the specific driving tasks. These had to be familiar, relevant and require drivers to perceive the unfolding driving conditions in order to manoeuvre the vehicle appropriately through a process of closed-loop vehicle control. Most importantly, the tasks had to allow an objective and empirical assessment of driver performance against fixed goals, facilitating a validation method geared to the requirements of the particular driving tasks. Furthermore, they had to demand both longitudinal and lateral vehicle handling. In combination, the driving tasks and empirical technique provided a specific yet significant contribution towards the more elusive and all-embracing definition of simulator validation of Rolfe et al. (1970).

8.2. Focus

Ideally, a simulator would faithfully reproduce the complete range of dynamic cues experienced during driving. However, driving demands a dynamic representation of motion that far exceeds the limited displacement capability of a conventional motion system workspace (Stewart, 1965). To achieve this, a Motion Drive Algorithm (MDA) filters the vehicle motion before positional commands are sent to the motion system. A number of different MDAs, reviewed in section 2.4, have been exploited for use in driving simulation. A common theme is their collective reliance on tilt-coordination to recreate the low frequency motion cues, first realised in the original development of the classical MDA for flight simulation (Conrad & Schmidt, 1969). However, the demands on tilt-coordination in driving simulation are much more challenging than for commercial aviation. In flight, the majority of manoeuvres involving significant longitudinal acceleration, and consequently the requirement for sizeable tilt-coordination, are limited to a small part of the overall simulation, i.e. take-off and

landing. Furthermore, in well-executed flight, turns are infrequent and coordinated. Car drivers, on the other hand, witness a rapidly changing longitudinal and lateral specific force during both accelerating/braking and in curve negotiation.

The flexible and elegant nature of the classical MDA lends itself well to coping with the expansive and varied nature of driving, which is one of the reasons it enjoys such wide-spread use in driving simulation (Colombet, Dagdelen, Reymond, Pere, Merienne & Kemeny, 2008). It contains various parameters whose value can be adjusted to tune the algorithm and thus the subsequent perception of motion. Further evidence of its applicability to driving was provided by Grant, Blommer, Artz & Greenberg (2009), who in comparing it to alternatives concluded that "for general driving manoeuvres, a well-tuned classical algorithm is likely [to be] superior".

Frequently, objective methodologies provide a useful off-line appraisal of the classical MDA's effectiveness. These are based on an assessment of the frequency response of the transfer function describing the algorithm's behaviour. Flattening the transfer function in gain provides a response of the MDA that closely matches its demand throughout a vehicle's typical frequency range. This provides an accurate perception of the magnitude of the motion cues achieved during vehicle handling (Reid & Nahon, 1986b). Flattening the transfer function in phase minimises latency and hence any timing discrepancies between control input and perceived vehicle response. Such a lagged simulator is notoriously difficult to handle and requires extra mental effort on the part of the operator to deal with (Reid & Nahon, 1988).

When the outputs of tilt-coordination are limited to the accepted angular motion perception threshold of the semi-circular canals in the human vestibular system, an operator will interpret motion platform tilt exclusively as linear acceleration (Groen & Bles, 2004). However, such limiting results in an irregular and uneven MDA transfer function. Scaling the specific forces generated by the platform is one straight-forward and relatively successful method to re-flatten

the frequency response (Reid & Nahon, 1986b). Hence, the validation technique presented in the three-stage experimental design focussed on an optimisation of the classical algorithm for the characteristic driving tasks, with particular focus on the specific force / tilt rate error trade-off.

The system transfer function can be supplemented to include not just the behaviour of the MDA, but also a model of human perception. By ensuring that any MDA gain or phase lags occur outside the typical frequencies of human perception, the performance of the overall system can be maximised. Hosman & Stassen (1999) used such a technique in their development of a visual-vestibular model of pilot behaviour during a tracking task. Their perceptual model suggests that closed-loop vehicle control is significantly enhanced by the vestibular perception of motion. It provides the driver with the stimuli required to more accurately perceive vehicle movement than the visual system alone does, such that the most appropriate control inputs are made to maintain tracking task performance. Hosman & Stassen's work informed the present study in the selection of the specific longitudinal and lateral driving tasks selected. These were designed, as much as possible in the context of driving, to resemble such tracking tasks. An additional benefit was the immediate and effective step control input required at the start of the tracking task, by its nature sweeping a large expanse of the vehicle's typical frequency range.

The absence of similar transfer function-style models of driver perception prevented a comparable off-line evaluation and tuning of the classical MDA. Hence, a driver-in-the-loop evaluation was employed for a series of MDA manipulations. The algorithm's subsequent role in driving simulator validity was also assessed. Such validity extends to the concept of internal simulator fidelity and the behavioural correspondence of drivers between real and virtual environments (Kaptein, Theeuwes & van der Horst, 1996). Internal validity is lost if driver behaviour is specifically affected by the limitations of the simulator, including misperceptions of motion stimuli.

8.3. Observed results

8.3.1. Stage 1

Not only is scaling the specific forces a straight-forward method to flatten a MDA's frequency response, it is also a useful defence against the frequent overestimation of physical platform motion with respect to simulated visual motion. In their study of F-16 pilots witnessing a simulated take-off run as passive observers, Groen, Valenti Clari & Hosman (2001) suggested that unity scale-factors were rejected as too powerful due to a "visual-vestibular discrepancy". They proposed that the incongruity was actually a result of an underestimation of visual cues but manifested, however, as an over-estimation of vestibular cues. Berger, Schulte-Pelkum & Bülthoff (2010) suggested that a confounding factor existed in Groen et al.'s (2001) observations, through their use of too simplistic a representation of the visual scene, the runway lacking in any "clearly perceptible size cues". To address this, Berger et al. (2010) tasked their passive observers with rating the "believability" of motion cues as participants were "moved" through a randomly textured ground plane populated with familiar, life-size mages of people. Rather than the preference for scaled motion asserted by Groen et al.'s (2001) sample of pilots, Berger et al.'s (2010) observers deemed that the most believable simulation occurred when the motion cues corresponded to the accompanying visual cues on a 1:1 basis.

Analogous to the research of Groen et al. (2001) and Berger et al. (2010), Stage 1 employed drivers who took part as passive observers. Therefore, by assessing just the maximum perceptible scale-factor, like the studies mentioned, Stage 1 also only considered motion system Bode gain. Hence, simply the magnitude of the perceived specific force rather than any latency in its development could be considered. Both previous studies had additionally shown that different scale-factors in translational motion platform movement and tilt-coordination can complement each other to produce the most realistic combined perception of motion. Hence, Stage 1 was split into two phases. The first investigated maximum perceptible scale-factor for motion platform translation (or more accurately the maximum perceptible scale-factor closest to

unity). A second, complimentary phase deciphered the equivalent for platform tilt.

Where Stage 1 superseded the scope of Groen et al.'s (2001) and Berger et al.'s (2010) investigations was in its regard not only to longitudinal but also to lateral motion. Furthermore, in pre-scripting vehicle control inputs, it utilised the full dynamic range of the simulation, including the vehicle dynamics model. By controlling movement through the virtual environment in this way, it minimised some other aspects known to affect the overestimation of vestibular cues, such as the sensitivity of observers to the rate of change of linear (Grant & Haycock, 2008) or rotational accelerations (Hosman & Stasson, 1999). Finally, by using unfiltered motion in the simulation of the pre-scripted vehicle manoeuvres, confounding scaling due to the intrinsic performance of the classical MDA could be eliminated.

Whilst naturally influenced by Groen et al.'s (2001) and Berger et al.'s (2010) studies, the fundamental aim of Stage 1 was to ensure that, during the optimisations of the classical MDA in Stages 2 and 3, those motion cueing conditions incorporating a high scale-factor did not unnecessarily utilise precious actuator stroke through overly-scaled motion. The results were determined using a robust and well-established Just Noticeable Difference methodology, requiring participants to discriminate between scaled and unscaled motion using a Levitt 1 up / 3 down technique (Levitt, 1971). This culminated in a convergence on the maximum perceptible scale-factor that could be sensed by at least 79% of the sample population. This consisted of 20 experienced drivers, randomly selected and well balanced demographically. High and low frequency driver manoeuvres were pre-scripted to allow for unfiltered motion cueing that required both longitudinal and lateral platform movement exclusively in either translation or tilt. The observed maximum perceptible scale-factors did not differ in terms of the modality of the manoeuvres. However, there were slight, but statistically significant, differences detected between translation (0.9) and tilt (0.87). Nevertheless, the variation in maximum perceptible scale-factor of just 0.03 between the two degrees-of-

freedom of platform movement is practically negligible. To all extent and purposes, the results indicated that any scale-factor of linear acceleration in any direction need never exceed 0.9.

Of the two studies, Stage 1 probably more closely resembled that of Berger et al. (2010) than that of Groen et al. (2001). Accordingly, the results were more closely aligned to the former's insinuation that unity scale-factors are most appropriate in providing a convincing perception of the magnitude of motion cues. However, Stage 1 differed from both in that participants were not required to rate the believability or realism of the motion cues, simply to discriminate between those that were scaled and those that were not. Hence, rather than emulating the previous studies, which concluded implementation strategies for MDA based merely on the perceived magnitude of motion cues, Stage 1 was able to inform Stages 2 and 3 to reach such conclusions based also on the inherent MDA phase lag and its subsequent impact on simulator controllability.

8.3.2. Stage 2

Every motion system has its own physical displacements limits defined by the constraints of its individual actuators and the movement they are able to afford. Like all other algorithms, the actuator movement commanded by the classical MDA must respect these limits to avoid the false cues associated with full extension, felt by drivers as unanticipated jolts in the expected smooth motion cues.

Through the use of maximum perceptible scale-factors gleaned during Stage 1, Stage 2 addressed the first stage in the optimisation of the classical MDA in driving simulation by pinpointing the most suitable Motion Reference Point location. Since the vestibular system is located in the inner-ear, the ideal MRP location is typically centred on the head of the observer (Reid & Nahon, 1985). However, due to the geometric constraints of the hexapod, commonly used in many moving-base driving simulators (including UoLDS), moving the MRP up to this point requires significantly longer actuator strokes to achieve the same

degree of tilt. Therefore, MRP location constrains the maximum tilt angle achievable and subsequently the effective maximum specific force possible for driving manoeuvres in the simulator.

Previous attempts to investigate the influence of MRP location in the perception of motion in driving simulators are scarce, probably since they are mainly based on the very limited number of motion platform designs that actually differ geometrically from the hexapod. Fischer & Werneke (2008) had drivers undertake a series of emergency stops in the inverted hexapod DLR driving simulator. MRP was located either just above or well below drivers' heads, differing by 1.75m between the two conditions. The higher MRP location was observed to play a minor role in improving the subjective rating of realism during the sustained period of braking. Fischer & Werneke (2008) also manipulated tilt-coordination such that, during the braking manoeuvre, it was either rate-limited at the accepted perceptual threshold or effectively unlimited. They reported a clear preference in the participant ratings of both the magnitude and timing of the unlimited condition. The study resulted in the Fast Tilt-Coordination algorithm, developed and tested by Fischer, Lorenz, Wildfeuer & Oeltze (2008). In this assessment, the driving scenario required braking on the approach to a roundabout, followed by the negotiation of three-quarters of its circular section. With both longitudinal and lateral demands now incumbent on the MDA, participants still rated rapid tilt located above the head as the most realistic. No significant differences in driving performance were observed.

In its achievement of maximally-scaled motion cues without any unnecessary depletion of precious actuator extension, Stage 2 manipulated MRP-Location as one of two factors in a repeated-measures experimental design. The other independent variable was the limiting of platform tilt rate in the specific force / tilt rate error perceptual trade-off. Whilst it is acknowledged that this trade-off is influenced by other issues such as overall scale-factor, onset filter performance and available platform translational displacement, at this stage these were held constant prior to their deeper investigation during Stage 3.

The permutation of two levels in each of MRP-Location and Maximum-Tilt-Rate necessitated four different motion cueing conditions resulting in two different classical MDA parameter sets. The corresponding motion cueing was experienced by participants undertaking two familiar and common driving tasks both longitudinally in braking and laterally in steering.

The longitudinal scenario developed for Stage 2 involved braking at a set of traffic-lights. Car following on the approach to the traffic-lights was exploited in order to sufficiently control the degree of braking required as the traffic-lights changed to red. The quasi tracking task required participants to brake as smoothly and consistently as possible to maintain a constant distance headway to the lead vehicle as it responded to the red light, slowing at a constant linear deceleration of 0.15g. The lateral scenario required participants to maintain the same linear acceleration whilst taking a circular left-hand bend at pre-defined and automatically controlled speed. Here, the tracking task was to maintain the centre of the driving lane throughout the curve negotiation.

The classical MDA parameter sets were each tuned to achieve the best possible perception of motion during driving task performance. As part of this objective off-line optimisation, the classical algorithm was modelled in MATLAB/Simulink. The tuning was carried out, given the constraints of the independent variables, by flattening the resulting transfer function output of the modelled algorithm to the greatest extent possible.

Eighteen experienced drivers took part in Stage 2, with both their subjective assessments of realism and objective task performance analysed in a Paired Comparison, comprising of all possible combinations of the various motion cueing conditions. The combinations were balanced for order and carry-over effects (Russell, 1980).

The significance of these results varied considerably depending on the modality of the driving task in question. In braking, whilst participants expressed no preference for a MRP location close to the head, such placement of the MRP

did result in marginally better longitudinal task performance. During the same manoeuvres, they also consistently and strongly favoured the development of slow tilt rate over one that arose more rapidly. However, the fondness for a slow tilt rate was not borne out by the performance metrics, which indicated, conversely, that the driving task was achieved more accurately in rapid-tilt motion cueing conditions.

The lateral task did not show any such substantial and sizeable differences. Participants demonstrated no partiality towards any of the motion cueing conditions and only for a single performance metric, minimum time-to-line-crossing, was anything approaching a robust effect revealed. That result confirmed high Maximum-Tilt-Rate as the most likely to produce more accurate steering performance, although its impact was far from substantial in terms of the amount of that improvement.

By and large, the findings of Stage 2 opposed those of Fischer & Werneke (2008) and Fischer, Lorenz, Wildfeuer & Oeltze (2008) whose drivers favoured rapid tilt rates, also demonstrating a weak predilection towards a high MRP location. Whilst the dramatic nature of the emergency stop task required by Fischer & Werneke (2008) may have influenced participants desire for a fast acting motion cue, the preferences expressed during the more mundane roundabout negotiation are harder to explain away. Maybe the limited size (N=10) of a demographically similar sample (all young drivers aged 20-25) played some role in the preference toward the more “punchy” fast-tilt motion cueing conditions even in the more unremarkable of the two scenarios?

8.3.3. Stage 3

Even though MRP location showed no impact on participant ratings, it did display a marginal effect on performance during the longitudinal task. Hence, it was maintained in the higher position during Stage 3’s fuller evaluation of the perceptual trade-off of specific force and tilt rate error. Three elements critical to this trade-off, and hence the implementation of the classical MDA in driving

simulation, were manipulated as two-level, independent factors in a repeated-measures, paired comparison design. Those factors were the availability of extended translational motion platform displacement through the exploitation of UoLDS's XY-table, the selection of classical MDA filter settings that intrinsically limited the rate of tilt-coordination and the overall scaling of the specific force witnessed by the driver during motion cueing.

The extended surge and sway capabilities allowed a flattening of the classical MDA's transfer function through a reduction in the first-order and second-order high-pass filters' cut-off frequencies. Such a technique results in a more accurate perception of the high-frequency motion cues associated with the onset of a manoeuvre, since a greater proportion of these are allowed to pass through the filter. This sustains the cue for a longer duration, but naturally requires significantly greater platform excursion to do so. Using the large amplitude vertical motion capability of the NASA Ames Vertical Motion Simulator (VMS), Schroeder, Chung & Hess (2000) investigated onset cues in a sample of helicopter pilots controlling their aircraft's vertical movement between two points 32 feet (9.75m) apart. Similar to the pre-scripted driving manoeuvres used during Stage 1, the nature of the "bob up/down" flying task could be simulated within the available motion envelope of the VMS without any need for washout. Hence, Schroeder et al.'s (2000) experimental manipulations were first-order high-pass cut-off frequency and overall scale-factor. They reported that improving the off-line MDA performance by lowering the filter's cut-off resulted in a significantly greater degradation in the pilots' tracking task performance compared to a reduction in scale-factor. Similarly, Groen, Valenti Clari & Hosman's (2001) take-off study also concluded that their fixed-wing pilots were more tolerant to variations in scale-factor rather than filter frequency. The conclusion of both was that the down-scaling of motion is the most desirable method of flattening the MDA's transfer function.

Previous studies on the development of tilt-coordination in driving simulation have struggled to show such definite results. On one hand, there is the inclination for rapid tilt resulting in a low specific force / high tilt rate error,

affirmed by both Fischer & Werneke (2008) and Fischer, Lorenz, Wildfeuer & Oeltze (2008). On the other, there is the evidence offered by Grant, Blommer, Artz & Greenberg (2009). In this study using Ford's VIRRTEX simulator, drivers were tasked with a series of lane changes on a straight carriageway. Six different conditions of motion cueing were compared, including four in which the classical MDA parameter sets were manipulated to compare and contrast varying amounts of lateral specific force and roll rate error. Improved subjective ratings of motion cueing realism were reported by reducing roll rate error at the expense of specific force error. Grant et al. (2009) also evaluated driver performance by analysing the variation of steering wheel angle whilst drivers made their lane changes. The rank ordering of the parameter sets was supported by both the objective and subjective data, the former demonstrating greater statistical power.

These conflicting studies shaped the novel and original approach of Stage 3. Its aim was to investigate the three factors independently in a regulated manner, allowing an investigation of any main effects and potential interaction between the factors. The permutation of two levels in each of XY-table availability, Maximum-Tilt-Rate and Scale-Factor necessitated eight different conditions of motion cueing and classical MDA parameter sets. Exactly as in Stage 2, these conditions were experienced by participants undertaking two typical driving tasks in both braking and steering, each with explicit performance requirements. The parameter sets were tuned to achieve their best possible off-line optimisation of predicted perceived motion during driving task performance. Eighteen experienced drivers took part, with both their subjective assessments of motion cueing realism and objective task performance analysed in a Paired Comparison.

For the longitudinal task, the participant sample demonstrated reliable ratings of motion cueing realism, the observed 59.4% being very much on a par with the 61% overall consistency reported during Grant et al.'s (2009) lane-change study. During the braking manoeuvres, motion cues that resulted from slow tilt-coordination were rated as significantly more realistic than those that emanated

from a rapid development of tilt angle. However, this was the case only when the slow tilt was supplemented by extended motion platform translation, made available by the XY-table.

Drivers' impression of improved realism when platform tilt rate was low was not unexpected. The finding concurs with the application of tilt-coordination in flight simulation, routinely limited to the commonly accepted perceptual thresholds (Groen & Bles, 2004). The fact that this impression was also strengthened for motion cueing conditions that allowed additional platform surge is also consistent with the improved frequency response and hence the minimal sag in the perceived specific force that these conditions afford. What was more unexpected was the lack of any significant inclination toward the lower of the two scale-factors, as had been expressed by the pilots in Groen, Valenti Clari & Hosman's (2001) take-off study. The only possible reason for this is the added benefit of the additional surge motion of the XY-table. The superior onset cueing that this surge allowed improved the transfer functions of the motion cueing conditions $XY_{on}Tilt_{lo}SF_{hi}$ and $XY_{on}Tilt_{lo}SF_{lo}$ to such an extent that their difference became imperceptible during the braking task. In other words, drivers were more tolerant to variations in scale-factor than they were to variations in filter frequency, just like Schroeder et al.'s (2000) helicopter pilots.

Groen et al.'s (2001) study did not benefit from sizeable platform translation and hence, during take-off roll, the fixed-wing pilots would have experienced motion cues that more closely resembled Stage 3's four XY_{off} motion cueing conditions. Although, in the present study, these did not differ significantly for the braking drivers at 95% confidence, the difference between $XY_{off}Tilt_{hi}SF_{hi}$ and $XY_{off}Tilt_{lo}SF_{lo}$ almost reached this level. Had it done so, it would have exactly concurred with Groen et al's (2001) "XY-less" findings that slow tilt and low scale-factors best achieve the perception of magnitude of linear longitudinal acceleration in simulation.

In terms of tilt rate, the objective results for Stage 3's longitudinal task contrasted entirely with the subjective ratings. In accordance with the task

demands, drivers demonstrated smoother braking and less variation in following distance during the manoeuvre when experiencing conditions of rapid tilt rather than when tilt developed more slowly. Additionally, motion cues that were effectively unscaled also resulted in a better accomplished braking task. However, more in line with the realism ratings, both behavioural metrics revealed a more accurate performance when participants experienced extended translational motion. The size of these main effects of all three factors on both dependent variables was highly convincing.

The interactions of the other factors with tilt rate also proved to be reasonably strong. When tilt rate was low, in line with the accepted thresholds of tilt perception, braking was equally smooth regardless of the scale-factor selected. Increasing tilt rate to a value well above perceptual threshold generally improved performance, but by a greater degree when the scale-factor was also high. A similar interaction was observed for the general improvement in task performance in conditions of rapid tilt. This improvement was more considerable when the onset motion cues experienced during braking were enhanced by the extra translational capacity of the XY-table.

This interaction of platform translation and tilt-rate is arguably the most important, an assertion followed up in the conclusions of this chapter. With no additional platform translation, the simulator behaves as a traditional hexapod. As such, the improvement in task performance whilst braking under conditions of rapid tilt is consistent with the preference of drivers experiencing Fischer & Werneke's (2008) emergency stop study. However, with the enhanced onset cueing that the extra surge allowed, the performance differences became less clearly related to tilt rate.

For the lateral task, the participant sample again demonstrated reliable ratings of motion cueing realism, observed at slightly lower figure of 55.8%. This was an early indication of the greater difficulty that participants had in differentiating the effects of the motion cueing conditions whilst steering than they were able to under braking. This may have been due to different visual-

vestibular influences between the two tasks. Potentially, the visually sparse longitudinal braking scenario places more of a reliance on the accurate perception motion cues in order to support the closed-loop control task. In comparison, the lateral scenario, is awash with visual stimuli through the more significant optic flow apparent during the steering manoeuvre; hence, it becomes less reliant on motion for accurate task execution.

One potential flaw in terms of assessing participant's consistency of realism ratings may have resulted from the lack of an assessment of the function of each individual's vestibular system prior to any of the experimental stages. However, no specific gender or age effects on vestibular function appear evident in the literature. Furthermore, in the evaluation each participant's coefficient of consistence across the experimental stages, no pattern was evident to suggest that any individual steadily made inconsistent ratings of realism. Hence, it is considered unlikely that any interactions of vestibular health and motion rating exist in the data presented.

On the whole, perceived realism was enhanced when motion cues were scaled by 50%, especially when supplemented by the extended motion platform translation capabilities afforded by the XY-table. However, manipulating tilt rate had no impact on participant ratings.

In line with the longitudinal task, the three independent factors all demonstrated a significant main effect on task performance in terms of the dependent behavioural variables selected. However, unlike the braking task measures, they did not all exhibit statistical significance simultaneously. When tilt rate was rapid, participants did display improved task performance. However, this result was discernible only through a reduction in the variation of lateral acceleration; the effect was not confirmed by an assessment of either lane position variation or minimum time-to-line-crossing during the negotiation of the curve. Similarly, extra motion platform sway benefitted precise steering as measured by lane position variation, a finding also not duplicated in either of the

other two metrics. Finally, minimum time-to-line-crossing alone illustrated any adverse effects of motion scaling on task accuracy.

Certain interactions of the experimental factors were also significant, but more persistent across two of the three dependent variables involved. For lane position variation, the availability of XY-table sway and Maximum-Tilt-Rate demonstrated one such interaction. With the XY-table in operation, task performance differed little as tilt rate was increased from sub to super-threshold. However, without any additional sway motion, the already degraded performance became worse still with reducing tilt rate. XY and Scale-Factor also interacted. When XY-table sway was available, a reduction in scale-factor had little impact on participants' ability to accurately execute the task. Without such platform movement, lane tracking was worse, poorer still with unscaled motion as opposed to when it was scaled. Equivalent interactions of XY and Maximum-Tilt-Rate and XY and Scale-Factor were also observed when assessing lateral task performance in terms of the proximity of lane excursions, as measured by minimum time-to-line-crossing. These results support the previously reported main effect, advocating the potential benefit of the XY-table.

A consistent theme in the results observed in both of Stage 3's driving tasks was the lack of consistency between the subjective perception of realism and the objective measures of task performance. Such an issue did not crop up during Grant et al.'s (2009) impeccably administered lane-change study, which reported that perceived realism correlated well with lateral task performance. The nature of this steering task was generally dictated by relatively high frequency steering inputs, demanding a similarly high frequency response of the motion cueing. The present study, on the other hand, utilised a lane keeping rather than a lane changing task, characterised by a dominant low frequency domain. Its results undeniably demonstrate that more significant differences exist between the perception and performance with motion cues under longitudinal tasks compared to lateral tasks. That Grant et al. (2009) did not employ a longitudinal task and the fact that the lateral task existed in an

altogether different frequency range could easily explain the observed perception/performance correlation differences between the two studies.

The lack of perception/performance consistency reported here leads to a dilemma as how best to handle the specific force / tilt rate error trade-off when making use of the classical MDA in research driving simulation applications. When large motion platform translations are made possible by a XY-table, the motion cues most realistic to drivers stem from the reduction of tilt rate errors at the expense of specific force errors. The same is true, admittedly not as clear cut statistically, even when onset cues are handled less effectively without such additional translation capabilities of the motion system. However, the motion cues that are most beneficial in terms of the successful accomplishment of longitudinal and lateral driving tasks doubtlessly originate from the reduction of specific force errors at the expense of tilt rate errors.

8.4. Study limitations

Perhaps the major limitation to this work is the fact that only two specific driving tasks were selected. The analysis of these tasks informed the subsequent assessment of the classical MDA achieved during Stages 2 and 3. From these tasks, conclusions on simulator validity and ideal motion platform operational range are made that are naturally restricted to the individuality of those tasks. However, the identification of a suitably wide-ranging definition and classification of such tasks is another challenge altogether and one that outside the scope of the present work.

A similar scope-driven limitation was in the selection of the single MDA manipulated for assessment: namely the classical algorithm. Several alternative MDAs exist for application in driving simulation, discussed in detail in section 2.4. Whilst there is, occasionally, strong evidence for their superiority, particularly for the Lane Position Algorithm over even an optimally tuned classical filter, it is normally limited to specific, relatively high frequency driving tasks (e.g. Grant et al., 2009). The classical MDA was selected primarily due to

its flexible and well-understood characteristics, a result of its long-standing nature (Conrad & Schmidt, 1969) and common use in driving simulation (Colombet et al., 2008). Clearly, the present study would have benefitted further from its comparison against alternatives. However, it was felt that an original, robust and wide-ranging study optimising its use for typical longitudinal and lateral driving tasks was lacking in the existing literature. The present study has attempted to address this gap.

Stage 1 suffered from the fact that the perception of maximum scale-factor was made without any attempt to simulate the high frequency rotational accelerations associated with the vehicle's natural response to the pre-scripted driver inputs. Whilst these were validated against the equivalent CarSim outputs and displayed through the visual system, they were not mimicked by the motion system. Potentially, the maximum perceptible scale-factors in translation and tilt could have been slightly higher had these motions also been simulated.

Rotational acceleration motion cues were, however, introduced for the manoeuvres resulting from the driving tasks employed in Stages 2 and 3. But during the paired comparisons, these cues were not manipulated experimentally in any way between the various scenario pairs. To have done so would have been advantageous, resulting in a classical algorithm optimised not only for linear acceleration, but also for rotational cues. However, scope constraints prevented such an over-complication of the experimental design. Whilst the rotational cues were tuned for their best possible and consistent representation in the experimental stages, it was decided that in terms of the perception of motion, perceived specific force was likely to be more influential on ratings of realism and on task performance than the depiction of perceived rotational acceleration. This decision was made based on there being no existing evidence to the contrary.

Another limitation was the choice of only two levels of the manipulated independent variables. This judgment was made to prevent the experiment from becoming unwieldy, especially with regard to managing realistic demands of the

participant sample. For Stage 3, to have increased the number of levels in each experimental factor to three would have necessitated an eye-watering 351 scenario pairs. Even with two levels, there are already grounds to question the continued motivation of drivers throughout a study that required them to negotiate the same manoeuvre on 56 separate occasions, even though this was mitigated by breaks and split over two separate driving sessions.

A further shortcoming was the fact that the driving scenarios had to be choreographed carefully to ensure that the longitudinal and lateral manoeuvres achieved a consistent level of linear acceleration. Furthermore, the braking task had to commence with the lead vehicle at a pre-defined distance ahead of the simulator driver. To achieve this, driving speed was controlled automatically at the start of each scenario. Participants were not advised of this fact, simply that they had to press the accelerator pedal to initiate the driving scene. Although full control resumed before the start of the data collection period, many reported anecdotally that they were unconvinced that they had been in full command all along. Although a necessary evil, the speed controller did have the potential to disturb participants' feelings of being fully in charge of the handling of their vehicle.

Trace-fading, the potential for participants to lose their working memory of the various presentations of the motion cueing conditions, in turn affecting their ability to make reliable ratings of realism, was discussed in section 4.2.2. Ideally, the inter-stimulus interval would have presided in the accepted 5s – 10s range of sensory memory (Davidson, 1972). However, the methodology employed at each of the three stages required a physical re-positioning of the motion system of upto 5m between comparison pairs. In order to make this movement imperceptible, such repositioning was slow and therefore took longer than sensory memory period, typically some 15s – 20s. Whilst this is clearly an inherent limitation to the methodology selected, such a concern is mitigated somewhat by the generally acceptable level of participant response consistency, comparable at least to Grant et al.'s (2009) lane-change study.

Finally, there is the lack of any real-world equivalent data with which to compare the observed driver behavioural measures between natural and virtual environments. Whilst this study does not purport to prove an absolute validity in terms of the exact matching of driver performance to comparable driving scenarios in reality and in the simulator, which according to Kaptein, Theeuwes & van der Horst (1996) is in practice an almost unattainable objective, it does demonstrate the relative effects of the manipulations of the various motion cueing conditions. With regard to the objective of achieving an optimisation of the classical algorithm most suitable to specific yet typical driving tasks, the study has been a success. More full conclusions can be found later in section 8.6, but for one, it would appear that the availability of XY-table translation significantly improves the effectiveness of classical motion cueing. However, XY-tables present a significant financial outlay. Therefore, the investigation would have been further enhanced by the ability to draw some conclusions on the cost-benefit structure of motion system characteristics against real driving data.

8.5. Potential for further study

Early in Chapter 1, it was mentioned that no international legislator exists to assess validity in terms of the specific characteristics of the many and varied subsystems that make up an individual driving simulator. Maybe in a research environment, such legislation is unnecessary given the wide range of studies that are frequently undertaken. To effectively standardise the plethora of driving tasks and scenarios that such studies may demand is not only a daunting task, it is also one that would restrict the potential for driving simulator investigations over a range of facilities, depending on their perceived merit. Surely the defence of a particular study and the apparatus used to make its conclusions is the responsibility of the individual researcher, rather than a mysterious body that arbitrarily decides on the worth (or lack of it) of the scientific equipment involved? For all of its failings, peer review remains an appropriate means of quality control.

Investigations requiring the use of research driving simulators seldom differ significantly in the scenarios they employ or in the metrics by which they define driver behaviour. By defining a variety of such scenarios, analogous to the driving task demands exploited during Stages 2 and 3, not only would the measurement of equivalent real-world data be possible but the scenario demands would typify the simulator characteristics required. These characteristics would identify the success of respective simulators in recreating the perceptions necessary to allow equivalent behaviour between real and the virtual conditions they construct. Furthermore, simulators could be compared on a relative basis.

By developing the experimental design and expanding on the scenario definitions used in this study, further work would be able to address and appropriately manage common incongruities that already exist in driving simulation. Such issues include the mental effort required of simulator drivers to maintain their desired driving performance, simulator sickness or the misperceptions of visual, vestibular or auditory stimuli. Effectively the suitability of a particular simulator to a individual research question could be made objectively rather than by some macho drive for the biggest, boldest and most expensive facility. Rather than searching for the proverbial needle in the validation haystack, the simulator engineer would be able to answer the more straight-forward yet pertinent of research questions, “how well does yours achieve the driving task?”

8.6. Conclusions and final thoughts

8.6.1. Summary of main findings

With its three-stage experimental plan, this study has attempted to provide a robust, defendable and original investigation into a topic area that is sparsely populated in the driving simulation literature. Given the caveat that its conclusions can only be drawn for the specific longitudinal and lateral driving

tasks examined, the following can be drawn from the various stages of the present investigation:

- Scale-factors over 0.9 for motion platform translation or tilt are unnecessary. Above this point, motion cues cannot be perceptibly differentiated from unscaled motion.
- Drivers are not able to perceive a relocation of Motion Reference Point to a position close to the head. Such placement does, however, result in marginally smoother braking, in line with the longitudinal task requirements employed in this study.
- Especially when complemented by extended motion platform translation, braking cues that result from sub-threshold tilt-coordination are rated as more realistic than those emanating from a rapid development of tilt angle.
- Conversely, in line with the longitudinal task requirements of this study, braking is performed more smoothly in conditions of rapid, above-threshold tilt-coordination.
- Braking is smoother with the improved onset cueing made possible by extended motion platform surge.
- Braking is smoother when longitudinal motion cues are effectively unscaled.
- Especially when complemented by extended motion platform sway, the perceived realism of steering cues is enhanced when motion cues are scaled by 50%. Realism is not influenced by the rate limiting of tilt-coordination.
- Cornering is smoother in conditions of rapid, above threshold tilt-coordination.
- Lane position is less varied during cornering with the improved onset cueing made possible by extended motion platform sway.
- Lane encroachments are less likely during cornering when lateral motion cues are effectively unscaled.

8.6.2. Implications for simulator design

Motion platforms exist in various guises. Specifications stretch from relatively cheap, small systems limited in their available displacement to those more costly, but affording the simulation engineer a much more expansive representation of the dynamic range of typical driving. By comparing subjective assessments of realism and objective measures of performance, the main objective of this work was to investigate the most appropriate motion cueing to achieve both a strong perceived correlation between real and virtual conditions (perceptual validity) and behavioural correspondence (behavioural validity). Generally, drivers consider scaled motion cues developed at a low tilt rate most realistic. Conversely, unscaled cues presented at rapid tilt rates appear to foster more accurate driving task performance.

These results do suggest an apparent conflict. However, armed with the data summarised in the bulleted list above, design implications for research driving simulators can be drawn. In terms of fidelity and motion cueing, the most appropriate tuning depends on the specific focus of the driving simulator. The fundamental characteristics of the simulator should maximise its internal validity, a concept introduced at the start of this chapter. Internal validity is lost if driver behaviour is specifically affected by the limitations of the simulator (Kaptein, Theeuwes & van der Horst, 1996). Consequently, should driver behavioural research be the simulator's focus, it is logical to place the importance of behaviour and performance over that of perceived realism. Therefore, the first main theoretical contribution of this work is that optimal motion cueing (resolution of the specific force / tilt rate error trade-off) in a research driving simulator is achieved by minimising specific force error at the expense of tilt rate error.

However, before we jump to too hasty a main conclusion, it should be remembered that earlier in this discussion, it was argued that the interaction of motion platform translation capability and tilt-rate was the most noteworthy. This interaction occurred repeatedly, observed in both the performance metrics used in the longitudinal task and two of the three lateral task measures. When the

XY-table was operational, driving task performance varied little between sub-threshold and more rapid tilt-coordination. However, while the XY-table was inactive, both driving tasks were better achieved with a high platform tilt rate.

This interaction supports the second main theoretical contribution. In a small motion system, without the benefit of the XY-table, the constraints of internal validity force the hand of the simulation engineer to minimise specific force error at the expense of tilt rate error. However, a more expansive motion platform, characterised by greater translational capacity, affords the luxury of achieving motion cues that not only bring about accurate driving task performance, but also attain maximum perceived realism. In such a system, the apparently conflicting goals of perceptual and behavioural validity can be aligned much more closely. Whether the benefits of such a system can actually outweigh its cost will have to be the focus of a future thesis.

REFERENCES

Adler, H.E., Howes, D.H. & Boring, E.G. (1966). Elements of Psychophysics. Holt, Rinehart & Winston.

Advani, S.K., Hosman, R.J.A.W. & Haeck, N. (2002). Integrated design of a motion cueing algorithm and a motion-base mechanism for a Wright Flyer Simulator. AIAA Modeling and Simulation Technologies Conference. Monterey, 5th-8th August 2002. AIAA 2002-4690.

Alicandri, E., Roberts, K. & Walker, J. (1986). A validation study of the DoT/FHWA simulator (HYSIM). Report FHWA/RD-86/067, Federal Highway Administration, U.S. Department of Transportation.

Allen, R.W., Klein, R.H. & Ziedman, K. (1979). Automobile research simulators: a review and new approaches. Transportation Research Board, 706, pp. 9-15.

Allen, R.W., Mitchell, D.G., Stein, A.C. & Hogue, J.R. (1991). Validation of real-time man-in-the-loop simulation. Proceedings of the Strategic Highway Research Program and Traffic Safety On Two Continents Conference, Swedish Road and Traffic Research Institute, Linköping, Sweden, 18th – 20th September 1991.

Allerton, D.J. (2009). Principles of flight simulation. Wiley-Blackwell. ISBN 0470754362.

Alm, H. (1995). Driving simulators as research tools – a validation study based on the VTI driving simulator. GEM Validation Studies, DRIVE II, project V2065, GEM (Generic Evaluation Methodology for Integrated Driving), VTI report ref. GEM/TR/TRC/MK950327, VTI, Sweden.

Bailey, A.C., Jamson, A.H., Wright, S. & Parkes, A.M. (1999). Recent and future development of the Leeds Driving Simulator. Proceedings of the Driving Simulation Conference, DSC '99, Paris, France, pp. 45-61.

Berger, D.R., Schulte-Pelkum, J. & Bülthoff, H.H. (2010). Simulating believable forward accelerations on a Stewart motion platform. ACM Transactions on Applied Perception, 7(1), pp. 5:1-5:27.

Bernard, J. & Clover, C. (1995). Tire modeling for low-speed and high-speed calculations. SAE Technical Paper Series 950311, Society of Automotive Engineers, Warrendale, PA, USA.

Berthoz, A., Pavard, B. & Young, L.R. (1975). Perception of linear horizontal self- motion induced by peripheral vision (linear vection) basic characteristics and visual-vestibular interactions. Experimental Brain Research, 23, pp. 471–489.

Berthoz, A. & Droulez, J. (1982). Linear self motion perception. In A. H. Wertheim, W. A. Wagenaar, & H. W. Leibowitz (Eds.), Tutorials on human motion perception, pp. 157–199. Plenum Press.

Berthoz, A. (2000) The brain's sense of movement, Harvard University Press. ISBN 0674009800.

Bertollini, G.P., Johnston, C.M., Kuiper. J.W., Kukula, J.C., Kulczycka, M.A. & Thomas, W.E. (1994). The General Motors driving simulator. Society of Automobile Engineers, Warrendale, PA, USA.

Blaauw, G.J. (1982). Driving experience and task demands in simulator and instrumented car: a validation study. Human Factors, 24(4), pp. 473–486.

Blakemore, M.R. & Snowdon, R.J. (1999). The effect of contrast upon perceived speed: a general phenomenon? Perception, 28(1), pp. 33-48.

Blakemore, M.R. & Snowdon, R.J. (2000). Textured backgrounds alter perceived speed. Vision Research, 40(6), pp. 629-638.

Blana, E. & Golias, J. (2002). Differences between vehicle lateral displacement on the road and in a fixed-base simulator. Human Factors, 44, pp. 303-313.

Boer, E.R., Kuge, N. & Yamamura, T. (2001). Affording realistic stopping behaviour: a cardinal challenge for driving simulators. Proceedings of the First Human-Centered Transportation Simulation Conference, Iowa City, 4th – 7th November 2001.

Bosch Rexroth-Hydraudyne (2006). University of Leeds electric 8-DoF motion system EMotion-2500-8DOF-500-MK1-XY; site acceptance tests. Document ID NL000584-02-39-0000-ATP-0001, Rexroth Hydraudyne B.V., Systems & Engineering, Boxtel, Netherlands.

Bradley, R.A. & Terry, M.E. (1952). Rank analysis of incomplete block designs: I. The method of paired comparisons. Biometrika, 39(4), pp. 324-345.

Brandt, T., Koenig, E. & Dichgans, J. (1973). Differential effects of central versus peripheral vision on egocentric and exocentric motion perception," Experimental Brain Research, 16(5), pp. 476–491.

Bray, R.S. (1985). Visual and motion cueing in helicopter simulation. NASA Technical Report, NASA-TM-86818.

Bremmer, F. & Lappe, M. (1999). The use of optical velocities for distance discrimination and reproduction during visually simulated self motion. Experimental Brain Research, 127(1), pp. 33-42.

Brookhuis, K.A., de Vries, G. & de Waard, D. (1991). The effects of mobile telephoning on driving performance. Accident Analysis and Prevention, 23(4), pp. 309-316.

Burchill, P. (2003). Simple X202 steering model: production version. Internal Jaguar Land Rover report.

Bürki-Cohen, J., Sparko, A.L. & Go, T.H. (2007). Training value of a fixed-base flight simulator with a dynamic seat. Proceedings of the AIAA Modelling and Simulation Technologies Conference and Exhibit, Hilton Head, South Carolina, 20th – 23rd August 2007. AIAA 2007-6564.

Capustiac, A., Hesse, B., Schramm, D. & Banabic, D. (2010). A human centered control strategy for a driving simulator. International Journal of Mechanical & Mechatronics Engineering, 11(1), pp.45-52.

Chapron, T. & Colinot, J.P. (2007). The new PSA Peugeot-Citroën advanced driving simulator: overall design and motion cue algorithm. Proceedings of the Driving Simulation Conference North America (DSC-NA 2007). Iowa City, 12th – 14th September 2007.

Chen, L.D., Papelis, Y., Watson, G. and Solis, D. (2001). NADS at the University of Iowa: a tool for driving safety research. Proceedings of the 1st Human-Centered Transportation Simulation Conference, Iowa, 4th – 7th November 2001.

Clark, B. & Graybiel, A. (1966). Factors contributing to the delay in the perception of the oculogravic illusion. American Journal of Psychology, 79, pp. 377-388.

Colombet, F., Dagdelen, M., Reymond, G., Pere, C., Merienne, F. & Kemeny, A. (2008). Motion cueing: what is the impact on the driver's behaviour? Proceedings of the Driving Simulation Conference 2008 (DSC Europe 2008), Monaco, 31st January – 1st February 2008.

Conrad, B. & Schmidt, S. F. (1969). The calculation of motion drive signals for piloted flight simulators. NASA Technical Report, NASA-CR-73375.

Conrad, B., Schmidt, S.F. & Douvillier, J. G. (1973). Washout circuit design for multi-degrees-of-freedom moving base simulators. Proceedings of the American Institute of Aeronautics and Astronautics Visual and Motion Simulation Conference, Palo Alto (CA), 10th September - 12th September 1973, paper number AIAA-1973-929.

Cremer, J.F., Kearney, J.K. & Papelis, Y. (1995). Hierarchical Concurrent State Machines: a framework for behavior and scenario control in virtual environments. ACM Transactions on Modeling and Computer Simulation, 5(3), pp. 242-267.

Crowell, J.A., Banks, M.S., Shenoy K.V. & Andersen R.A. (1998). Visual self-motion perception during head turns. Nature Neuroscience, 1(8), pp. 732-737.

Dagdelen, M., Reymond, G., Kemeny, A., Bordier, M. & Maïzi, N. (2009). Model-based predictive motion cueing strategy for driving simulators. Control Engineering Practice, 17(9), pp. 995-1003.

David, H.A. (1988). The method of paired comparisons. Charles Griffin & Company. ISBN 0852642903, second edition (first edition 1963).

Davidson, P. W. (1972). Haptic judgments of curvature by blind and sighted humans. Journal of Experimental Psychology, 93(1), pp. 43-55.

Davis, B.T. & Green, P (1995). Benefits of sound for driving simulation: an experimental evaluation. Technical report UMTRI-95-16, University of Michigan, Ann Arbor, Michigan.

Den Hartog, J.P. (1961). Mechanics. Dover Publications. ISBN 0486607542.

Drosdol, J. & Panik, F. (1985). The Daimler-Benz driving simulator: a tool for vehicle development. SAE Technical Paper Series 850334, Society of Automotive Engineers, Warrendale, PA, USA.

Duncan, B. (1995). Calibration trials of the TRL driving simulator. TRL Report PA/3079/95. Transport Research Laboratory, Crowthorne, U.K.

Dykstra, O. (1956). A note on the rank analysis of incomplete block designs – applications beyond the scope of existing tables. Biometrics, 12(3), pp. 301-306.

van Egmond, A. A. J., Groen, J. J. & Jongkees, L. B. W. (1949). The mechanics of the semicircular canal. Journal of Physiology, 110(1-2), pp. 1-17.

Fischer, M. & Werneke, J. (2008). The new time-invariant motion cueing algorithm for the DLR dynamic driving simulator. Proceedings of the Driving Simulation Conference (DSC Europe 2008), Monaco, 31st January - 1st February 2008.

Fischer, M., Lorenz, T., Wildfeuer, S. & Oeltze, K. (2008). The impact of different motion cueing aspects concerning the perceived and subjectively rated motion feedback during longitudinal and lateral vehicle control tasks. Proceedings of the Driving Simulation Conference (DSC Asia/Pacific 2008), Seoul, 10th – 12th September 2008.

Foley, J.D. van Dam, A., Feiner, S.K. & Hughes, J.F. (1990). Computer graphics principles and practice. Addison-Wesley. ISBN 0201121107.

Forsythe, G.E., Malcolm, M.A. & Moler, C.B. (1977). Computer methods for mathematical computations. Prentice-Hall. ISBN 0131653326.

Freeman, J.S., Watson G., Papelis, Y.E., Lin, T.C., Tayyab, A., Romano, R.A. & Kuhl, J.G. (1995). The Iowa Driving Simulator: an implementation and application overview. SAE Technical Paper Series 950174. Society of Automobile Engineers, Warrendale, PA, USA.

Gibson, J.J. & Crooks, L.E. (1938). A theoretical field-analysis of automobile driving. American Journal of Psychology, 51(3), pp. 453–471.

Gibson, J.J. (1950). The Perception of the Visual World. Greenwood Publishing Group. ISBN 0837178363.

Gillespie, T.D. (1992). Fundamentals of vehicle dynamics. SAE International. ISBN 1560911999.

Godthelp, H. & Konings, H.J.M. (1981). Levels of steering control; some notes on the time-to-line crossing concept as related to driving strategy. Proceedings of the First European Annual Conference on Human Decision Making and Manual Control, Delft, The Netherlands, 25th – 27th May 1981, pp. 343-356.

Gogel, W.C. & Tietz, J.D. (1979). A comparison of oculomotor and motion parallax cues of egocentric distance. Vision Research, 19(10), pp. 1161-1170.

Goldstein, H. (1980). Classical mechanics. Addison-Wesley. ISBN 0201029189

Grant, P.R. & Reid, L.D. (1997). Motion washout filter tuning: rules and requirements. Journal of Aircraft, 34(2), pp. 145-151.

Grant, P.R. & Nasri, A. (2005). Actuator state based adaptive motion drive algorithm. Proceedings of the Driving Simulation Conference 2005 (DSC North America 2005), Orlando, FL, 30th November – 2nd December 2005.

Grant, P.R. & Lee, P.T.S (2007). Motion-visual phase error detection in a flight simulator. Journal of Aircraft, 44(3), pp. 927-935.

Grant, P.R. & Haycock, B. (2008). Effect of jerk and acceleration on the perception of motion strength. Journal of Aircraft, 45(4), pp.1190-1197.

Grant, P.R., Blommer, M., Artz, B. & Greenberg, J. (2009). Analysing classes of motion drive algorithms based on paired comparison techniques. Vehicle System Dynamics, 47(9), pp. 1075-1093.

Greenberg, J.A. & Park, T.J. (1994). The Ford driving simulator. SAE Technical Paper Series 940176. Society of Automobile Engineers, Warrendale, PA, USA.

Greenberg, J., Artz, B. & Cathey, L. (2002) The effect of lateral motion cues during simulated driving. Proceedings of the Driving Simulation Conference – North America (DSC-NA 2003), Dearborn, Michigan, 8th – 10th October 2003.

Groeger, J.A., Carsten, O.M.J., Blana, E. & Jamson, A.H. (1997). Speed and distance estimation under simulated conditions. In: A.G. Gale, I.D. Brown, C.M. Haslegrave & S.P. Taylor (Eds.), Vision in Vehicles VII. Elsevier, North Holland. ISBN 0080436714.

Groen, E.L., Howard, I.P. & Cheung, S.K. (1999). Influence of body roll on visually induced sensations of self-tilt and rotation. Perception, 28(3), pp. 287-297.

Groen, E.L., Valenti Clari, M.S. & Hosman, R.J.A.W (2001). Evaluation of perceived motion during a simulated takeoff run. Journal of Aircraft, 38(4), pp. 600-606.

Groen, E.L. & Bles, W. (2004). How to use body tilt for the simulation of linear self motion. Journal of Vestibular Research, 14(4), pp. 375-385.

Gundry, J. (1976). Man and motion cues. Proceedings of the Third Flight Simulation Symposium, Royal Aeronautical Society, pp 1-19.

Guo, K., Ding, H., Zhang, J., Lu, J. & Wang, R. (2004). Development of a longitudinal and lateral driver model for autonomous vehicle control. International Journal of Vehicle Design, 36 (1), pp. 50-65.

Guo, L.W., Cardullo, F.M. Telban, R.J., Houck, J.A. & Kelly, L.C. (2003). The results of a simulator study to determine the effects on pilot performance of two different motion cueing algorithms and various delays, compensated and uncompensated. Proceedings of the AIAA Modeling and Simulation Technologies Conference and Exhibition, Austin, 11th-14th August 2003. AIAA 2003-5676.

Harms, L. (1993). Driving performance on a real road and in a driving simulator: results of a validation study. In Gale, A.G., Brown, I.D., Haslegrave, C.M. & Taylor, S.P. (Eds.): Vision in Vehicles IV. Elsevier, North Holland. ISBN 0444893628.

Harris, J.M. & Bonas, W. (2002). Optic flow and scene structure do not always contribute to the control of human walking. Vision Research, 42(13), pp. 1619-1626.

Harris, L. R., Jenkin, M. & Zikovitz, D. C. (2000). Visual and non-visual cues in the perception of linear self motion. Experimental Brain Research, 135(1), pp. 12–21.

Hess, R.A. & Malsbury, T. (1991). Closed loop assessment of flight simulator fidelity. Journal of Guidance, Control and Dynamics, 14(1), pp. 191–197.

Hess, R.A. & Marchesi, F. (2009). Analytical assessment of flight simulator fidelity using pilot models. Journal of Guidance, Control and Dynamics, 32(3), pp. 760-770.

van Hofsten, C. (1976). The role of convergence in visual space perception. Vision Research 16(2), pp. 193-198.

Hosman, R.J.A.W. & Stassen, H. (1999). Pilot's perception in the control of aircraft motions. Control Engineering Practice, 7(11), pp. 1421–1428.

Hosman, R.J.A.W. & van der Vaart, J.C. (1981). Effects of vestibular and visual-motion perception on task performance. Acta Psychologica, 48, pp. 271–281.

Howard, I.P. & Templeton, W.B. (1966). Human spatial orientation. John Wiley & Sons. ISBN 0471416622.

Howard, I.P. & Rogers, B.J. (1995). Binocular vision and stereopsis. Oxford University Press. ISBN 0195084764.

Howarth, P.A. (1999). Oculomotor changes with virtual environments. Applied Ergonomics, 30(1), pp. 59-67.

Jackson, S.W., Crick, J.L., White, A.D. & Shuttleworth, A. (1999). An assessment of the requirements for automotive ride and handling simulation. Defence Evaluation and Research Agency, Farnborough, U.K. DERA Report CR990280.

Jamson, A.H. (2000). Driving simulator validity: issues of field of view and resolution. Proceedings of the Driving Simulation Conference (DSC2000), Paris, 4th – 6th September 2000.

Jamson, A.H., Horrobin, A.J. & Auckland, R.A. (2007). Whatever happened to the LADS? Design and development of the new University of Leeds Driving Simulator. Proceedings of the Driving Simulation Conference North America (DSC-NA 2007). Iowa City, 12th – 14th September 2007.

Jex, H. R., Magdaleno, R. E. & Junker, A. M. (1978). Roll tracking effects of g-vector tilt and various types of motion washout. NASA Technical Report, NASA-CP-2060.

Käding, W. & Hoffmeyer, F. (1995). The advanced Daimler-Benz driving simulator. SAE Technical Paper Series 952279. Society of Automobile Engineers, Warrendale, PA, USA.

Kaptein, N.A., Theeuwes, J. & van der Horst, A.R.A. (1996). Driving simulator validity: some considerations. Transportation Research Record, 1550, pp. 30-36.

Kemeny, A. & Panerai, F. (2003). Evaluating perception in driving simulation. Trends in Cognitive Sciences, 7(1), pp. 31-37.

Kendall, M.G. & Babington-Smith, B. (1940). On the method of paired comparisons. Biometrika, 31(4), pp. 324-345.

Kennedy, R. S., Lane, N. E., Lilienthal, M. G., Berbaum, K. S. & Hettinger, L. J. (1992). Profile analysis of simulator sickness symptoms: Application to virtual environment systems. Presence: Teleoperators and Virtual Environments, 1(3), pp. 295-301.

Land, M.F. & Lee, D.N. (1994). Where we look when we steer. Nature, 369(6483), pp. 742-744.

Land, M.F. & Horwood, J. (1995). Which parts of the road guide steering? Nature, 377(6547), pp. 339-340.

Lappe, M., Bremmer, F & van den Berg, A.V. (1999). Perception of self-motion from visual flow. Trends in Cognitive Sciences, 3(9), pp. 329-336.

Larson,P., Väljamäe, A., Västfjäll, D. & Kleiner, M. (2004). Perception of self-motion and presence in auditory virtual environments. Proceedings of the 7th Annual Workshop of Presence, Valencia, Spain.

Leal-Loureiro, B.D.C. (2009). Motion cueing in the Chalmers Driving Simulator: a model predictive control approach. Master of Science Thesis, Department of Signals and Systems, Chalmers University of Technology, Report No. EX057/2009.

Lee, A.T. & Bussolari, S.R. (1989). Flight simulator platform motion and air transport pilot training. Aviation, Space and Environmental Medicine, 60(2), pp 136-140.

Lee, D.N. (1976). A theory of visual control of braking based on information about time-to-collision. Perception, 5(4), pp. 437-459.

Levitt, H. (1971). Transformed up-down methods in psychoacoustics. Journal of the Acoustical Society of America, 49(2), pp.467-477.

Lichtenberg, B.K., Young, L.R. & Arrot, A.P. (1982). Human ocular counter-rolling induced by varying linear accelerations. Experimental Brain Research, 48, pp. 127-136.

Loomis, J.M. & Knapp, J.M. (1999). Visual perception of egocentric distance in real and virtual environments. In: L.J.Hettinger & M.W. Haas (Eds.), Virtual and adaptive environments, Erlbaum.

Loomis, J.M. (2010). Visual control of driving and flying: importance of optic flow rules, perceptual representation of 3-D space, and internal models of vehicle dynamics. Proceedings of the Driving Simulation Conference 2010 (DSC Europe 2010), Paris, 9th – 10th September 2010.

McKnight, A.J. & Hunter, H.G. (1966). An experimental evaluation of a driver simulator for safety training. Technical Report. No. 66-9, Human Resources Research Organization, Alexandria, VA, USA.

McLane, R.C. & Wierwille, W.W. (1975). The influence of motion and audio cues on driver performance in an automobile simulator. Human Factors, 17(5), pp. 488-501.

McLean, J.R. & Hoffmann, E.R. (1975). Steering reversals as a measure of driver performance and steering task difficulty. Human Factors, 17(3), pp. 248-256.

McRuer, D.T. & Jex, H.R. (1967). A review of quasi-linear pilot models. IEEE Transactions on Human Factors in Electronics, 8(3), pp. 231 -249.

Mann, H.B. & Whitney, D.R. (1947). On a test of whether one of two random variables is stochastically larger than the other. Annals of Mathematical Statistics, 18(1), pp. 50-60.

Melcher, G.A. & Henn, V. (1981). The latency of circular vection during different accelerations of the optokinetic stimulus. Perception and Psychophysics, 30(6), pp. 552-556.

Mesland, B.S. (1998). About linear self-motion perception. Ph.D. Thesis, Department of Biology, Utrecht University, The Netherlands.

Nahon, M. A. & Reid, L. D. (1990). Simulator Motion-Drive Algorithms: A designer's perspective. AIAA Journal of Guidance, Control and Dynamics, 13(2), pp. 356-362.

Nahon, M.A., Reid, L.D. & Kirdeikis, J. (1992). Adaptive simulator motion software with supervisory control. AIAA Journal of Guidance, Control and Dynamics, 15(2), pp. 376-383.

Noether, G.E. (1960). Remarks about paired comparisons. Psychometrika, 25(4), pp. 357-367.

Nordmark, S. (1984). VTI Driving Simulator – mathematical model of a four-wheeled vehicle for simulation in real time. VTI Report 267A, VTI, Swedish National Road and Transport Research Institute, Lindköping.

Nordmark, S., Lidström, M. & Palmkvist, G. (1984). Moving base driving simulator with wide angle visual system. SAE Technical Paper Series 845100, Society of Automotive Engineers, Warrendale, PA, USA.

Nordmark, S., Janson, H., Palmkvist, G. & Sehammar, H. (2004). The new VTI driving simulator: multi-purpose moving base with high performance linear motion. Proceedings of the Driving Simulation Conference (DSC 2004), Paris, 8th -10th September 2004.

Padfield, G. & White, M. (2005). Measuring simulation fidelity through an adaptive pilot model. Aerospace Science and Technology, 9(5), pp. 400-408.

Pacejka, H.B. & Besselink, I.J.M. (1997). Magic Formula tyre model with transient properties. Vehicle System Dynamics, 27(S1), pp.234-249.

Pacejka, H. B. (2005). Tyres and vehicle dynamics. Butterworth-Heinemann. ISBN 0750669187.

Panerai, F., Cornilleau-Peres, V. & Droulez, J. (2002). Contribution of extra-retinal signals to the scaling of object distance during self-motion. Perception and Psychophysics, 64(5), pp. 717-731.

Parrish, R.V., Dieudonne, J.E., Bowles, R.L. & Martin, D.J. (1975). Coordinated adaptive washout for motion simulators. Journal of Aircraft, 12(1), pp. 44-50.

Porat, B. (1997). A Course in Digital Signal Processing. New York: John Wiley. ISBN 0471149616

Pouliot, N.A., Gosselin, C.M. & Nahon, M.A. (1998). Motion simulation capabilities of three-degree-of-freedom flight simulators. Journal of Aircraft, 35(1), pp. 9-17.

Rasmussen, J. (1983). Skills, rules, and knowledge: Signals, signs, and symbols, and other distinctions in human performance models. IEEE Transactions on Systems, Man and Cybernetics, 13(3), pp. 257-266.

Reid, L. D. & Nahon, M. A. (1985). Flight Simulation Motion-Base Drive Algorithms: Part 1 – Developing and Testing the Equations. University of Toronto Institute for Aerospace Studies Report 296, University of Toronto.

Reid, L. D. & Nahon, M. A. (1986a). Flight Simulation Motion-Base Drive Algorithms: Part 2 – Selecting the System Parameters. University of Toronto Institute for Aerospace Studies Report 307, University of Toronto.

Reid, L. D. & Nahon, M. A. (1986b). Flight Simulation Motion-Base Drive Algorithms: Part 3 – Pilot Evaluations. University of Toronto Institute for Aerospace Studies Report 319, University of Toronto.

Reid, L. D. & Nahon, M. A. (1988). Response of airline pilots to variations in flight simulator motion algorithms," Journal of Aircraft, 25(7), pp. 639-646.

Reymond, G. & Kemeny, A. (2000) Motion cueing in the Renault driving simulator. Vehicle System Dynamics, 34(4), pp. 249-259.

Reymond, G., Kemeny, A., Droulez, J. & Berthoz, A. (2001). Role of lateral acceleration in curve driving: driver model and experiments on a real vehicle and a driving simulator. Human Factors, 43(3), pp. 483-495.

Riecke, B.E., Schulte-Pelkum, J., Caniard, F. & Bülthoff, H.H. (2005). Influence of auditory cues on the visually-induced self-motion illusion (circular vection) in virtual reality. Proceedings of the 8th Annual Workshop of Presence, New York.

Riecke, B.E., Väljamäe, A. & Schulte-Pelkum, J. (2009). Moving sounds enhance the visually-induced self-motion illusion (circular vection) in virtual reality. ACM Transactions on Applied Perception, 6(2), article 7, pp. 7:1-7:27.

Riemersma, J.B.J., van der Horst, A.R.A. & Hoekstra, W. (1990). The validity of a driving simulator in evaluating speed-reducing measures. Traffic Engineering and Control, 35, pp. 416-420.

Rogers, B. & Graham, M. (1979). Motion parallax and an independent cue for depth perception. Perception, 8(1), pp. 125-134.

Rolfe, J.M., Hammerton-Frase, A.M., Poulter, R.F. & Smith, E.M.B. (1970). Pilot response in flight and simulated flight. Ergonomics, 13(6), pp. 761-68.

Russell, K.G. (1980). Balancing carry-over effects in round robin tournaments. Biometrika, 67(1), pp.127-131.

SAE (2008). SAE J670 – Vehicle dynamics terminology. Society of Automotive Engineers, Vehicle Dynamics Standards Committee, Warrendale, PA, USA.

Salaani, K.M. & Heydinger, G.J. (1998). Powertrain and brake modelling of the 1994 Ford Taurus for the National Advanced Driving Simulator. SAE Technical Paper Series 981190, Society of Automotive Engineers, Warrendale, PA, USA.

Salaani, K.M., Heydinger, G.J. & Grygier, P. (2002). Modeling and implementation of steering system feedback for the National Advanced Driving Simulator. Technical Paper Series 2002-01-1573, Warrendale, PA, USA.

Sakamoto, S., Osada, Y., Suzuki, Y. & Gyoba, J. (2004). The effects of linearly moving sound images on selfmotion perception. Acoustical Science and Technology, 25(1), pp. 100-102.

Sayers, M.W. (1993). AUTOSIM. Vehicle System Dynamics, 22(2), S1, pp. 53-56.

Sayers, M.W. & Han, D.S. (1996). A generic multibody vehicle model for simulating handling and braking. Vehicle System Dynamics, 25(1), S1, pp. 599-613.

Sayers, M.W. & Riley, S.M. (1996). Modelling assumptions for realistic multibody simulations of the yaw and roll behaviour of heavy trucks. SAE Technical Paper Series 960173. Society of Automobile Engineers, Warrendale, PA, USA.

Schroeder, J.A. (1999). Helicopter flight simulation motion requirements. NASA Technical Report, NASA-TP-1999-208766.

Schroeder, J.A., Chung, W.W.Y. & Hess, R.A. (2000). Evaluation of a motion fidelity criterion with visual scene changes. Journal of Aircraft, 37(4), pp. 580-587.

Segel, L. (1956). Theoretical prediction and experimental substantiation of the response of the automobile to steering control. Proceedings of the Automobile Division of the Institution of Mechanical Engineers, 1956, (7), pp. 310–330.

Shirachi, D. K. & Shirley, R. S. (1981). Visual/motion cue mismatch in a coordinated roll maneuver. NASA Technical Report, NASA CR-166259.

Siegler, I., Reymond, G., Kemeny, A. & Berthoz, A. (2001). Sensorimotor integration in a driving simulator: contribution of motion cueing in elementary driving tasks. Proceedings of the Driving Simulation Conference (DSC2001), Nice, 5th – 7th September 2001.

Sinacori, J. B. (1977). The determination of some requirements for a helicopter flight research simulation facility. NASA technical report, NASA-CR-152066.

Sinclair, R.J. & Burton, H. (1996). Discrimination of vibrotactile frequencies in a delayed pair comparison task. Perception & Psychophysics, 58(5), pp. 680-692.

Sivan, R., Ish-shalom, J. & Huang, J.K. (1982). An optimal control approach to the design of moving flight simulators. IEEE Transactions on Systems, Man and Cybernetics, 12, pp. 818-827.

Stanney, K. M., Mourant, R. R. & Kennedy, R. S. (1998). Human factors issues in virtual environments: a review of the literature. Presence, 7(4), pp. 327–351.

Student (1908). The probable error of a mean. Biometrika, 6(1), pp. 1-25.

Stewart, D. (1965). A platform with six degrees of freedom. Proceedings of the Institution of Mechanical Engineers 1965-66, 180(1), pp. 371-378.

Soma, H., Hiramatsu, K., Satoh, K. and Uno, H. (1996). System architecture of the JARI driving simulator and its validation. Proceedings of the Symposium on the Design and Validation of Driving Simulators, Valencia, Spain, 21st May 1996.

Suetomi, T., Horiguchi, A., Okamoto, Y. & Hata, S (1990). The Driving Simulator with large amplitude motion system. SAE Technical Paper Series 910113. Society of Automobile Engineers, Warrendale, PA, USA.

Suikat, R. (2005). The new dynamic driving simulator at DLR. Proceedings of the Driving Simulation Conference - North America (DSC-NA 2005), Orlando, 30th November – 2nd December 2005.

Takeuchi, T. & De, V. (2000). Velocity discrimination in scotopic vision. Vision Research, 40, pp. 2011-2024.

Telban, R.J., Cardullo, F.M. & Houck, J.A. (2002). A nonlinear, human-centered approach to motion cueing with a neurocomputing solver. Proceedings of the AIAA Modeling and Simulation Technologies Conference and Exhibit, Monterey, CA, 5th-8th August 2002. Paper number AIAA 2002-4692.

Thurstone, L.L. (1927). A law of comparative judgement. Psychological Review, 34(4), pp. 273-286.

Tomaske, W. (1999). A Modular Automobile Road Simulator (MARS) for on and off-road conditions. Proceedings of the Driving Simulation Conference (DSC '99), Paris, 7th – 8th July 1999.

Valente Pais, A.R., Wentink, M., van Paassen, M.M. & Mulder, M. (2009). Comparison of three motion cueing algorithms for curve driving in an urban environment. Presence, 18(3), pp. 200-221.

Väljamäe, A., Larson, P, Västfjäll, D. & Kleiner, M. (2006). Vibrotactile enhancement of auditory induced self-motion and spatial presence. Journal of Acoustic Engineering Society, 54(10), pp. 954-963.

Vander, A.J., Sherman, J.H. & Luciano, D.S. (1975). Human physiology: the mechanisms of body function. McGraw-Hill. ISBN 0070669546.

Wald, G. (1945). Human vision and spectrum. Science, 101(2635), pp. 653-658.

Watts, G.R. and Quimby, A.R. (1979). Design and validation of a driving simulator for use in perceptual studies. Report no. TRRL LR 907, Transport and Road Research Laboratory, Crowthorne, U.K.

Wann, J. & Land, M.J. (2000). Steering with or without the flow: is the retrieval of heading necessary? Trends in Cognitive Sciences, 4(8), pp. 319-324.

Wertheim, A. H. (1994). Motion perception during self-motion: the direct versus inferential controversy revisited," Behaviorial and Brain Sciences, 17(2), pp. 292–355.

Wetink, M., Bles, W. Hosman, R. & Mayrhofer, M. (2005). Design & evaluation of spherical washout algorithm for Desdemona simulator. Proceedings of the AIAA Modeling and Simulation Technologies Conference and Exhibit, San Francisco, 15th – 18th August 2005. AIAA 2005-6501.

Wickens, C. D. & Flach, J. (1988). Information processing. In: E. L. Wiener & D. C. Nagel (Eds.). Human factors in aviation. San Diego: Academic Press, pp. 111-155.

Wierwille, W.W., Casali, J.G. & Repa, B.S. (1983). Driver steering reaction time to abrupt-onset crosswinds as measured in a moving-base driving simulator. Human Factors, 25(1), pp. 103-116.

Wilcoxon, F. (1945). Individual comparisons by ranking methods. Biometrics Bulletin, 1(6), pp. 80-83.

van Winsum, W. & Godthelp, H (1996). Speed choice and steering behaviour in curve driving. Human Factors, 38(3), pp. 257-268.

van Wolffelaar, P.C. (1996). Traffic generation and scenario control in the TRC simulator. Workshop on Scenario and Traffic Generation for Driving Simulation, Orlando, 6th – 7th December, 1996.

Wojcik, C.K. & Hulbert, S.F. (1965). The driving simulator – a research tool. Paper number 65-WA/HUF-13, American Society of Mechanical Engineers.

Young, L.R. (1969). On adaptive manual control. Ergonomics 12(4), pp. 635-675.

Young, L. R., Dichgans, J., Murphy, R. & Brandt, T. (1973). Interaction of optokinetic and vestibular stimuli in motion perception. Acta Oto-Laryngologica, 76, pp. 24–31.

APPENDIX 1 –

PARTICIPANT BRIEFING (STAGE 1)

PARTICIPANT BRIEFING (STAGE 1)

Background

The study in which you have been invited to participate, seeks to investigate the most realistic way to simulate motion in the driving simulator. It has been designed in three stages, each looking at different aspects of the motion system. During each stage, you will be presented with a series of short driving scenarios, some involving braking/accelerating, others involving cornering. During the this stage, you will not be required to actually drive the simulator but just to experience the simulation as though you were the driver. However, in following two stages you will be in full control of the vehicle.

Today's study

Today's study will be split into two 25-minute sessions in the simulator, one involving cornering through a long chicane and the other involving braking and accelerating during car following. Although you will be sitting in the driver's seat, you will not be required to actually drive the simulator in either session; all you will be requested to do is rate your perception of the feel of the simulation. Between each session there will be a short break.

The chicane-cornering session consists of a number of paired scenarios. In each scenario, the driving scene is a wide test-track with cones marking out a path for the vehicle through the chicane. As the visual display fades up into the scenario, you will find yourself "driving" at a constant 60mph. The vehicle will follow the path of the cones as though you were smoothly steering to the right and then back to the left in order to straighten up. The scenario should feel a bit like a S-shaped curve before fading back out. During the scenario, it is important to imagine as though you were handling the vehicle as described here.

This driving situation is presented twice, forming a scenario pair. During each pair, the motion system will behave differently. In one of the pairs, the acceleration of the simulator will exactly match that of a real vehicle in such a scenario. In the other, movement of the simulator will be scaled down so that the simulated accelerations are lower than they would be in the real situation. You are required to indentify in which of the pairs matches reality, i.e. the unscaled condition. The impression of acceleration will appear stronger in this condition. The visual scene will reinforce the illusion, but it is important that your answer is based on the perceived level acceleration that you feel in the simulator.

The braking/accelerating session also consists of a number of paired scenarios. This time, the visual scene will fade into a typical country road with you "driving" at the speed limit of 60mph. There will be another vehicle in front of you, also travelling at 60mph. After a few seconds, this lead vehicle will begin to slow down gently, denoted by the illumination of its brakelights. At this point, the simulator will also slow down, as though you had also gently applied the brakes in an attempt to keep a constant gap to the lead vehicle. After several seconds of braking, the lead vehicle will slowly accelerate back to 60mph (its brakelights will turn off), followed by the simulator as though you were accelerating to once again close the gap and maintain a constant following distance to the lead vehicle. At the end of the manoeuvre, the visual scene will fade back out. It is important to imagine as though you were handling the vehicle as described here. Once again, the visual scene will reinforce the illusion and the speedometer in the simulator cab will show how driving speed changes during the scenario.

Just as in the chicane-cornering scenario, the movement of the simulator will be presented both in a 1:1 relationship and in a scaled down version where you will experience a feeling of acceleration and

PTO

deceleration at a reduced level from reality. Once more, your task is to identify the higher level of acceleration in the unscaled condition.

Some participants will undertake the braking/accelerating car following session before the chicane cornering session, whilst others the chicane cornering session before the braking/accelerating car following session. The researcher will let you know in which order you will experience the sessions.

While the visual scene has faded out as well as when the scenario starts, you may feel some small jolts through the motion system. Please ignore this motion. When rating the perceived accuracy of the motion cue, consider only the motion that that you feel during the actual chicane or braking/accelerating manoeuvres.

You will be given an opportunity to experience the two scenarios with the researcher in attendance in order to fully demonstrate the requirements of the study. Please feel free as many questions as you like and to clarify anything that is not obvious to you.

Wellbeing

Although today's study has been carefully designed to minimise any potential problems, there is a small risk that the repeated scenarios may introduce feelings of motion discomfort. As you have driven the simulator in the past, it is highly unlikely that any such issues will arise. However, if at any point you do feel unwell or nauseous, please do not be embarrassed to withdraw from the study. We would rather this than make you feel ill! Simply inform the researcher over the intercom and we will stop the simulation immediately. The researcher will then escort you back to the briefing area and remain with you whilst any symptoms subside.

Ethics, safety and confidentiality

As with all our research, this study is subject to the strict ethical guidelines of the British Psychological Society and the requirements of the Data Protection Act. In particular please note that:

- At no time now, nor in the future, will any information that you provide be published in such a manner that might allow you to be identified as an individual.
- You are free to withdraw from the study at any time without having to give any reason for your decision.
- Video footage, which may include images of your face, may be used during the dissemination of this research project to the scientific community. We will **not** make such footage available to any other organisation.

Multi-staged experiment

Your results from this first stage will feed through into the two later stages that you have also kindly volunteered for. In order to achieve meaningful results from this study, it is important that each stage is completed.

In total, you will make five visits to the simulator and each will take around one hour. At the end of your fifth and final visit you will receive £50 as a token of appreciation for your commitment.

Finally, we would like to thank you very much for expressing an interest in this work and we hope that you will enjoy the time spent at the simulator. Your contribution is much appreciated. If you have any questions, please feel free to ask.

APPENDIX 2 –

PARTICIPANT BRIEFING (STAGES 2 & 3)

PARTICIPANT BRIEFING (STAGES 2 AND 3)

Today's stage

Today's stage is similar to the previous sessions in that short scenarios will be presented in pairs. However, this time you will actually be controlling the simulator. You will be participating in two 25-minute sessions, one involving cornering and the other involving braking. This time, both scenarios require you to achieve a particular driving task, as well as rate your perceived quality of the feel of the simulator. Between each session there will be a short break.

In the braking scenarios, the visual scene will only fade up when you are ready. When prompted by the researcher, signal you readiness by depressing the accelerator pedal. At this point, the visual scene will fade in and you will find yourself on a two-lane urban road, travelling at 40mph. Ahead of you will be a lead vehicle. You task is to try and drive as smoothly as possible, keeping a constant distance between you and the lead vehicle throughout the scenario. After a few seconds, you will notice a traffic light ahead change from green to amber to red. As in a typical U.K. urban traffic light, the amber phase will remain illuminated for 3s before the red light appears. The moment the traffic light changes to red, the lead vehicle will start to brake as through it were about to stop at the lights. The continuation of your task is to brake at the same time as the lead vehicle, decelerating as smoothly as possible and always keeping a constant distance between you and the lead vehicle. After a few seconds on red, the traffic light will change to red/amber and then to green. The moment you see the red/amber phase, your task is over and you can stop braking. A few seconds later the scene will fade out.

As in the previous stage, this scenario will be presented to you in pairs. You will be given an opportunity to practice the scenario as many times as you like with the researcher present with the motion system switched off. This is followed by four practice pairs with you alone in the vehicle and with the motion system switched on.

During each pair, the motion system will behave differently. As well as the task of maintaining a constant distance to the lead vehicle, you will also be asked to rate which of the two scenarios in the pair felt, in your opinion, the more realistic. The specific question you will be answering is: "was the simulation of motion more accurate in the first or second presentation of the scenario pair?". Your response will be either "first" or "second". It is **very important** that your answer is based on your perception of the realism of motion that you feel during the scenario, rather than how well you think you performed during in the braking task.

Between scenario pairs and as the visual scene fades up, you may feel some movement of the motion system. Please disregard this and make your ratings based only of the behaviour of the simulator during the scenario itself.

In the cornering scenario, again the visual scene will only fade up when you are ready. When prompted by the researcher, signal your readiness by depressing the accelerator pedal. You will now find yourself on an empty three-lane motorway, travelling at just over 70mph. Ahead of you is a bend to the left. Again, your task is to drive as smoothly as possible, but this time keeping as close as you can to the middle of the lane that you are in throughout the curve. After you have negotiated the curve, the scene will fade out. Again, you will be given an opportunity to practice the scenario with the researcher present (no motion) and alone (with motion).

This driving situation is also presented twice, forming a scenario pair and again you will be requested to decide which of the two felt the more realistic. It is important that your answer is based on your

PTO

perception of the realism of the motion cue that you feel rather than your ability to keep the vehicle in lane and your performance in the task.

Wellbeing

The fact that you had no problems in stage 1 means that it is highly unlikely that you will have any feelings of motion discomfort during this stage. However, as you are now in control of the vehicle and hence the behaviour of the motion system, you still need to be aware of this risk. If at any point you do feel unwell or nauseous, please do not be embarrassed to withdraw from the study. We would rather this than make you feel ill! Simply inform the researcher over the intercom and we will stop the simulation immediately.

Ethics, safety and confidentiality

As with all our research, this study is subject to the strict ethical guidelines of the British Psychological Society and the requirements of the Data Protection Act. In particular please note that:

- At no time now, nor in the future, will any information that you provide be published in such a manner that might allow you to be identified as an individual.
- You are free to withdraw from the study at any time without having to give any reason for your decision.
- Video footage, which may include images of your face, may be used during the dissemination of this research project to the scientific community. We will **not** make such footage available to any other organisation.

Multi-staged experiment

Your earlier results have fed into this stage. Correspondingly, your results from this stage will feed through into the final stage that you have also kindly volunteered for. In order to achieve meaningful results from this study, it is important that each stage is completed.

This and each of your next visits to the simulator will take around one hour. At the end of your fifth and final visit you will receive £50 as a token of appreciation for your commitment.

Finally, we would like to thank you very much for expressing an interest in this work and we hope that you will enjoy the time spent at the simulator. Your contribution is much appreciated. If you have any questions, please do not hesitate to ask.